

MD thesis

**Improving the detection of abnormal visual
function in glaucoma using High Spatial
Resolution Perimetry and Motion
Displacement Threshold testing**

Mark Westcott FRCOphth.

1999

Supervisors

Professor F W Fitzke PhD

Professor R A Hitchings FRCS FRCOphth.

Institutions:

Institute of Ophthalmology, Bath Street London EC1.

Moorfields Eye Hospital; City Road, London EC1



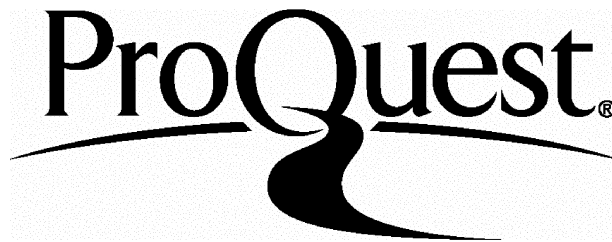
ProQuest Number: U122170

All rights reserved

INFORMATION TO ALL USERS

The quality of this reproduction is dependent upon the quality of the copy submitted.

In the unlikely event that the author did not send a complete manuscript and there are missing pages, these will be noted. Also, if material had to be removed, a note will indicate the deletion.



ProQuest U122170

Published by ProQuest LLC(2015). Copyright of the Dissertation is held by the Author.

All rights reserved.

This work is protected against unauthorized copying under Title 17, United States Code.
Microform Edition © ProQuest LLC.

ProQuest LLC
789 East Eisenhower Parkway
P.O. Box 1346
Ann Arbor, MI 48106-1346

1. Abstract

Primary open angle glaucoma is a major cause of blindness and visual disability. The introduction to this thesis summarises evidence that automated perimetry is not sensitive enough to detect early glaucomatous damage. This thesis investigates two novel tests of visual function which are Motion Displacement Threshold (MDT) testing and High Spatial Resolution Perimetry (HSRP).

In chapter 4, motion reaction times are shown to be abnormally elevated in glaucoma patients as a function of threshold elevation. Their potential use as a marker for reliability is outlined. Chapter 5 reports that analysis of the slope of the frequency-of-seeing curve improves the sensitivity of the MDT test compared with analysis of the threshold alone.

Chapter 6 describes the technique of High Spatial Resolution Perimetry (HSRP) and investigates its spatial resolution, repeatability and clinical use in glaucoma.

Chapter 7, elevated Motion Displacement Thresholds (MDTs) are identified in glaucoma. These are shown to coexist in some cases with fine scale scotomas identified using HSRP. This suggests that an underlying factor contributing to MDT abnormalities in addition to selective magnocellular loss or reduced redundancy is sensitivity loss on a spatial scale too small to be measured by conventional perimetry. This led to the hypothesis that the orientation of the MDT stimulus could have a significant effect on motion threshold glaucoma, and that stimulus orientation might be incorporated in order to improve the sensitivity of the test. This hypothesis was tested in chapter 8, which identified increasing elevation of motion threshold for a line stimulus moving perpendicular to the retinal nerve fibre layer compared to a line stimulus moving parallel to the retinal nerve fibre layer in some glaucoma patients.

The clinical significance of these studies is summarised in chapter 9 and future developments to improve the MDT and HSRP tests are discussed.

2. Table of contents

1. Abstract	2
2. Table of contents	3
3. List of figures	8
4. Acknowledgements	11
5. Outline of thesis	12
1. CHAPTER 1 Glaucoma	13
1.1 Definition	13
1.2 Classification	13
1.2.1 Concepts	13
1.2.2 Primary Open Angle Glaucoma (POAG)	14
1.3 Epidemiology	14
1.3.1 Prevalence	15
1.3.2 Incidence	16
1.3.3 Risk factors	16
1.4 Aetiology	19
1.4.1 Pathogenesis	19
1.4.2 Mechanical theories	20
1.4.3 Vascular theory	21
1.4.4 Apoptosis	22
1.4.5 Genetic factors	23
1.5 Treatment	23
1.6 Summary	24
2. CHAPTER 2 Visual function in glaucoma	26
2.1 The anatomy of the visual pathway	26
2.1.1 Introduction	26
2.1.2 The retinal ganglion cell	26
2.1.3 Parallel visual pathways	27
2.1.4 Visual function and parallel pathways	28
2.2 Measurement of visual function in glaucoma	30
2.2.1 Fundamentals of perimetry	30

2.2.2 History of perimetry _____	30
2.2.3 Kinetic perimetry _____	31
2.2.4 Static perimetry _____	31
2.2.5 Automated perimetry _____	31
2.2.6 The Humphrey Field Analyzer (HFA) _____	32
3. CHAPTER 3 Aims of research: Improving the detection of abnormal visual function in glaucoma _____	34
3.1 Limitations of conventional automated perimetry in detecting early damage _____	34
3.2 Rationale for using other psychophysical tests _____	35
3.2.1 Introduction _____	35
3.2.2 Selective ganglion cell loss in glaucoma _____	36
3.2.3 Reduced redundancy _____	37
3.3 Motion Perception perimetry in glaucoma _____	38
3.3.1 Introduction _____	38
3.3.2 Line displacement thresholds _____	38
3.3.3 Random dot kinetograms _____	40
3.4 Other psychophysical tests _____	42
3.4.1 Short Wavelength Automated perimetry (SWAP) _____	42
3.4.2 Flicker perimetry _____	43
3.4.3 High-pass resolution perimetry _____	43
3.4.4 Frequency doubling perimetry _____	44
3.5 Aims and plan of research _____	44
3.5.1 Motion sensitivity _____	45
3.5.2 High Spatial Resolution Perimetry _____	45
4. CHAPTER 4 Differences in the reaction times for motion detection between normals and glaucoma. _____	46
4.1 Background _____	46
4.2 Purpose _____	47
4.3 Method _____	47
4.3.1 Subjects _____	47
4.3.2 Motion Displacement Testing _____	48
4.3.3 Recording of reaction times _____	48
4.4 Results _____	48
4.4.1 Motion thresholds _____	48
4.4.2 Reaction times _____	49

4.4.3 The relationship between reaction time and stimulus displacement _____	49
4.4.4 Are the prolonged reaction times in glaucoma patients accounted for by threshold elevation? _____	53
4.5 Discussion _____	54
5. CHAPTER 5 Characteristics of Frequency-of-Seeing curves for a motion stimulus in glaucoma eyes, glaucoma suspect eyes, and normal eyes. _____	55
5.1 Background _____	55
5.2 Purpose _____	56
5.3 Method _____	56
5.3.1 Subjects _____	56
5.3.2 Testing strategy _____	57
5.3.3 Analysis _____	58
5.4 Results _____	61
5.4.1 Discriminating between the glaucoma eyes and normal eyes using threshold and slope abnormalities. _____	61
5.4.2 The relationship between slope and the 50% seen threshold _____	64
5.5 Discussion _____	67
6. CHAPTER 6 High spatial resolution automated perimetry in glaucoma _____	69
6.1 Background _____	69
6.2 Purpose _____	69
6.3 Methods _____	70
6.3.1 Subjects _____	70
6.3.2 Technique of fine matrix mapping (FMM) _____	70
6.3.3 Examination protocols _____	71
6.3.4 Statistical analysis _____	72
6.4 Results _____	73
6.4.1 High Spatial Resolution Perimetry of the blind spot. _____	73
6.4.2 High Spatial Resolution Perimetry in patients with retinal nerve fibre layer defects. _____	75
6.4.3 Clinical evaluation of High Spatial Resolution Perimetry _____	78
6.5 Discussion _____	87
7. CHAPTER 7 Abnormal Motion Displacement Thresholds are associated with Fine Scale Luminance Sensitivity Loss in Glaucoma. _____	89
7.1 Background _____	89

7.2 Purpose	90
7.3 Methods	91
7.3.1 Subjects	91
7.3.2 Motion Displacement Testing	92
7.3.3 High Spatial Resolution Perimetry	95
7.3.4 Analysis	96
7.4 Results	96
7.4.1 Motion Displacement Thresholds (MDTs)	96
7.4.2 High Spatial Resolution Perimetry Luminance thresholds	97
7.4.3 Comparison between abnormal Motion Displacement Thresholds and abnormal High Spatial Resolution Perimetry thresholds.	98
7.5 Discussion	104
8. CHAPTER 8 <i>The effect of stimulus orientation on Motion Displacement Thresholds in glaucoma.</i>	107
8.1 Background	107
8.2 Purpose	107
8.3 Methods	110
8.3.1 Subjects	110
8.3.2 Examination protocol	110
8.3.3 Analysis	111
8.4 Results	112
8.4.1 Motion Displacement Thresholds	112
8.4.2 Effect of stimulus orientation on motion threshold	113
8.5 Discussion	116
9. CHAPTER 9 <i>Discussion and summary</i>	118
9.1 High spatial resolution automated perimetry	118
9.1.1 Implications of findings	118
9.1.2 Clinical applications	119
9.1.3 Future modifications	119
9.2 Motion Displacement threshold testing	120
9.2.1 Reaction times for motion detection	120
9.2.2 Frequency of seeing analysis for motion detection	122
9.2.3 Association of abnormal Motion Displacement Thresholds with fine scale luminance sensitivity loss in Glaucoma.	126

9.2.4 Stimulus orientation and motion threshold	127
9.3 Summary	128
10. APPENDIX: Supporting publications	131
10.1 Peer reviewed published papers	131
10.2 Papers under review	131
11. REFERENCES	132

3. List of figures

<i>Figure 4.1a Relationship between reaction time and stimulus displacement for glaucoma eyes and controls. Reaction times were significantly prolonged in glaucoma eyes for displacements 12-18 min. arc.</i>	51
<i>Figure 4.1b Same data as figure 4.1a, replotted to show the relationship between reaction time as a function of distance in min. arc from threshold. There are now no significant differences between the groups.</i>	51
<i>Figure 4.2a Relationship between reaction time and stimulus displacement for suspect eyes and controls, showing a trend of prolonged reaction times eyes for displacements 12-18 min. arc in suspect eyes (not significant).</i>	52
<i>Figure 4.2b Same data as figure 4.2a, replotted to show the relationship between reaction time as a function of distance in min. arc from threshold. This abolishes any differences between the two groups.</i>	52
<i>Figure 5.1a Humphrey 24-2 from normal control aged 69 (right), showing site of motion testing (arrow) with 4 closest Humphrey test locations. Above is subject's normal motion frequency-of-seeing curve. Black circles represent raw data points with probit-fitted curve (solid black curve), and 95% C.I. (dashed black curve). Dashed black line indicates 50% seen threshold, with interquartile ranges (dashed gray lines), within mean +2 SD of control group.</i>	59
<i>Figure 5.1b Humphrey 24-2 of a glaucoma patient aged 69 with an inferior arcuate scotoma (right). Arrow indicates site of motion testing on greyscale plot, with 4 closest Humphrey 24-2 test locations (box) showing normal threshold sensitivity, within 95% population limits on Statpac2 output. Above is motion frequency-of-seeing curve of same patient, with elevated threshold (11.6 min. arc) and abnormally shallow slope (elevated interquartile range of 7.6 min. arc). Compare with figure 5.1a.</i>	60
<i>Figure 5.2 Receiver operating characteristic (ROC) curve for the motion thresholds (gray line) and the logistic regression model incorporating the interquartile range (black line) for normal versus glaucoma eyes (top) and normal versus suspect eyes (bottom).</i>	62
<i>Figure 5.3 Relationship between calculated interquartile range and threshold of motion frequency-of-seeing curves for all subjects. The solid line represents the least-squares linear fit through the data. Dashed lines represent cut-offs below which all of control values for motion threshold (vertical) and interquartile range (horizontal) lie. Off scale refers to a single glaucoma eye with marked shallowing of the frequency of seeing curve with an interquartile range of 25 min. arc., off the y scale.</i>	64
<i>Figure 5.4 Top shows the frequency-of-seeing curve of a glaucoma suspect with a normal 50% seen motion threshold of 8.4 min. arc and a normal slope (interquartile range of 4.2 min. arc).</i>	66
<i>Figure 5.4 Middle shows the frequency-of-seeing curve from a glaucoma suspect with a similar motion threshold of 8.6 min. arc, with shallowing of the slope, signified by an interquartile range of 6.8 min. arc, which lies outside our normal range.</i>	66

<i>Figure 5.4 Bottom shows the frequency-of-seeing curve from a glaucoma eye with more extreme shallowing of the slope, with an abnormal interquartile range of 9.6 min. arc, although the motion threshold remains normal at 8.5 min. arc.</i>	66
<i>Figure 5.5 Frequency-of-seeing curve of glaucoma eye from patient aged 75 with elevated threshold (13.2 min. arc) and normal slope, indicated by interquartile range of 5.1 min. arc (normal range up to 6 min. arc).</i>	67
<i>Figure 6.1 Contour plot of luminance sensitivity from fine matrix maps performed over blind spot of a normal control, superposed with a fundal Scanning Laser Ophthalmoscope image (inverted) of the subject. Contour lines represent isoluminant points, in 1 dB increments. Note steep sensitivity gradients at the edge of the blind spot as well as more subtle linear defects corresponding in location and extent to the major retinal vascular trunks exiting the optic disc.</i>	74
<i>Figure 6.2a Top figure is a fundal scanning laser ophthalmoscope image (inverted) obtained from a patient showing a retinal nerve fibre layer defect. Bottom figure shows high spatial resolution luminance contour plots which have been superimposed. The sensitivity loss corresponds closely to the extent of the retinal nerve fibre layer defect.</i>	76
<i>Figure 6.2b shows a Humphrey 30-2 greyscale and statpac2 total deviation plot, and adjacent FMMs, which reveal an obvious superior arcuate extending from the blind spot, not shown by the Humphrey 30-2.</i>	77
<i>Figure 6.3a Humphrey 30-2 of glaucoma eye. Boxes indicate superior and inferior sites of FMM.</i>	79
<i>Figures 6.3b & d Pointwise difference versus mean plots for first and second FMM in the superior location, for raw (b) and Gaussian filtered (d) thresholds.</i>	79
<i>Figures 6.3c & e Corresponding plots for raw (c) and filtered thresholds (e) of the FMMs in the inferior location. Dashed lines indicate pointwise limits of agreement, represented as 2 SD, between the first and second FMMs.</i>	79
<i>Figure 6.4a SD of pointwise differences of first and second FMM versus mean sensitivity of first and second FMM using raw thresholds</i>	82
<i>Figures 6.4b Same axis for figure 6.4a, but using Gaussian filtered thresholds. The effect of filtering has been to reduce the magnitude of the SD by a factor of approximately 2, representing a twofold improvement in repeatability. Lines indicates the least squares linear fit of the data, excluding 1 outlier.</i>	82
<i>Figure 6.5a Humphrey 30-2 greyscale and Statpac2 total deviation plot from glaucoma eye, with site of FMM indicated by box.</i>	84
<i>Figure 6.5b Resulting FMMs obtained from same patient at the location indicated on figure 6.5a. Plots of Gaussian filtered sensitivity thresholds of first (left figure) and repeat (right figure) reproducible threshold profiles reveal a steep sensitivity gradient from severely depressed sensitivity, represented as elevated area, to normal sensitivity.</i>	84
<i>Figure 6.6a Humphrey 30-2 greyscale and Statpac2 total deviation plot from glaucoma eye. Box indicates site of FMM which overlaps 4 Humphrey 30-2 test locations with normal threshold sensitivity.</i>	86

<i>Figures 6.6b & c Three-dimensional plots of Gaussian filtered luminance sensitivity thresholds of first and second FMMS. Elevated areas indicate repeatable luminance defects, not seen in the FMM of an equivalent area of field from age matched normal controls (figure 6.6d).</i>	86
<i>Figure 7.0a Picture of a subject performing a MDT test.</i>	94
<i>Figure 7.0b Close up picture of the monitor showing the line stimulus used for the MDT test.</i>	94
<i>Figure 7.1 Humphrey 24-2 from a glaucoma subject showing inferior arcuate scotoma. Arrow indicates site of motion testing within area of normal Humphrey 24-2 field, overlapped by site of High Spatial Resolution Perimetry (box). Adjacent HSRP matrix map is abnormal: elevations represent area of depressed thresholds. Motion frequency-of-seeing curve (bottom) shows grossly abnormal motion response.</i>	99
<i>Figure 7.2 Humphrey 24-2 from a glaucoma subject showing inferior arcuate scotoma. Arrow indicates site of motion testing within area of normal Humphrey 24-2 field, overlapped by site of High Spatial Resolution Perimetry (box). Adjacent HSRP shows abnormal matrix map. Subtle elevations represent areas of abnormally depressed thresholds. Motion frequency-of-seeing curve (bottom) shows dip at 10 min. arc. The 50% seen threshold is 4.2 min. arc, within the control range.</i>	100
<i>Figures 7.3 Humphrey 24-2 from a glaucoma subject showing superior arcuate scotoma. Arrow indicates site of motion testing within area of normal Humphrey 24-2 field, overlapped by site of High Spatial Resolution Perimetry (box). Adjacent HSRP matrix map is normal, with normal mean threshold sensitivities, and uniform threshold profile (normal uniformity index). Motion frequency-of-seeing curve (bottom) shows grossly abnormal motion response.</i>	101
<i>Figure 7.4 Humphrey 24-2 from a normal control. Arrow indicates site of motion testing within area of normal Humphrey 24-2 field, overlapped by site of High Spatial Resolution Perimetry (box). Adjacent HSRP matrix map is normal with uniform luminance profile (mean threshold sensitivity and uniformity index within control range). Normal motion frequency-of-seeing curve (below) with 50% seen threshold within control range.</i>	102
<i>Figure 7.5 Relationship between subjects' Motion Displacement Threshold and HSRP matrix map mean threshold. The solid line represents the least-squares linear fit through the data. Arrow indicates 1 outlier off the y-scale.</i>	103
<i>Figures 8.1a, b & c Left eye motion test in superotemporal field: vertical line stimulus shown in white superimposed on fundus image. The arrow shows the direction of the stimulus displacement in relation to a hypothetical slit-like scotoma orientated along the axis of the retinal nerve fibre layer shown in black.</i>	109
<i>Figure 8.2 Scatterplot of subjects' thresholds for stimulus motion perpendicular vs. motion parallel to retinal nerve fibres, with the line of unity.</i>	113
<i>Figure 8.3 Difference versus mean plot of motion thresholds for stimulus motion perpendicular and parallel to retinal nerve fibres. Subjects with normal motion thresholds lie to left of vertical reference line of 8.6 min. arc.</i>	114
<i>Figure 8.4 Proportional difference versus mean plot of motion thresholds for stimulus motion perpendicular and parallel to retinal nerve fibres.</i>	115

4. Acknowledgements

I would like to acknowledge the encouragement and patience of my supervisors Professor Fitzke (Institute of Ophthalmology) and Professor Hitchings (Moorfields Eye Hospital). I am especially indebted to Fred and Roger for their wisdom and for imparting me with a sound scientific training. I also thank both supervisors who as well as being ever accessible for advice, allowed me the freedom to pursue work which I found very interesting.

I would like to thank Dr David Crabb (Institute of Ophthalmology 1993-97) who provided expert statistical advice and assisted in the statistical analysis in chapters 5 and 6.

Thanks to Ananth Viswanathan (Institute/Moorfields 1995-97) for his programming help which greatly facilitated the analysis of the study described in chapter 4.

Thank you also to Andrew McNaught, whose collaboration culminated in the study described in chapter 6.

I would like to thank Ted Garway-Heath (Institute/Moorfields 1995-97) and Isobelle Antunes of the ocular hypertension unit for their assistance in recruiting subjects to undergo High Spatial Resolution Perimetry to provide data for the studies in chapters 6 & 7.

I gratefully acknowledge the generous support of the *Friends of Moorfields Charity* which provided the main project grant. I am also indebted to Mr R P Crick and the *International Glaucoma Association* for generously providing me with travel grants to attend international conferences in vision research and present my work.

Finally I thank Sandrine for her love and support during the writing of this thesis.

5. Outline of thesis

Chapter 1 summarises the classification, epidemiology, aetiology, and treatment of glaucoma. **Chapter 2** describes the anatomy and physiology of the visual system, and outlines the history of perimetry. **Chapter 3** discusses the limitations of conventional perimetry in detecting early glaucomatous damage and gives an account of the use of other psychophysical testing in glaucoma. **Chapters 4 to 8** describe the results of 5 experimental studies in this thesis. **Chapter 4** investigates possible differences in reaction time between controls and glaucoma patients for a motion stimulus. **Chapter 5** details the improvement in the sensitivity of the MDT test obtained with the use of frequency-of-seeing analysis, as compared against the use of threshold analysis alone. **Chapter 6** investigates the use of High Spatial Resolution Perimetry in glaucoma. **Chapter 7** tests the hypothesis that elevated Motion Displacement Thresholds coexist with fine scale depressions of Humphrey threshold. **Chapter 8** describes a study to investigate the effect of stimulus orientation on motion thresholds.

The results of these studies are summarised and discussed in **Chapter 9**.

1. CHAPTER 1

Glaucoma

1.1 Definition

There is no universally agreed definition for glaucoma. One approach is to consider glaucoma as a group of conditions, characterized by damage to the optic nerve head in association with a diagnostic pattern of visual field loss, for which elevation of intraocular pressure is a major risk factor. Recent major epidemiological studies do not include the demonstration of an elevated IOP (i.e. above 21 mm Hg.) as part of the case definition for open angle glaucoma (Mitchell *et al.*, 1996; Tielsch *et al.*, 1991). Instead intraocular pressure is more usefully thought of as a continuous risk factor, which is only one of several that have been identified.

Subjects who have normal visual fields, but have risk factors for the development of glaucoma such as the presence of optic disc damage or elevated intraocular pressure, may be defined as glaucoma suspects since they are at risk of developing the disease in the future.

1.2 Classification

1.2.1 Concepts

Glaucoma is classified into primary or secondary. Primary glaucoma occurs in the absence of any coexisting or antecedent ocular disease. Secondary glaucomas occur as conditions which are secondary to another ocular or systemic disease. Causes of secondary glaucoma include uveitis, cataract, and trauma, and account for only approximately 5% of all glaucomas.

All glaucomas can also further be subdivided according to whether the aqueous drainage angle is open (trabeculum visible on gonioscopy) or closed (trabeculum obscured by normal or pathological structures).

Finally, the congenital glaucomas represent a separate rare group of disorders characterized by congenital malformations of the drainage angle of varying degree, which may be accompanied by ocular or systemic malformations.

1.2.2 Primary Open Angle Glaucoma (POAG)

The commonest form of glaucoma in the Western world is primary open angle glaucoma. These patients have by definition cupping of the optic nerve head and visual field loss, with an open aqueous drainage angle of normal appearance.

Patients with primary open angle glaucoma frequently remain asymptomatic until extensive and unrecoverable visual field loss has occurred. An important characteristic of the disease is the progressive deterioration of the visual field with constriction of the visual field which may lead ultimately to blindness. Although the intraocular pressure may be raised at the time of diagnosis, major epidemiological studies have consistently shown that only about half of newly detected cases of POAG have an elevated intraocular pressure (commonly defined as ≥ 21 mm Hg.) at the time of screening (Sommer *et al.*, 1991b). In addition, a significant proportion of patients diagnosed as having POAG on the basis of optic nerve head cupping and visual field damage never have elevated IOPs. For example, in the Baltimore eye survey, 21% of patients confirmed as POAG failed to demonstrate elevated intraocular pressures above 21 mm Hg. on further follow up (Sommer, *et al.*, 1991b). Many clinicians classify these patients as **Normal Tension Glaucoma (NTG)**, particularly if diurnal measurements of IOP fail to demonstrate any elevation of IOP above 21 mm Hg.

1.3 Epidemiology

Glaucoma is the third most common cause of blindness in the world, after cataract and age related macular degeneration, and is estimated to be responsible for approximately 5.2 million blind people worldwide (Thylefors and Negrel, 1994). It is estimated that glaucoma will be the second commonest cause by the year 2000, when it will be the most important cause of irreversible visual disability. In the U.K., estimates based on the prevalence of Coffey *et al.* suggest that there are approximately 250,000 known sufferers in the UK, with probably another 250,000 undiagnosed (Coffey *et al.*, 1993).

In the United States there are probably 2 million glaucoma sufferers, of whom 120,000 are blind (Leske, 1983). Guzman suggested that the economic burden of glaucoma rivals that for cataract, despite the considerably lower prevalence of the disease compared to cataract (Guzman *et al.*, 1992). In the US for example, direct health care costs from glaucoma are estimated at about US\$ 2 billion (£1.2 billion) and indirect costs at about US\$ 500 million (£300 million).

1.3.1 Prevalence

Hollows and Graham conducted an epidemiological study that has subsequently become a benchmark for studies of glaucoma prevalence (Hollows and Graham, 1966). Their study was the first to examine a large proportion of a defined population using comprehensive case finding methods. They also included extensive visual field testing as part of the case definition, although this was not performed on all subjects. They studied a sample of 4231 from Ferndale in Wales (age range 40-70 years) and found a prevalence of POAG of 0.5% in the population studied.

Leibowitz et al reported a prevalence of POAG of 1.4% from a sample of 2631 of the 3977 members of the Framingham (Massachusetts) Heart Study population still living in 1973-1975 (age range 52-85 years) (Leibowitz *et al.*, 1980) .

Although these studies were population-based, they were not true random samples of the population at risk. More recent studies based on the evaluation of multiple risk factors within a random sample of the population have suggested a higher prevalence.

The Baltimore Eye Survey surveyed 5308 black and white urban American subjects aged 40 years or older to give a prevalence of 1.3% among the white population (Sommer, et al., 1991b). The Beaver Dam study reported a slightly higher prevalence for POAG of 2.1% in a non-urban sample of 4926 predominantly white subjects in Wisconsin (age range 43-84 years).

A study by Coffey et al reported a prevalence of 1.9% in a sample of 2186 subjects aged over 50 in the rural community of Roscommon in the West of Ireland (Coffey, et al., 1993).

The highest prevalence of POAG reported for an urban population was 2.4%, from the Blue Mountain Study (Mitchell, et al., 1996). However this sample consisted of an older population with a higher proportion of people over 75 years of age. Despite differences in case detection and definition of POAG in these studies, it is notable how well the

prevalence rates agree among white populations of equivalent ages. An important finding that all these studies consistently highlight is the fact that at least 50% or more of the glaucoma within the community is undiagnosed. They also emphasize the poor performance of IOP as a screening test, as only half of newly detected cases of POAG have raised IOP ≥ 21 mm. Hg. (Coffey, et al., 1993; Klein *et al.*, 1992; Sommer, et al., 1991b).

1.3.2 Incidence

There are major difficulties in estimating the incidence of glaucoma. The difficulties of reliable early detection present problems in deciding at what point the disease becomes manifest. This is illustrated by the observation that pathological changes at the optic disc and nerve fibre layer can occur many years before the development of a repeatable visual field defect (Quigley *et al.*, 1980; Sommer *et al.*, 1991a; Zeyen and Caprioli, 1993). The incidence of glaucoma can only be determined by prospective long-term studies, ideally of a truly representative random sample of a population. It is hoped that longitudinal follow-up of the Baltimore and Beaver Dam studies will provide estimates of the incidence of glaucoma in the future.

1.3.3 Risk factors

The epidemiological studies described above have greatly improved our understanding of the risk factors which predispose an individual to POAG. These studies have consistently highlighted the multifactorial nature of the disease. Thus an individual's risk of POAG is best considered as the combination of a number of risk factors, although the exact magnitude of risk attributable to a specific risk factor remains a matter of debate.

1.3.3.i Intraocular pressure

Of all the risk factors that have been identified in the large epidemiological studies described above, IOP consistently remains a major risk factor.

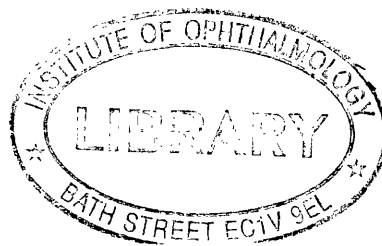
Leske (1983) suggested that the overall risk of developing POAG is approximately five times higher in subjects with IOPs > 21 mm Hg than in subjects with lower IOPs (Leske, 1983). However, rather than an absolute cut-off, more recent approaches have assessed the level of IOP in terms of being a continuous a risk factor.

The Baltimore Eye Survey identified a clear log-linear relationship between the prevalence of POAG and the level of the screening IOP (Sommer, et al., 1991b). This relationship reached high levels of significance and existed both for all cases of POAG and for untreated previously undiagnosed POAG in the community. For example, for subjects with screening IOPs in the 19-21 mm Hg range, the prevalence of POAG was 1.8%. In subjects with IOPs in the 22-29 mm Hg. range the prevalence was 8.3% and with IOPs above 29 mm Hg. this rose to 25%. A clear relationship between IOP and prevalence was also identified for a black population in the Barbados Eye Study (Leske *et al.*, 1995).

Both studies made the important observation that even low levels of IOP were associated with a small but definite risk of POAG. Although this risk was small, the fact that the majority of the population had low screening IOPs resulted in significant numbers of POAG below 21 mm Hg. This finding of a continuous relationship between IOP and prevalence may explain the significant numbers of POAG cases identified with screening pressures below 21 mm Hg. in every major epidemiological study to date. An important finding of many studies is that they have consistently identified a significant proportion of undiagnosed POAG using accepted disc and field criteria in subjects with screening IOPs below 21 mm Hg., emphasising the poor performance of IOP as a screening measure (Coffey, et al., 1993; Klein, et al., 1992; Sommer, et al., 1991b).

1.3.3.ii Age

Epidemiological studies of POAG prevalence have identified age as a major risk factor, which may be as important as IOP. For example, the Beaver Dam eye study indicated that the prevalence of POAG increased with age from 0.9% in subjects 43 to 54 years of age to 4.7% in people 75 years of age or older (Klein, et al., 1992). Similar results were obtained in the Roscommon study showing that the 70-79 year old age band have a 4.5 times increased risk compared to the 50-59 age group (Coffey, et al., 1993). By comparison, the Baltimore study identified an eightfold increase for the same age groups (Sommer, et al., 1991b). Prevalence rates for older age groups may be even higher, as suggested by the Blue Mountain Study (Mitchell, et al., 1996). This study reported an exponential increase in POAG prevalence with age, with a prevalence rising to 10.2% in people aged 85 years or older.



1.3.3.iii Race

Being of African, African-American, or Afro-Caribbean origin is a significant risk factor. The Baltimore Eye Survey showed that black Americans had strikingly higher rates of POAG, compared to whites at every age (Tielsch, et al., 1991). For example, the prevalence rates for blacks ranged from 1.2% in those aged 40 to 49 years to 11.3% in those aged 80 years or older. In whites for the same age groups the rates ranged from 0.9% to 2.2%. The Barbados Eye Study found even higher prevalence rates of POAG in an entirely Afro-Caribbean population (Leske *et al.*, 1994). Age-adjusted comparisons showed that the prevalence rates for the Barbados Eye study were 7 times that of the Baltimore Eye Survey whites, and 1.5 times that of the Baltimore Eye Survey black participants.

1.3.3.iv Family history

A number of studies have shown that a family history is an important risk factor in the development of POAG (Leske, et al., 1995; Tielsch *et al.*, 1994). The Baltimore Eye Survey showed a significant age-adjusted association of POAG with a family history of glaucoma (Tielsch, et al., 1994). This was higher in siblings (odds ratio = 3.69) than in parents (odds ratio = 2.17) or children (odds ratio = 1.12). However there was evidence for selection bias, as the odds-ratios were between two and three times higher for subjects who had prior knowledge of their glaucoma diagnosis than for those who first received their diagnosis at the time of the study examination.

1.3.3.v Other factors

Although diabetes was previously thought of as an independent risk factor for POAG, results from large population-based studies have failed to find evidence of an association between diabetes and POAG (Sommer, et al., 1991b; Tielsch *et al.*, 1995).

At present, the role of blood pressure as a risk factor is unclear. Some studies have demonstrated an association between a decrease in systemic blood pressure, either due to a hypotensive crisis or due to anti-hypertensive therapy, and the development of POAG (Leske, 1983). The Framingham study and the Barbados study (Leske, et al., 1995) have reported an association between persons with a low BP/IOP ratio and POAG risk, although this may simply be a measure of the strong association between IOP and POAG.

There is some evidence that myopia is a risk factor for POAG (Wilson *et al.*, 1987) but recent studies have suggested there is no direct link (Quigley *et al.*, 1994).

The majority of epidemiological studies have not shown any association of POAG with gender (Coffey, *et al.*, 1993; Klein, *et al.*, 1992; Tielsch, *et al.*, 1991). The exceptions are the Framingham and Barbados Eye Studies, which identified a preponderance of males with POAG.

Another factor which has been investigated is whether or not there is a significant association between migraine and POAG, which remains a matter of debate. For example, although a positive association between migraine and Normal Tension Glaucoma (NTG) has been reported (Phelps and Corbett, 1985), results from the Beaver Dam study found no association between POAG and a history of migraine (Klein, *et al.*, 1992). However the relationship between migraine and POAG is complex and may be modified by age, as shown by the recent Blue Mountain study which did find a significant association between headache and POAG (odds ratio 2.5) in the 70-79 age group, although not for other age groups (Wang *et al.*, 1997).

1.4 Ætiology

1.4.1 Pathogenesis

The pathogenesis of glaucoma is still unknown. Primary Open Angle Glaucoma (POAG) is an optic neuropathy consisting of characteristic changes to the appearance of the optic nerve head associated with loss of visual function. A remarkably constant feature of established glaucoma is the excavation of the optic nerve head tissues known as cupping. This was first described by von Graefe and is the feature which most easily distinguishes glaucoma from other optic neuropathies that produce similar field defects (von Graefe, 1856). Histological studies have shown that cupping of the optic disc is primarily the result of backward and lateral displacement of the connective tissue beams of the lamina cribrosa. The loss of visual function in glaucoma has been shown to be a result of accelerated ganglion cell death (Quigley *et al.*, 1981). Although the exact cause of glaucomatous ganglion cell death is unknown, a number of mechanisms have been proposed. These mechanisms broadly fall into two major classes: mechanical or vascular.

A full discussion of the extensive and controversial literature is beyond the scope of this MD. A recent comprehensive review is given by Hayreh (Hayreh, 1994).

1.4.2 Mechanical theories

The hypothesis that glaucomatous optic neuropathy is produced mechanically by raised IOP was first postulated by von Graefe nearly 140 years ago (von Graefe, 1857). In human eyes with secondary glaucoma, elevations of intraocular pressure are clearly associated with optic nerve cupping. In other primates, optic nerve cupping can be obtained experimentally in eyes with chronic elevation of intra-ocular pressure obtained using laser damage to the trabecular meshwork. This remains the only method of inducing glaucomatous changes of the optic nerve that resemble those seen in human POAG (Pederson and Gaasterland, 1984). Using this primate model, Pederson et al have examined the development of optic disc cupping with chronic elevation of IOP. They reported that the degree of neuronal loss was more marked in eyes with higher levels of IOP and in eyes with a longer exposure to an elevated IOP (Pederson and Gaasterland, 1984). Histological examination of these eyes shows posterior bowing of the lamina cribrosa, with associated local interruption of axonal transport at this level. According to the mechanical theory, it is proposed that mechanical compression of the axons by raised intraocular pressure occurs as they traverse the lamina cribrosa, resulting in ganglion cell death.

Post mortem studies of glaucomatous human eyes by Quigley et al have shown similar changes, characterised by posterior bowing of the lamina cribrosa with associated stretching, distortion and compression of the lamellar sheets (Quigley, et al., 1981). This is associated with reductions in optic nerve axon density throughout the optic nerve, which is more severe in the superior and inferior poles. This led Quigley to propose that the characteristic visual field defects in glaucoma result from regional differences in the structure of the scleral lamina cribrosa and their susceptibility to mechanical damage (Quigley, et al., 1981).

A number of investigators have addressed the question of whether ganglion cell death in glaucoma is dependent in some way on IOP by investigating the correlation of IOP with visual function. A number of studies have provided clinical evidence to suggest that the absolute level of IOP and the level of fluctuation of the IOP correlates with the degree of visual field deterioration (Mao *et al.*, 1991; Migdal *et al.*, 1994; Smith, 1986; Sommer,

et al., 1991b; Vogel *et al.*, 1990; Weber *et al.*, 1993) and with the extent of glaucomatous optic nerve damage (Airaksinen *et al.*, 1992). Other studies have failed to show an unequivocal relationship between IOP and progressive deterioration in the visual field (Chauhan and Drance, 1992; Holmin and Krakau, 1982; O'Brien *et al.*, 1991). It has become apparent from these studies that for a given level of intra-ocular pressure elevation, there exists considerable individual variability in the susceptibility to developing glaucomatous optic nerve change and visual field deterioration. This clinical observation has recently been supported experimentally by Harwerth *et al.* They investigated the relationship between visual field deterioration and intraocular pressure elevation in 18 monkeys with laser induced unilateral glaucoma. They found that visual field defects occurred above a certain "threshold" of IOP elevation, with the absolute level of threshold IOP elevation varying considerably between eyes. However once visual damage occurred, the rate of visual field progression occurred at more or less uniform rates (Harwerth and Smith, 1997).

1.4.3 Vascular theory

The observations that approximately half of glaucomatous eyes present with IOPs less than 21 mm Hg., and that a proportion of these develop progressive glaucoma despite IOPs within the normal range, suggest that other factors must play major roles in the pathogenesis of glaucoma. A major theory to explain pressure independent ganglion cell death is the vascular theory, which was first proposed by Jaeger only 1 year after von Graefe's mechanical theory (Jaeger, 1858). He postulated that impairment of the circulation in the short posterior ciliary arteries was responsible for the damage to the optic nerve head in glaucoma. Recent research has concentrated on the importance of autoregulation of optic nerve head blood flow. Pillunat *et al.* and Robert *et al.* have found evidence to suggest defective autoregulation in optic nerve head blood flow in POAG and NTG (Pillunat *et al.*, 1987; Robert *et al.*, 1989). Defective autoregulation has also been proposed to explain the reported association between nocturnal hypotension and those patients who show progressive visual field damage in normal tension glaucoma patients treated for systemic hypertension (Graham *et al.*, 1995; Hayreh *et al.*, 1994). It is postulated that the presence of marked nocturnal dips of BP may lead to hypoperfusion of the optic nerve head, with consequent ischaemic disc damage.

Another mechanism that has been postulated to account for the reduction in ocular blood flow in some patients is vasospasm. A number of studies have identified the presence of peripheral vasospasm (e.g. migraine, chronic cold hands and feet) as a risk factor for glaucoma, particularly for normal tension glaucoma (Drance *et al.*, 1988; Phelps and Corbett, 1985).

A number of techniques have been used to attempt to obtain an indirect measure of optic nerve head blood flow. These have been limited by the difficulties of obtaining sensitive and reproducible measurements and may not measure the posterior ciliary circulation which is of prime importance.

Abnormalities of blood flow have been reported in normal tension glaucoma using the ocular pulse to measure blood flow (James and Smith, 1991) and colour Doppler ultrasonography to measure blood flow velocity (Butt *et al.*, 1995).

1.4.4 Apoptosis

Quigley has recently postulated that apoptosis may be an important IOP independent mechanism for ganglion cell death in glaucoma (Quigley *et al.*, 1995). Apoptosis was first described by Kerr who identified a unique form of active cell death which differs from necrosis by its absence of inflammation (Kerr *et al.*, 1972). This process requires the transcription of messenger RNA to initiate a cascade of programmed cell death. Apoptosis has been shown to be important in embryogenesis (Young, 1984), and in preventing carcinogenesis (Kerr *et al.*, 1994). The ocular importance of apoptosis is suggested by the fact that half the initial population of ganglion cells die by apoptosis during normal foetal development. Apoptosis has been shown to play an important role in some experimental inherited retinal dystrophies (Papermaster and Nir, 1994). Levin *et al.* reported evidence of apoptosis in the ganglion cell layer of an eye of a patient with acute ischaemic optic neuropathy (Levin and Louhab, 1996). Quigley has shown that apoptosis is associated with ganglion cell death in experimental glaucoma and postulates that this mechanism may play an important part in the progressive loss of ganglion cells in human glaucoma (Quigley, *et al.*, 1995). However the techniques to identify apoptosis remain controversial and further investigations are required to ascertain what role apoptosis has in the pathogenesis of glaucoma.

1.4.5 Genetic factors

The mechanism by which genes influence the susceptibility to POAG is as yet unknown. Teikari and Airaksinen have recently shown that IOP and the dimensions of the optic nerve head are genetically determined (Teikari and Airaksinen, 1992). This suggests that genetic factors may influence the facility of aqueous outflow and the susceptibility of the optic disc to the development of glaucomatous change. Other evidence confirming the importance of genetic factors in determining the susceptibility to glaucoma is the identification of a number of pedigrees with autosomal dominant inheritance POAG (Kitsos *et al.*, 1988). Sheffield *et al.* have recently published the first mapping of a gene causing an autosomal dominant form of juvenile open angle glaucoma (JOAG) in a pedigree (Sheffield *et al.*, 1993). They used linkage analysis to identify positive linkage to a region on the long arm of chromosome 1. Subsequently, other investigators have also demonstrated linkage to this region. However, this linkage appears to be associated with rare juvenile onset primary open angle glaucoma (JOAG) and the genetic relationship between JOAG and POAG is not known. The later onset of POAG and the undoubted genetic heterogeneity of POAG presents major difficulties in the mapping of POAG genes.

1.5 Treatment

It is beyond the scope of this thesis to give an exhaustive account of the various treatments for glaucoma. For a more detailed account of the therapeutic rationale for glaucoma the reader is referred to the following reviews (Hitchings, 1992; Hitchings, 1995; Luntz and Harrison, 1994).

In brief, the therapeutic rationale for the treatment of POAG has concentrated on attempts to manipulate the known risk factors. Treatments of POAG have historically been preoccupied with attempts to lower a patient's IOP in the assumption that this will alter the rate of progression of the disease. The mainstay of current treatment is topical medical therapy to reduce aqueous secretion (e.g. beta blockers) or improve the aqueous outflow (e.g. miotics). Argon laser trabeculoplasty may be a useful adjunctive therapy in lowering IOP, but will only work in a proportion of patients for a limited period of time (Shingleton *et al.*, 1993).

Surgical treatment (known as trabeculectomy or filtration surgery) commonly involves making a guarded corneoscleral channel to allow a controlled flow of aqueous into the subconjunctival space. Results from recent trials have shown filtration surgery to be superior to medical or laser treatment in reducing IOP and preserving vision (Migdal, et al., 1994). Recently there have been major advances in surgical techniques to improve the long-term success of drainage surgery. One advance is the use of perioperative antiproliferative agents to modify the local healing response and reduce scarring at the site of surgery (Khaw and Migdal, 1996). A number of trials have shown that the perioperative application of these agents can achieve a significant lowering of IOP in the long-term after surgery, compared with previous techniques (Goldenfeld *et al.*, 1994). Despite these advances, postoperative subconjunctival scarring still remains the most important cause of subsequent failure of drainage surgery (Khaw and Migdal, 1996).

In normal tension glaucoma, treatment has been aimed at further lowering IOP (deJong *et al.*, 1989; Hitchings *et al.*, 1995; Schulzer, 1992) or correcting for presumed abnormal vascular circulation at the optic nerve head (Kitazawa *et al.*, 1989; Netland *et al.*, 1993). With regard to the efficacy of medical treatment of POAG, Rossetti have emphasized the fact that only a fraction (16/102) of published trials were properly designed to assess the effectiveness of treatment by comparing active treatment with an untreated or placebo group. Of such trials, only 3 trials investigated the effect of treatment on long-term visual function, and their cumulative results failed to show a protective effect of treatment (Rossetti *et al.*, 1993). The authors concluded that there was a need for a more evidence based and critical assessment of current treatment in glaucoma. This situation may be improved once the results are known from a number of large scale prospective treatment trials with defined end points which include visual function.

1.6 Summary

Primary open angle glaucoma (POAG) is a disease characterized by characteristic damage to the optic nerve head in association with progressive visual field loss. It is a major cause of blindness and visual disability throughout the world. In the UK alone, it is estimated that there are approximately 250, 000 known sufferers, with a similar number again undiagnosed. Although the pathogenesis of glaucoma is not fully understood, two theories have remained predominant. The mechanical theory proposes that mechanical compression of the axons by raised intraocular pressure occurs as they traverse the

lamina cribrosa. Alternatively, the vascular theory postulates that an abnormality in blood flow to the optic nerve head is the main cause of nerve fibre damage. However, it is likely that the pathogenesis is multifactorial. This is supported by recent epidemiological evidence which has identified a number of risk factors. These factors include increasing age, elevated IOP, being of Afro-Caribbean origin, and having a family history of glaucoma.

The mainstay of treatment for POAG depends upon lowering IOP using medicine, laser or surgery in the assumption that modulating this risk factor alters the rate of progression of the disease. Less commonly, medical treatment has been used for correcting for presumed abnormal vascular circulation at the optic nerve head, particularly in normal tension glaucoma.

2. CHAPTER 2

Visual function in glaucoma

2.1 The anatomy of the visual pathway

2.1.1 Introduction

This section will examine the anatomy of the visual system and discuss the concept of parallel visual processing in the human visual system. An understanding of the visual pathways provides the framework in which to develop more sensitive tests of early visual damage in glaucoma.

2.1.2 The retinal ganglion cell

The main pathway of visual information in the primate retina is from the photoreceptors to the bipolar cells, which in turn synapse to the ganglion cells, either directly or via amacrine cells or other bipolar cells.

Ganglion cells are defined as visual neurons having long axons that project to the brain via the optic nerve. There are approximately 1.1 - 1.3 million ganglion axons (fibres) in the adult human optic nerve (Balazsi *et al.*, 1984; Potts *et al.*, 1972). The number of ganglion fibers declines with age throughout life, although the individual variation in the total nerve fibre count makes it extremely difficult to estimate the normal rate of age-related decline. Frisen used pooled histological study data to estimate a retinal ganglion cell loss of approximately 5,000 per year (Frisen, 1991). The axons of the ganglion cells become myelinated at the lamina cribrosa, and undergo partial decussation at the optic chiasm, to synapse with second order neurons at the dorsal lateral geniculate nucleus (dLGN).

The ganglion cell is of fundamental importance in glaucoma because the major histological abnormality in glaucoma is an absolute reduction in the number of ganglion cell axons in the optic nerve, as a consequence of ganglion cell death (Quigley *et al.*, 1982).

Physiological studies in cats and primates suggested that retinal ganglion cells could be separated into 2 major classes, called “X” and “Y” cells (Lennie, 1980). These cells were found to correspond to anatomically distinct classes of ganglion cells. The anatomical equivalents of the “X” cells have confusingly been called B or β cells in primates, or **midget cells** in humans. To avoid confusion it is easier to refer to midget cells as **P-cells**, as these cells project to the parvocellular layers of the dorsal lateral geniculate nucleus (dLGN).

The anatomical equivalents of the “Y” cells are A or α cells in primates, and parasol cells in humans. I shall refer to these cells as **M-cells** as these cells project to the magnocellular layers of the dLGN.

P-ganglion cells constitute 80% of the retinal ganglion cells in primates, and are found at highest density in the fovea (Perry *et al.*, 1984). Characteristic features of P-cells include the presence of small dendritic fields, small to medium sized axon diameters, and projections to the parvocellular dLGN (Leventhal *et al.*, 1981).

M-ganglion cells constitute only 10% of the retinal ganglion cells and are evenly distributed across the retina. Typically M-cells are characterized by the presence of large dendritic fields, faster conducting large axon diameters, and projections to the magnocellular dLGN (Leventhal, et al., 1981).

2.1.3 Parallel visual pathways

Physiological evidence suggests that the morphological differences between the P-cells and M-cells reflect distinct differences in function (Livingstone and Hubel, 1987).

For example, M-cells have high contrast sensitivity, and respond optimally to low spatial frequency stimuli (<1 cycle/deg.). M-cells also lack spectral selectivity, i.e. they are not tuned to a particular waveband or colour (De-Monasterio, 1979; Derrington and Lennie, 1984; Kaplan and Shapley, 1982; Marrocco, 1976; Perry, et al., 1984).

P-cells have much smaller receptive fields, and respond optimally to high spatial frequency stimuli. They have low contrast sensitivity and do show spectral selectivity (De-Monasterio, 1979; Derrington and Lennie, 1984; Kaplan and Shapley, 1982; Marrocco, 1976; Perry, et al., 1984).

These different properties of the M-cells and P ganglion cells are conserved by anatomically and functionally distinct pathways throughout the human visual system.

The anatomic separation of M-cells and P-cells is most evident in the dLGN, which is sharply delineated into 6 layers: retinal P-cells synapse with second order neurons in the dorsal 4 layers (parvocellular layers), M-cells synapse in the ventral 2 layers.

The parvocellular layers of the dLGN project to layer IVC beta (the “striate” cortex), and then to layer III of the primary visual cortex (Brodmans area 17 or V-1). Parvocellular connections of layer III project widely, with major projections to Brodmans area 18, to the dorsal lateral parietal cortex and the inferotemporal cortex. Magnocellular dLGN projects to layers IVC alpha and IVB of the primary visual cortex. From layer IVB, there are projections to layer III, as well as direct connections to the middle temporal cortex, otherwise known as MT. For the sake of simplicity, only the major connections of the parallel pathways have been considered here.

2.1.4 Visual function and parallel pathways

There is considerable evidence that fundamental visual processing occurs via the separate pathways of the parvocellular and magnocellular systems. This segregation of visual processing is broadly maintained throughout the visual system, although recent evidence suggests that there is some mixing of the parallel pathways in the higher visual centres (Merigan and Maunsell, 1993).

The concept of separate processing streams is of fundamental importance, and is a basis for understanding the development of more sensitive tests of visual function in glaucoma. The following section details some of the evidence for parallel processing as it applies to the following aspects of visual function.

2.1.4.i Contrast sensitivity and visual acuity

Experimental work in primates suggests that contrast sensitivity at low and medium spatial frequencies is principally a function of the magnocellular system, which is far more sensitive than the parvocellular system at these frequencies (Derrington and Lennie, 1984).

Contrast sensitivity at very high spatial frequencies is likely to be a function of the parvocellular system (Merigan, 1989). This includes visual acuity, which is a function of the high spatial resolution sensitivity of P-cells concentrated at the fovea.

2.1.4.ii Motion sensitivity

There is extensive evidence to suggest that motion sensitivity is principally carried out by the magnocellular system. Experimentally induced lesions of the magnocellular dLGN in primates results in profound losses of motion sensitivity to fast moving gratings (Merigan *et al.*, 1991; Merigan and Maunsell, 1990). Other experimental work in primates has shown that the perception of line displacement motion is primarily a function of magnocellular ganglion cells (Lee, 1993; Lee *et al.*, 1993; Schiller *et al.*, 1990a; Schiller *et al.*, 1990b).

Further evidence has been provided from psychophysical experiments by Livingstone and Hubel. They demonstrated that human motion sensitivity was characterized by high contrast sensitivity and colour insensitivity, both of which are known properties of the magnocellular system (Livingstone and Hubel, 1988).

However a number of recent studies have shown that the parvocellular system also makes an important contribution to motion acuity. Studies in humans of the motion reversal effect (the apparent reversal of the direction of motion of a high frequency grating) provide estimates of the sampling density of receptors. Comparisons with the known retinal densities of magnocellular and parvocellular ganglion cells allow the contribution of the two pathways to be assessed. Several such studies have shown that motion acuity in the periphery (30 to 40 degrees eccentricity) is limited by the density of parvocellular cells rather than magnocellular cells (Anderson *et al.*, 1995; Galvin *et al.*, 1996). Some authors have suggested that parvocellular cells play an important role in limiting motion acuity across the entire field (Anderson, et al., 1995). Physiological studies have also shown that P-cells in the visual cortex respond well to moving stimuli.

2.1.4.iii Flicker sensitivity

Like contrast, flicker sensitivity may be mediated by both the magnocellular and parvocellular pathways, depending on the stimulus conditions. Low spatial frequencies modulated at high flicker frequencies are believed to be mediated by the magnocellular system, whereas low flicker frequencies of high spatial frequency gratings are likely to be mediated by the parvocellular system.

2.1.4.iv Colour sensitivity

Primate colour perception appears to be primarily mediated by the parvocellular system. This is supported by evidence from primate studies which showed that toxicant induced damage to the parvocellular pathway resulted in substantial reductions in colour sensitivity (Merigan, 1989).

2.2 Measurement of visual function in glaucoma

2.2.1 Fundamentals of perimetry

The visual field is defined as the portion of space from which light can enter the eye, reach the retina, stimulate the photoreceptors and evoke a sensation of light. Perimetry is defined as the study and measurement of the visual field, and is the technique used to identify disturbances in the visual field. It is therefore essential for diagnosing and monitoring glaucomatous visual field damage.

The oldest and most established techniques of perimetry use tests of the light sensitivity across the visual field. These tests measure the luminance sensitivity which is the ability of the eye to perceive the brightness difference between a test target and the background. This luminance sensitivity is greatest at the fovea, and declines with increasing distance towards the periphery. The decline in sensitivity with eccentricity has been described as the “hill of vision”, which was first coined by Traquair (Traquair, 1931).

2.2.2 History of perimetry

The first systematic attempt to reliably assess the visual field was by von Graefe (von Graefe, 1856). He used a board with a central fixation target and an illuminated target, which was moved from seeing to non seeing parts of the field. In 1869, Landesburg used an early perimeter to provide the first description of an arcuate scotoma, one of the hallmarks of glaucoma. Further descriptions of arcuate scotomas were provided by Bjerrum who used a flat screen perimeter, otherwise known as a campimeter (Bjerrum, 1889). Using Bjerrum’s method of perimetry, Rönne first described the glaucomatous nasal step and recognised that this distribution related to the anatomical arrangement of the retinal nerve fibre layer (Rönne, 1909). Further contributions were made by Traquair,

who provided a classification for the evolution of glaucomatous defects (Traquair, 1931).

2.2.3 Kinetic perimetry

A significant advance was made by Goldmann who developed a bowl perimeter to allow full control of the luminance of the background and stimulus (Goldmann, 1945). The Goldmann perimeter is commonly used to perform kinetic perimetry. Kinetic perimetry is performed by moving the stimulus from areas of the visual field where it cannot be seen to where it can be seen. Lines called isopters are drawn to connect points which show the same sensitivity to differences between stimulus and background. An overall contour map of the field can be generated using different stimuli to obtain different isopters. Goldmann perimetry became the clinical standard in glaucoma and was only superseded in the last decade by the developments in static automated perimetry.

2.2.4 Static perimetry

An alternative approach to kinetic perimetry is the technique of static perimetry. Stimuli are presented at fixed locations in the visual field and at varying levels of luminance. Static perimetry was first described by Sloan using an arc perimeter and by Harms using a bowl perimeter (Harms, 1940; Sloan, 1939). Static perimetry has a number of important advantages over kinetic perimetry as it can be made operator independent, and lends itself to automation and numerical analysis. However, the potential benefits of static perimetry have only been realized with the development of fully automated perimetry.

2.2.5 Automated perimetry

In automated perimetry the entire decision-making process of the test is controlled by a computer, thus eliminating any bias by the examiner. Automated perimetry is now the predominant and preferred method of perimetry for glaucoma in clinical practice and research.

Early examples of automated perimeters were the Octopus (Spahr, 1973), and the Competer (Heijl and Krakau, 1975).

The Humphrey Field Analyzer was introduced in the mid 1980s by Heijl (Heijl, 1985). Since this time, a wide range of automated perimeters has become available, including updated versions of the Humphrey Field Analyzer, the Octopus and the Henson perimeters. These machines offer a number of different test programs which utilize either suprathreshold or threshold static examination strategies. Suprathreshold strategies present stimuli at intensities calculated to be above the patient's threshold at that location, and are useful for rapid screening of the visual field. Alternatively, full threshold strategies can be used to obtain quantitative estimates of the threshold at each location by presenting stimuli which change luminance in a stepwise way. Full threshold strategies have the advantage of allowing a quantitative assessment of the visual field. This allows changes in the threshold to be assessed over time, although a disadvantage is they are more time consuming and demanding for the patient. The use of full threshold perimetry is now widely accepted as the mainstay technique for diagnosing and monitoring visual field loss in glaucoma.

I have used full threshold testing programs on the Humphrey Field Analyzer for the research in this thesis. Details of the test strategy that was used are given in the following section. Comprehensive surveys of the instrumentation and test strategies currently available are given by Lachenmayr (Lachenmayr and Vivell, 1993) and Henson (Henson *et al.*, 1996).

2.2.6 The Humphrey Field Analyzer (HFA)

2.2.6.i Specification

The Humphrey field analyzer is a bowl perimeter that performs fully automated static perimetry under constant photopic background conditions of 31.5 apostilbs. The standard projected stimulus is a white size III stimulus, which can be varied in luminance over a range of over 5.1 log units (range 0.08 to 10,000 apostilbs). The threshold is measured in terms of sensitivity, ranging from 0-50 dB, where 0 dB represents maximum stimulus brightness.

2.2.6.ii Test pattern and test strategy

The HFA 24-2 and 30-2 test programs are most commonly used in the management of patients with glaucoma, and were used for the testing of patients in this thesis. These

tests consist of a matrix of test locations covering the central 24 and 30 degrees of visual field respectively. The distance between the test locations is 6 degrees, and none of the test locations lies on the horizontal or vertical meridians.

Alternatively the “custom grid” program allows the experimenter to apply a matrix of test locations to a particular area of field, using test locations separated by smaller distances, for instance by 2 degrees. This program was used in my investigations of High Spatial Resolution Perimetry.

The standard strategy used by the Humphrey for full threshold testing is a 4/2 dB two reversal staircase procedure. The algorithm initially determines the threshold twice at each of four primary seed locations situated at 9 degrees eccentricity. The starting luminance of the primary locations is 25 dB. The final 2 dB crossing of threshold can occur in either the ascending or descending direction and the threshold is taken as the luminance intensity of the last seen stimulus. The initial starting luminance of the secondary locations is 2 dB higher than the expected threshold value derived from the knowledge of the sensitivity of the primary locations and of the slope of the hill of vision. Fixation is also monitored during the test using the Heijl and Krakau technique, which involves the presentation of a suprathreshold stimulus within the site of the predetermined blind spot (Heijl and Krakau, 1975). If this is seen then a loss of fixation is indicated. The patient’s performance is also assessed by the frequency of false positive and false negative results.

A television camera in the HFA 630 also allows the operator to continuously monitor the patient’s fixation during the test procedure.

3. CHAPTER 3

Aims of research: Improving the detection of abnormal visual function in glaucoma

3.1 Limitations of conventional automated perimetry in detecting early damage

Automated perimetry is at present regarded as the “gold standard” test of visual function in glaucoma, and is essential to the diagnosis and management of glaucoma. However, a major limitation with the use of automated perimetry as a standard is the fact that it is not sensitive to early glaucomatous damage. This section will examine evidence from clinical, histological and psychophysical studies to support this conclusion.

Prior to the introduction of automated perimetry, there was considerable evidence to suggest that glaucomatous disc changes and nerve fibre layer defects could often be detected clinically a considerable time before the development of glaucomatous visual field defects measured with manual perimetry. For example, Pederson and Anderson were able to show that progressive enlargement of the optic cup typically preceded visual field loss by several years in ocular hypertensive patients (Pederson and Anderson, 1980). Airaksinen and colleagues were able to measure rates and patterns of neuroretinal loss in patients converting to glaucoma, and concluded that such disc changes could be detected before field changes could be detected on the Friedmann perimeter (Airaksinen, et al., 1992).

Other investigators have shown that both observed cup disc changes and retinal nerve fibre layer defects can precede the onset of field defects detected by manual perimetry by several years (Quigley *et al.*, 1992; Quigley, et al., 1980; Sommer, et al., 1991a).

Although these later studies did include some patients who had undergone automated perimetry, all used manual Goldmann perimetry as the final arbiter of definite conversion of the field to glaucoma.

A study by Katz et al showed that automated perimetry could detect glaucomatous visual field loss before manual Goldmann perimetry in the majority of patients by at least 1 year (Katz *et al.*, 1995). Although this suggests that automated perimetry should be more

sensitive in detecting early visual damage, clinical studies continue to show that glaucomatous optic disc changes could be identified in patients before detectable visual field loss. Zeyen and Caprioli investigated 15 POAG patients who had initially unilateral field loss with longitudinal follow up (mean 6.1 years). Of the 15 contralateral ocular hypertensive eyes, 8 eyes showed progressive disc changes determined by planimetry. Of these 8 eyes, only 2 (25%) showed a deterioration by conventional automated perimetry (Zeyen and Caprioli, 1993).

Further evidence is provided by histological studies that have investigated the relationship between perimetric damage and the degree of ganglion cell death. Quigley reported that up to 50% of the optic nerve fibres could be lost in glaucomatous eyes before there was any evidence of visual field loss determined by Goldmann manual kinetic perimetry (Quigley, et al., 1982). A later study of 6 glaucomatous eyes that had undergone automated perimetry showed that 40% nerve fibre loss was associated with approximately 10 dB sensitivity loss, and 20% loss with 5 dB loss (Quigley *et al.*, 1989). This finding suggests that a considerable proportion of retinal ganglion cells may be lost in glaucoma before a field defect can be reliably detected using conventional white-on-white perimetry.

The final body of evidence is provided by psychophysical studies which have identified a wide variety of abnormalities of visual function before the appearance of conventional Humphrey field abnormalities. The clinical evidence and the possible theoretical basis for these findings is crucial to understanding the rationale for the research work described in this thesis, and is therefore discussed in detail in the following section.

3.2 Rationale for using other psychophysical tests

3.2.1 Introduction

The limitations of conventional perimetry outlined above have prompted the search for alternative methods which might be more sensitive in detecting early abnormalities of visual function.

This has resulted in the development of alternative psychophysical tests, each aimed at isolating and testing particular aspects of visual function. Two principal hypotheses must be considered in relation to the rationale for using a selective test of ganglion cell

function. These are the selective cell death hypothesis and the concept of reduced redundancy.

3.2.2 Selective ganglion cell loss in glaucoma

The hypothesis of selective ganglion loss in early glaucoma was first proposed by Quigley as a result of histological studies of the optic nerves of primates with laser induced chronic glaucoma (Quigley *et al.*, 1987). The results of these studies suggested that although glaucomatous losses occurred for all sizes of ganglion cells, losses were proportionately greater for larger diameter ganglion cells (large optic nerve fibres) compared with small diameter fibers. Similar findings were identified in human post mortem studies that compared the size and distribution of surviving axon fibers in glaucomatous eyes with control eyes (Quigley *et al.*, 1988). In the glaucoma eyes, size distribution plots showed a significant loss of large fibres relative to smaller fibres (Quigley, *et al.*, 1988). The most vulnerable parts of the nerve (the superior and inferior poles) had a higher proportion of the larger fibres and were consequently more likely to suffer damage. However, the preferential loss was found to be uniformly present throughout the optic nerve, including the least damaged zones. Quigley *et al.* postulated two reasons for preferential loss of large diameter fibers, firstly their vulnerable location in the nerve, and secondly their greater intrinsic susceptibility.

Since magnocellular cells are associated with larger mean diameters, this “selective loss hypothesis” would imply a preferential loss of magnocellular function. Tests that have been designed to selectively test this pathway include tests of motion, flicker or temporal modulation perimetry, and scotopic sensitivity. Abnormalities of all these modalities have been found to occur early in glaucoma. These findings can be interpreted as providing evidence for the selective magnocellular loss hypothesis.

Further histological evidence in support for the hypothesis of selective cell death was provided by Chaturvedi *et al.*, who compared cell counts of human autopsy LGN material in 5 glaucoma patients and 5 age matched controls (Chaturvedi *et al.*, 1993). They found a significant reduction in the cell counts of the magnocellular layers of the dLGN in the patients compared to the controls. There were no statistically significant differences in the parvocellular layers.

The hypothesis of selective cell loss has recently been criticized by Morgan, who hypothesized that non selective cell shrinkage may account for the above findings.

However, this analysis was based on entirely theoretical reasoning and has not been substantiated by any experimental evidence (Morgan, 1994).

3.2.3 Reduced redundancy

One problem with the selective magnocellular cell loss theory is that many studies have identified early losses of visual function believed to be mediated by the parvocellular system. These include high-pass resolution perimetry, pattern discrimination perimetry, and short-wavelength automated perimetry (SWAP). This finding is difficult to reconcile with the selective magnocellular loss theory.

This diversity of psychophysical abnormalities found in early glaucoma has lead Johnson to observe how *non-selective* the deficits are between the parvocellular and magnocellular systems.

Johnson has proposed the hypothesis of reduced redundancy to account for the nature of early psychophysical losses that have been reported in glaucoma (Johnson, 1994). This hypothesis is not contrary to the concept of selective loss. In addition to considering differential losses of different ganglion cell populations, this theory takes into account the degree of inherent redundancy present in a specific population of ganglion cells. The redundancy theory predicts that a test which isolates a very sparse population of ganglion cells (so called *selective tests*) will identify the earliest loss as this system has little physiological redundancy. Non-selective tests such as conventional white on white perimetry stimulate large populations of ganglion cells with considerable receptive field overlap. Tests of these populations will identify losses later because of their greater inherent redundancy.

This theory predicts a sequential progression of different functional losses in any region of the visual field. The order would depend on the relative degree of redundancy of each function. Johnson predicts that blue-on-yellow deficits should appear first, followed by magnocellular losses (motion, flicker), followed by conventional automated perimetric defects (Johnson, 1994). The occurrence of a wide variety of selective test deficits, including blue-on-yellow, flicker, and motion, before conventional field loss appears to support this hypothesis. However, a rigorous test of this hypothesis can only be provided by longitudinal studies which subject glaucoma patients and suspects to a battery of different psychophysical tests to prospectively sequence the occurrence of defects. At present such studies are lacking, and such data remains to be seen.

3.3 Motion Perception perimetry in glaucoma

3.3.1 Introduction

The first report of impaired motion perception in glaucoma was by Fitzke et al (Fitzke *et al.*, 1987). Since then, this finding has been confirmed by number of researchers, who have identified motion perception losses using a variety of different stimuli and test strategies.

Abnormalities of motion perception have been shown to occur early in glaucoma. This finding has been interpreted as being consistent with the selective magnocellular ganglion cell death, as proposed by Quigley, which hypothesizes that there is selective damage to the larger fibre diameter ganglion cell in early glaucoma. Since magnocellular cells are associated with larger mean fibre diameters, the “selective loss hypothesis” would imply a preferential loss of magnocellular function, which includes motion sensitivity.

Alternatively, the presence of abnormalities of motion sensitivity before conventional perimetric defects would be consistent with the reduced redundancy hypothesis, as described earlier in this chapter.

3.3.2 Line displacement thresholds

Fitzke et al first identified motion sensitivity defects in glaucoma using a line displacement test (Fitzke, et al., 1987). This test uses a line stimulus presented at 15 degrees eccentricity in the superotemporal field, which undergoes sudden oscillatory displacements. Frequency of seeing curves are generated for a test of 10 presentations each of 10 different displacements in 2 minute arc intervals from 0-18 minutes of arc. A probit fit analysis is applied, and the threshold is taken as the minimum displacement corresponding to 50% seen level (the Motion Displacement Threshold or **MDT**). Therefore a high value of MDT indicates that only large displacements of the stimulus are seen consistently, indicating a low motion sensitivity.

The technique for measuring motion sensitivity for the purposes of this thesis was that described by Fitzke et al (for details see chapters 4,5,7,8).

Fitzke et al showed that the Motion Displacement Thresholds (MDTs) of glaucoma patients with existing field defects were significantly elevated compared to controls. In this study, the mean MDT of 16 glaucoma eyes was 9.7 minutes of arc, compared to a mean of 3.2 minutes of arc for 38 normal eyes (Fitzke, et al., 1987).

Elevated displacement thresholds were also identified in a proportion of ocular hypertensive patients with normal automated visual fields (Fitzke, et al., 1987).

Subsequent work by the same group showed that Motion Displacement Thresholds are relatively resistant to the confounding effects of media opacity, refractive blur and pupil size (Fitzke *et al.*, 1989). These properties are clinically beneficial and appear to be shared by other hyperacuity tasks (Whitaker and Buckingham, 1987).

The clinical usefulness of this technique of measuring line displacement thresholds in glaucoma has been demonstrated in a study which showed that abnormalities of motion sensitivity could precede conventional field loss (Baez *et al.*, 1995). Motion Displacement Thresholds were measured in 51 patients with confirmed normal tension glaucoma, with strictly unilateral field loss. In 22 eyes of 51 patients with normal fields at presentation, one or more of the Humphrey 24-2 test locations showed significant field deterioration. An initially normal MDT test showed a sensitivity of 73% and specificity of 90% in predicting field deterioration within the cluster of four Humphrey locations closest to the MDT test site. However the sensitivity was only 40% for predicting field deterioration for all Humphrey test locations, including locations distant from the MDT test site, although the specificity remained high.

3.3.2.i Correlation of MDT with optic disc parameters

Ruben et al identified a significant negative correlation between MDT and neuroretinal rim area in 50 patients with ocular hypertension (Ruben and Fitzke, 1994). The finding of an association between early loss of neural tissue at the disc with this early loss of visual function is significant as both may precede conventional visual field changes.

3.3.2.ii Other studies of displacement threshold perimetry

Johnson et al have reported preliminary results for a multilocation displacement test using 2 degree diameter targets presented in a grid similar to the Humphrey 30-2.

They have identified elevated Motion Displacement Thresholds in glaucoma patients, which in most cases appear to be more extensive than conventional field deficits (Johnson *et al.*, 1995).

This finding suggests that motion displacement testing may detect earlier losses of visual function. However longitudinal studies are required to ascertain the proportion of these patients which develop conventional visual field progression.

3.3.3 Random dot kinetograms

3.3.3.i Central field random dot kinetogram testing

An alternative method of investigating motion sensitivity in glaucoma involves the use of random dot kinetograms.

A random dot display typically consists of an array of randomly moving dots to provide a perception of random noise. A proportion of dots are replotted at a fixed spatial offset to provide the coherent motion signal. The percentage of moving dots to randomly moving dots is known as the coherence, and can be varied to produce graded intensities of motion signals.

Silverman et al performed random dot kinetogram testing of the central field to measure motion thresholds. He identified a 70% elevation of the foveal motion coherence thresholds in primary open angle glaucoma patients, and 40% elevation in ocular hypertensives. These patients therefore require a higher proportion of moving dots (coherence) relative to background noise to reliably detect motion (Silverman *et al.*, 1990).

Trick *et al.* found significant elevations of direction discrimination thresholds for low velocity (4.2 deg/sec), and high velocity (12.5 deg/sec) random dot kinetograms tested in the central 24.5 degrees of field (Trick *et al.*, 1995).

These studies all used random dot kinetograms to test large areas of the central field. One potential drawback of this type of motion testing is that it may be poorly sensitive to early focal glaucomatous losses. This may explain the poor performance of a central random dot kinetogram test in early glaucoma reported by Graham et al (Graham *et al.*, 1996). They compared the sensitivity and specificity of a battery of psychophysical tests performed on 43 patients with early glaucoma. Motion measurements were performed using a random dot kinetogram test to measure motion coherence thresholds of the central field, adapted from the test described by Silverman (Silverman, et al., 1990). The tests with the highest sensitivity and specificity were the pattern electroretinogram and isoluminant letter acuity tests, followed by SWAP and high pass resolution perimetry. Tests such as the motion test, flicker contrast and flash electroretinogram performed poorly, with the motion test performing little better than chance.

This finding supports previous work by Bullimore et al, who found that random dot kinetogram testing of coherence thresholds and maximum displacement thresholds

(Dmax) did not discriminate between patients and controls (Dmax refers to the maximum displacement for apparent motion. Displacements larger than Dmax elicit the perception of two unrelated patterns).

Instead they reported better results using smaller field sizes to measure minimum displacement thresholds, which were significantly elevated in glaucoma patients. Mean minimum displacement thresholds were more than twice that for controls, and 10 out of 15 glaucoma patients had elevated Dmin outside the normal range (Bullimore *et al.*, 1993).

3.3.3.ii Random dot kinetogram testing of focal areas of field

Following the work of Bullimore, a number of workers have used random dot kinetogram testing to test focal areas of the visual field. One approach has been to measure focal motion sensitivity by presenting circles of moving random dots, of 50% coherence, of varying sizes within a background of random noise (Wall and Ketoff, 1995; Wall and Montgomery, 1995). The subject indicates the perceived centre of the stimulus using a light pen. This technique allows motion size thresholds to be measured, and these have been shown to be significantly elevated in glaucoma patients and in patients. Wall et al have recently reported nerve bundle-like defects of motion size thresholds in individual ocular hypertensive patients. However as a group the size thresholds of the ocular hypertensive patients did not differ significantly from controls (Wall *et al.*, 1997).

Alternatively random dot kinetograms have been used to measure coherence thresholds in focal areas of the visual field. Preliminary results have recently been reported by Bosworth (*et al.*, 1997), who found that motion coherence thresholds were significantly poorer within areas of conventional Humphrey field loss compared to areas of field sparing. However, they did not report whether motion thresholds in areas of field sparing were impaired compared to age matched controls.

3.4 Other psychophysical tests

3.4.1 Short Wavelength Automated perimetry (SWAP)

SWAP (otherwise known as blue-on-yellow perimetry) uses a blue stimulus on a yellow background to isolate and measure the sensitivity of the short-wavelength pathway. This pathway is mediated by a subpopulation of P-pathway ganglion cells believed to be the bistratified ganglion cells. These cells have slightly larger mean diameters and it is postulated that they may be susceptible to selective loss. They are also relatively sparsely distributed, comprising only 1-2% of total ganglion cell pool. Thus it is postulated that functional losses may occur early in the blue pathway because of the reduced redundancy of this system (Johnson, 1994). SWAP is usually performed on the Humphrey Field Analyzer using a size V stimulus with a yellow background.

The use of SWAP in glaucoma has now been under investigation for 10 years, and a full review of the extensive literature is beyond the scope of this thesis. In POAG patients, SWAP defects have been shown to correspond with, and often overlap conventional white on white defects (Johnson *et al.*, 1993a; Sample and Weinreb, 1992). SWAP defects have also been shown to correspond to the retinal nerve fibre layer pattern. The greater extent of SWAP deficits compared with conventional perimetric deficits appears to be most marked in POAG patients who undergo progression of their conventional field loss (Johnson *et al.*, 1993b).

In ocular hypertensive patients, a longitudinal study of 76 subjects showed that of nine patients with initial SWAP defects, 5 developed conventional field defects within 5 years (a sensitivity of 100 %, specificity of 94 %) (Johnson, et al., 1993a). Sample et al reported significantly larger SWAP defects in suspect eyes that subsequently converted over at least 1 year of follow up (Sample *et al.*, 1993).

Unfortunately SWAP has a number of major disadvantages which may seriously limit its clinical usefulness. These include a shorter dynamic range, and a greater short-term fluctuation (Wild *et al.*, 1996; Wild *et al.*, 1995). Wild et al have also shown that SWAP has a greater long-term fluctuation compared with white-on-white perimetry (Wild *et al.*, 1997). This would be expected to make the identification of progressive field loss more difficult using SWAP perimetry compared with conventional perimetry.

Another problem with SWAP is the individual variation in the degree of absorption of short wavelengths by the lens. The accepted method of correcting for this requires the

measurement of dark adapted thresholds which are time consuming and clinically impractical. Sample et al have attempted to address this problem using an approach similar to the Glaucoma Hemifield Test to avoid the need for such correction, although this analysis has yet to be replicated (Sample *et al.*, 1994b).

3.4.2 Flicker perimetry

Flicker perimetry has been shown to identify early abnormalities of visual function in glaucoma. High frequency flicker is believed to be mediated by the magnocellular cell pathway, whereas low frequency flicker is believed to be mediated by the parvocellular pathway (Schiller, et al., 1990a).

One threshold measure that has been used is the “critical flicker fusion frequency”, which is the highest frequency of flicker that can be detected for a target at 100% contrast. A cross-sectional study by Lachenmeyer showed increasing depth of flicker fusion defects relative to conventional perimetric defects, with increasing level of IOP in glaucoma patients (Lachenmayr and Drance, 1992).

An alternative threshold measure is to determine the minimum contrast needed to detect a flickering stimulus maintained at a constant frequency (temporal modulation perimetry). Casson et al reported that temporal modulation defects were more extensive than conventional field defects in ocular hypertension and early glaucoma. In a prospective follow-up, temporal modulation defects at the 8 and 16 Hz frequencies performed best in predicting the locality of subsequent conventional field deterioration (Casson *et al.*, 1993).

Finally, flicker perimetry has the clinically useful properties of being very resistant to the effects of blur and cataract (Lachenmayr and Gleissner, 1992).

3.4.3 High-pass resolution perimetry

Another test that has been used to investigate early abnormalities of visual function is high-pass resolution perimetry. This is a test of peripheral spatial resolution, and was first pioneered by Frisen as a test of parvocellular pathway function (Frisen, 1995). Frisen has suggested theoretical reasons for a close relationship between the high pass resolution threshold and the number of functioning retinocortical neural channels. The test uses a ring-shaped target with a bright core and dark borders, and is quick to perform. Various sizes of rings are presented in the field, and the threshold is the minimum size of the ring

when it is first seen. The agreement between high pass resolution defects and conventional field defects has been reported as moderately good, ranging from 67% to 77% in glaucoma patients (Chauhan *et al.*, 1993a; Sample *et al.*, 1992). However Sample *et al.* found no differences in high pass resolution thresholds in ocular hypertensive patients and age matched normal controls (Sample, et al., 1992). At present there are no results on the long-term usefulness of high pass resolution perimetry in predicting conversion of ocular hypertensives to glaucoma.

3.4.4 Frequency doubling perimetry

There has recently been considerable interest in the use of the frequency doubling illusion as a screening method for glaucoma. The frequency doubling illusion, as originally described by Kelly, occurs when a low spatial frequency grating (<1 cyc/deg) undergoes rapid counterphase flicker (i.e. the light bars become dark and vice versa). Under these conditions a normal physiological illusion occurs in that the grating appears to be twice its actual frequency (Kelly, 1981). The stimulus characteristics required for this illusion suggest that the frequency doubling response is mediated by the magnocellular pathway, via a subset of M-cells with non-linear response properties (Johnson and Samuels, 1997; Maddess and Henry, 1992). Johnson & Samuels have investigated the screening ability of a frequency doubling contrast threshold test of discrete locations of the visual field, and reported a sensitivity of 93% at 100% specificity against the Humphrey perimeter (Johnson and Samuels, 1997). However this degree of separation could only be achieved using a frequency doubling test that sampled a relatively large number (16) of test locations in the visual field. Nevertheless this test appears promising as a screening test and further studies are awaited.

3.5 Aims and plan of research

The limitations of conventional Humphrey perimetry in detecting early glaucomatous damage have been described above. The aim of this thesis is to investigate further the early abnormalities of visual function in glaucoma using line displacement motion sensitivity testing and High Spatial Resolution Perimetry.

3.5.1 Motion sensitivity

The investigations of line displacement motion sensitivity in glaucoma have previously been described in this chapter. The research in this thesis describes further investigations into aspects of motion sensitivity which have not yet been explored. These aspects are the application of reaction time and frequency-of-seeing curve analysis, and the effect of stimulus orientation. The purpose of this is to investigate the physiological basis of motion sensitivity in glaucoma and to see if the sensitivity of motion testing in detecting early glaucoma can be improved.

3.5.2 High Spatial Resolution Perimetry

The principal aim of this research was to see if fine scale scotomas exist in glaucoma within areas of field which appear normal with conventional perimetry, and to investigate whether such fine scale scotomas coexist with abnormal motion sensitivity.

The presence of fine scale scotomas would suggest that the principal limitation of conventional Humphrey 24-2 in detecting early glaucoma is its inadequate spatial resolution.

An additional aspect of this investigation was to investigate the clinical practicality of the technique and the repeatability of the field measurements.

4. CHAPTER 4

Differences in the reaction times for motion detection between normals and glaucoma.

4.1 Background

The study of reaction times to visual stimuli has made important contributions to the understanding of a number of diseases. For example, Regan and colleagues have identified a significant delay in the perception of visual stimuli during electrophysiological studies of optic neuritis (Regan *et al.*, 1976). This delay was present in both perimetrically normal and abnormal areas of the visual field, and was found to be a more sensitive index of disease than perimetry alone. A study by Wall and Montgomery reported significantly prolonged reaction times and elevated motion thresholds using a random dot kinetogram test in patients with idiopathic intracranial hypertension (Wall and Montgomery, 1995).

In glaucoma, the study of reaction times during conventional perimetry has received some attention by (Flammer *et al.*, 1984b). They studied covariates of long term fluctuation in normals, glaucoma suspects and controls. The mean test reaction time was one factor significantly associated with the higher long-term fluctuation seen in glaucoma patients compared to controls. Increasing prolongation of reaction time was correlated with decreasing light differential sensitivity (Flammer, et al., 1984b). A more recent study of reaction time for a perimetric stimulus has been reported by Wall and colleagues, who investigated the relationship between reaction time and the psychometric function for a Humphrey stimulus (Wall *et al.*, 1996). They used frequency-of-seeing curves generated by a customized Humphrey in perimetrically normal and abnormal areas of the field. They found no significant differences in reaction time between normals and glaucoma patients. However in this study, reaction times were only reported at the threshold and at a suprathreshold stimulus.

In contrast with conventional perimetry, studies of motion detection in glaucoma have concentrated on motion threshold differences, and reaction time has received little attention. A study by Wall & Ketoff failed to identify significant prolongation of reaction

times in the presence of elevated motion detection thresholds in glaucoma patients (Wall and Ketoff, 1995). However this study did not specifically investigate the relationship between reaction time and threshold.

4.2 Purpose

The aim of this study was to confirm whether or not prolongation of reaction time for a motion stimulus occurs in glaucoma. A subsequent aim was to investigate the relationship between any prolongation of reaction time, if identified, and elevation of the motion threshold. The analysis was based on reaction times recorded from the motion testing of the study which is described in chapter 7. This was performed by obtaining frequency-of-seeing curves using a line displacement stimulus, whilst recording reaction times to all responses made throughout the psychometric function. One potential benefit of an improved understanding of reaction time abnormalities in glaucoma is that it may enable novel methods to assess subject reliability to be developed for motion testing, similar to those described by (Olsson *et al.*, 1997) for conventional perimetry (see discussion).

4.3 Method

The reaction time data for this study was obtained during the study described in detail in chapter 7 and readers are referred to this chapter for a full description. A summary of this study with details pertinent to the investigation of reaction time is given below.

4.3.1 Subjects

The study consisted of 18 Patients with Primary Open Angle Glaucoma in one eye and suspect glaucoma in the fellow eye, and 18 age-matched normal controls.

The mean Humphrey 24-2 MD for the glaucoma eyes was -5.8 ± 2.5 dB, range -11.1 to -3.0 dB, which was significantly different ($P < 0.0001$) from the glaucoma suspect eyes (mean MD -1.7 dB ± 1.7 dB, range -4.2 to +1.3 dB) and the controls (mean MD -0.5 dB ± 1.3 dB, range -2.7 to +2.5 dB). The mean MD of the glaucoma suspect eyes was not statistically different from the control mean MD.

The mean age of the 18 patients was 59.7 ± 12.2 years, with a range 30.6 - 78.8 years. The distribution of the 18 control ages was very similar, with a mean age of 57.8 ± 11.5

years, with a range of 31.3 - 74.9 years (non-significant difference in mean age, $P = 0.63$).

All patients and controls had a corrected visual acuity in both eyes of $\geq 6/9$ achieved with less than ± 4 dioptres spherical equivalent and less than 2 dioptres of astigmatism.

4.3.2 Motion Displacement Testing

Motion Displacement Threshold (MDT) testing was performed using a line stimulus undergoing displacements 0-18 min. arc. presented in the superotemporal field. (see chapter 7 for complete description). Patients underwent motion testing in the POAG eye and the glaucoma suspect fellow eye in a randomised order, separated by a suitable rest break. Controls underwent motion testing in one randomly chosen eye.

4.3.3 Recording of reaction times

Subjects were informed that the response measure of interest was the detection of motion, and were unaware that reaction times were being recorded. The experimenter avoided giving any cues that might influence an individual's response time. Reaction times were recorded for all stimuli presented and corresponded to the time interval between the onset of stimulus movement until the response button held in the subject's right hand was depressed.

4.4 Results

4.4.1 Motion thresholds

The results of the motion threshold testing are shown in table 4.1.

The MDTs of the glaucoma eyes were markedly greater than controls ($P < 0.0001$) and the glaucoma suspect fellow eyes ($P < 0.0034$). The MDTs of the suspect eyes were moderately elevated as a group compared to the controls, which just reached significance ($P = 0.046$).

Group	Normals (18 eyes)	Glaucoma suspects (18 eyes)	Glaucoma patients (15 eyes)
Threshold (min. arc)	6.1 ± 1.6 (2.3 - 8.2)	8.5 ± 3.9 (4.6 - 18.4)	15.3 ± 12.9 (4.2 - 57.6)
Mean Reaction time (msec.)	1160 ± 140 (940 - 1430)	1220 ± 310 (780 - 1760)	1370 ± 220 (980 - 1680)

Table 4.1 Summary statistics for the motion threshold and the subjects' mean reaction time during the test, by group. Values shown are mean ± 1 SD. Figures in brackets indicate minimum and maximum values. Only 15/18 glaucoma eyes tested had a measurable motion threshold.

4.4.2 Reaction times

We analyzed 2570 reaction times in total, and summary statistics are shown in table 4.1. The mean reaction times during the motion test for the glaucoma eyes ranged from 980 msec. to 1680 msec. with a group mean of 1370 msec., and were significantly prolonged ($P = 0.0075$) compared to the control eyes which ranged from 940 msec. to 1430 msec., with a group mean of 1160 msec. This represents a mean delay of 210 msec. in the reaction time between glaucoma and control eyes.

The mean reaction times of the suspect eyes ranged from 780 msec. to 1760 msec. with a group mean intermediate between the glaucoma and controls of 1220 msec.. This did not differ significantly with the control mean ($P = .85$).

We derived cut-offs for the motion threshold and the mean reaction time, using mean + 2 SD of the control values. Using these cut-offs, 11/15 (73%) of the glaucoma eyes and 4/18 (22%) of the glaucoma suspects had elevated motion thresholds above the control mean + 2 SD of 9.2 min arc. 8/15 (53%) of the glaucoma eyes and 6/18 (33%) of the glaucoma suspect eyes had a prolonged mean reaction time, above the control mean + 2 SD of 1440 msec.

4.4.3 The relationship between reaction time and stimulus displacement

Figures 4.1a & 4.2a show the relationship between reaction time as a function of stimulus displacement for the groups. Reaction times were longest for the glaucoma

group, and shortest for the controls for all displacements, with glaucoma suspect eyes intermediate. Because variances were dissimilar between groups, we used non parametric tests which showed that the prolonged reaction times were statistically significant at the $P < 0.05$ level for displacements 12-18 min. arc in the glaucoma eyes compared to controls (figure 4.1a). There were no statistically significant differences between the reaction times between glaucoma suspects and controls at any of the displacements (figure 4.2a). Displacements below 12 min. arc had too few responses in the glaucoma eyes for meaningful analysis.

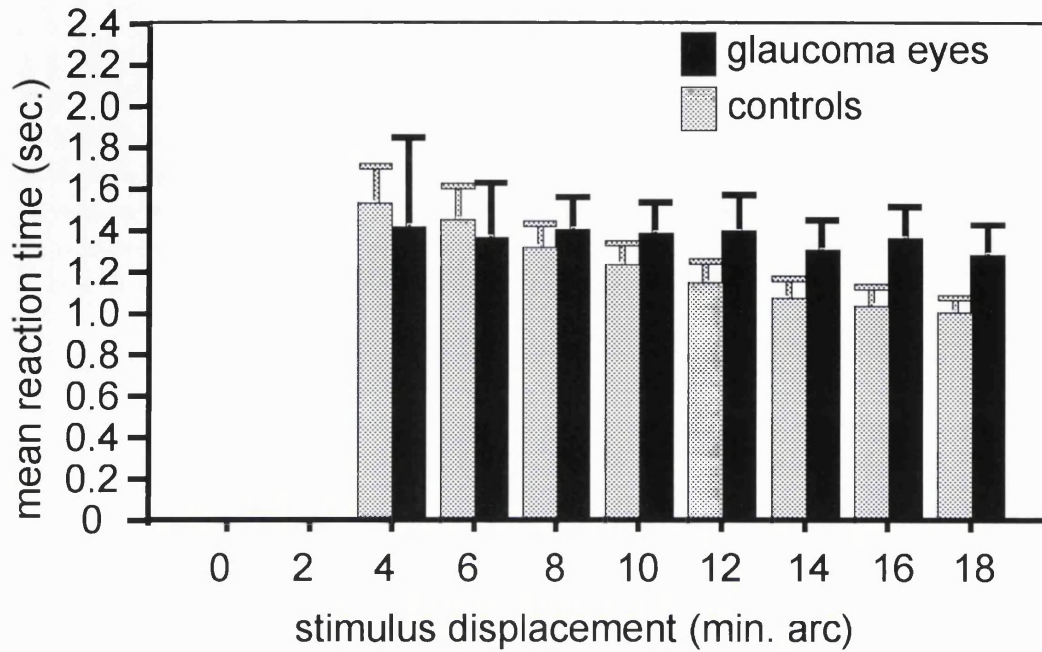


Figure 4.1a Relationship between reaction time and stimulus displacement for glaucoma eyes and controls. Reaction times were significantly prolonged in glaucoma eyes for displacements 12-18 min. arc.

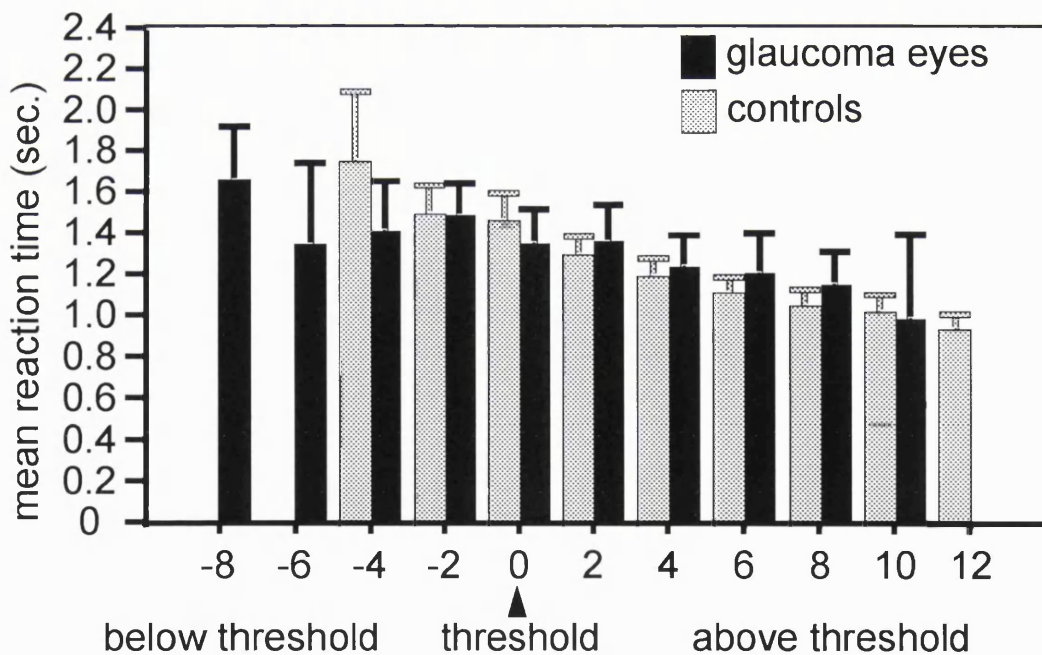


Figure 4.1b Same data as figure 4.1a, replotted to show the relationship between reaction time as a function of distance in min. arc from threshold. There are now no significant differences between the groups.

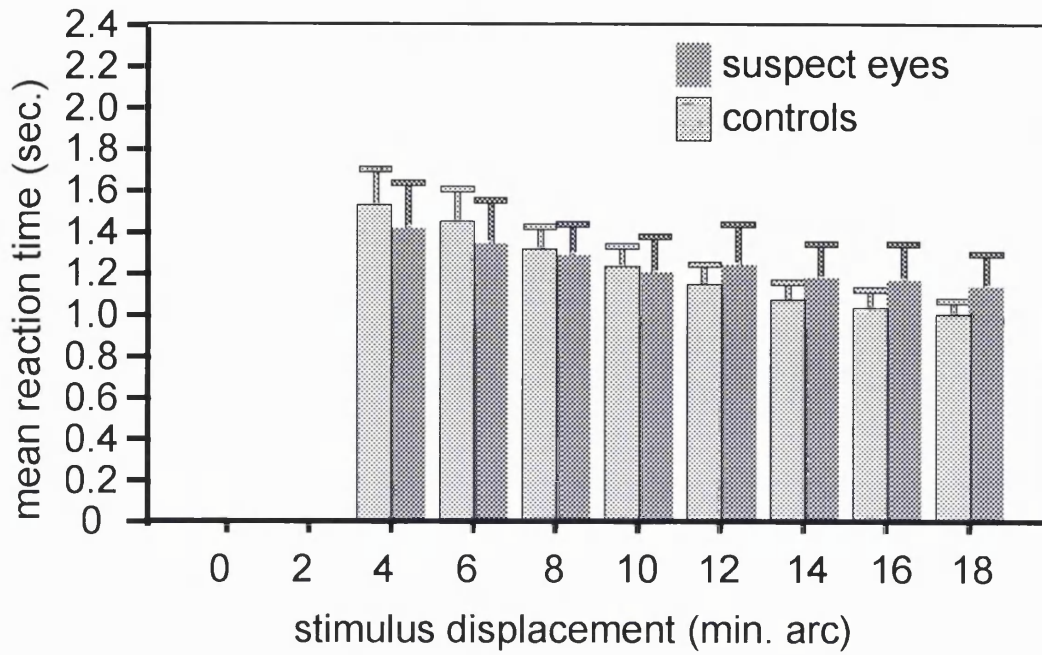


Figure 4.2a Relationship between reaction time and stimulus displacement for suspect eyes and controls, showing a trend of prolonged reaction times eyes for displacements 12-18 min. arc in suspect eyes (not significant).

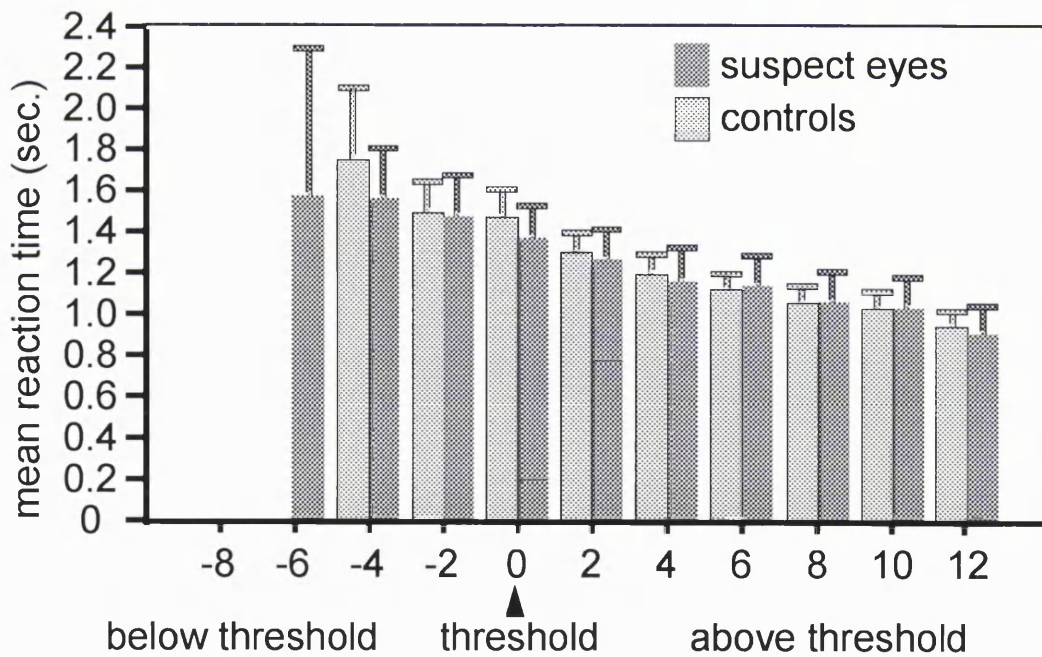


Figure 4.2b Same data as figure 4.2a, replotted to show the relationship between reaction time as a function of distance in min. arc from threshold. This abolishes any differences between the two groups.

4.4.4 Are the prolonged reaction times in glaucoma patients accounted for by threshold elevation?

Although figures 4.1a & 4.2a show the relationship between reaction time and displacement, they do not take account of the threshold elevation of the glaucoma eyes. We therefore corrected for threshold elevation by plotting reaction time as a function of distance from threshold (figures 4.1b & 4.2b). This results in a substantial reduction in any differences in reaction times we identified. After correcting for the elevated thresholds of the glaucoma eyes, there were no significant differences in the reaction times at any of the displacements, including the threshold displacement, (shown as the 0 min. arc interval on the x abscissae of figures 4.1b & 4.2b) or suprathreshold displacements.

Therefore reaction times at threshold did not differ significantly between the groups, and are in close agreement.

(table 4.2).

Group	Normals (18 eyes)	Glaucoma suspects (18 eyes)	Glaucoma patients (11 eyes)
Reaction time at threshold (msec.)	1470 \pm 270 (1000-2000)	1350 \pm 330 (850 - 1970)	1360 \pm 270 (980 - 1800)

Table 4.2 Summary Statistics for the reaction time at threshold displacement, showing no significant differences between the groups at the $P < 0.05$ level. Values shown are mean \pm 1 SD. Figures in brackets indicate minimum and maximum values.

We investigated the relationship between the mean reaction time at each displacement, as a function of distance from threshold (see figures 4.1b & 4.2b) and achieved a very good fit using the simplest linear fit model. Using this model, we obtained a significant negative correlation between the mean reaction time at each displacement, as a function of distance from threshold for all 3 groups. The goodness of fit (R^2) was 0.91 in the controls ($P < 0.001$), and 0.98 for glaucoma suspect eyes ($P < 0.001$). A slightly less goodness of fit was obtained with the glaucoma eyes, ($R^2 = 0.82$, $P < 0.001$) and the slope to the regression line was shallowest in the glaucoma eyes, although the difference in the regression line slope was not statistically significant between the groups.

4.5 Discussion

Investigations into abnormalities of Motion Displacement Threshold in glaucoma have concentrated on motion threshold differences and reaction time (RT) has received little attention. Wall et al were unable to identify significant prolongation of reaction times in the presence of the elevated Motion Displacement Threshold thresholds in glaucoma patients, although they did not specifically investigate the relationship between RT and threshold (Wall and Ketoff, 1995). We have shown that glaucoma eyes have prolonged mean reaction times during motion testing compared to controls. Prolongation of reaction times for a motion stimulus has been reported for other visual disorders. Wall et al reported a reaction time prolongation of approximately 100 msec. in the responses of patients with Benign Intracranial Hypertension undergoing motion perimetry (Wall and Montgomery, 1995). They suggested that the most likely cause of the reaction time elevation in the patients was as a consequence of a prolonged decision time relating to uncertainty of stimulus perception.

Recently Wall et al have investigated reaction times in glaucoma using frequency of seeing curves generated by a customized Humphrey in perimetrically normal and abnormal areas of the field. However, they only reported reaction times for threshold and 0 dB (suprathreshold) stimuli, which did not differ significantly from normals.

The MDT testing in the study described in this chapter has the advantage of recording reaction time for all the stimuli presented during a subject's motion test. This allows us to study mean reaction times which were found to be elevated in the glaucoma patients compared to controls. In addition, the relationship between prolongation of reaction time and elevation of motion threshold can be examined by re-analysing reaction times as a function of distance from threshold. We found that the motion reaction times at threshold were equivalent across the groups. This finding is similar to that reported for luminance stimuli. Reasons for the reaction time delay in glaucoma and the equivalence at threshold are discussed in chapter 9.

5. CHAPTER 5

Characteristics of Frequency-of-Seeing curves for a motion stimulus in glaucoma eyes, glaucoma suspect eyes, and normal eyes.

5.1 Background

Previously published investigations of motion sensitivity losses in glaucoma have concentrated on differences in the motion thresholds between groups. Although Silverman reported a qualitative lessening of the slope of the psychometric curve of motion in some patients with glaucoma (Silverman, et al., 1990), there has been no detailed analysis of frequency-of-seeing curves for motion response in glaucoma to date. Frequency-of-seeing curves describe the relationship between the probability of seeing a stimulus and a stimulus parameter such as intensity (luminance stimulus) or stimulus displacement (motion stimulus). The S-shaped frequency-of-seeing curve has been shown to describe the relationship between luminance sensitivity and variability in automated perimetry (Chauhan and House, 1991; Chauhan *et al.*, 1993b; Henson, et al., 1996; Olsson *et al.*, 1993; Wall, et al., 1996; Weber and Rau, 1992). The threshold is usually defined as the stimulus intensity at which 50% of the stimuli will be seen. In addition the steepness of the frequency-of-seeing curve can be calculated to provide a measure of the intratest variability around the threshold at that test location. A steep gradient represents little variability, whilst shallow gradients indicate large intratest variability. A number of researchers have found a significant correlation between threshold and the slope of the frequency-of-seeing curve for luminance stimuli (Chauhan and House, 1991; Chauhan, et al., 1993b; Henson, et al., 1996; Olsson, et al., 1993; Wall, et al., 1996; Weber and Rau, 1992). These studies have reported a shallowing of the slope of the frequency-of-seeing curve in glaucoma patients with decreased sensitivities, reflecting an abnormally high intratest variability. In addition, Chauhan et al have shown that glaucoma patients have widely differing frequency-of-seeing curves for similar thresholds and were able to identify patients who had normal Humphrey field

thresholds, but who had an abnormally shallow slope of the frequency-of-seeing curve (Chauhan, et al., 1993b).

5.2 Purpose

This study tests the hypothesis that frequency-of-seeing analysis can characterise additional differences between the motion response of normal subjects and glaucoma patients beyond that achieved by measuring thresholds alone.

The identification of these differences may allow us to improve the sensitivity and specificity of motion testing in glaucoma.

5.3 Method

5.3.1 Subjects

Eyes with an established diagnosis of POAG were eligible for this study if they had documented evidence of an intra-ocular pressure > 21 mm Hg. on at least one occasion in association with glaucomatous optic disc cupping, in conjunction with a glaucomatous visual field defect on the Humphrey 24-2 field test. A field was defined as glaucomatous on the Humphrey 24-2 if at least one hemifield contained a cluster of a minimum of three adjacent depressed points on the STATPAC2 pattern deviation plot with one point having a probability of $P < 1\%$ and 2 adjacent points having a probability of $P < 2\%$ (Piltz *et al.*, 1991). We evaluated the Humphrey 24-2 field at the MDT test site using the field thresholds of the four locations nearest the MDT test site (see Figure 5.1a). We defined the Humphrey 24-2 field at the motion test site as being abnormal if the field thresholds of at least 1 of these 4 locations was contiguous with a hemifield cluster of depressed locations, according to the above criteria.

Glaucoma suspect eyes were eligible if they had at least one of the following: glaucomatous optic disc cupping, clinical evidence of retinal nerve fibre layer defects, or a documented intra-ocular pressure > 21 mm Hg on at least one occasion, in the presence of a normal Humphrey 24-2 field (defined as normal or borderline Glaucoma Hemifield Test in the absence of any clusters of depressed locations in either hemifield). We excluded any eyes with significant ocular pathology other than glaucoma, including evidence of cataract or secondary glaucoma, and eyes which were being treated with

topical miotics. We recruited suitably age-matched controls if they had no significant ocular history, had a normal ocular examination with an IOP less than 21 mm Hg. and had normal Humphrey HFA 24-2 fields (defined as a normal Glaucoma Hemifield Test with global indices within 95% C.I. for normal subjects with no hemifield clusters of depressed points). All Humphrey 24-2 fields met standard reliability criteria of < 20 % fixation losses, < 33 % false negatives, < 33 % false positives. All patients and controls had a corrected visual acuity in the tested eye of $\geq 6/9$ achieved with less than ± 4 dioptres spherical equivalent and less than 2 dioptres of astigmatism. We tested 29 control subjects and 42 patients. The controls underwent testing in one randomly selected eye. 27 patients had one eye meeting either POAG ($n = 14$) or glaucoma suspect criteria ($n = 13$) and underwent testing in this eye only. 15 patients had POAG in one eye and a glaucoma suspect fellow eye, and underwent testing of both eyes in a randomised order. Because these patients were contributing both eyes to the study, we performed 2 independent analyses of the data: the first using data from both eyes of these patients, then reanalyzing using data from only 1 eye selected at random from each of these patients. We present the data using both eyes of these patients, as all statistically significant results reported in this study were confirmed using both analyses, and did not differ at the $P = 0.005$ level of significance.

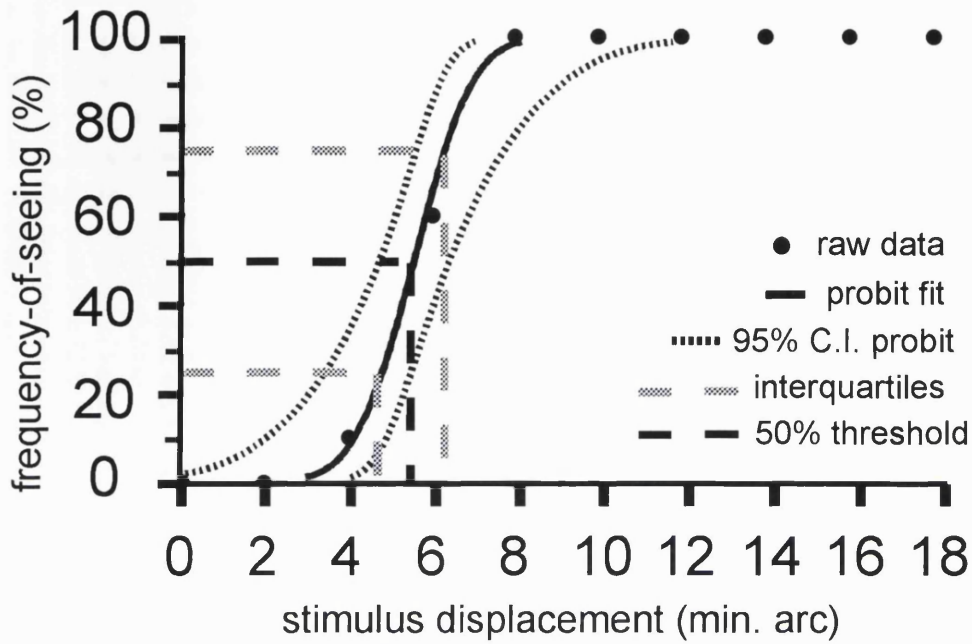
The mean age of the controls was 58.7 ± 10.5 years, with a range 31.3 - 74.9 years. The mean age of patients with glaucoma suspect eyes tested was 60.9 ± 11.5 years (range 30.6 - 78.8 years) and POAG eyes tested was 62.9 ± 10.7 years (range 30.6 - 78.8). Analysis of variance showed no statistically significant differences between the group's ages at the 0.05 level. The MD range of the Humphrey 24-2 fields from the glaucoma eyes was -14.2 to -1.3 dB, (median -4.6 dB), and the glaucoma suspect eyes from -4.2 dB to +1.8 dB (median -0.7 dB). These were significantly lower than the Humphrey 24-2 MDs of the control eyes (range -2.7 to +2.5 dB, median 0.05 dB) at the $P = 0.05$ level.

5.3.2 Testing strategy

We measured motion sensitivity using a line displacement test presented in the superotemporal field to obtain Motion Displacement Thresholds (MDT). The experimental set up was identical to that used in the studies in chapters 4 and 7 (for a detailed description see chapter 7).

5.3.3 Analysis

We generated frequency-of-seeing curves of the subject's responses to the motion stimulus, and the data were imported to SPSS for Windows, (release 6.0, SPSS Inc. Chicago) for further analysis. We performed probit analysis of the data using SPSS and the Motion Displacement Threshold (MDT) was defined as the displacement corresponding to a 50% frequency-of-seeing of the probit fitted curve. We used the interquartile range as a measure of the slope of the frequency-of-seeing curve, as this measure has previously been used by other investigators (Chauhan, et al., 1993b). The interquartile range is the stimulus displacement interval that corresponds to 25% to 75% frequency-of-seeing of the probit fitted curve. Figure 5.1 shows the motion frequency-of-seeing curve from a normal control, with the calculated parameters.



Right HFA 24-2
TOTAL DEVIATION

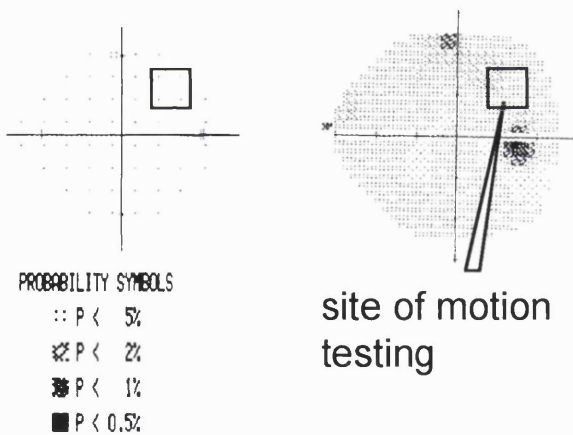
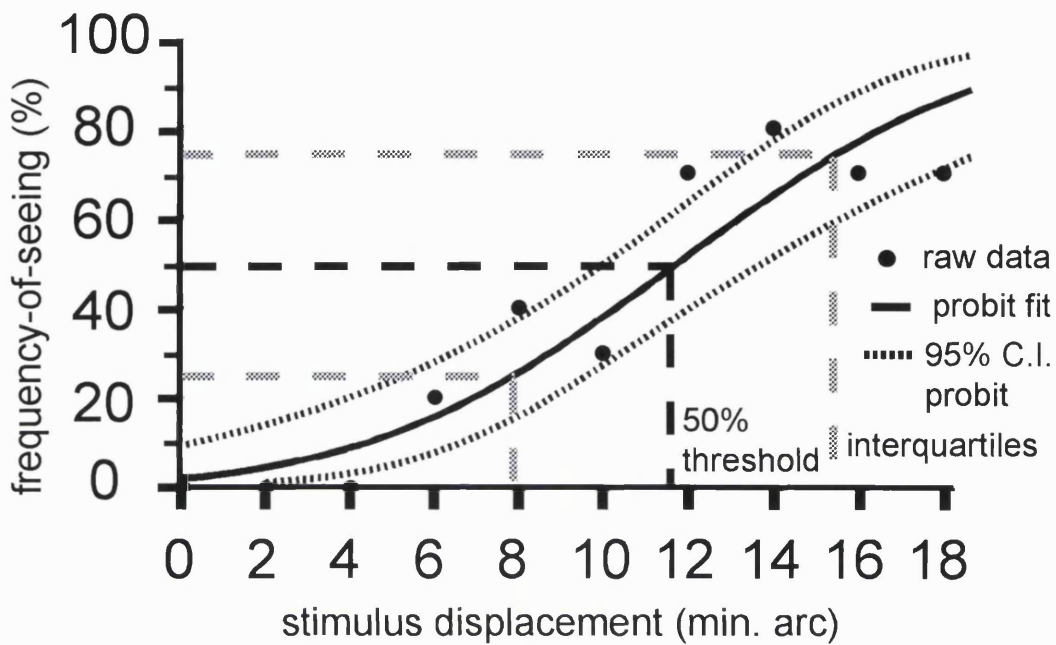
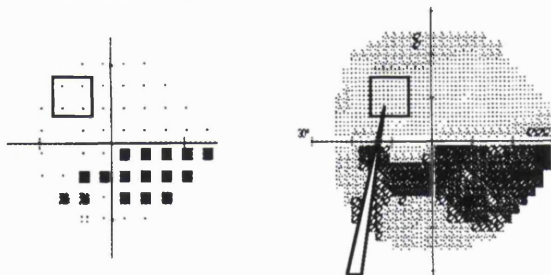


Figure 5.1a Humphrey 24-2 from normal control aged 69 (right), showing site of motion testing (arrow) with 4 closest Humphrey test locations. Above is subject's normal motion frequency-of-seeing curve. Black circles represent raw data points with probit-fitted curve (solid black curve), and 95% C.I. (dashed black curve). Dashed black line indicates 50% seen threshold, with interquartile ranges (dashed gray lines), within mean +2 SD of control group.





Left HFA 24-2
TOTAL DEVIATION



PROBABILITY SYMBOLS

- ∴ P < 5%
- ⊗ P < 2%
- ⊗ P < 1%
- P < 0.5%

site of motion
testing

Figure 5.1b Humphrey 24-2 of a glaucoma patient aged 69 with an inferior arcuate scotoma (right). Arrow indicates site of motion testing on greyscale plot, with 4 closest Humphrey 24-2 test locations (box) showing normal threshold sensitivity, within 95% population limits on Statpac2 output. Above is motion frequency-of-seeing curve of same patient, with elevated threshold (11.6 min. arc) and abnormally shallow slope (elevated interquartile range of 7.6 min. arc). Compare with figure 5.1a.

To characterize the extent to which the slope provides additional information we analysed the data according to a stepwise logistic regression model incorporating both the motion thresholds and the interquartile ranges, and their squared terms. The results of the logistic regression analysis were used to generate a receiver operating characteristic (ROC) curve which was compared to the ROC curve generated using the motion threshold alone. The ROC curve is a plot of sensitivity versus 1 - specificity for each possible cut-off across the measurement range of the variables, and is useful in comparison of 2 or more test parameters (Graham, et al., 1996).

5.4 Results

Table 5.1 shows the summary statistics of the 50% seen motion thresholds and the interquartile ranges of the probit fitted frequency-of-seeing curves for the controls, glaucoma suspect and glaucoma eyes.

Group	Normals (29 eyes)	Glaucoma suspects (28 eyes)	Glaucoma patients (29 eyes)
Motion Threshold (min. arc)	5.9 + 1.7 (2.6 - 8.9)	8.7 + 3.4 (5.0 - 17.6)	12.9 + 5.8 (5.2 - 34.2)
Interquartile range (min. arc)	3.3 + 1.4 (1.0 - 5.9)	5.3 + 2.3 (2.1 - 9.6)	8.4 + 4.7 (4.2 - 25.5)

Table 5.1. Summary statistics for the frequency-of-seeing curves, by group. Values shown are mean \pm 1 SD. Figures in brackets indicate minimum and maximum values.

The MDTs in the glaucoma eyes ($P < 0.0001$) and in the glaucoma suspect eyes ($P < 0.001$) were significantly elevated compared to controls. The interquartile ranges were also significantly elevated in the glaucoma eyes ($P < 0.0001$) and in the glaucoma suspect eyes ($P < 0.005$) compared to the controls.

5.4.1 Discriminating between the glaucoma eyes and normal eyes using threshold and slope abnormalities.

To investigate the separation between the glaucoma eyes and the controls we plotted a ROC curve of the motion threshold compared with the logistic regression model incorporating the interquartile range (see figure 5.2 top).

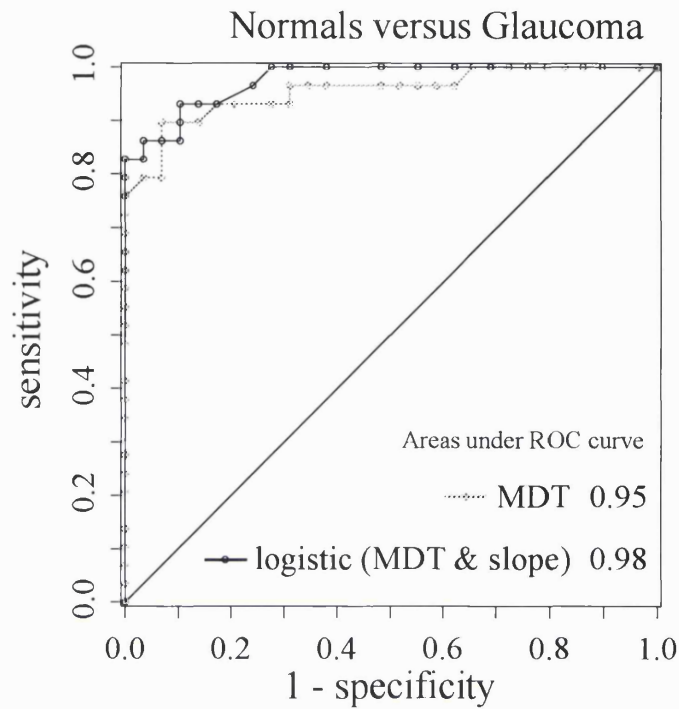
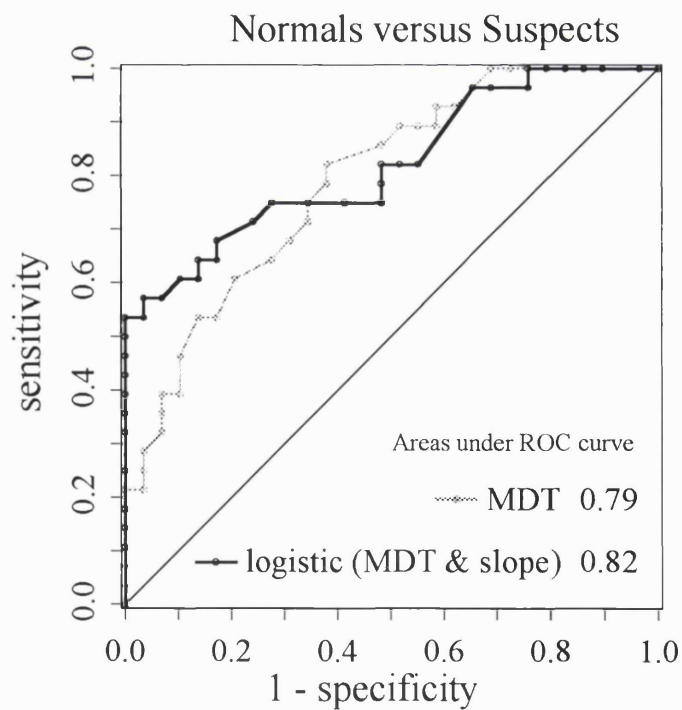


Figure 5.2 Receiver operating characteristic (ROC) curve for the motion thresholds (gray line) and the logistic regression model incorporating the interquartile range (black line) for normal versus glaucoma eyes (top) and normal versus suspect eyes (bottom).



A motion threshold cut-off of 9.0 min. arc identified 22/29 glaucoma eyes as abnormal, with a sensitivity of 76% and a specificity of 100%. The logistic regression model identified 24/29 glaucoma eyes as abnormal with a sensitivity of 83% at 100% specificity. Thus in the glaucoma eyes, only 2 additional eyes were identified as abnormal on the basis of an abnormal interquartile range, whereas they would have been classified as normal on the basis of threshold alone. Of the 24/29 eyes classified as abnormal by the regression model, 17/24 eyes had normal Humphrey 24-2 field thresholds at the motion test site. One such example is shown in figure 5.1b, which shows an abnormal frequency-of-seeing curve with an elevated threshold and interquartile range, indicating an abnormally shallow slope, obtained in a region of field with normal Humphrey 24-2 thresholds.

In the glaucoma suspects the motion threshold alone identified 6/28 suspect eyes as abnormal, with a sensitivity of 21% at 100% specificity. The logistic regression model identified 15/29 glaucoma suspect eyes as abnormal resulting in a sensitivity of 54% with 100% specificity. All 29 suspect eyes had normal Humphrey 24-2 fields according to our enrollment criteria. Thus amongst suspects, abnormal ranges without abnormal thresholds were more common, accounting for 9 of the 15 abnormal results. The difference between the proportion of suspects identified as abnormal using the regression model compared to the threshold alone was statistically significant (proportion test $P < 0.05$). Thus abnormal slopes would seem to indicate early progression of the disease which may not be measurable by the threshold alone. This is shown schematically in figure 5.3 which shows the relationship between the interquartile range and the threshold. The top left-hand quadrant contains the 9 suspect and 2 glaucoma eyes which could be diagnosed as abnormal on the basis of an abnormal interquartile range when consideration of the threshold alone would class them as normals.

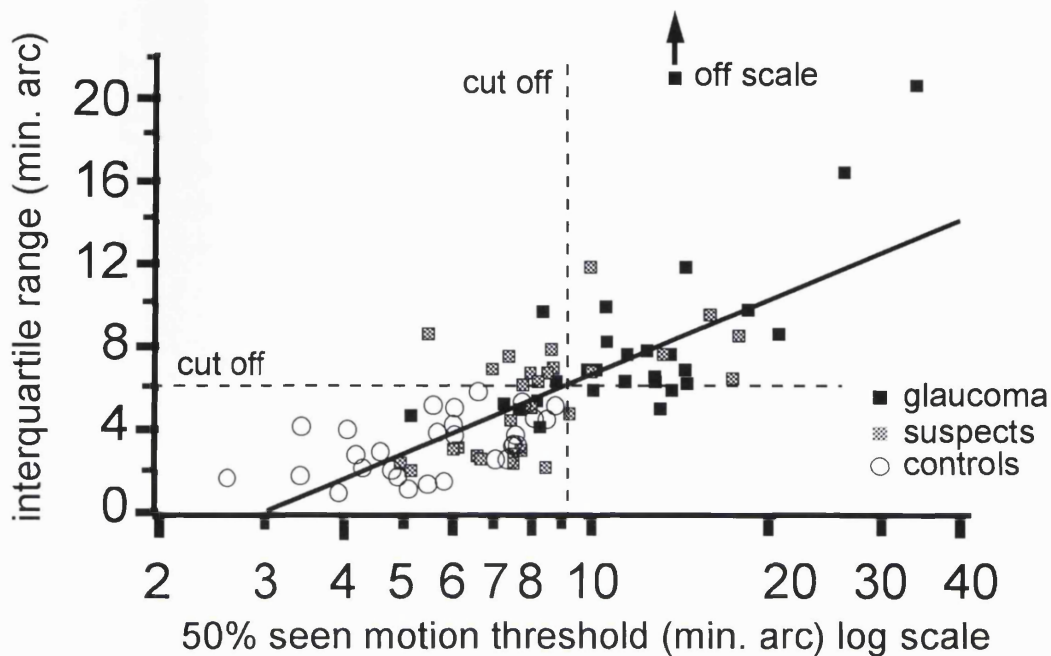


Figure 5.3 Relationship between calculated interquartile range and threshold of motion frequency-of-seeing curves for all subjects. The solid line represents the least-squares linear fit through the data. Dashed lines represent cut-offs below which all of control values for motion threshold (vertical) and interquartile range (horizontal) lie. Off scale refers to a single glaucoma eye with marked shallowing of the frequency of seeing curve with an interquartile range of 25 min. arc., off the y scale.

5.4.2 The relationship between slope and the 50% seen threshold

Figure 5.3 shows the relationship between the slope, as measured by the interquartile range of the motion frequency-of-seeing curve, and the 50% seen threshold. There was a significant correlation between the threshold and the interquartile range for all subjects ($P < 0.0001$, $r^2 = 0.56$, excluding 1 outlier $r^2 = 0.71$). Analysis within groups showed a significant correlation between the threshold and the interquartile range at $P < 0.005$ for the controls ($R^2 = 0.27$), glaucoma suspect eyes ($R^2 = 0.32$) and for the glaucoma patients ($R^2 = 0.41$).

Although the correlation between threshold elevation and shallowing of the slope of the frequency-of-seeing curve was statistically significant, the degree of correlation was low, and we observed considerable variation in the slope of the frequency-of-seeing curve for a given threshold value, both within and between the subject groups. This is illustrated in figure 5.4 which shows the frequency-of-seeing curves of 3 patients with similar motion

thresholds with markedly different interquartile ranges. Although these subjects had essentially the same thresholds (8.4 to 8.6 min. arc) the interquartile ranges increased roughly in proportion to the seriousness of their glaucoma: extending from a normal value of 4.2 min. arc for a suspect eye (figure 5.4 top) to 9.6 min. arc in a glaucoma eye (figure 5.4 bottom).

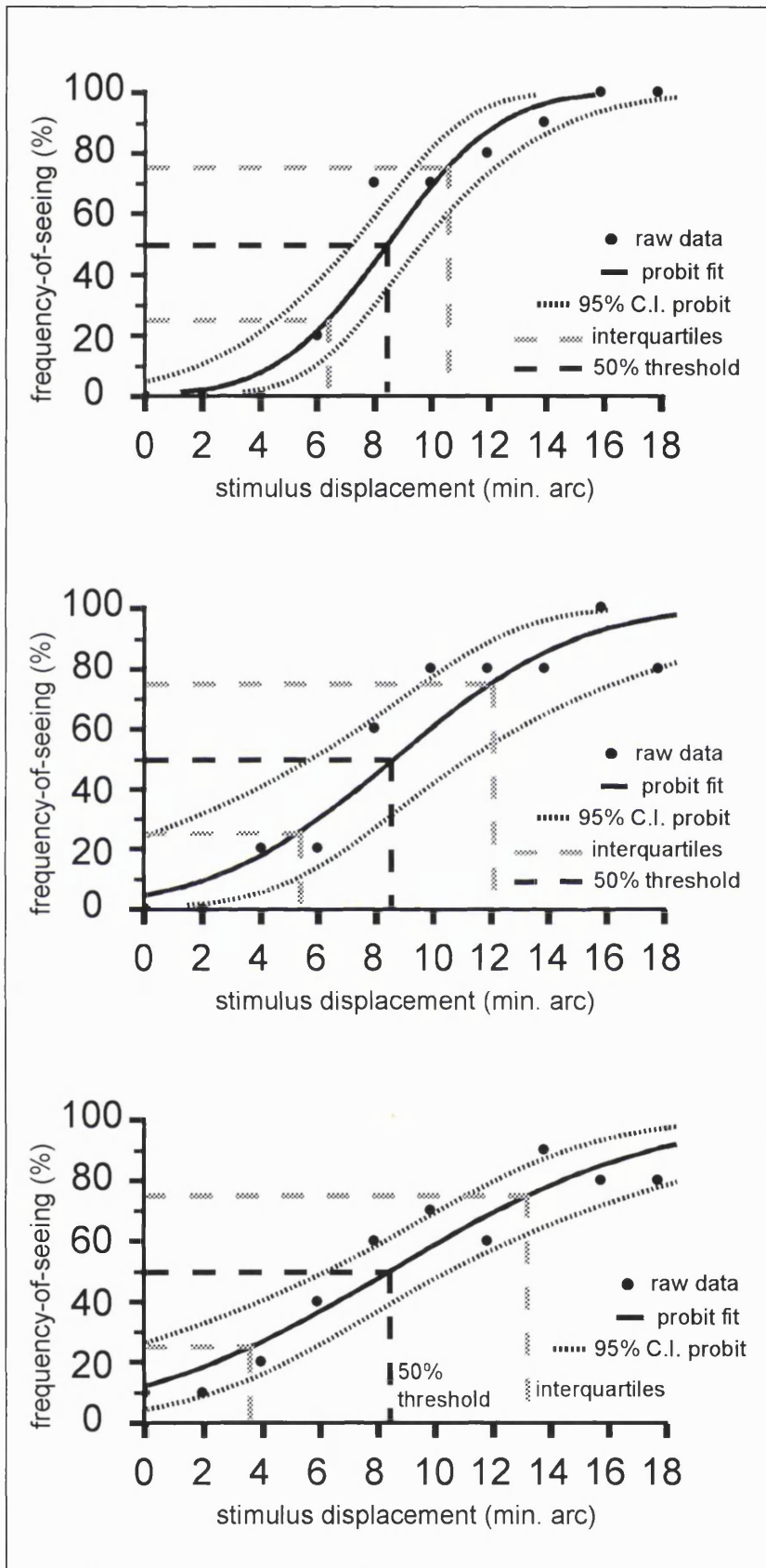


Figure 5.4 Top shows the frequency-of-seeing curve of a glaucoma suspect with a normal 50% seen motion threshold of 8.4 min. arc and a normal slope (interquartile range of 4.2 min. arc).

Figure 5.4 Middle shows the frequency-of-seeing curve from a glaucoma suspect with a similar motion threshold of 8.6 min. arc, with shallowing of the slope, signified by an interquartile range of 6.8 min. arc, which lies outside our normal range.

Figure 5.4 Bottom shows the frequency-of-seeing curve from a glaucoma eye with more extreme shallowing of the slope, with an abnormal interquartile range of 9.6 min. arc, although the motion threshold remains normal at 8.5 min. arc.

We identified 4 eyes that had abnormal motion thresholds and normal slopes. Figure 5.5 illustrates the frequency-of-seeing curve obtained from a glaucoma eye with an abnormal motion threshold (13.2 min. arc) and a normal slope (interquartile range of 5.1 min. arc).

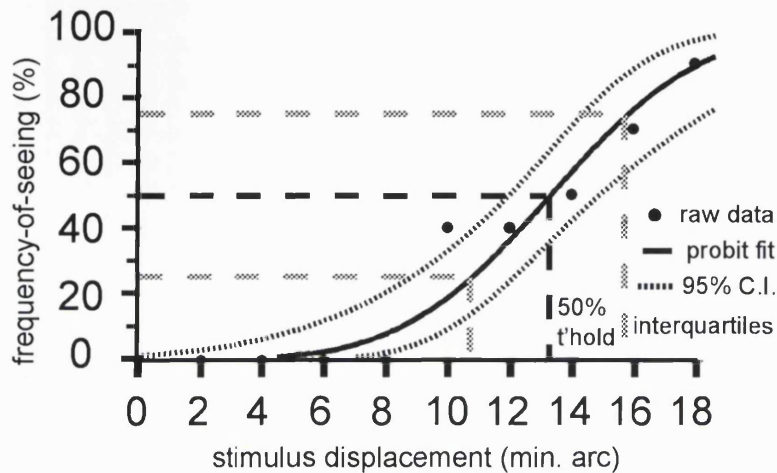


Figure 5.5 Frequency-of-seeing curve of glaucoma eye from patient aged 75 with elevated threshold (13.2 min. arc) and normal slope, indicated by interquartile range of 5.1 min. arc (normal range up to 6 min. arc).

5.5 Discussion

The aim of this study was to examine the characteristics of frequency-of-seeing curves for a motion stimulus in normals, glaucoma suspects and glaucomatous eyes.

We have found a correlation between the slope of the frequency-of-seeing curve and the motion threshold, with increasing threshold elevation associated with shallowing of the slope of the frequency-of-seeing curve, signifying a higher threshold variability. However the degree of association was low, and we identified considerable variation in the slope of the frequency-of-seeing curves for a given motion threshold.

A significant finding was the fact that analysis of the interquartile range in addition to the motion threshold achieved a significantly greater separation of suspects from controls than could be obtained by analyzing the motion threshold alone. This is reflected by the improvement in the sensitivity of the motion test in the suspects at 100% specificity from 21% using threshold alone to 54% using both variables. The improvement in separation was most marked in patients with only moderately elevated thresholds or with thresholds

within the normal range. For example, only 6/28 (21%) of the glaucoma suspects had abnormally elevated motion thresholds outside our normal range. Of the remaining 22 eyes with normal thresholds, analysis of the interquartile range identified an abnormal shallowing of the slope in a further 9 eyes.

In the glaucoma eyes, abnormally elevated thresholds and interquartile ranges coexisted in a high proportion (72%). Because of the greater proportion of threshold abnormalities in this group, analysis of the interquartile range only identified 2 additional eyes as abnormal, compared with the threshold analysis alone.

The finding in this study of a correlation between the motion threshold and slope of the frequency-of-seeing curve is analogous to that for conventional perimetry, which has been reported by a number of workers (Chauhan and House, 1991; Chauhan, et al., 1993b; Henson, et al., 1996; Olsson, et al., 1993; Wall, et al., 1996; Weber and Rau, 1992). The considerable individual differences that we identified in the motion frequency-of-seeing curves of patients with similar motion thresholds are similar to the findings of Chauhan et al. for a luminance stimulus.

Our results indicate that an abnormal shallowing of the slope of the motion frequency-of-seeing curve may represent one of the earliest changes in glaucoma, and may occur before identifiable threshold elevation. This finding suggests that measures of intratest variability may be an important component of future motion tests in glaucoma. Further longitudinal studies are required to investigate whether frequency-of-seeing analysis can improve the sensitivity and specificity of motion testing in predicting conventional field deterioration.

Our findings suggest that the analysis of intratest variability in motion testing can identify important additional differences between glaucoma patients and controls. This may lead to improvements in our understanding of the earliest abnormalities of motion sensitivity in glaucoma.

6. CHAPTER 6

High spatial resolution automated perimetry in glaucoma

6.1 Background

Conventional automated perimetry threshold examinations have a relatively low spatial resolution with 6 degrees separating adjacent test locations in the Humphrey 24-2 or 30-2 programmes. Perimetry performed at higher resolution may obtain a more detailed picture of the field in selected areas of the visual field which may be of particular interest to the clinician.

We have developed a technique to perform High Spatial Resolution Perimetry using a Humphrey perimeter to generate a fine matrix map (FMM) of a specified region of the visual field within an acceptable test time. This technique of fine matrix mapping has been applied to the study of a number of diseases (Chen *et al.*, 1990; Chen *et al.*, 1992; Chuang *et al.*, 1987; Fitzke and Kemp, 1989).

6.2 Purpose

The purpose of this study was to investigate the use of High Spatial Resolution Perimetry in glaucoma. The study investigated the question of whether High Spatial Resolution Perimetry can identify fine scale scotomas beyond the resolution of conventional perimetry. We also investigated the use of image processing techniques to improve the repeatability of the high spatial resolution luminance measurements. These techniques have already been shown to substantially improve the repeatability of conventional perimetry, with no additional cost in test time (Fitzke *et al.*, 1995; Fitzke and Kemp, 1989).

6.3 Methods

6.3.1 Subjects

We prospectively recruited patients with an established diagnosis of POAG, glaucoma suspects, and suitably age matched normal controls. All subjects were phakic and had uncorrected visual acuity of $>6/9$ in at least one eye. All glaucoma patients had documented intraocular pressure >21 mm Hg on at least one occasion before treatment, and evidence of asymmetrical glaucomatous field loss relative to the horizontal meridian on the most recent Humphrey 24-2 or 30-2 field. Glaucoma suspects had documented intraocular pressure >21 mm Hg on at least one occasion, and a normal visual field. A field was defined as normal if there were no clusters of significantly depressed locations in either hemifield on the pattern deviation plot of the 24-2 or 30-2 programmes of the Humphrey Field Analyser. According to previously established criteria (Piltz, et al., 1991), a cluster was defined as being significantly depressed if it contained a minimum of three adjacent depressed test locations on the pattern standard deviation plot, with at least 1 location having a probability of abnormality of $p < 0.01$ and 2 locations of $p < 0.05$, excluding the peripheral ring of the HFA 30-2. Suitably age-matched controls were recruited if they had no significant ocular history, had a normal ocular examination with an IOP less than 21 mm Hg and had normal Humphrey HFA 24-2 fields, according to the above criteria.

6.3.2 Technique of fine matrix mapping (FMM)

To perform fine matrix mapping perimetry the co-ordinates of four interlaced 5 x 5 grids of 25 locations (with a separation between adjacent points of 2 degrees) are entered in the "custom grid" feature of a Humphrey automated perimeter. Each grid is offset relative to the other grids by one degree: either in the x ,y ,or x and y axes. The patient undergoes examination using each of the four grids sequentially, using a target size III on a standard Humphrey bowl illumination of 31.5 apostilbs. Accuracy of fixation is monitored in the same way as conventional perimetry.

The data are converted into IBM format files which are merged using custom software to produce a single matrix with a separation between test locations of 1 degree. This fine matrix map (FMM) of 100 locations subtends a visual angle of 9 degrees by 9 degrees, approximately the area occupied by 4 locations in the 30-2 program. The numerical

matrix is then used to generate a surface or contour plot showing the size and location of luminance sensitivity gradients across the grid. In addition to analysis of the raw data, the FMM thresholds underwent spatial processing using a 3 by 3 Gaussian (normal) filter. This technique has been used to filter conventional Humphrey 30-2 field data and fine matrix maps, and has been described in detail previously (Fitzke, et al., 1995; Fitzke and Kemp, 1989).

6.3.3 Examination protocols

6.3.3.i High Spatial Resolution Perimetry of the blind spot.

We investigated the resolution of our technique by obtaining fine matrix maps of the blind spot of a normal control. Luminance contour plots were imaged with a Confocal Laser Scanning Ophthalmoscope (C.L.S.O.), using Argon 488 nm light, (Zeiss instruments) and superposed using the fovea and the optic disc as fundal landmarks.

6.3.3.ii High Spatial Resolution Perimetry in patients with retinal nerve fibre layer defects.

2 Glaucoma patients with clinical evidence of focal retinal nerve fibre layer defects which did not correspond to a scotoma on conventional perimetry underwent High Spatial Resolution Perimetry. Contour plots of the luminance sensitivity were superposed to C.L.S.O. images of the retinal nerve fibre layer defects.

6.3.3.iii Clinical evaluation of High Spatial Resolution Perimetry

Further evaluation of High Spatial Resolution Perimetry was performed in glaucomatous eyes, glaucoma suspect eyes and normal controls. Each glaucoma patient underwent Humphrey field examination using the 30-2 program. One eye only was chosen for examination. If both eyes satisfied the above inclusion requirements, the eye showing the greatest contrast in defect depth / sizes across the horizontal midline was chosen. The two sites of fine matrix mapping were chosen as mirror image pairs across the horizontal meridian, and were performed at two eccentricities: the supero and inferotemporal site (figure 6.3a), or the superior paracentral (figure 6.5a) and inferior paracentral sites.

Each subject underwent examination first at one site with each of the four constituent 25 location grids performed successively with a short, standardised rest between each. The

patient was then tested at the mirror image retinal location using the same protocol of 4 successive grids of 25 locations. The patient was then allowed a rest of at least 2 hours and then the whole protocol was repeated at the original retinal locations to assess intertest fluctuation and reproducibility. The time required for each constituent grid varied between each patient depending on the number of Humphrey stimuli presented which was related to the defect size and depth. Excluding the brief rest between grids, the test time required on the Humphrey to obtain a FMM in the glaucoma patients was clinically acceptable and ranged from 8 to 26 minutes, with a mean of 20 minutes.

Glaucoma suspects were tested according to the same protocol using the mirror image pair of Fine Matrix Maps (FMMs) in the supero and inferotemporal site. In the absence of conventional field abnormalities, we chose this site as it has been reported to be one of the locations of early visual field defects in glaucoma suspects. We investigated the repeatability of the FMMs in age-matched normal controls, using the same test sites, except that the testing was confined to either the superior or the inferior location of the mirror image pair.

Three-dimensional surface plots of the FMMs for matched locations in the visual field were compared between groups. Quantitative analysis of the raw and Gaussian filtered thresholds was performed, and the repeatability of the FMMs was assessed using the technique described by Bland and Altman (see below).

6.3.4 Statistical analysis

The repeatability of the FMMs was investigated using the technique described by Bland and Altman (Bland and Altman, 1986). This technique has been applied to investigate the repeatability of a number of measurements of ocular components (Rudnicka *et al.*, 1992; Zadnik *et al.*, 1992), and has also been used to assess the repeatability of visual field measurements (Fitzke, *et al.*, 1995; Flanagan *et al.*, 1993). To assess the repeatability of the first and second FMMs, the numeric difference between the first and second threshold sensitivities is calculated for each test location, and plotted versus the mean of the sensitivities for that location. The difference between the first and second threshold can be calculated on a pointwise basis, and the repeatability can be represented on a graphical plot of the spread and distribution of the pointwise differences. The repeatability of the FMMs is defined as the SD of the pointwise differences between the first and second FMM.

6.4 Results

6.4.1 High Spatial Resolution Perimetry of the blind spot.

Figure 6.1 shows the results of performing High Spatial Resolution Perimetry around the blind spot of a normal subject. A contour map of the luminance sensitivity profile has been superimposed onto a fundal Confocal Scanning Laser Ophthalmoscope image (using Argon 488 nm. light, Zeiss instruments) obtained from the same eye. Accurate superposition was achieved by aligning anatomical landmarks such as the centre of the disc and fovea with the corresponding perimetric landmarks such as centre of the blind spot and fixation, which are plotted by the Humphrey Field Analyzer. The resulting aligned contour map reveals well defined steep luminance sensitivity gradients at the edge of the blind spot as well as more subtle linear relative defects corresponding in location and extent to the major retinal vascular trunks exiting the optic disc. The diameters of the retinal arterioles at the disc margin are approximately 100 microns, while that of the retinal veins are about 130 microns (Wessing and Von Noorden, 1969). 100 microns corresponds to a visual angle of approximately 0.3 degrees. This degree of resolution compares well with other reported techniques of High Spatial Resolution Perimetry, which have also identified angioscotoma associated with the major retinal vascular trunks (Safran *et al.*, 1995).

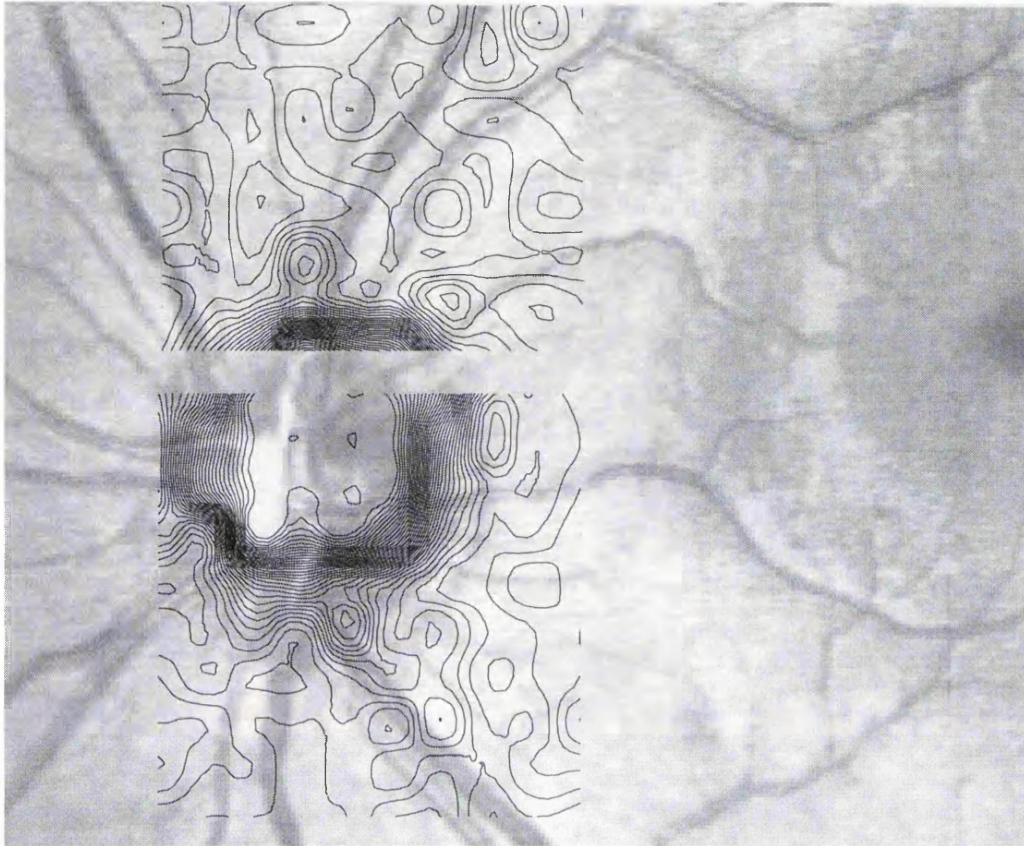
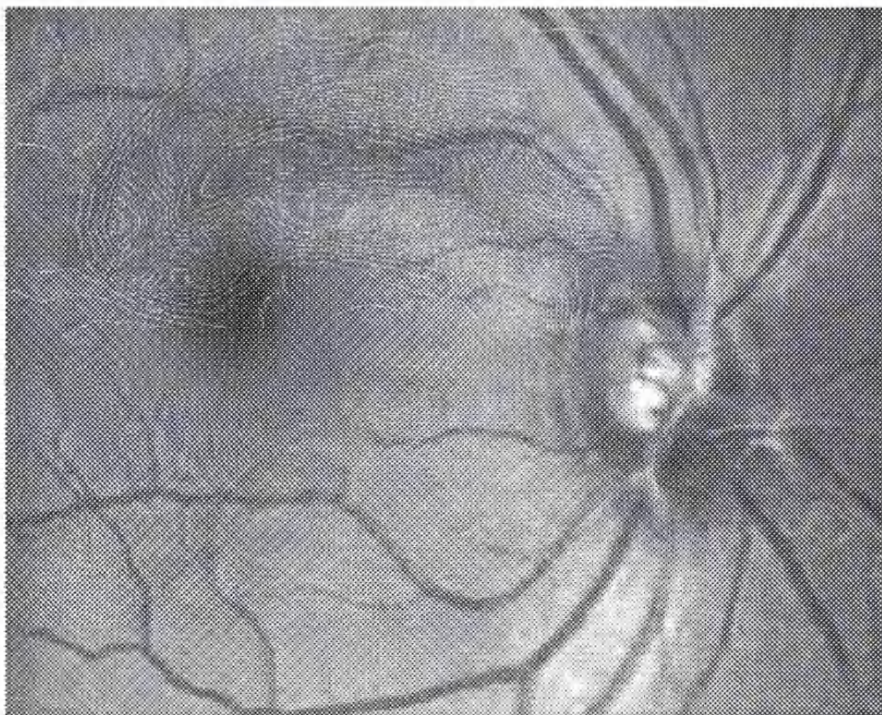
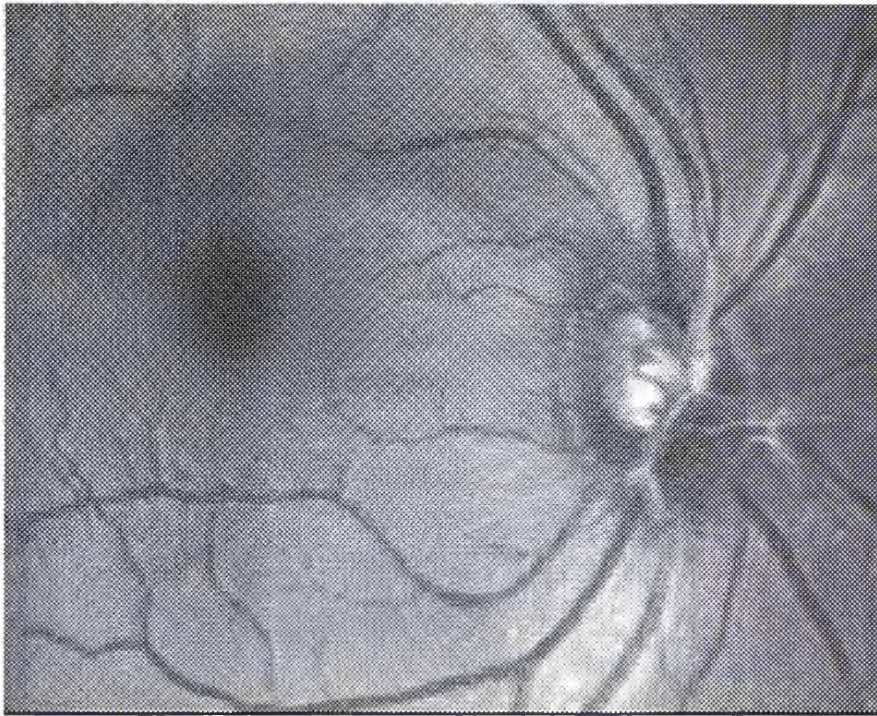


Figure 6.1 Contour plot of luminance sensitivity from fine matrix maps performed over blind spot of a normal control, superposed with a fundal Scanning Laser Ophthalmoscope image (inverted) of the subject. Contour lines represent isoluminant points, in 1 dB increments. Note steep sensitivity gradients at the edge of the blind spot as well as more subtle linear defects corresponding in location and extent to the major retinal vascular trunks exiting the optic disc.

6.4.2 High Spatial Resolution Perimetry in patients with retinal nerve fibre layer defects.

Figures 6.2 illustrates the results of High Spatial Resolution Perimetry performed in a glaucoma patient in an area of the visual field corresponding to a clinically visible focal retinal nerve fibre layer defect. The aligned contour map shows contour lines (figure 6.2a) indicating a region of steep luminance sensitivity loss which corresponds closely with the extent of the retinal nerve fibre layer defect imaged using the Scanning Laser Ophthalmoscope. A three dimensional surface plot of the luminance sensitivity (figure 6.2b) reveals an obvious scotoma which is not apparent on the conventional Humphrey 24-2. The scotoma extends into the nasal field, in a region where the threshold sensitivities of the corresponding Humphrey 24-2 test locations are within the 95% population limits, according to STAPAC2.

Figure 6.2a Top figure is a fundal scanning laser ophthalmoscope image (inverted) obtained from a patient showing a retinal nerve fibre layer defect. Bottom figure shows high spatial resolution luminance contour plots which have been superimposed. The sensitivity loss corresponds closely to the extent of the retinal nerve fibre layer defect.



Right eye, glaucoma suspect.

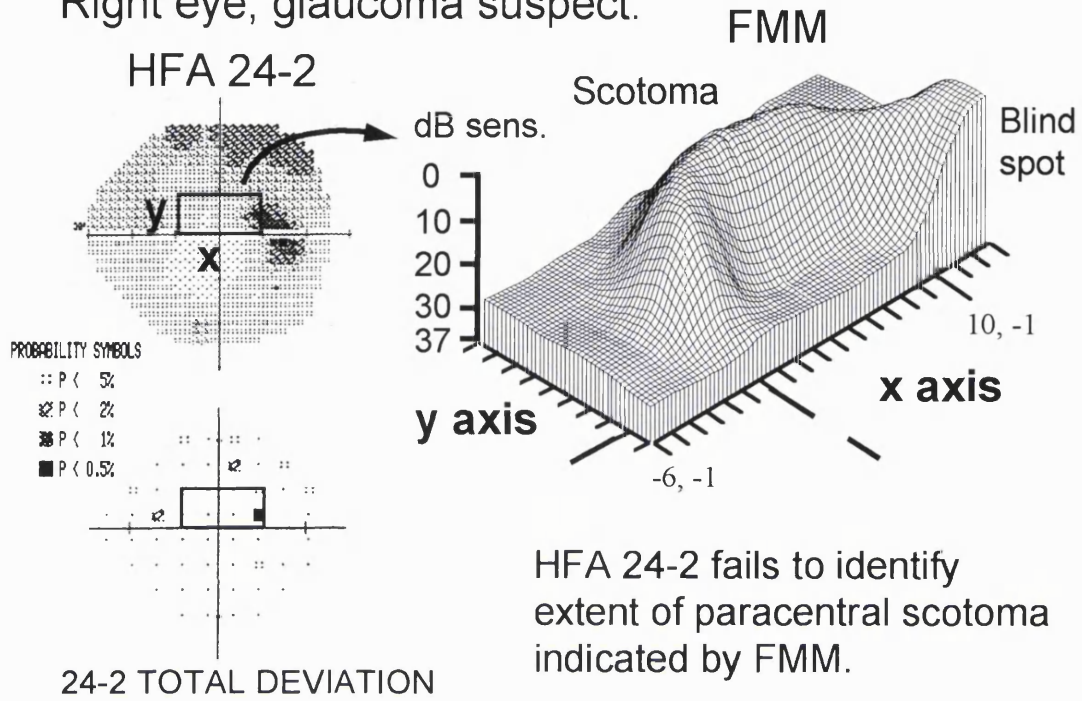


Figure 6.2b shows a Humphrey 30-2 greyscale and statpac2 total deviation plot, and adjacent FMMs, which reveal an obvious superior arcuate extending from the blind spot, not shown by the Humphrey 30-2.

6.4.3 Clinical evaluation of High Spatial Resolution Perimetry

We tested 6 eyes of 6 glaucoma patients (4 eyes in mirror image supero and inferotemporal sites, 2 eyes in mirror image supero and inferoparacentral sites), 4 eyes of 4 glaucoma suspects (3 eyes in mirror image supero and inferotemporal sites, 1 eye in inferotemporal only) and 6 eyes of 6 normal subjects (4 eyes in superotemporal site, 1 eye in inferotemporal site, 1 eye in inferoparacentral site). The mean ages by group were 64 ± 4 years for the glaucoma patients, 58 ± 7 years for the glaucoma suspects, and 65 ± 6 years for the controls. These differences were not statistically significantly different.

Bland Altman plots of the pointwise differences versus the pointwise means between the baseline and the repeat FMM were plotted for each subject at each location tested. The mean of the pointwise differences and the SD of the pointwise differences were calculated to provide summary statistics of repeatability for each individual. The mean of the pointwise differences reflects any systematic difference, (bias) between the baseline and the subsequent FMM as might be expected if there was a considerable fatigue effect or learning effect. The repeatability of the first and second FMM is defined as the SD of the pointwise differences with lower values indicating better repeatability. The mean ± 2 SD indicates the limits of agreement between the first and the second FMM.

Figures 6.3b-e show the Bland Altman plots of the first and second FMMs performed for one glaucoma patient in two mirror image locations (figure 6.3a) of the field. The superotemporal FMM overlaps an area of depressed sensitivity on the Humphrey 30-2, whilst the inferotemporal FMM overlaps an area of normal Humphrey 30-2 threshold sensitivity.

HFA 30-2 GREYSCALE

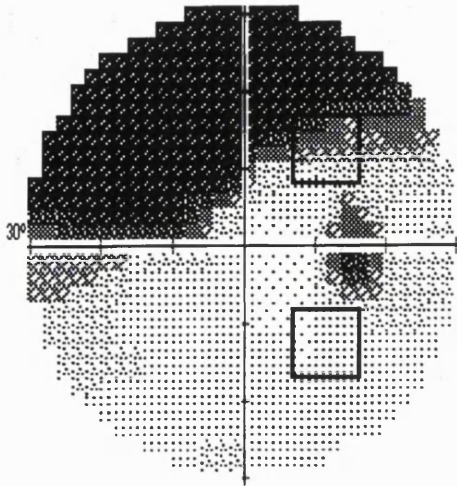
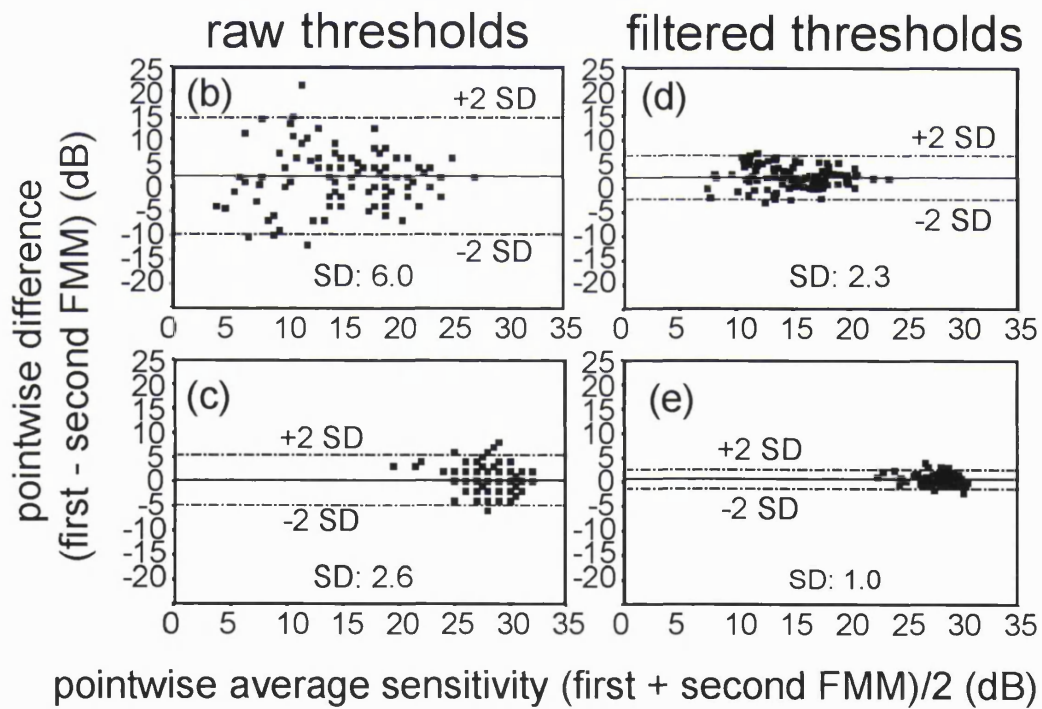


Figure 6.3a Humphrey 30-2 of glaucoma eye. Boxes indicate superior and inferior sites of FMM.



Figures 6.3b & d Pointwise difference versus mean plots for first and second FMM in the superior location, for raw (b) and Gaussian filtered (d) thresholds.

Figures 6.3c & e Corresponding plots for raw (c) and filtered thresholds (e) of the FMMs in the inferior location. Dashed lines indicate pointwise limits of agreement, represented as 2 SD, between the first and second FMMs.

The repeatability between the first and second FMMs is poorest, as indicated by the higher pointwise SD in the location of depressed threshold sensitivity (figure 6.3b), compared to the location of normal threshold sensitivity (figures 6.3c). The effect of Gaussian filtering the FMMs has been to substantially reduce the SDs, (figures 6.3d & e) representing an improved repeatability by a factor of 2 between the baseline and the second FMMs. The mean pointwise difference remains the same for the raw and Gaussian filtered data, and is close to zero in all the plots.

Figure 6.4a shows the repeatability of the first and second FMMs for all the subjects: the SD of the pointwise differences has been plotted against the mean threshold sensitivity of the first and second FMMs for each subject. The SD values are highest for the glaucoma patients, indicating poorer repeatability, compared to the controls. The one outlier was a glaucoma patient who had FMMs performed in a region of absolute sensitivity loss on the Humphrey 30-2. In this patient only 1 test location had a measurable sensitivity and the remaining test locations had no measurable in either baseline or the repeat FMM, with a consequent zero pointwise difference between the majority of points. Figure 6.4a illustrates the negative correlation between the SD and the mean grid sensitivity which was highly significant ($P = 0.0001$, $R^2 = 0.91$). Thus the repeatability was poorest in the FMMs with greater degrees of threshold sensitivity loss.

Figure 6.4b shows a similar correlation between the pointwise SD and the mean threshold sensitivity for the Gaussian filtered thresholds.

Note that the values of the SD have been reduced by a factor of approximately 2. Designated limits of pointwise agreement between the first and the second FMMs can be defined as the mean ± 2 SD, according to Bland Altman (Bland and Altman, 1986). The limits of agreement for all the Gaussian filtered FMM pairs are below 5 dB: thus for each FMM pair, the difference between the first and second (repeat) sensitivity thresholds will be less than 5 dB at 95 out of 100 test locations, which we believe is clinically acceptable.

Calculated values for the means of the pointwise differences between the first and second, representing any overall bias between the first and the second grids were smallest for controls (mean -0.09 dB, range -0.58 dB to 0.50 dB). The means of the pointwise

differences for the glaucoma patients were higher, (mean 0.37 dB, range -6.70 dB to 3.00 dB), although they still remained small: 11 of 12 repeated FMMS had a mean difference of less than 4 dB. In addition there was no systematic departure from the zero in any of the groups, indicating that there is no significant bias between the first and second FMMS which we might have expected if there was a significant learning or fatigue effect.

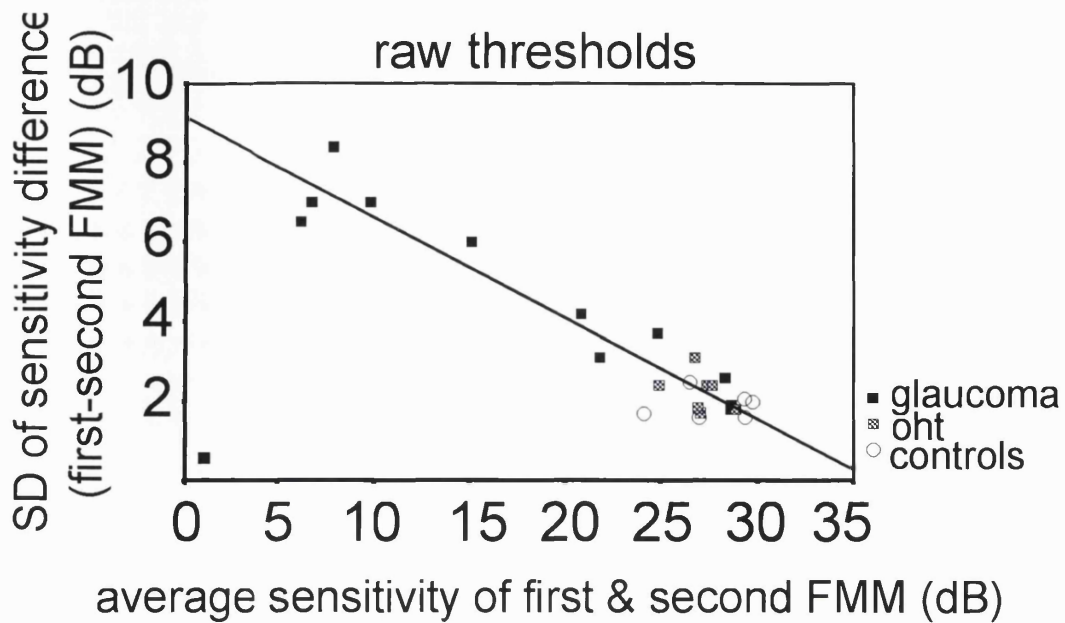
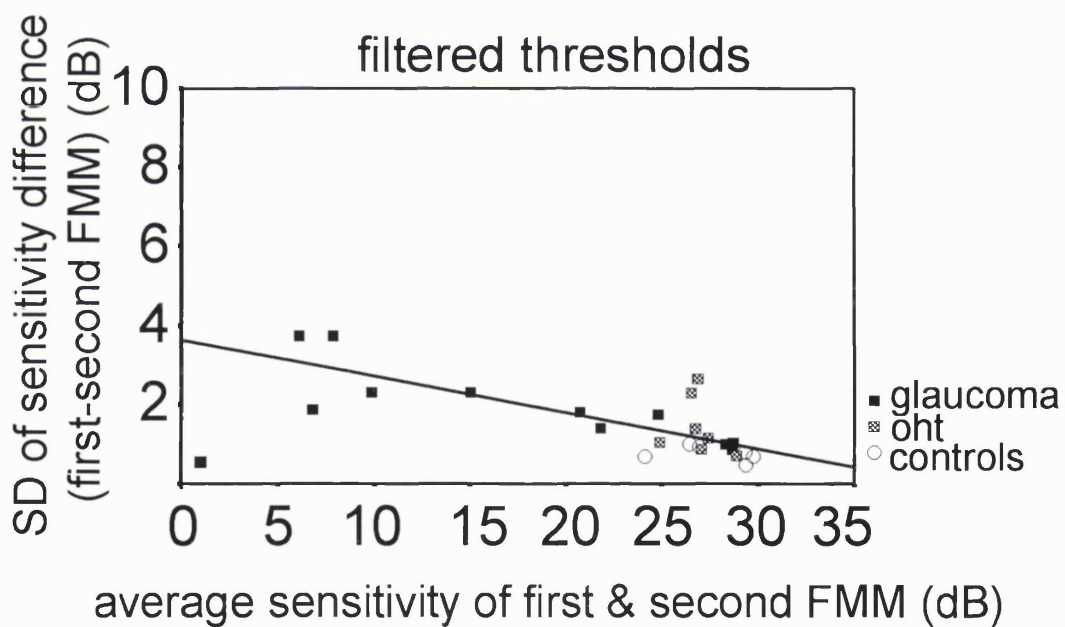


Figure 6.4a SD of pointwise differences of first and second FMM versus mean sensitivity of first and second FMM using raw thresholds

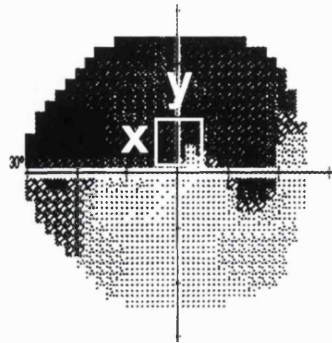


Figures 6.4b Same axis for figure 6.4a, but using Gaussian filtered thresholds. The effect of filtering has been to reduce the magnitude of the SD by a factor of approximately 2, representing a twofold improvement in repeatability. Lines indicates the least squares linear fit of the data, excluding 1 outlier.

FMMs obtained from High Spatial Resolution Perimetry in glaucoma patients at sites already known to be abnormal from the 30-2 examination revealed a complex profile of sensitivity loss which was not revealed by the low spatial resolution of the conventional

Humphrey 30-2 or 24-2 programs. Figure 6.5a shows Humphrey 30-2 greyscale and Statpac2 total deviation plots from a glaucoma patient who underwent High Spatial Resolution Perimetry at the site indicated. Figure 6.5b shows three-dimensional surface plots of the first FMM and the repeat FMM which have undergone filtering. Both surface plots show the complex profile of the scotoma, which reveals a steep sensitivity gradient from severely depressed to normal sensitivity. Much of the detail is reproducible.

HFA 30-2 GREYSCALE



TOTAL DEVIATION

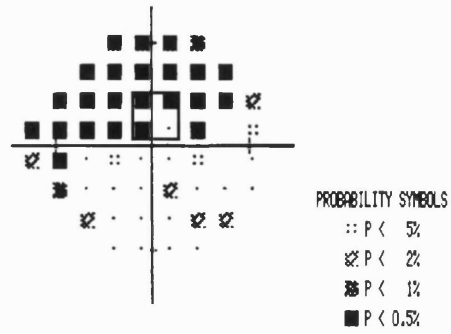


Figure 6.5a Humphrey 30-2 greyscale and Statpac2 total deviation plot from glaucoma eye, with site of FMM indicated by box.

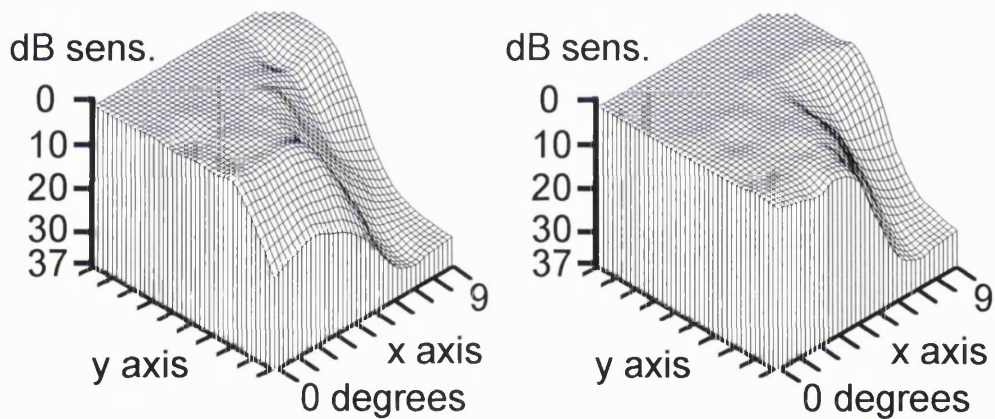


Figure 6.5b Resulting FMMs obtained from same patient at the location indicated on figure 6.5a. Plots of Gaussian filtered sensitivity thresholds of first (left figure) and repeat (right figure) reproducible threshold profiles reveal a steep sensitivity gradient from severely depressed sensitivity, represented as elevated area, to normal sensitivity.

In 2 glaucomatous eyes of 2 patients fine matrix mapping in an area of normal sensitivity on the Humphrey 30-2 revealed an obvious reproducible defect that was not apparent with conventional perimetry. Illustrated by figures 6.6a-d. High Spatial Resolution Perimetry identified a localised reproducible scotoma, represented as an elevated area on the first FMM (figure 6.6b) and second FMM (figure 6.6c). The FMMs were performed in an area of field overlapped by 4 Humphrey 24-2 test locations which have normal threshold sensitivity (figure 6.6a). Figure 6.6d shows a surface plot of a FMM from a normal control for comparison, which shows a uniform luminance profile.

figure a

HFA 30-2 GREYSCALE

TOTAL DEVIATION

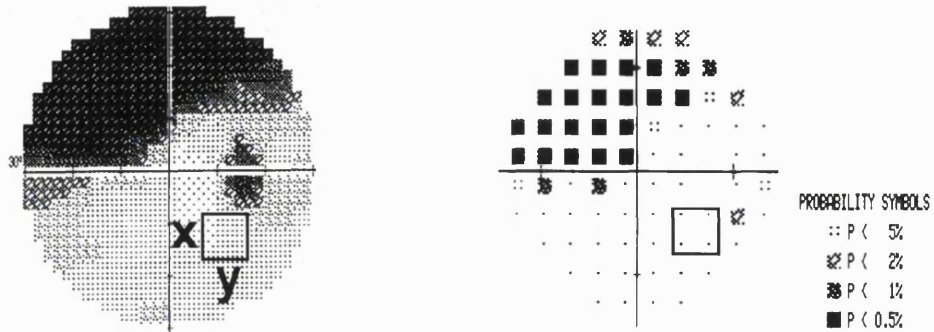
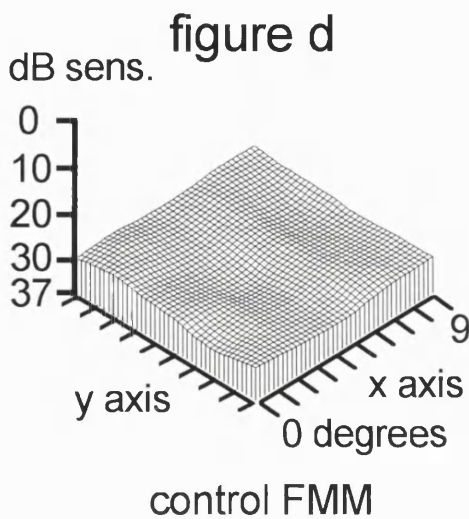
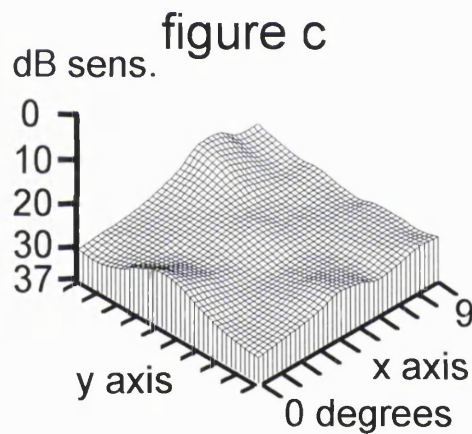
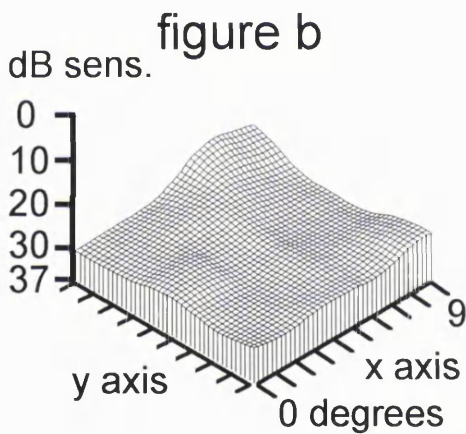


Figure 6.6a Humphrey 30-2 greyscale and Statpac2 total deviation plot from glaucoma eye. Box indicates site of FMM which overlaps 4 Humphrey 30-2 test locations with normal threshold sensitivity.



Figures 6.6b & c Three-dimensional plots of Gaussian filtered luminance sensitivity thresholds of first and second FMMs. Elevated areas indicate repeatable luminance defects, not seen in the FMM of an equivalent area of field from age matched normal controls (figure 6.6d).

6.5 Discussion

A number of investigators have used High Spatial Resolution Perimetry to detect scotomas beyond the resolution of conventional perimetry (Sturmer, 1985; Weber and Dobek, 1986). Airaksinen et al has used High Spatial Resolution Perimetry to identify scotomas corresponding to retinal nerve fibre layer defects in glaucoma suspects who have normal conventional perimetry (Airaksinen and Heijl, 1983). In addition, High Spatial Resolution Perimetry has also been shown to be clinically useful in defining residual small central isles of field in advanced glaucoma, which may be too small for conventional perimetry to map (McNaught *et al.*, 1995; Weber *et al.*, 1989). However, a major disadvantage of some of these studies is that they have been arduous for patients and have required an extremely long test time. The aim of this study was to investigate high resolution perimetry in a group of normal, glaucoma and glaucoma suspect eyes using the technique of fine matrix mapping performed on a Humphrey Automated perimeter. This identified glaucomatous luminance loss which was not revealed by the lower spatial resolution of the conventional Humphrey 30-2 or 24-2 programs. The testing protocol was well tolerated and all subjects performed the test within a test time of 30 minutes, which we believe is clinically acceptable. Previous investigations of High Spatial Resolution Perimetry have demonstrated that one of the earliest perimetric disturbances in glaucoma is an elevated intra test variability in some regions, even though the mean threshold sensitivity at the location may still remain normal (Heijl, 1993; Sturmer, 1985). A number of studies have shown that the inter-test variability of conventional threshold perimetry is higher in glaucoma than normals (Flammer *et al.*, 1984a; Flammer *et al.*, 1984c; Holmin and Krakau, 1979; Werner *et al.*, 1982). In addition the degree of inter-test variability has been found to correlate with the degree of sensitivity loss (Flammer, et al., 1984a). Our results confirm that a similar correlation exists between inter-test variability and sensitivity loss in High Spatial Resolution Perimetry, as has been suggested by other workers (Sturmer, 1985). One advantage of the technique described in this chapter was the improvement in repeatability which was obtained with the use of image processing techniques.

In summary, we have described a technique for performing High Spatial Resolution Perimetry which is clinically practical and can be performed on an unmodified Humphrey Automated Perimeter. We have identified glaucomatous luminance loss which was not

revealed by the lower spatial resolution of the conventional Humphrey 30-2 or 24-2 programs, and have obtained a substantial improvement in the repeatability of the technique by using image processing techniques.

7. CHAPTER 7

Abnormal Motion Displacement Thresholds are associated with Fine Scale Luminance Sensitivity Loss in Glaucoma.

7.1 Background

Histological evidence has shown that a substantial number of retinal ganglion cell axons may be lost in glaucoma before a visual field defect can be detected using conventional methods of full threshold automated perimetry (Quigley, et al., 1982; Quigley, et al., 1989).

This finding has prompted the search for more sensitive tests of early glaucomatous visual damage. A large number of different functional deficits have been identified in early glaucoma using psychophysical tests to isolate a particular aspect of visual function (see chapter 3).

One such test is motion perception (see chapter 3). Previous work at the Institute of Ophthalmology and Moorfields Eye Hospital has used a line displacement test to show that Motion Displacement Thresholds (MDTs) are significantly elevated in glaucoma (Fitzke, et al., 1987; Fitzke, et al., 1989; Ruben *et al.*, 1994).

Other investigators have used random dot kinetograms to test motion perception. Initial investigations used these to simultaneously test large areas of the central visual field, and have reported elevated motion thresholds in glaucoma patients (Bullimore, et al., 1993; Silverman, et al., 1990; Trick, et al., 1995). One criticism of this type of testing is that it may perform poorly in patients with early focal scotomas (Bosworth *et al.*, 1997). Graham and colleagues recently reported that random dot kinetogram testing of central field performed little better than chance in identifying patients with early focal glaucomatous field defects (Graham, et al., 1996). Recently Bosworth and colleagues performed focal random dot kinetogram testing on 14 patients, and were able to show that motion coherence thresholds were significantly poorer in areas of known visual field loss compared to eccentrically matched areas of relative field sparing (Bosworth, et al.,

1997). However they did not comment on whether coherence thresholds in areas of relative field sparing differed from controls. One limitation of random dot kinetograms is the inherently low spatial resolution of the test, which is limited by the size of the smallest area that can be tested. In the test described by Bosworth and colleagues, the size of the test region was 7.4 degrees, which may encompass 4 Humphrey test locations.

An alternative approach is to use line stimuli to measure Motion Displacement Thresholds. The higher spatial resolution of a line stimulus has the advantage of making it possible to evaluate small localized regions of field. Previous research at the Institute of Ophthalmology and Moorfields Eye Hospital has used a line displacement test to demonstrate elevated Motion Displacement Thresholds in glaucoma (Fitzke, et al., 1987; Fitzke, et al., 1989; Ruben, et al., 1994) and has shown that abnormally elevated Motion Displacement Thresholds can occur in areas of normal Humphrey 24-2 visual field.

These findings have been confirmed by other workers using both Line Displacement tests (Johnson, et al., 1995) and Random Dot Kinetograms (Wall and Ketoff, 1995).

The significance of elevated Motion Displacement Thresholds within areas of normal Humphrey field was demonstrated by Baez and colleagues, who showed that elevated motion thresholds could predict the future development of conventional visual field loss at the same locality in initially perimetrically normal fellow eyes of normal tension glaucoma patients (Baez, et al., 1995). Elevated Motion Displacement Thresholds have also been correlated with glaucomatous optic disc changes in ocular hypertensive patients, before scotomata can be detected using conventional visual field assessment (Ruben and Fitzke, 1994).

7.2 Purpose

The finding of abnormal Motion Displacement Thresholds in areas of normal Humphrey field raises the question of whether motion abnormalities coexist with fine scale depressions of Humphrey threshold which may not be identifiable with conventional Humphrey field testing.

The aim of this study is to test the hypothesis that elevated Motion Displacement Thresholds coexist with fine scale depressions of Humphrey threshold, which may predate the appearance of scotomas detected with conventional perimetry.

A number of investigators have used High Spatial Resolution Perimetry to identify fine scale scotomas in apparently normal areas of the field on the Humphrey 24-2, although these results were not examined in the context of other psychophysical abnormalities.(Sturmer, 1985; Tuulonen *et al.*, 1993).

In this study, High Spatial Resolution Perimetry was performed using the technique described in chapter 6.

We investigated a group of patients with unilateral POAG, as this group offers the advantage of allowing us to study both glaucomatous eyes and fellow suspect eyes that are at high risk of developing glaucoma in the future (Gliklich *et al.*, 1989; Hitchings and Anderton, 1983; Zeyen and Caprioli, 1993). The selection of this well defined group of patients for our study facilitates the assessment of the significance of any psychophysical abnormalities found in our suspect group.

7.3 Methods

7.3.1 Subjects

18 POAG patients and 18 normal controls were prospectively recruited for this study.

Patients were eligible if they had an established diagnosis of POAG in one eye, with at least 2 Humphrey 24-2 fields with a localized glaucomatous visual field defect, and a normal Humphrey HFA 24-2 field in the fellow eye. To define a scotoma we used the pattern deviation plot on the Humphrey 24-2, according to a cluster definition used in a number of previous studies (Graham, et al., 1996; Wall and Ketoff, 1995). A scotoma required a minimum cluster of three adjacent points depressed on the pattern deviation plot at the $P < 0.02$ level (or at least 5 dB), with one of the points depressed at the $P < 0.01$ level (or at least 10 dB); or two adjacent points depressed $P < 0.01$ level (or at least 10 dB). In addition, the cluster of abnormal points could not cross the horizontal meridian.

All fields had to meet standard reliability criteria of $< 20\%$ fixation losses, $< 33\%$ false negatives, $< 33\%$ false positives. All patients had documented evidence of an intra-ocular pressure > 21 mm Hg. on at least one occasion in the glaucoma eye with glaucomatous optic disc cupping characterized by a vertical cup/disc ratio ≥ 0.6 , or cup disc asymmetry between the two eyes of greater than 0.2.

15/18 of the glaucomatous eyes, and 10/18 of the glaucoma suspect eyes were being treated with topical antihypertensives. Patients currently using miotics were excluded, as were patients with significant ocular pathology other than glaucoma or evidence of secondary glaucoma.

Suitably age-matched controls were recruited if they had no significant ocular history, had a normal ocular examination with an IOP less than 21 mm Hg and had normal Humphrey HFA 24-2 fields, with no identifiable clusters of depressed points according to the above definition.

The mean Humphrey 24-2 MD for the glaucoma eyes was -5.8 ± 2.5 dB, range -11.1 to -3.0 dB, which was significantly different ($P < 0.0001$) from the glaucoma suspect eyes (mean MD -1.7 ± 1.7 dB, range -4.2 to +1.3 dB) and the controls (mean MD -0.5 ± 1.3 dB, range -2.7 to +2.5 dB).

The mean age of the 18 patients was 59.7 ± 12.2 years, with a range 30.6 - 78.8 years. The mean age of the 18 controls was 57.8 ± 11.5 years, with a range of 31.3 - 74.9 years. This difference was not statistically significant ($P = 0.63$).

All patients and controls had a corrected visual acuity in both eyes of $\geq 6/9$ achieved with less than ± 4 dioptres spherical equivalent and less than 2 dioptres of astigmatism.

7.3.2 Motion Displacement Testing

We measured motion sensitivity using a line displacement test presented in the superotemporal field to obtain Motion Displacement Thresholds (MDT). This site was chosen as previous results have identified significantly elevated Motion Displacement Thresholds at this location in glaucoma patients, with good separation between patients and controls (Fitzke, et al., 1987; Fitzke, et al., 1989). The MDT test was performed using a computer generated line stimulus, 2 degree by 2 min. arc in size, presented on a monochrome monitor (Phillips green monochrome P31 monitor, pixelation 480 x 640, frame rate 50 Hz). The line stimulus was presented in the superotemporal field at 15 degrees eccentricity on the 30 degree meridian. The luminance of the background was set to 7 cd/m^2 and the stimulus was 27 cd/m^2 , thereby obtaining a stimulus contrast of 59% relative to background. The background was viewed at a distance of 1.24 m, and subtended 8 by 10 degrees.

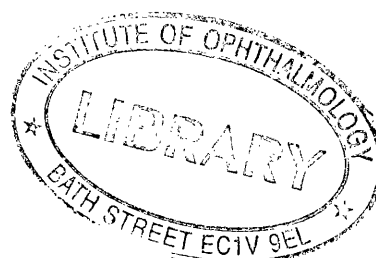
The subject viewed a fixation target and was instructed to press a response button when movement was seen. A warning tone was sounded which was followed by 1.5 seconds

during which the stimulus was stationary. During the following 2 seconds, the stimulus (if it were to move), would undergo instantaneous oscillatory displacements at 2.5 Hz. beginning at a random time after the start of this interval. If the subject pressed the response button before stimulus movement had begun, then this was counted as a false positive response.

After a suitable instruction period, subjects underwent a test which consisted of 10 presentations each of 10 different displacements in 2 minute arc intervals from 0-18 minutes of arc presented in a random order. The test includes 10 presentations of a 0 min. arc displacement (stationary target catch trials) and if the subject pressed the button to 0 min. arc displacement then this was recorded as a false positive response.

The experimenter observed the subject for the duration of the test to ensure reliable fixation throughout the test. Frequency-of-seeing curves were generated, and the data were fit by probit analysis. The Motion Displacement Threshold (MDT) was taken as the displacement corresponding to a 50% frequency-of-seeing of the fitted curve.

Figure 7.0a shows a subject performing the MDT test, and a close up picture of the stimulus presented on the monitor is shown in figure 7.0b.



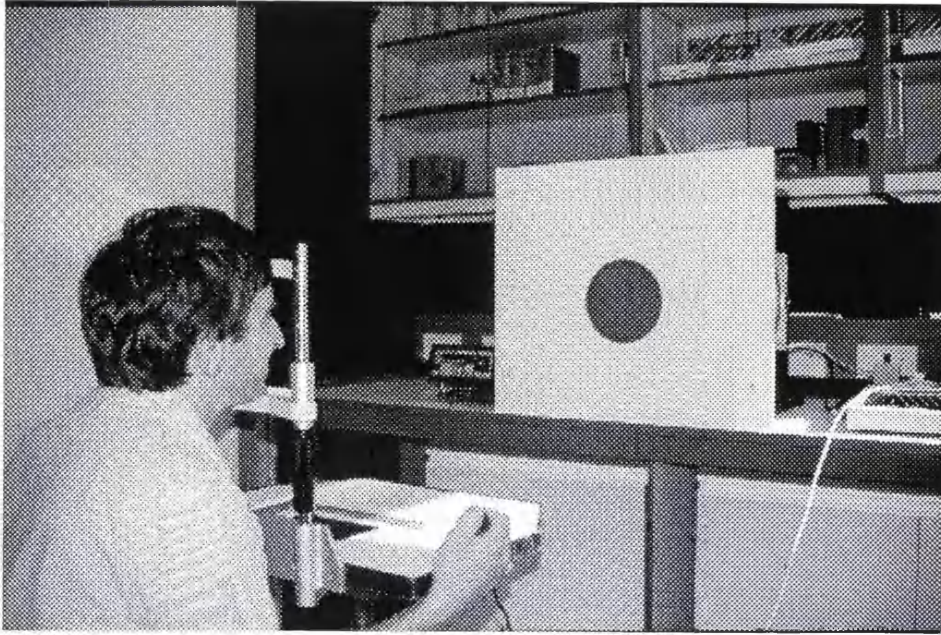


Figure 7.0a Picture of a subject performing a MDT test.

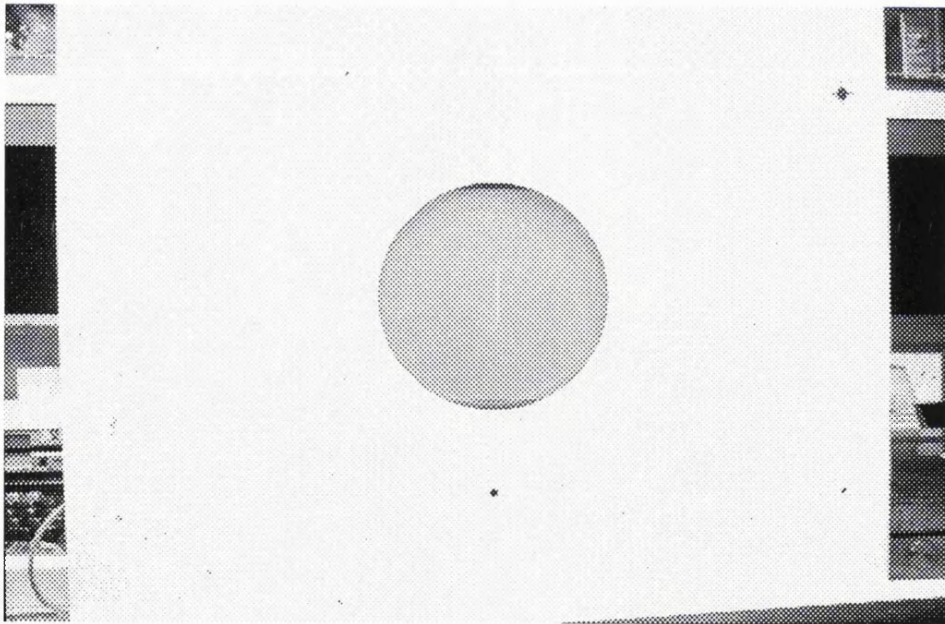


Figure 7.0b Close up picture of the monitor showing the line stimulus used for the MDT test.

7.3.3 High Spatial Resolution Perimetry

High Spatial Resolution Perimetry (HSRP) was performed in the same region of the superotemporal field by measuring the Humphrey visual field thresholds across a 10 by 10 matrix of 100 Humphrey test locations separated by 1 degree. The site of motion displacement testing falls within this area. The technique to perform High Spatial Resolution Perimetry has been extensively described in chapter 6. Briefly 4 “custom grid” programs of the Humphrey are applied using a standard Humphrey to define four custom test programs, each consisting of 5 by 5 locations separated by 2 degrees, with the coordinates of each custom test program offset to the other by one degree in the x, y, or x and y axis. The 4 custom test programs were applied in succession in a randomised order using target size III on a standard Humphrey bowl illumination of 31.5 apostilbs. Custom software was used to merge the custom test programs to generate a single fine matrix map of the thresholds of 100 test locations separated by 1 degree covering an area of 9 by 9 degrees and extending from Humphrey coordinates 7, 7 to 16,16 (for a right eye).

The High Spatial Resolution Perimetry was performed without near correction, as the refraction at this eccentricity is difficult to ascertain and near correction could induce prismatic and edge effects which would be difficult to standardize during the test procedure. However, the distribution of refractive errors was closely comparable between the groups of eyes tested: the median distance refraction (spherical equivalent) of the control eyes was 0 dioptres, range: -1.75 to +2.13 D, the median for glaucoma suspect eyes was 0 D, range: -2.00 to +2.00 D, and for glaucoma eyes 0 D, range: -2.13 to +2.00 D.

We analyzed each subject’s fine matrix map by calculating the mean threshold sensitivity of the 100 test locations. We derived an additional measure to describe the uniformity of thresholds within each matrix map. This uniformity index (UI) was calculated as the standard deviation (SD) of the threshold values.

In addition, spatial image processing of the HSRP thresholds using a Gaussian filter was performed and three-dimensional surface plots were generated for display purposes.

Patients underwent Motion Displacement Threshold testing and High Spatial Resolution Perimetry in both eyes. The controls underwent Motion Displacement Threshold testing and High Spatial Resolution in one randomly chosen eye. Since learning and fatigue may

be influenced by the order of the eye tested, the glaucoma and glaucoma suspect eye were tested in a randomised order to avoid introducing any consistent order effects.

7.3.4 Analysis

The level of statistical significance was set at $P < 0.05$. Because each patient underwent testing in both eyes in this study, we performed 2 independent analyses of the data: the first using data from both eyes of the patients, then reanalyzing using data from only 1 eye selected at random from each patient. We present the data using both eyes of these patients, as all statistically significant results reported in this study were confirmed using both analyses, and did not differ at the $P = 0.05$ level of significance.

7.4 Results

7.4.1 Motion Displacement Thresholds (MDTs)

We were able to record Motion Displacement Thresholds in all 18 control eyes and 18 glaucoma suspect eyes. We obtained motion measurements in 15/18 glaucoma eyes, the remaining 3 eyes of 3 patients had such grossly impaired motion perception that the patients did not perceive motion in any of the stimuli presented.

Table 7.1 shows the mean and SD of the MDTs by group. There was a statistically significant elevation of the MDTs of the glaucoma eyes compared to the controls ($P < 0.0001$), and glaucoma suspect fellow eyes ($P < 0.0034$).

There was a moderate elevation of the MDTs of the suspect eyes as a group compared to the controls, which was significant ($P = 0.046$).

At the location tested, 11/15 (73%) of the glaucoma eyes had abnormally elevated MDTs above mean $+1.96$ SD of the controls ($= 9.2$ min. arc). Only 5/15 (33%) of these eyes had a scotoma cluster on the Humphrey 24-2 field involving the test locations closest to the MDT site.

For the glaucoma suspect eyes, 4/18 (22%) had abnormally elevated MDTs above mean $+1.96$ SD of the controls. By definition, all these eyes had normal Humphrey fields with no glaucomatous clusters on the pattern deviation plots.

There were no controls with MDT thresholds above the mean $+1.96$ SD of the control group.

Group	Mean MDT (min. arc)	SD	Minimum	Maximum
Glaucoma	15.3	12.9	4.2	57.6
Suspects	8.5	3.9	4.6	18.4
Controls	6.1	1.6	2.3	8.2

Table 7.1. Summary statistics for the Motion Displacement Threshold Thresholds (MDTs) by group.

7.4.2 High Spatial Resolution Perimetry Luminance thresholds

Mean sensitivities for each fine matrix map were calculated (table 7.2). This mean sensitivity was significantly lower in the glaucoma patients compared to both the controls and the suspects at the $P < 0.05$ level (Post-Hoc Student-Newman-Keuls tests).

The control group mean was found to be 27.9 dB. We defined abnormal as 1.96 SD below this (23.5 dB). Using this cut-off, 13/18 of glaucoma patients had mean matrix thresholds below this level.

Group	matrix map mean threshold (dB)	matrix map uniformity index (dB)
Controls	Mean 27.9, SD 2.2 (r 22.8 - 30.5)	Mean 1.8, SD 0.33 (r 1.3 - 2.5)
Suspects	Mean 26.6, SD 2.5 (r 23.2 - 31.9)	Mean 2.0, SD 0.42 (r 1.3 - 2.8)
Glaucoma	Mean 21.6, SD 3.4 (r 15.2 - 27.1)	Mean 4.1, SD 2.25 (r 1.4 - 9.5)

Table 7.2 Summary statistics of High Resolution Perimetry thresholds by group.

We derived a “uniformity index” (UI) to assess the degree of uniformity of the matrix thresholds, which was calculated as the SD of the matrix thresholds. In normals, the threshold plots were flat, and as a consequence the UIs were low. Areas of scotoma would result in hills and valleys on the threshold plot, and would give rise to a high UI. The UIs of the glaucoma group were significantly higher than those of controls and suspects at the $P < 0.05$ level, indicating greater spatial variability in the High Spatial Resolution thresholds in the glaucoma patients. The control values for the UI ranged from 1.3 - 2.5 dB, mean 1.8 dB, SD 0.33 dB. We defined the UI as abnormal if it exceeded the control mean + 1.96 SD (= 2.4 dB). 12 of the 13 eyes previously identified as having abnormally low mean matrix threshold had an abnormal UI index. We also

identified 1 additional glaucoma eye with an abnormal UI in the presence of a normal mean threshold.

7.4.3 Comparison between abnormal Motion Displacement Thresholds and abnormal High Spatial Resolution Perimetry thresholds.

8 glaucoma eyes had scotomas on the Humphrey 24-2 field involving the test locations closest to the MDT site. All were abnormal with High Spatial Resolution Perimetry.

7/8 eyes had abnormally elevated MDTs.

The remaining 10 glaucoma eyes had no scotomas on the Humphrey 24-2 field which involved any of the test locations closest to the MDT site. (table 7.3). 6/10 had abnormal High Spatial Resolution Perimetry, and of these 4 had abnormally elevated MDTs. An example is shown in figure 7.1, which shows an abnormal HSRP matrix map (abnormally depressed mean sensitivity and an abnormally high uniformity index). This eye has an abnormally elevated Motion Displacement Threshold at the location tested.

2 glaucoma eyes had abnormal High Spatial Resolution Perimetry, with normal MDTs (an example is shown in figure 7.2).

4/10 had normal High Spatial Resolution Perimetry, and of these, 3 had abnormally elevated MDTs. An example is shown in figure 7.3, which shows a normal HSRP matrix map (normal mean sensitivity and a normal uniformity index) with a coexisting elevated MDT. For comparison, figure 7.4 shows a normal HSRP matrix map and normal MDT obtained from a control eye.

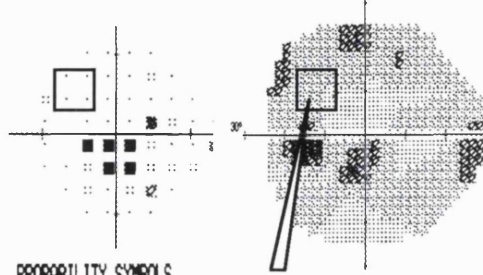
1 glaucoma eye had normal High Spatial Resolution Perimetry and normal Motion Displacement Thresholds at the site tested.

	Normal HSRP (eyes)	Abnormal HSRP (eyes)
Normal MDT (eyes)	1	2
Abnormal MDT (eyes)	3	4

Table 7.3. Number of eyes with respective MDT and HSRP abnormalities, out of 10 glaucoma eyes which did not show scotomas involving any of the test locations closest to the MDT site on the Humphrey 24-2.

Left HFA 24-2

TOTAL DEVIATION



PROBABILITY SYMBOLS

- P < 5%
- ◐ P < 2%
- ◑ P < 1%
- P < 0.5%

site of motion testing

HSRP matrix

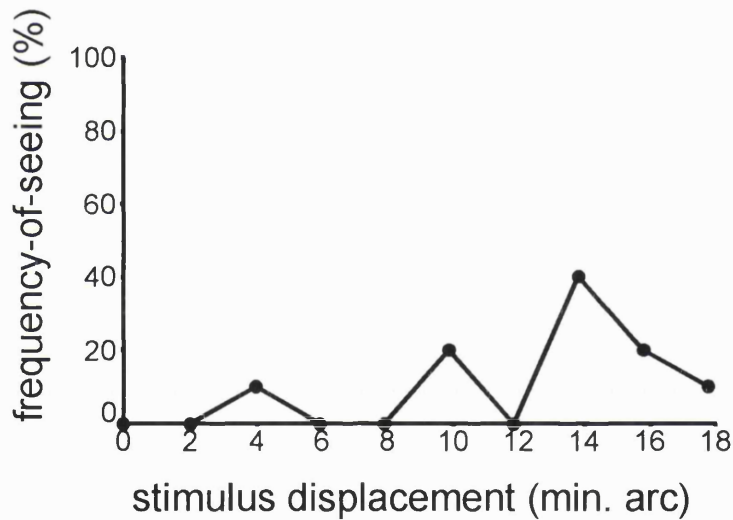
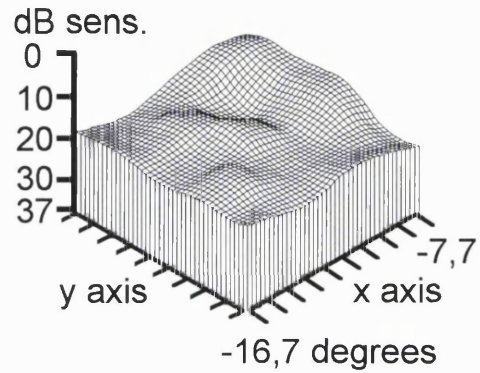
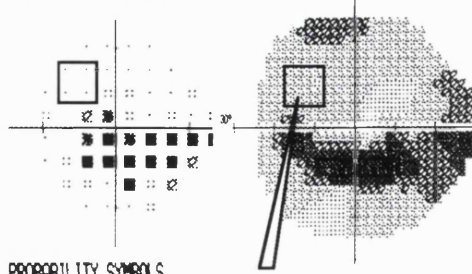


Figure 7.1 Humphrey 24-2 from a glaucoma subject showing inferior arcuate scotoma. Arrow indicates site of motion testing within area of normal Humphrey 24-2 field, overlapped by site of High Spatial Resolution Perimetry (box). Adjacent HSRP matrix map is abnormal: elevations represent area of depressed thresholds. Motion frequency-of-seeing curve (bottom) shows grossly abnormal motion response.

Left HFA 24-2

TOTAL DEVIATION



PROBABILITY SYMBOLS

- ∴ P < 5%
- ⊗ P < 2%
- ⊗ P < 1%
- P < 0.5%

site of motion testing

HSRP matrix

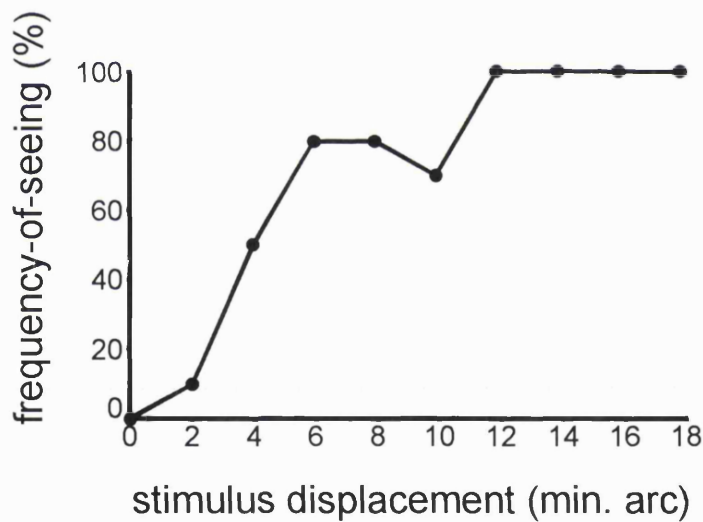
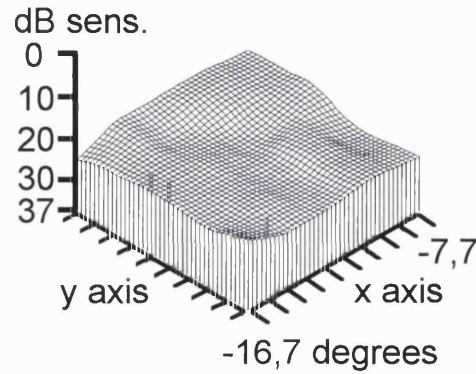
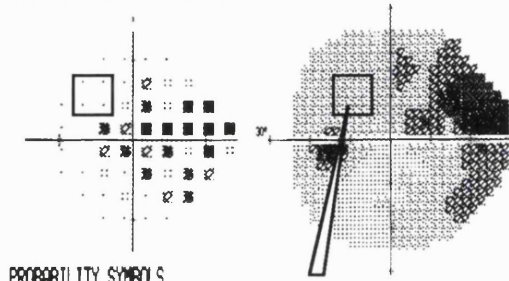


Figure 7.2 Humphrey 24-2 from a glaucoma subject showing inferior arcuate scotoma. Arrow indicates site of motion testing within area of normal Humphrey 24-2 field, overlapped by site of High Spatial Resolution Perimetry (box). Adjacent HSRP shows abnormal matrix map. Subtle elevations represent areas of abnormally depressed thresholds. Motion frequency-of-seeing curve (bottom) shows dip at 10 min. arc. The 50% seen threshold is 4.2 min. arc, within the control range.

Left HFA 24-2

TOTAL DEVIATION

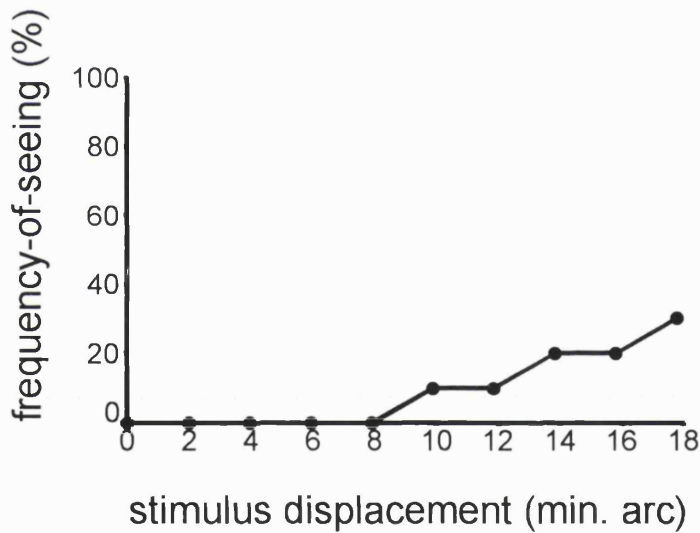
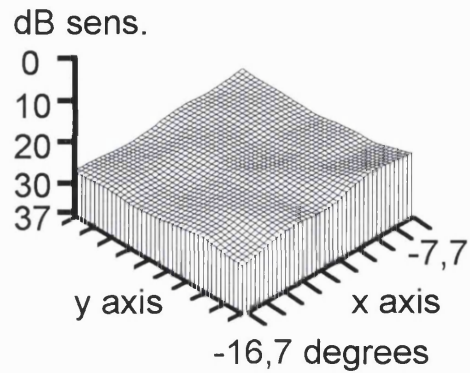


PROBABILITY SYMBOLS

- ∴ P < 5%
- ⊗ P < 2%
- ⊗ P < 1%
- P < 0.5%

site of motion testing

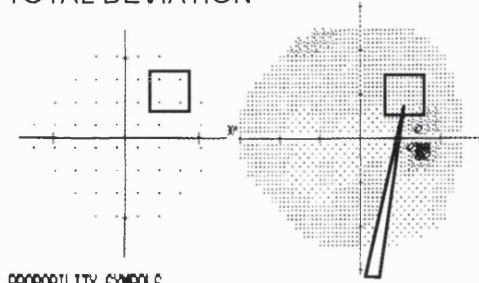
HSRP matrix



Figures 7.3 Humphrey 24-2 from a glaucoma subject showing superior arcuate scotoma. Arrow indicates site of motion testing within area of normal Humphrey 24-2 field, overlapped by site of High Spatial Resolution Perimetry (box). Adjacent HSRP matrix map is normal, with normal mean threshold sensitivities, and uniform threshold profile (normal uniformity index). Motion frequency-of-seeing curve (bottom) shows grossly abnormal motion response.

Left HFA 24-2

TOTAL DEVIATION



PROBABILITY SYMBOLS

- ∴ P < 5%
- ⊗ P < 2%
- ⊗ P < 1%
- P < 0.5%

site of motion testing

HSRP matrix

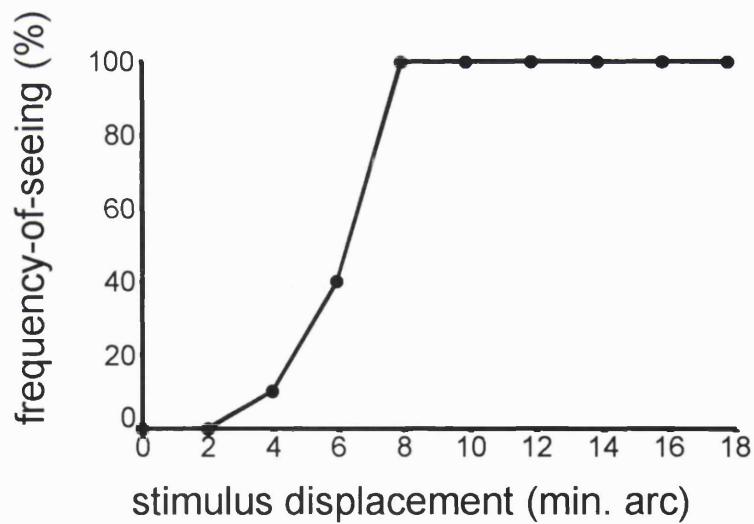
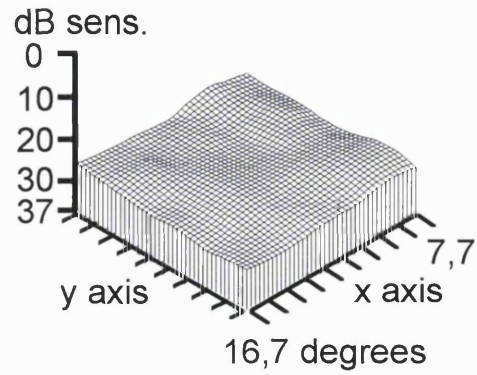


Figure 7.4 Humphrey 24-2 from a normal control. Arrow indicates site of motion testing within area of normal Humphrey 24-2 field, overlapped by site of High Spatial Resolution Perimetry (box). Adjacent HSRP matrix map is normal with uniform luminance profile (mean threshold sensitivity and uniformity index within control range). Normal motion frequency-of-seeing curve (below) with 50% seen threshold within control range.

All 18 glaucoma suspect eyes had normal Humphrey 24-2 fields with no glaucomatous clusters according to our criteria. 3/18 had an abnormal High Spatial Resolution Perimetry, with normal Motion Displacement Thresholds. The remaining 15 suspect eyes had normal High Spatial Resolution Perimetry. However, 4 of these eyes had elevated MDTs.

For the controls, 1/18 had abnormally depressed HSRP mean threshold sensitivity of 22.8 dB, below our cut-off of 23.5, and 2.3 SD below the control group mean. The subject's motion tests and Humphrey 24-2 were both normal. None of the remaining controls had MDTs and HSRP outside the control group mean ± 2 SD.

There was a statistically significant correlation between the motion thresholds and the mean High Spatial Resolution Perimetry matrix thresholds, ($P = 0.0001$, $r^2 = 0.24$; excluding 2 outliers: $r^2 = 0.30$), (figure 7.5).

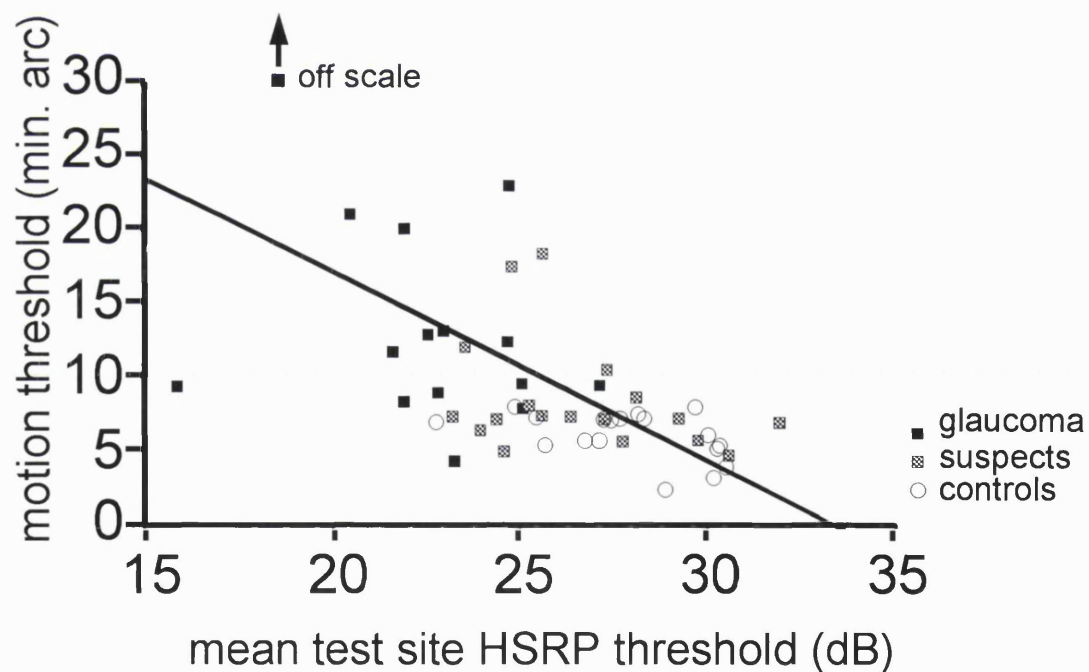


Figure 7.5 Relationship between subjects' Motion Displacement Threshold and HSRP matrix map mean threshold. The solid line represents the least-squares linear fit through the data. Arrow indicates 1 outlier off the y-scale.

7.5 Discussion

This aim of this study is to test the hypothesis that abnormal Motion Displacement Thresholds coexist with scotomas on a finer scale than is measurable by conventional Humphrey perimetry. We identified 10 glaucoma eyes with normal Humphrey 24-2 field nearest the MDT test site. Of these 7 had abnormally elevated Motion Displacement Thresholds and 6 had fine scale scotomas detected with High Spatial Resolution Perimetry. This result suggests that glaucomatous elevations of Motion Displacement Threshold may be present in areas of normal Humphrey 24-2 field, and this may coexist with measurable scotomas beyond the resolution of conventional Humphrey perimetry in some, but not all patients.

We identified 2 glaucoma eyes with abnormal HSRP in the presence of a normal motion 50% threshold test. Whilst it is possible that these defects may be non-glaucomatous, and secondary to the influence of refractive error or media absorption, we were unable to identify such factors in our patients. Further studies will be required to confirm this and to examine for additional unrecognized factors which may be responsible for this. A further proportion of the glaucoma patients (30%) had Motion Displacement Thresholds defects in areas of field with no detectable scotomas, measured with conventional perimetry or High Spatial Resolution Perimetry. One possible explanation would be the existence of scotomas beyond the resolution of our technique. The maximum displacement of the motion stimulus is less than 0.3 degrees, whilst the High Spatial Resolution Perimetry has been performed by measuring field thresholds across a grid at 1 degree intervals. Thus we cannot exclude the possibility of abnormal Motion Displacement Thresholds coexisting with scotomas beyond the resolution of our technique.

In order to avoid artifacts due to the trial frame, we elected to perform Motion Displacement testing and High Spatial Resolution Perimetry without near correction.

Motion Displacement Thresholds have been shown to be relatively unaffected by refractive errors (Fitzke, et al., 1989; Whitaker and Buckingham, 1987), and the subjects had low refractive errors. Refractive error would be expected to globally suppress Humphrey field threshold sensitivity (Goldstick and Weinreb, 1987). The uniformity index (UI) we used reflects focal threshold depression, which would not be expected to

be affected by refractive error. 13/14 of the glaucoma eyes identified as abnormal with the HSRP had an abnormal Uniformity Index. Refractive changes would not be expected to account for these localized threshold abnormalities, as in general the effect of refractive error is to smear out localized abnormalities.

One finding of this study was that over half of the glaucoma eyes with abnormal motion sensitivity had normal Humphrey 24-2 field at the motion test site. This finding has also been reported by Johnson et al, who identified elevated Motion Displacement Thresholds in glaucoma in areas appearing normal on conventional perimetry (Johnson, et al., 1995). I shall examine two major hypotheses to explain this finding.

One hypothesis which has been invoked to account for the occurrence of early abnormalities of motion perception before conventional field defects is the “selective loss hypothesis”.

Quigley has hypothesized that there is selective damage to the larger diameter optic nerve fibres in early glaucoma (Quigley, et al., 1988). Since magnocellular cells are associated with larger mean diameters, the “selective loss hypothesis” would imply a preferential loss of magnocellular function. The evidence for this is described in chapter 3.

Johnson has proposed an alternative hypothesis based on the concept of reduced redundancy to explain the presence of a variety of psychophysical abnormalities of visual function (including motion perception) in glaucoma before conventional perimetric field defects (Johnson, 1994). According to the reduced redundancy theory, the poor performance of conventional perimetry may be a consequence of the non-selective nature of the stimulus, which stimulates a broad spectrum of retinal ganglion cells. The large overlap in ganglion cell receptive fields results in considerable redundancy, that may mask early losses if all classes of ganglion cells are stimulated (Johnson, 1994). Tests that stimulate only a subpopulation of ganglion cells to isolate one aspect of visual function may identify the earliest losses.

Psychophysical evidence for both the selective cell hypothesis and the reduced redundancy hypothesis depends upon comparisons of the extent and the sequence of occurrence of selective losses of visual function, compared with non selective losses identified with conventional perimetry (Johnson, 1994; Sample *et al.*, 1994a).

An important finding of this study was that elevations of Motion Displacement Threshold may coexist with scotomas beyond the resolution of conventional Humphrey perimetry. This finding demonstrates the importance of considering the spatial resolution of the tests, which must be taken into account when making comparisons between tests. The differing spatial resolution of the tests may be as significant as any intrinsic differences that may exist in the sensitivity of a broad spectrum stimulus such as the Humphrey stimulus, compared with more selective stimuli such as motion stimulus. In summary, the results of this study suggest that a principal limitation of conventional Humphrey 24-2 perimetry in detecting early glaucoma is its inadequate spatial resolution.

8. CHAPTER 8

The effect of stimulus orientation on Motion Displacement Thresholds in glaucoma.

8.1 Background

Previous studies that have reported elevated Motion Displacement Thresholds in glaucoma have used a vertical line stimulus which undergoes horizontal displacements (Fitzke, et al., 1987; Fitzke, et al., 1989; Johnson, et al., 1995). The results of the studies outlined in chapters 4,5, and 7 were obtained using the test described by Fitzke et al (Fitzke, et al., 1987). Other stimuli that have been used are random dot kinetograms, using stimuli in which the signal component moves in either a horizontal direction or one of four cardinal directions (Bullimore, et al., 1993; Silverman, et al., 1990; Wall and Ketoff, 1995).

8.2 Purpose

This aim of this study was to investigate the effect of the orientation of the stimulus motion on the displacement thresholds in normals and glaucoma.

Although mediated by motion sensitive pathways, line displacement thresholds may in addition be influenced by local retinal luminance sensitivity loss. Previous investigators have identified the existence of fine slit-like scotomas, beyond the resolution of conventional perimetry, that correspond to the orientation of retinal nerve fibre layer defects (Tuulonen, et al., 1993).

This study tests the hypothesis that displacements of a line stimulus into a slit-like scotoma would contribute to impaired motion sensitivity, and that this effect would depend on the orientation of the line stimulus relative to the orientation of the slit-like scotoma.

It is hypothesized that the motion sensitivity of a line stimulus moving in a parallel direction to the nerve fibre layer would be less influenced by an underlying fine slit-like scotoma orientated along the axis of the nerve fiber, as illustrated by figure 8.1a, than a

stimulus moving perpendicular to the retinal nerve fibre layer (RNFL) and thus into the slit-like scotoma (figure 8.1b).

The aim of this study is to test the hypothesis.

figure 8.1a

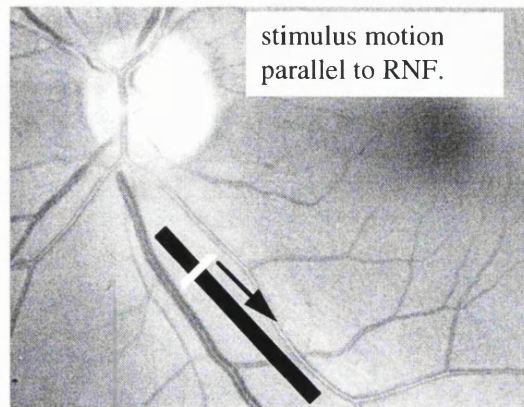


figure 8.1b

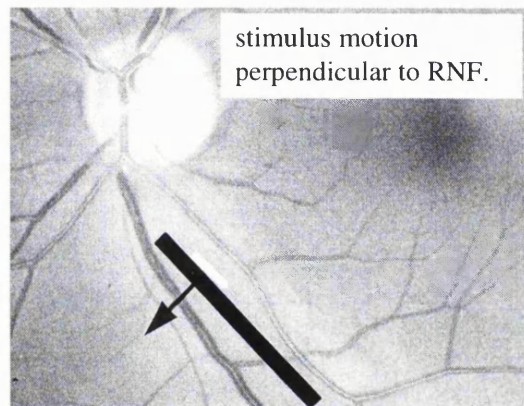
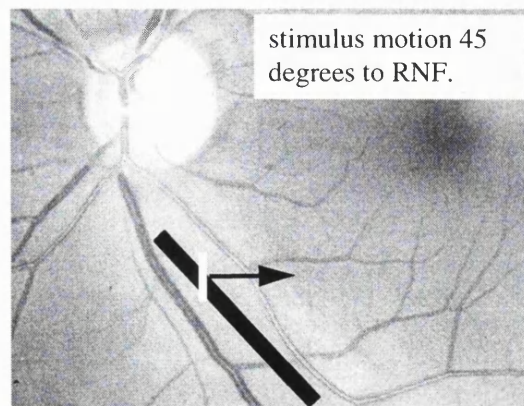


figure 8.1c



Figures 8.1a, b & c Left eye motion test in superotemporal field: vertical line stimulus shown in white superimposed on fundus image. The arrow shows the direction of the stimulus displacement in relation to a hypothetical slit-like scotoma orientated along the axis of the retinal nerve fibre layer shown in black.

8.3 Methods

8.3.1 Subjects

17 patients with an established diagnosis of primary open angle glaucoma and 8 age-matched normal controls were prospectively recruited for this study. All patients had documented intraocular pressures above 21 mm Hg, glaucomatous optic disc cupping and early but reproducible glaucomatous visual field defects on the program 24-2 of the Humphrey Visual Field Analyzer. All controls had a normal ocular examination, intraocular pressures under 21 mm Hg and normal Humphrey 24-2 fields (normal glaucoma hemifield test and global indices within 95% C.I. for normal subjects) in both eyes.

All patients and controls had a corrected visual acuity in both eyes of $\geq 6/9$ achieved with less than ± 4 dioptres spherical equivalent and less than 2 dioptres of astigmatism. Patients with significant ocular pathology other than glaucoma were excluded.

The glaucoma patients had a mean age of 64.9 years with a SD of 7.4, and the control group 58.9 with a SD of 9.8. (non-significant difference at 0.05 level).

The patients had early glaucomatous Humphrey 24-2 field loss with repeatable focal arcuate losses or a nasal step usually limited to one hemifield. The mean of the MDs of the Humphrey 24-2 fields of the glaucoma group was -4.87 dB, SD +3.37 dB, (range +3.37 to -10.10 dB) which was significantly different from the control mean MD of -0.65 dB, SD +1.11 dB (range +1.11 to -2.24 dB). (T-test significant at $p < 0.001$).

15/17 of the patients had normal Humphrey thresholds at the 4 closest Humphrey test locations to the motion test site, according to our definition (see analysis section), whilst 2 patients had scotomas extending into the motion test site.

8.3.2 Examination protocol

The test set-up to measure Motion Displacement Thresholds was the same as that described in detail in Chapter 7. Briefly, a line stimulus is presented in the superotemporal or inferotemporal fields. The line stimulus undergoes instantaneous oscillatory displacements of magnitudes 0 - 18 min. arc. Frequency-of-seeing curves are generated for 10 magnitudes of displacement from 0 to 18 min. arc each presented 10

times. A probit fit analysis is applied and the displacement corresponding to 50% seen is taken as the threshold.

A gimbal system was constructed to enable the monitor to be rotated through 360 degrees. This allowed us alter the orientation of the line and hence the direction of the stimulus motion to an accuracy of within 1 degree whilst keeping all other properties of the test constant. Patients underwent motion measurements in one glaucomatous eye in either the superotemporal location (14 patients) or in the inferotemporal location (3 patients). Controls underwent motion sensitivity testing in 1 randomly chosen eye, all in the superotemporal location. All subjects underwent an initial baseline motion sensitivity test with the stimulus in the vertical position undergoing horizontal motion (designated 0 degrees axis). This was followed by tests with the stimulus rotated counterclockwise by 45 degrees, 135 degrees and 0 degrees (i.e. baseline again) with appropriate rest breaks in a randomised order to avoid any consistent bias in learning or fatigue.

8.3.3 Analysis

Motion measurements were classified according to the direction of stimulus movement with respect to the orientation of the retinal nerve fibres at the test site. Figures 8.1a, 8.1b and 8.1c show the position of the stimulus for a motion test in the superotemporal field of the left eye: movement along the 135 degrees meridian is labeled as “motion parallel” to the retinal nerve fibres, stimulus movement along the 45 degree meridian is labeled as “motion perpendicular” to the retinal nerve fibres, and stimulus movement along the 0 degree meridian is labeled as “motion at 45 degrees” to the retinal nerve fibre layer. This analysis is a valid assumption, assuming that the orientation of the retinal nerve fibres at the test location lies between 22.5 degrees and 90 degrees from the horizontal reference line.

We evaluated the Humphrey 24-2 luminance at the test site by examining the threshold sensitivities at the 4 Humphrey 24-2 test locations closest to the motion site. We defined the Humphrey 24-2 threshold at the motion test site as being abnormal if at least 1 of these 4 locations was contiguous with a hemifield cluster of depressed locations consisting of at least 3 adjacent depressed points on the STATPAC2 pattern deviation plot with one point having a probability of $P < 1\%$ and 2 adjacent points having a probability of $P < 2\%$ (Piltz, et al., 1991).

8.4 Results

8.4.1 Motion Displacement Thresholds

Table 8.1 shows the mean Motion Displacement Thresholds for the glaucoma and control groups for the orientations tested. The motion tests are classified according to the direction of the stimulus movement relative to the orientation of the retinal nerve fibres (RNF).

direction of motion relative to RNF	controls (min. arc)	glaucoma (min. arc)	controls vs. glaucoma
45 degrees (1)	6.4 ± 1.2	11.7 ± 3.8	t = 5.18 p < 0.001
45 degrees (2)	5.0 ± 1.5	10.0 ± 4.3	t = 4.25 p < 0.001
perpendicular	5.2 ± 1.8	11.3 ± 5.2	t = 4.32 p < 0.001
parallel	5.6 ± 1.5	9.8 ± 3.7	t = 3.04 p = 0.006

Table 8.1. Mean Motion Displacement Thresholds and standard deviations in min. arc. for glaucoma and control groups by orientation, with statistical comparison between groups using Student's T-test.

The means of the motion thresholds of the controls lie within our normal range of values for this test for all orientations tested (Fitzke, et al., 1989).

The means of the Motion Displacement Thresholds of the glaucoma group were significantly elevated compared to the means of the control group for all orientations tested.

There was a statistically significant negative linear correlation between the motion thresholds and the mean of the Humphrey sensitivity thresholds at the 4 Humphrey 24-2 test locations nearest the test site although the degree of correlation was poor ($r^2 = 0.22$, $p = 0.02$). There was no significant linear correlation between the motion thresholds and the Humphrey MD.

8.4.2 Effect of stimulus orientation on motion threshold

To illustrate the individual orientation dependent variability we plotted the thresholds for stimulus motion perpendicular to the RNF against stimulus motion parallel to the RNF for all subjects (Figure 8.2).

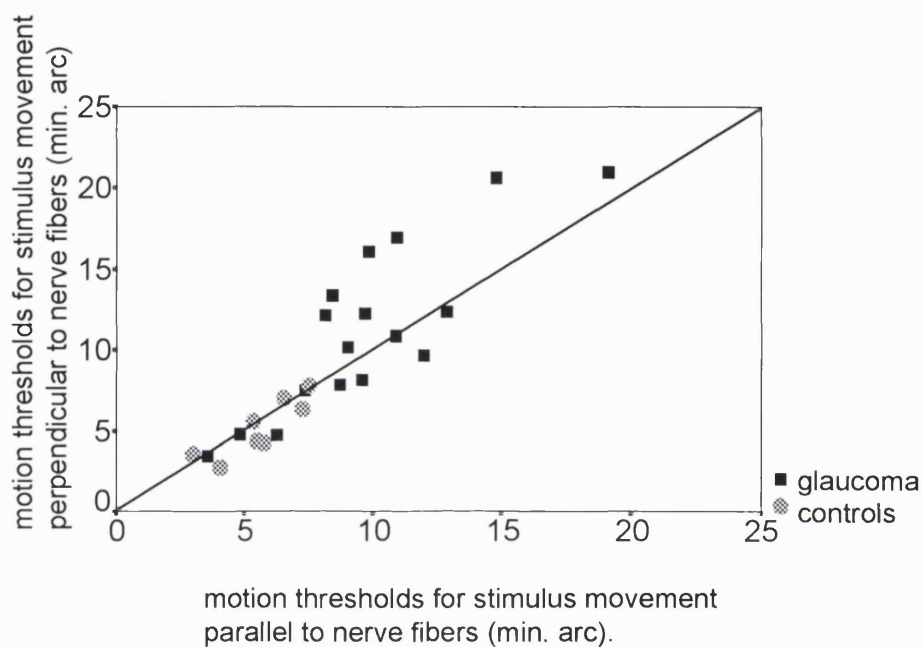


Figure 8.2 Scatterplot of subjects' thresholds for stimulus motion perpendicular vs. motion parallel to retinal nerve fibres, with the line of unity.

For quantitative analysis, we plotted the difference in the thresholds for stimulus motion perpendicular and parallel to the RNF versus the mean of the thresholds (figure 8.3). The zero on the y ordinate represents no difference between the motion threshold for motion perpendicular and parallel to the retinal nerve fibre layer.

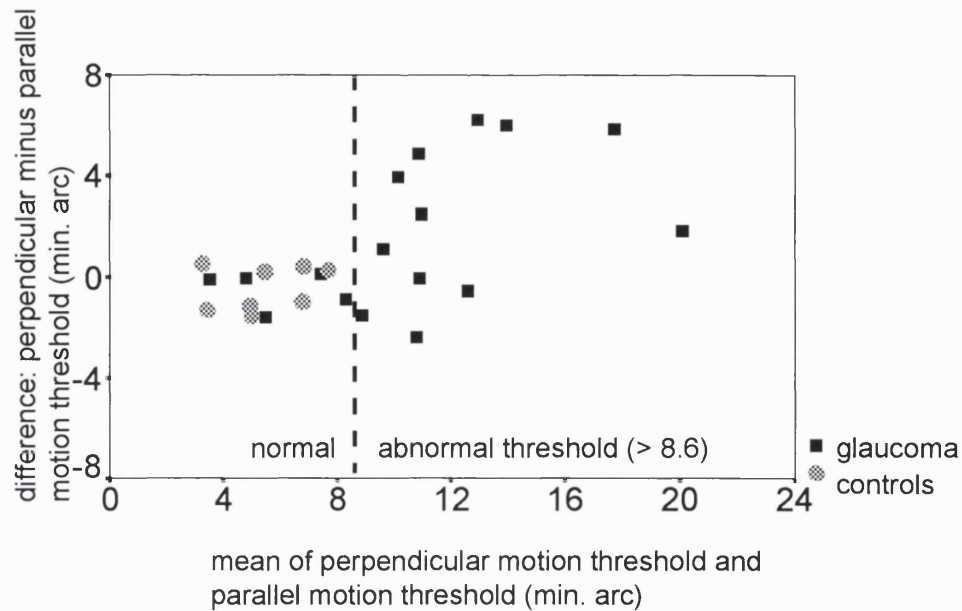


Figure 8.3 Difference versus mean plot of motion thresholds for stimulus motion perpendicular and parallel to retinal nerve fibres. Subjects with normal motion thresholds lie to left of vertical reference line of 8.6 min. arc.

For subjects with normal motion thresholds (up to 8.6 min. arc, equivalent to mean + 2 SD of controls), there is no orientation dependence, with all differences lying close to the zero ordinate.

In contrast, in patients with abnormally elevated motion thresholds (above 8.6 min. arc), a number of the patients lie a considerable distance above the zero ordinate, with the motion threshold for stimulus motion perpendicular to the nerve fibre layer more severely elevated compared to motion parallel to the nerve fibre layer.

Figure 8.3 also shows a trend of increasing elevation of motion threshold for stimulus motion perpendicular compared to parallel to the nerve fibre layer (data points above zero ordinate) in patients with more pronounced threshold elevations. A Spearman rank correlation test showed that this was highly statistically significant ($\rho = 0.55$, $p < 0.005$). Thus increasing threshold elevation is associated with increasing elevation of the motion threshold for motion perpendicular compared to parallel to the nerve fibre layer.



However this analysis does not take into account smaller differences in the thresholds which may be proportionally more important at the lower range of threshold values.

To correct for this we calculated the proportional difference in the thresholds for perpendicular and parallel stimulus motion according to:

Proportional difference (Pn) = perpendicular – parallel motion threshold / perpendicular + parallel motion threshold.

A proportional difference value of 0 represents no difference between the perpendicular and parallel thresholds, + 1 represents maximally elevated perpendicular threshold relative to parallel, -1 maximally elevated parallel threshold relative to perpendicular.

Figure 8.4 is a plot of the proportional difference vs. the mean of the perpendicular and parallel thresholds for all subjects. A ranked Spearman correlation test again showed a significant positive correlation between the proportional difference (Pn) and the mean for all subjects (Spearman ranked correlation coefficient Rho = 0.555, p = 0.004).

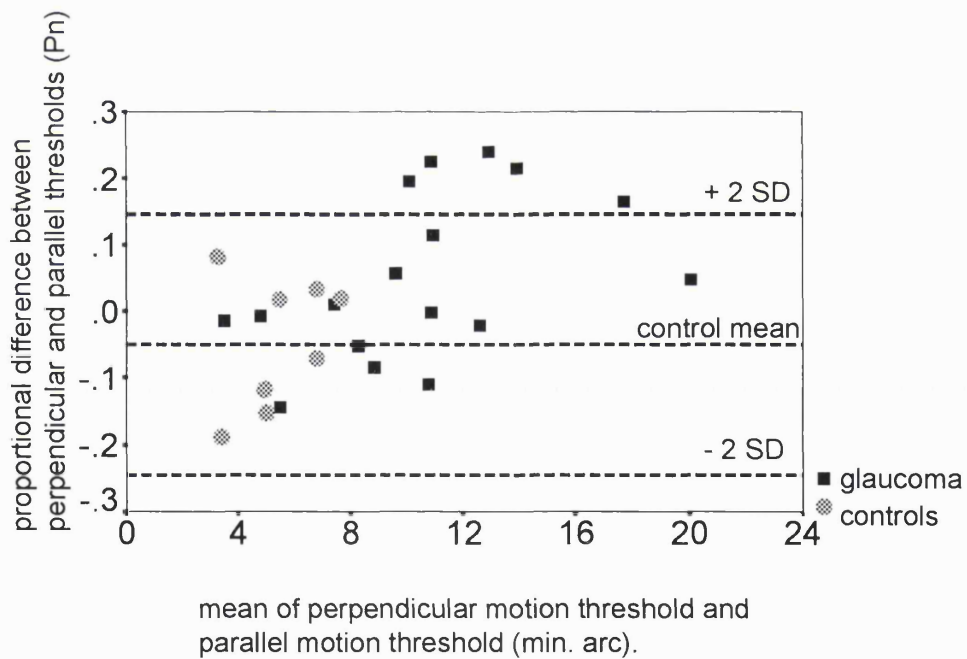


Figure 8.4 Proportional difference versus mean plot of motion thresholds for stimulus motion perpendicular and parallel to retinal nerve fibres.

Reference lines indicate the mean +2 SD of the proportional difference of the controls, with no controls lying outside this range. However, 5 of the glaucoma patients lie above the control mean +2 SD. These patients have a proportionally elevated motion threshold

of at least 15% for stimulus motion perpendicular to the RNF compared to stimulus motion parallel to the RNF. No patients have a proportional difference below the mean - 2 SD of the controls. We reviewed the results to identify any distinguishing characteristics of these 5 patients who showed the most pronounced orientation effect. There was no consistent order in the sequence of the tests performed in the 5 which may have influenced the results. Of these 5 patients with the most pronounced orientation effect, 1 had a scotoma extending to the 4 Humphrey 24-2 test locations closest to the site of motion testing, 1 had a nasal Humphrey field defect distant to the motion test site, and 3 patients had normal Humphrey field in the hemifield of the motion test. Although there was a weak correlation between the motion threshold and the Humphrey luminance at the motion test site, there was no significant correlation between the difference in the motion thresholds of the orientations tested and the Humphrey luminance at the motion test site.

8.5 Discussion

The aim of this study was to investigate the effect of stimulus orientation on Motion Displacement Threshold thresholds in controls and patients with POAG. We performed tests of motion sensitivity using a line displacement test, with the line stimulus orientated parallel or perpendicularly to the orientation of the retinal nerve fibre layer corresponding to the site of motion testing. We did not identify any clinically significant differences between the thresholds at perpendicular and parallel orientations in the controls, or in patients with normal motion thresholds. In patients with elevated motion thresholds, there was more marked threshold elevation for stimulus movement perpendicular to the nerve fibre layer compared to movement parallel to the nerve fibre layer. This difference was statistically significantly greater for patients with more pronounced threshold elevations.

In 5 patients the motion thresholds for stimulus motion perpendicular to the retinal nerve fibre layer were proportionately elevated by over 15% compared with motion parallel to the nerve fibre layer. This proportional elevation exceeded the 95% confidence limits we obtained with our controls. We did not identify any patients who demonstrated a proportional elevation of the threshold for motion parallel compared to perpendicular of this magnitude.

Although factors such as fatigue and learning may affect an individual's performance during the tests we think this is unlikely to explain this effect as the order in which the motion tests were performed was randomised, and we could not find any consistent order effects in the test sequence in these patients. There were no differences in the degree of astigmatic and spherical error in these patients (which was low in all groups), nor were there marked differences in the Humphrey sensitivity thresholds at the test site between the patients who showed an orientation effect and those who did not.

We hypothesize that this effect is explained by the interaction of the stimulus with fine slit-like luminance loss orientated along the retinal nerve fibres, on a much finer scale than is identifiable with conventional perimetry. We postulate that the motion sensitivity of a line stimulus in a parallel direction to the nerve fibre layer would be less influenced by fine slit-like luminance loss orientated along the axis of the nerve fiber, as illustrated by figure 8.1a, than a stimulus moving perpendicular to the nerve fiber layer and thus into the luminance loss (figure 8.1b). According to this hypothesis, any effect of orientation on the motion threshold may be predicted by the underlying orientation of the retinal nerve fibre layer at the site of testing. The results of this study are based on a small number of subjects, and further work is required to investigate for any orientation effect in other locations of the visual field.

In summary, this study has identified an orientation dependence sensitivity to motion in some patients with glaucoma. This effect has not been reported previously and may be useful in improving the sensitivity and specificity of motion sensitivity testing in identifying early glaucomatous damage.

9. CHAPTER 9

Discussion and summary

9.1 High spatial resolution automated perimetry

9.1.1 Implications of findings

Chapter 6 investigated the use of High Spatial Resolution Perimetry in glaucoma. Previous investigators have performed perimetry at higher spatial resolution than conventional perimetry, and have identified subtle scotomas beyond the resolution of conventional perimetry (Sturmer, 1985; Weber and Dobek, 1986). High Spatial Resolution Perimetry has also been shown to identify scotomas that correspond to retinal nerve fibre layer defects in glaucoma suspects who have normal conventional perimetry (Airaksinen and Heijl, 1983; Tuulonen, et al., 1993). This suggests that High Spatial Resolution Perimetry may have a number of distinct clinical advantages over conventional perimetry in the detection of the earliest glaucomatous field defects. However, previous techniques of High Spatial Resolution Perimetry have been arduous for patients and have been limited by long testing times (Airaksinen and Heijl, 1983; Sturmer, 1985). Another recognized problem of High Spatial Resolution Perimetry has been a high intratest variability, with a corresponding poor repeatability of the threshold measurements (Sturmer, 1985). The high intra-test variability in areas of glaucomatous sensitivity loss has previously posed a significant limitation to the usefulness of High Spatial Resolution Perimetry. Attempts to improve the precision of the threshold measurements by repeating the measurements is unlikely to be practical in High Spatial Resolution Perimetry because of the already lengthy test times. Chapter 6 describes the use of image processing techniques (Fitzke and Kemp, 1989) as an alternative method to improve the repeatability. Image processing techniques have the advantage of requiring no extra test time, and have already been shown to improve the repeatability of conventional automated perimetry (Fitzke, et al., 1995). The application of a Gaussian filter to the High Spatial Resolution Perimetry threshold data resulted in a marked improvement (by a factor of 2) in the repeatability of the technique. We obtained good

reproducibility of the threshold profiles using this technique, and this has allowed us to obtain finer details of sensitivity loss which were not apparent on the lower spatial resolution of conventional perimetry.

9.1.2 Clinical applications

We believe that High Spatial Resolution Perimetry fine matrix mapping may be a useful clinical tool, and may have a diagnostic role in the more detailed evaluation of equivocal areas of visual field of glaucoma patients and suspects.

Previous studies have suggested that the test point density of conventional perimetry is not a limiting factor for the identification of the earliest glaucomatous field change. However these studies are inherently biased as they used conversion criteria based on the development of field defects measured at conventional resolution (Heijl, 1993). It remains to be determined whether the detection of conversion is improved by the use of High Spatial Resolution Perimetry. In addition, High Spatial Resolution Perimetry may have a role in identifying early progression of glaucomatous visual field defects. There is evidence to suggest that the progression of glaucomatous defects, as detected using conventional perimetry, is slow (Migdal, et al., 1994; Smith *et al.*, 1996). Using conventional perimetric programs with a spacing of 6 degrees between adjacent test points, progression of the advancing edge of a scotoma which is increasing in size must exceed 6 degrees visual angle before change is registered at a repeat examination. Perimetry performed using test locations separated by 1 degree offers the theoretical possibility that we may be able to identify advancement at the edge of a scotoma at an earlier stage than is possible with conventional perimetry.

9.1.3 Future modifications

Chapters 6 & 7 describe research into High Spatial Resolution Perimetry and the use of Gaussian image filtering techniques to improve the repeatability. However other widely used filters in image processing may have particular advantages useful to our technique. The properties of a median filter suggest that it may have advantages in preserving areas of abrupt change in the visual field, for instance a scotoma. Another filter is the Sobel filter, which could be used to accentuate the edges of a scotoma. Future work is required to investigate the usefulness of these filters. Another future improvement would be the development of a physiologically based custom filter which would be tailored according

to glaucomatous patterns of field loss. Humphrey thresholds of adjacent test locations are not spatially independent, and can be weighted according to common patterns of field loss. Such a custom filter is generated by giving each test location a weighting calculated from its degree of correlation with neighbouring points. Neighbouring test locations which follow an arcuate pattern are likely to be more highly correlated than distant points. Such a custom filter would be expected to follow an arcuate pattern, and respect the horizontal meridian. The application of a more physiological filter may be useful in improving the identification of early pathological field loss from non pathological noise in the field.

9.2 Motion Displacement threshold testing

9.2.1 Reaction times for motion detection

The study in chapter 4 investigated for differences in reaction time between glaucoma patients and controls during line displacement motion testing. It was found that the mean reaction times during motion testing of the glaucoma patients were significantly prolonged by approximately 200 msec. compared to controls. This compares with the delay of 100 msec. reported in glaucoma patients undergoing random dot kinetogram motion testing reported by Wall et al (Wall and Montgomery, 1995).

Possible causes for the reaction time prolongation in glaucoma can be examined by considering reaction time to be the combined time for (1) stimulus perception and signal conduction, (2) decision time relating to uncertainty of stimulus perception, and (3) motor reaction time.

The possibility of conduction delay can be investigated by calculating the total retinocortical pathway time, using known conduction velocities and assuming that maximal delay would be caused by total loss of faster conducting magnocellular ganglion cells. I have calculated that the maximal delay associated with total magnocellular ganglion cell dropout could only contribute to a delay of 20 msec.. This is clearly insufficient to explain the magnitude of the reaction time prolongation in our patients.

The possibility that prolonged reaction times in glaucoma are the result of a prolonged decision time has been suggested by Wall & Montgomery (Wall and Montgomery,

1995). This is a consequence of the greater stimulus uncertainty associated with the elevated motion threshold.

The study in chapter 4 has tested this possibility by measuring the reaction times to a motion target across the psychophysical response function. This enabled us to measure the reaction times at threshold, where all subjects have an equal 50% uncertainty of stimulus perception. The equivalence of reaction times at threshold across the groups suggests that the prolongation of reaction time in glaucoma is due to stimulus uncertainty associated with the elevated motion threshold in the glaucoma patients. Lastly, the possibility that the reaction time prolongation in the glaucoma patients represents a motor delay is unlikely, as glaucoma would not be expected to affect the motor system and the subjects were age-matched.

In summary, this study has shown that reaction times are prolonged for a motion stimulus in glaucoma as a consequence of the elevated motion threshold. A similar finding was reported by Wall et al using a conventional Humphrey perimetric stimulus (Wall, et al., 1996). On the basis of these two studies, one can postulate that any prolongation of total test reaction time to a variety of stimuli would be accounted for by elevation of threshold. The corollary of this is that the measurement of reaction time is unlikely to yield any additional information beyond that obtained by measuring threshold alone. However the analysis of reaction time may provide a useful marker of reliability, as discussed below.

9.2.1.i Future modifications

One potentially very useful benefit of reaction time analysis is the assessment of a subject's reliability.

One measure of a subjects' reliability during perimetry is the frequency of false positive responses, i.e. false responses by the subject when no response or a subliminal response is presented. The traditional method of estimating the frequency of false positive responses is to add catch trials to the test. Because the false positive rate in most patients is usually small (less than 10%), an accurate estimation of the false positive rate would require the presentation of a large number of catch trials which would lengthen the test to unacceptable limits. Because of these time constraints, the false positive rate is estimated by presenting a small number of catch trials, resulting in an inexact estimate of the "true" rate. Olsen et al have recently described a method of analysis which uses

reaction times to assess patient reliability in automated Humphrey perimetry (Olsson, et al., 1997). They divided the response time after onset of the stimulus into periods. One period is known as the response window which is the period when the subject would be expected to respond if the stimulus is perceived. There are also periods when no responses would be expected, which are known as listen times. One such period is from the onset of stimulus to the minimum reaction time, known to be 180 msec or more. The other period starts from a fixed time after the response window and lasts until the next stimulus exposure. Responses within these periods can be assumed to be false positive responses. Olsson et al have shown that the frequency of false positives obtained by reaction time analysis can be used to provide a measure of reliability during the test (Olsson, et al., 1997). Unlike the use of catch trials, this method has the advantage that no additional test time is required. Another significant advantage of reaction time analysis of Humphrey reliability is that the method samples much more of the field test (up to 15 times more) compared to catch trials.

One future modification of the MDT test would be to incorporate a similar reaction time analysis to estimate the false positive rate, eliminating the need to perform catch trials and thus shortening the test time. To perform this analysis, estimates of the response window and minimum reaction time would need to be obtained for each magnitude of displacement presented. The variation of these times with respect to stimulus intensities and location would have to be investigated. This would allow cut-offs to be derived for the minimum reaction time, and comparison of the subjects' reaction time would allow a false positive rate to be calculated.

9.2.2 Frequency of seeing analysis for motion detection

In chapter 5, frequency-of-seeing curve analysis was used to investigate the relationship between threshold and intratest variability for a motion stimulus.

Frequency-of-seeing analysis has previously been useful in investigating the relationship between the threshold and intratest variability in conventional perimetry. Several studies have shown a relationship between increasing threshold elevation and shallowing of the slope of the frequency-of-seeing curve, representing an elevated intratest variability (Chauhan and House, 1991; Chauhan, et al., 1993b; Henson, et al., 1996; Olsson, et al., 1993; Wall, et al., 1996; Weber and Rau, 1992). However frequency-of-seeing curves have received little attention for other stimuli, including motion stimuli.

The results in chapter 5 showed that the intratest variabilities were significantly elevated in the glaucoma patients and glaucoma suspects, compared to controls. There was also a significant correlation between the degree of motion threshold elevation and the degree of slope shallowing.

A significant finding was the fact that a proportion of patients had abnormal shallowing of the slope of the frequency-of-seeing curve, without abnormal elevation of the motion threshold. This suggests that alterations in the shape of the motion frequency-of-seeing curve occur early in glaucoma, and may precede threshold abnormalities. A similar finding was reported by Chauhan et al using frequency-of-seeing tests in conventional perimetry.

This finding highlights the importance of determining the variability at threshold at a given location, as abnormally high values may indicate the earliest abnormality in glaucoma. However, commonly used staircase algorithms do not directly measure threshold variability for all threshold test locations in the visual field. For instance, the widely used Humphrey full threshold algorithm only provides a global measure of threshold variability as the short term fluctuation (SF), which is calculated from 10 pre-determined test points where the threshold is determined twice. We have used frequency-of-seeing analysis to investigate the relationship between the threshold and intratest variability, as have several other studies (Chauhan and House, 1991; Chauhan, et al., 1993b; Henson, et al., 1996; Olsson, et al., 1993; Wall, et al., 1996; Weber and Rau, 1992). Although frequency-of-seeing analysis allows the determination of the slope and threshold, one drawback of a frequency-of-seeing analysis is the longer test times required, as compared with other staircase-based thresholding strategies. In MDT test used for this research, this time constraint would be a major limitation to the number of locations which could be tested at a single test session.

One novel approach to the problem of obtaining a measure of intratest variability within an acceptable test time has recently been described by Bengtsson and Olsson in their work on the new generation of algorithms called SITA, or Swedish Interactive Threshold Algorithms (Bengtsson *et al.*, 1997). This algorithm uses a prior model of the frequency-of-seeing curve at a given location to represent both the normal response and the abnormal response. Such models have been determined from a database of subject responses. The Humphrey SITA program presents stimuli in a staircase test procedure. From the start of the test, the prior models are constantly updated as the patients' own responses are used to refine the model. Post processing of the model is performed by

incorporating reliability data to recalculate the frequency-of-seen models, and the threshold is estimated. According to the authors, this new Humphrey thresholding strategy has three major advantages: firstly all the patients' responses are added to the model, both negative and positive. This utilises more of the data than the conventional Humphrey staircase algorithm, and has the statistical and theoretical advantages of providing a more accurate threshold estimation. Secondly, the shape of the subjects' response models can be used to provide the intratest variability at threshold for all locations tested. Thirdly, because the subjects' responses are incorporated within an existing model, current best estimates of the threshold are constantly available throughout the test. This allows the testing strategy to be terminated at a predetermined level of accuracy (Bengtsson, et al., 1997).

In summary, the newer generation of algorithms such as SITA may allow the identification of early shallowing of the slope of the frequency-of-seeing curve, in addition to threshold changes. This can be achieved with an acceptable test time. These strategies are likely to be used in motion testing and other psychophysical tests. One future development of the MDT test would be to use a similar strategy to allow multilocation MDT testing within an acceptable test time. The results of chapter 5 already provide preliminary data to generate age-matched prior models of frequency-of-seeing curves for normals and glaucoma patients. A staircase strategy displacement test would be used to update such models with the patients' own responses, and similar analysis to the SITA program would be applied.

Although the findings of chapter 5 demonstrate an increased variability in the motion response of patients with glaucoma compared with normals, the cause for this remains unknown. However a number of mechanisms have been proposed to explain the increased variability reported in glaucoma for conventional field testing, and similar mechanisms may be invoked to explain our findings for motion testing.

One hypothesis is that small inaccuracies of fixation in the presence of steep field threshold sensitivity profiles may account for the increased variability in glaucoma (Haefliger and Flammer, 1991; Henson and Bryson, 1991; Vingrys and Demirel, 1993). According to this hypothesis, small inaccuracies of fixation in the presence of a steep sensitivity profile result in the stimulus falling into and climbing of a scotoma. This would result in apparent large changes in sensitivity, which would manifest as an increased variability. This hypothesised mechanism applies to all methods of perimetry, including

motion perimetry. The degree of variability will depend on the magnitude of fixation instability and the number and steepness of the sensitivity gradients.

Henson has recently cast doubt on this hypothesis by measuring perimetric frequency-of-seeing curves both with and without fixation error correction in 14 glaucoma patients. He identified a positive correlation between the sensitivity and the slope of the frequency-of-seeing curve, with a shallowing of the curve associated with locations of lowered sensitivity. However a reanalysis using only those responses with good fixation had no significant effect on reducing the variability, either at normal locations or damaged field locations (Henson, et al., 1996).

Alternative mechanisms which are not dependent on fixation losses have been proposed to explain the changes in the slope of the psychophysical function. These include neural mechanisms related to factors such as fatigue (Brenton and Argus, 1987) and reduced number of nerve fibres (Flammer, et al., 1984c).

Our finding of an increased intratest variability in the motion testing of glaucoma patients can also be considered in terms of the concept of reduced redundancy, as postulated by Johnson et al (Johnson, 1994).

One prediction of the reduced redundancy hypothesis is that selective tests should exhibit greater threshold variability than non-selective tests, such as conventional perimetry (Johnson, 1994). This is because a selective test stimulates a sparser subpopulation of ganglion cells with minimal overlapping receptive fields, compared with a more non-selective test (Johnson, 1994). Further studies are required to investigate whether the degree of intratest variability that we have identified in our motion testing is proportionately greater than conventional perimetry. However this prediction of the reduced redundancy hypothesis has been supported by Wild et al, who have shown that the short-term variability of selective blue-on-yellow testing (SWAP) is higher than conventional perimetry (Wild, et al., 1995).

In summary, the implication of the findings of chapter 5 is that frequency-of-seeing analysis may improve the sensitivity and specificity of motion sensitivity testing in glaucoma, as compared with the analysis of threshold alone.

Longitudinal studies are required to investigate the value of slope abnormalities of the motion response in predicting subsequent conventional Humphrey field deterioration at that location.

9.2.3 Association of abnormal Motion Displacement Thresholds with fine scale luminance sensitivity loss in Glaucoma.

The study described in chapter 7 identified abnormal Motion Displacement Thresholds in areas of normal Humphrey field. In a proportion of patients these coexisted with fine scale depressions of Humphrey threshold which were not identifiable with conventional Humphrey field testing.

There are a number of interpretations of this:

a) The motion stimulus is specific for magnocellular ganglion cells and the motion abnormalities are indicative of magnocellular drop out. However, the coexistence of the motion abnormalities with fine scale scotomas suggests that the ganglion cell loss is not purely selective for the magnocellular system, but involves the parvocellular ganglion cells. This finding of fine scale scotomas in areas of normal Humphrey 24-2 suggests that the spacing of the test locations on the Humphrey 24-2 may be a limiting factor in the identification of the earliest scotomas. Progressive enlargement of these scotomas occurs until they are of a scale detectable by conventional perimetry.

b) The motion stimulus does not stimulate exclusively magnocellular ganglion cells, but also stimulates subpopulations of parvocellular ganglion cells. Recent research suggests that the perception of motion stimuli is not exclusively mediated by the magnocellular system, but also the parvocellular system (Merigan and Maunsell, 1993). As discussed in chapter 2, there is substantial evidence to suggest that P-cells must contribute to the perception of a wide range of motion stimuli throughout the visual field (Anderson, et al., 1995; Galvin, et al., 1996).

Accordingly, the line stimulus we used may stimulate ganglion cells of the parvocellular system in addition to ganglion cells of the magnocellular system. Although the Humphrey stimulus is believed to stimulate large classes of ganglion cells, the preponderance of P-cells suggests that glaucomatous loss of parvocellular cells is primarily responsible for producing a localized Humphrey field defect. Such loss may produce fine scale scotomas evident on High Spatial Resolution Perimetry, or larger scotomas on the conventional Humphrey field test. If P-cells contribute to motion acuity, then glaucomatous losses would be expected to produce a concomitant loss of line displacement sensitivity.

9.2.4 Stimulus orientation and motion threshold

The proposed effect of an underlying scotoma on the motion threshold obtained by line displacement testing is the basis for the investigations described in chapter 8. This study tested the hypothesis that the motion sensitivity of a line stimulus orientated perpendicularly to the nerve fibre layer, and moving in a parallel direction to the nerve fibre layer (see figure 8.1a), would be less influenced by fine slit-like luminance loss orientated along the axis of the nerve fibre than by a stimulus moving perpendicular to the NFL (see figure 8.1b). The results showed a significant trend of increasing elevation of motion threshold for stimulus motion perpendicular to the nerve fibre layer, compared to parallel, which is consistent with this hypothesis. In 5 patients the motion thresholds for stimulus motion perpendicular to the retinal nerve fibre layer were proportionately elevated by over 15%, compared with motion parallel to the nerve fibre layer. This exceeded the 95% confidence limits of controls.

This hypothesis is dependent on the existence of putative slit-like scotomas orientated along the retinal nerve fibre layer, of a width smaller than the length of the line stimulus (2 degrees). Evidence supporting the plausibility of scotomas on this spatial scale is supported by Tuulonen et al. They identified fine slit-like Humphrey field scotomas beyond the resolution of conventional perimetry that correspond to the orientation of retinal nerve fibre layer defects in 6 out of 8 patients (Tuulonen, et al., 1993)

Alternatively one can postulate the existence of fine arcuate losses of motion sensitivity orientated along the retinal nerve fibre layer in the absence of a coexisting Humphrey scotoma. This would be a result of ganglion cell loss selective to the magnocellular system. Wall et al have used size thresholds to measure motion sensitivity losses orientated along the nerve fibre layer in some ocular hypertensives with normal Humphrey fields (Wall, et al., 1997). Johnson has also reported motion sensitivity defects in an arcuate distribution which are more extensive than conventional Humphrey field losses (Johnson, et al., 1995). Both studies only compared the extent of motion deficits with conventional Humphrey field loss, and one cannot exclude the possibility of coexisting slit-like Humphrey scotomas beyond the resolution of conventional perimetry in these patients.

9.2.4.i Future modifications

The study in chapter 8 investigated the effect of stimulus orientation on motion threshold for a single test location in the superotemporal field. Further investigations are required to identify whether the motion threshold is significantly affected by stimulus orientation in other locations of the visual field. By considering the orientation of the line stimulus with respect to the known orientation of the retinal nerve fibre layer, predictions can be made regarding which orientations would be expected to show the greatest orientation effect at any given retinal location. These predictions can be tested experimentally to validate this hypothesis.

A future modification of the MDT test would be to develop a PC-driven multilocation test to allow threshold line displacement testing to be performed at multiple locations in the visual field. Line displacement motion thresholds would be obtained using stimuli orientated perpendicular and parallel to the retinal nerve fibre layer at the locations tested, and cut-offs derived from age matched normals would be used to identify abnormally elevated thresholds. An additional analysis would be performed on the difference in a patient's thresholds for parallel and perpendicular orientations. This would be compared with age and location specific norms to improve the discrimination between normals and abnormals. Further studies would be required to assess what effect any such orientation effect, if identified, would have upon the sensitivity and specificity of the motion test.

9.3 Summary

There is considerable evidence to suggest that a major limitation of automated perimetry is the fact that it is not sensitive to early glaucomatous damage. This finding has led to the development of more sensitive psychophysical tests, including motion sensitivity testing. This thesis investigated early abnormalities of motion sensitivity in glaucoma using a line displacement test.

This thesis has investigated three unexplored aspects of motion testing in glaucoma. The aspects studied are reaction times, frequency-of-seeing analysis and stimulus orientation (chapters 4,5,8).

The study of reaction times in chapter 4 provides the framework for the possible use of reaction times as a more efficient method of assessing reliability in motion testing.

In chapter 5, frequency-of-seeing analysis was shown to significantly improve the sensitivity of the motion test compared to analysis of the threshold alone. This finding has important implications for the development of future motion tests in glaucoma. A new generation of algorithms might be developed to allow the identification of early shallowing of the slope of the frequency-of-seeing curve, in addition to threshold changes. Such a development has already been initiated in conventional luminance testing with the introduction of the SITA Humphrey threshold programs, as outlined by Bengtsson (Bengtsson, et al., 1997).

In the study reported in chapter 7, a high proportion of glaucoma patients were found to have abnormal motion sensitivity in areas of field which appeared normal with conventional Humphrey perimetry. In addition it was found that abnormal motion sensitivity may coexist with fine scale scotomas beyond the resolution of conventional Humphrey perimetry. This finding has not been previously reported and demonstrates the importance of considering the spatial resolution of a test, which must be taken into account when making comparisons between motion and luminance tests. Although intrinsic differences may exist in the sensitivity of a broad spectrum stimulus such as the Humphrey stimulus compared with more selective stimulus such as motion stimuli, this finding suggests that a principal limitation of conventional Humphrey 24-2 perimetry in detecting early glaucoma is its inadequate spatial resolution. This would suggest caution in interpreting focal loss of motion sensitivity as *selective* until luminance sensitivity has been carefully measured at high spatial resolution.

The study in chapter 8 reports the finding of a significant effect of the line stimulus orientation on the motion threshold in some glaucoma patients, a finding which was not present in controls. A hypothesis was proposed to account for the apparent orientation effect based upon the interaction with the line stimulus with putative slit like scotomas orientated along the retinal nerve fibre layer. Further work is required to validate this finding, and to investigate for any orientation effect in other locations of the visual field in accordance with this hypothesis. Despite the range of stimuli that have been used in motion sensitivity testing, all reported studies of motion sensitivity in glaucoma have relied upon stimuli moving in cardinal directions. This is probably because it is technically simpler to generate such stimuli using a PC-driven monitor rather than for any physiological reason. It appears that the orientation of the motion stimulus warrants further investigation to confirm the presence of any orientation effect and to assess whether it significantly improves the sensitivity and specificity of motion testing in

glaucoma. This may have implications for the development of future motion testing, for example the development of a multilocational line displacement test.

10. APPENDIX: Supporting publications

10.1 Peer reviewed published papers

Westcott M, McNaught AI, Crabb D, Fitzke FW, Hitchings RA. High Spatial Resolution Perimetry in glaucoma. *British Journal of Ophthalmology* 1997, 81, 452-459.

Westcott MC, Fitzke FW, Hitchings RA. Stimulus orientation can effect motion sensitivity in glaucoma. *Perimetry Update* 1996/7 pp 35-42.

Westcott MC, Fitzke FW, Hitchings RA. Abnormal Motion Displacement Thresholds are associated with fine scale luminance sensitivity loss in glaucoma. *Vision research* (in print).

Westcott MC, Fitzke FW, Crabb DP, Hitchings RA. Characteristics of Frequency-of-Seeing Curves for a motion stimulus in glaucoma eyes, glaucoma suspect eyes, and normal eyes. *Vision research* (in print).

10.2 Papers under review

Westcott MC, Fitzke FW, Viswanathan AC, Hitchings RA. Reaction time prolongation for a motion stimulus in glaucoma subjects, and its relationship with elevation of the motion threshold. *Vision research*.

11. REFERENCES

- Airaksinen, P. J., and Heijl, A. (1983). Visual field and retinal nerve fibre layer in early glaucoma after optic disc haemorrhage. *Acta Ophthalmol Copenh* **61**, 186-94.
- Airaksinen, P. J., Tuulonen, A., and Alanko, H. I. (1992). Rate and pattern of neuroretinal rim area decrease in ocular hypertension and glaucoma. *Arch Ophthalmol* **110**, 206-10.
- Anderson, S. J., Drasdo, N., and Thompson, C. M. (1995). Parvocellular neurons limit motion acuity in human peripheral vision. *Proc Roy Soc Lond* **261**, 129-138.
- Baez, K. A., McNaught, A. I., Dowler, J. G., Poinoosawmy, D., Fitzke, F. W., and Hitchings, R. A. (1995). Motion detection threshold and field progression in normal tension glaucoma. *Br J Ophthalmol* **79**, 125-8.
- Balazsi, A. G., Rootman, J., Drance, S. M., Schulzer, M., and Douglas, G. R. (1984). The effect of age on the nerve fiber population of the human optic nerve. *Am J Ophthalmol* **97**, 760-6.
- Bengtsson, B., Olsson, J., Heijl, A., and Rootzen, H. (1997). A new generation of algorithms for computerized threshold perimetry, SITA. *Acta Ophthalmol Scand* **75**, 368-375.
- Bjerrum, J. (1889). Om en tilføelse til den sædvanlige synsfeltundersøgelse samt om synsfeltet ved glaukom. *Nordisk Ophthalmologisk Tidsskrift* **2**, 141-185.
- Bland, J. M., and Altman, D. G. (1986). Statistical methods for assessing agreement between two methods of clinical measurement. *Lancet* **1**, 307-10.
- Bosworth, C. F., Sample, P. A., and Weinreb, R. N. (1997). Motion perception thresholds in areas of glaucomatous visual field loss. *Vision Res.* **37**, 355-364.

- Brenton, R. S., and Argus, W. A. (1987). Fluctuations on the Humphrey and Octopus perimeters. *Invest Ophthalmol Vis Sci* **28**, 767-71.
- Bullimore, M. A., Wood, J. M., and Swenson, K. (1993). Motion perception in glaucoma. *Invest Ophthalmol Vis Sci* **34**, 3526-33.
- Butt, Z., McKillop, G., O'Brien, C., Allan, P., and Aspinall, P. (1995). Measurement of ocular blood flow velocity using colour Doppler imaging in low tension glaucoma. *Eye* **9**, 29-33.
- Casson, E. J., Johnson, C. A., and Shapiro, L. R. (1993). Longitudinal comparison of temporal-modulation perimetry with white-on-white and blue-on-yellow perimetry in ocular hypertension and early glaucoma. *J Opt Soc Am A* **10**, 1792-806.
- Chaturvedi, N., Hedley, W.-E. T., and Dreyer, E. B. (1993). Lateral geniculate nucleus in glaucoma. *Am J Ophthalmol* **116**, 182-8.
- Chauhan, B. C., and Drance, S. M. (1992). The relationship between intraocular pressure and visual field progression in glaucoma. *Graefes Arch Clin Exp Ophthalmol* **230**, 521-6.
- Chauhan, B. C., and House, P. H. (1991). Intratest variability in conventional and high-pass resolution perimetry. *Ophthalmology* **98**, 79-83.
- Chauhan, B. C., LeBlanc, R. P., McCormick, T. A., and Rogers, J. B. (1993a). Comparison of high-pass resolution perimetry and pattern discrimination perimetry to conventional perimetry in glaucoma. *Can J Ophthalmol* **28**, 306-311.
- Chauhan, B. C., Tompkins, J. D., LeBlanc, R. P., and McCormick, T. A. (1993b). Characteristics of frequency-of-seeing curves in normal subjects, patients with suspected glaucoma, and patients with glaucoma. *Invest Ophthalmol Vis Sci* **34**, 3534-40.
- Chen, J. C., Fitzke, F. W., and Bird, A. C. (1990). Long-term effect of acetazolamide in a patient with retinitis pigmentosa. *Invest Ophthalmol Vis Sci* **31**, 1914-8.

Chen, J. C., Fitzke, F. W., Pauleikhoff, D., and Bird, A. C. (1992). Functional loss in age-related Bruch's membrane change with choroidal perfusion defect .: *Invest Ophthalmol Vis Sci* **33**, 334-40.

Chuang, E. L., Sharp, D. M., Fitzke, F. W., Kemp, C. M., Holden, A. L., and Bird, A. C. (1987). Retinal dysfunction in central serous retinopathy .: *Eye* **1**, 120-5.

Coffey, M., Reidy, A., Wormald, R., Xian, W. X., Wright, L., and Courtney, P. (1993). Prevalence of glaucoma in the west of Ireland .: *Br J Ophthalmol* **77**, 17-21.

deJong, N., Greve, E. L., Hoyng, P. F., and Geijssen, H. C. (1989). Results of a filtering procedure in low tension glaucoma .: *Int Ophthalmol* **13**, 131-8.

De-Monasterio, F. M. (1979). Asymmetry of on- and off-pathways of blue-sensitive cones of the retina of macaques .: *Brain Res* **166**, 39-48.

Derrington, A. M., and Lennie, P. (1984). Spatial and temporal contrast sensitivities of neurones in lateral geniculate nucleus of macaque .: *J Physiol Lond* **357**, 219-40.

Drance, S. M., Douglas, G. R., Wijsman, K., Schulzer, M., and Britton, R. J. (1988). Response of blood flow to warm and cold in normal and low-tension glaucoma patients .: *Am J Ophthalmol* **105**, 35-9.

Fitzke, F. W., Crabb, D. P., McNaught, A. I., Edgar, D. F., and Hitchings, R. A. (1995). Image processing of computerised visual field data. .: *Br J Ophthalmol* **79**, 207-12.

Fitzke, F. W., and Kemp, C. M. (1989). Probing visual function with psychophysics and photochemistry .: *Eye* **3**, 84-9.

Fitzke, F. W., Poinosawmy, D., Ernst, W., and Hitchings, R. A. (1987). In “: Seventh International Visual Field Symposium” (E. L. Greve and A. Heijl, eds.), pp. 447-452. Martinus Nijhoff, Dordrecht.

Fitzke, F. W., Poinosawmy, D., Nagasubramanian, S., and Hitchings, R. A. (1989). In “: Perimetry Update 1989” (G. K. Kriegelstein, ed.), pp. 399-405. Kugler, Amsterdam.

Flammer, J., Drance, S. M., Fankhauser, F., and Augustiny, L. (1984a). Differential light threshold in automated static perimetry. Factors influencing short-term fluctuation .: *Arch Ophthalmol* **102**, 876-9.

Flammer, J., Drance, S. M., and Schulzer, M. (1984b). Covariates of the long-term fluctuation of the differential light threshold .: *Arch Ophthalmol* **102**, 880-2.

Flammer, J., Drance, S. M., and Zulauf, M. (1984c). Differential light threshold. Short- and long-term fluctuation in patients with glaucoma, normal controls, and patients with suspected glaucoma .: *Arch Ophthalmol* **102**, 704-6.

Flanagan, J. G., Wild, J. M., and Trope, G. E. (1993). The visual field indices in primary open-angle glaucoma .: *Invest Ophthalmol Vis Sci* **34**, 2266-74.

Frisen, L. (1991). High-pass resolution perimetry and age-related loss of visual pathway neurons .: *Acta Ophthalmol Copenh* **69**, 511-5.

Frisen, L. (1995). High-pass resolution perimetry central-field neuroretinal correlates .: *Vision Res* **35**, 293-301.

Galvin, S. J., Williams, D. R., and Coletta, N. J. (1996). The spatial grain of motion perception in human peripheral vision. . *Vision Res* **36**, 2251-2259.

Gliklich, R. E., Steinmann, W. C., and Spaeth, G. L. (1989). Visual field change in low-tension glaucoma over a five-year follow-up .: *Ophthalmology* **96**, 316-20.

Goldenfeld, M., Krupin, T., Ruderman, J. M., Wong, P. C., Rosenberg, L. F., Ritch, R., Liebmann, J. M., and Gieser, D. K. (1994). 5-Fluorouracil in initial trabeculectomy. A prospective, randomized, multicenter study .: *Ophthalmology* **101**, 1024-9.

Goldmann, H. (1945). Ein selbstregistrierendes Projektionskugelperimeter. *Ophthalmologica* , 71-79.

Goldstick, B. J., and Weinreb, R. N. (1987). The effect of refractive error on automated global analysis program G-1 .: *Am J Ophthalmol* **104**, 229-32.

Graham, S. L., Drance, S. M., Chauhan, B. C., Swindale, N. V., Hnik, P., Mikelberg, F. S., and Douglas, R. G. (1996). Comparison of psychophysical and electrophysiological testing in glaucoma. *Invest Ophthalmol Vis Sci* **37**, 2651-2662.

Graham, S. L., Drance, S. M., Wijsman, K., Douglas, G. R., and Mikelberg, F. S. (1995). Ambulatory blood pressure monitoring in glaucoma. The nocturnal dip. *Ophthalmology* **102**, 61-69.

Guzman, G., Javitt, J. C., and Glick, H. (1992). Glaucoma in the United States population: the economic burden of illness. *Invest Ophthalmol Vis Sci* **33 (suppl)**, 759.

Haefliger, I. O., and Flammer, J. (1991). Fluctuation of the differential light threshold at the border of absolute scotomas. Comparison between glaucomatous visual field defects and blind spots. *Ophthalmology* **98**, 1529-32.

Harms, H. (1940). Objektive perimetrie. *Ber. Deutsche Ophthalmologische Gesellschaft* **53**, 63-70.

Harwerth, R. S., and Smith, E. L. (1997). The relationship between visual defects and intraocular pressure in experimental glaucoma. *Invest Ophthalmol Vis Sci* **38 (suppl)**, 474.

Hayreh, S. S. (1994). Progress in the understanding of the vascular etiology of glaucoma. *Curr Opinion Ophthalmol* **5**, 26-35.

Hayreh, S. S., Zimmerman, M. B., Podhajsky, P., and Alward, W. L. (1994). Nocturnal arterial hypotension and its role in optic nerve head and ocular ischemic disorders. *Am J Ophthalmol* **117**, 603-24.

Heijl, A. (1985). The Humphrey Field Analyser: Concepts and clinical results. *Doc Ophthal Proc Ser* **43**, 55-64.

Heijl, A. (1993). Perimetric point density and detection of glaucomatous visual field loss. *Acta Ophthalmol Copenh* **71**, 445-50.

Heijl, A., and Krakau, C. E. T. (1975). An automatic perimeter for glaucoma visual field screening and control: Construction and clinical cases. *Graefe's Arch Clin Exp Ophthalmol* **197**, 13-23.

Henson, D. B., and Bryson, H. (1991). In "Perimetry Update" (R. P. Mills and A. Heijl, eds.), pp. 217- 220. Kugler & Ghendini, Amsterdam.

Henson, D. B., Evans, J., Chauhan, B. C., and Lane, C. (1996). Influence of fixation accuracy on threshold variability in patients with open angle glaucoma. *Invest Ophthalmol Vis Sci* **37**, 444-50.

Hitchings, R. A. (1992). Low tension glaucoma--its place in modern glaucoma practice. *Br J Ophthalmol* **76**, 494-6.

Hitchings, R. A. (1995). Therapeutic Rationale for normal-tension Glaucoma. *Curr op in ophthal* **6**, 67-70.

Hitchings, R. A., and Anderton, S. A. (1983). A comparative study of visual field defects seen in patients with low-tension glaucoma and chronic simple glaucoma. *Br J Ophthalmol* **67**, 818-21.

Hitchings, R. A., Wu, J., Poinoosawmy, D., and McNaught, A. (1995). Surgery for normal tension glaucoma. *Br J Ophthalmol* **79**, 402-6.

Hollows, F. C., and Graham, P. A. (1966). Intra-ocular pressure, glaucoma, and glaucoma suspects in a defined population. *Br J Ophthalmol* **50**, 570-86.

Holmin, C., and Krakau, C. E. (1979). Variability of glaucomatous visual field defects in computerized perimetry. *Albrecht Von Graefes Arch Klin Exp Ophthalmol* **210**, 235-50.

Holmin, C., and Krakau, C. E. (1982). Regression analysis of the central visual field in chronic glaucoma cases. A follow-up study using automatic perimetry. *Acta Ophthalmol Copenh* **60**, 267-74.

Jaeger, E. (1858). Ueber glaucom und seine heilung durch iridectomie. *Zeitscher Ges Aerzie zu Wien* **14**, 465-491.

James, C. B., and Smith, S. E. (1991). Pulsatile ocular blood flow in patients with low tension glaucoma. *Br J Ophthalmol* **75**, 466-70.

Johnson, C. A. (1994). Selective versus nonselective losses in glaucoma. *J. Glaucoma* **3**, S32-S44.

Johnson, C. A., Adams, A. J., Casson, E. J., and Brandt, J. D. (1993a). Blue-on-yellow perimetry can predict the development of glaucomatous visual field loss. *Arch Ophthalmol* **111**, 645-50.

Johnson, C. A., Adams, A. J., Casson, E. J., and Brandt, J. D. (1993b). Progression of early glaucomatous visual field loss as detected by blue-on-yellow and standard white-on-white automated perimetry. *Arch Ophthalmol* **111**, 651-6.

Johnson, C. A., Marshall, D., and Eng, K. M. (1995). In "Perimetry Update" (R. Mills and M. Wall, eds.), pp. 103-110. Kugler Publications, Amsterdam.

Johnson, C. A., and Samuels, S. J. (1997). Screening for glaucomatous visual field loss with frequency-doubling perimetry. *Invest Ophthalmol Vis Sci* **38**, 413-25.

Kaplan, E., and Shapley, R. M. (1982). X and Y cells in the lateral geniculate nucleus of macaque monkeys. *J Physiol Lond* **330**, 125-43.

Katz, J., Tielsch, J. M., Quigley, H. A., and Sommer, A. (1995). Automated perimetry detects visual field loss before manual Goldmann perimetry. *Ophthalmology* **102**, 21-6.

Kelly, D. H. (1981). Nonlinear visual responses to flickering sinusoidal gratings. *J Opt Soc Am* **71**, 1051-5.

Kerr, J. F., Winterford, C. M., and Harmon, B. V. (1994). Apoptosis. Its significance in cancer and cancer therapy [published erratum appears in *Cancer* 1994 Jun 15;73(12) 3108]. *Cancer* **73**, 2013-26.

Kerr, J. F., Wyllie, A. H., and Currie, A. R. (1972). Apoptosis a basic biological phenomenon with wide-ranging implications in tissue kinetics .: *Br J Cancer* **26**, 239-57.

Khaw, P. T., and Migdal, C. S. (1996). Current techniques in wound healing modulation in glaucoma surgery .*Current Opinion in Ophthalmology* **7**, 24-33.

Kitazawa, Y., Shirai, H., and Go, F. J. (1989). The effect of Ca²⁺ -antagonist on visual field in low-tension glaucoma .: *Graefes Arch Clin Exp Ophthalmol* **227**, 408-12.

Kitsos, G., Cote, G., and Psilas, K. (1988). [An example of dominant heredity in the transmission of primary open-angle glaucoma in a northwestern region of Greece] .: *J Fr Ophthalmol* **11**, 859-64.

Klein, B. E., Klein, R., Sponsel, W. E., Franke, T., Cantor, L. B., Martone, J., and Menage, M. J. (1992). Prevalence of glaucoma. The Beaver Dam Eye Study .: *Ophthalmology* **99**, 1499-504.

Lachenmayr, B., and Drance, S. (1992). The selective effects of elevated intraocular pressure on temporal resolution .: *German J Ophthalmol* **1**, 26-31.

Lachenmayr, B. J., and Gleissner, M. (1992). Flicker perimetry resists retinal image degradation .: *Invest Ophthalmol Vis Sci* **33**, 3539-42.

Lachenmayr, B. J., and Vivell, P. M. O. (1993). "Perimetry and its Clinical Correlations." Georg Thieme Verlag, Stuttgart.

Lee, B. B. (1993). Macaque ganglion cells and spatial vision .: *Prog Brain Res* **95**, 33-43.

Lee, B. B., Wehrhahn, C., Westheimer, G., and Kremers, J. (1993). Macaque ganglion cell responses to stimuli that elicit hyperacuity in man detection of small displacements .: *J Neurosci* **13**, 1001-9.

Leibowitz, H. M., Krueger, D. E., Maunder, L. R., Milton, R. C., Kini, M. M., Kahn, H. A., Nickerson, R. J., Pool, J., Colton, T. L., Ganley, J. P., Loewenstein, J. I., and

Dawber, T. R. (1980). The Framingham Eye Study monograph An ophthalmological and epidemiological study of cataract, glaucoma, diabetic retinopathy, macular degeneration, and visual acuity in a general population of 2631 adults, 1973-1975. *Surv Ophthalmol* **24**, 335-610.

Lennie, P. (1980). Parallel visual pathways a review. *Vision Res* **20**, 561-94.

Leske, M. C. (1983). The epidemiology of open-angle glaucoma a review. *Am J Epidemiol* **118**, 166-91.

Leske, M. C., Connell, A. M., Schachat, A. P., and Hyman, L. (1994). The Barbados Eye Study. Prevalence of open angle glaucoma. *Arch Ophthalmol* **112**, 821-9.

Leske, M. C., Connell, A. M., Wu, S. Y., Hyman, L. G., and Schachat, A. P. (1995). Risk factors for open-angle glaucoma. The Barbados Eye Study. *Arch Ophthalmol* **113**, 918-24.

Leventhal, A. G., Rodieck, R. W., and Dreher, B. (1981). Retinal ganglion cell classes in the Old World monkey morphology and central projections. *Science* **213**, 1139-42.

Levin, L. A., and Louhab, A. (1996). Apoptosis of retinal ganglion cells in anterior ischemic optic neuropathy. *Arch Ophthalmol* **114**, 488-91.

Livingstone, M., and Hubel, D. (1988). Segregation of form, color, movement, and depth anatomy, physiology, and perception. *Science* **240**, 740-9.

Livingstone, M. S., and Hubel, D. H. (1987). Psychophysical evidence for separate channels for the perception of form, color, movement, and depth. *J Neurosci* **7**, 3416-68.

Luntz, M. H., and Harrison, R. (1994). "Glaucoma surgery." World Scientific Publishing, New Jersey.

Maddess, T., and Henry, G. (1992). Performance of nonlinear visual units in ocular hypertension and glaucoma. *Clinical Vision Science* **7**, 371-383.

Mao, L. K., Stewart, W. C., and Shields, M. B. (1991). Correlation between intraocular pressure control and progressive glaucomatous damage in primary open-angle glaucoma. *Am J Ophthalmol* **111**, 51-5.

Marrocco, R. T. (1976). Sustained and transient cells in monkey lateral geniculate nucleus conduction velocities and response properties. *J Neurophysiol* **39**, 340-53.

McNaught, A. I., Westcott, M. C., Viswanathan, A. C., Fitzke, F. W., and Hitchings, R. A. (1995). Fine matrix mapping of foveal sensitivity loss in glaucoma. *Invest Ophthalmol Vis Sci* **36 (suppl)**, 1579.

Merigan, W. H. (1989). Chromatic and achromatic vision of macaques role of the P pathway. *J Neurosci* **9**, 776-83.

Merigan, W. H., Byrne, C. E., and Maunsell, J. H. (1991). Does primate motion perception depend on the magnocellular pathway? *J Neurosci* **11**, 3422-9.

Merigan, W. H., and Maunsell, J. H. (1990). Macaque vision after magnocellular lateral geniculate lesions. *Vis Neurosci* **5**, 347-52.

Merigan, W. H., and Maunsell, J. H. (1993). How parallel are the primate visual pathways? *Annu Rev Neurosci* **16**, 369-402.

Migdal, C., Gregory, W., and Hitchings, R. (1994). Long-term functional outcome after early surgery compared with laser and medicine in open-angle glaucoma. *Ophthalmology* **101**, 1651-6.

Mitchell, P., Smith, W., Attebo, K., and Healey, P. A. (1996). Prevalence of Open-angle Glaucoma in Australia. *Ophthalmology* **103**, 1661-1669.

Morgan, J. E. (1994). Selective cell death in glaucoma does it really occur? *Br J Ophthalmol* **78**, 875-9.

- Netland, P. A., Chaturvedi, N., and Dreyer, E. B. (1993). Calcium channel blockers in the management of low-tension and open-angle glaucoma. *Am J Ophthalmol* **115**, 608-13.
- O'Brien, C., Schwartz, B., Takamoto, T., and Wu, D. C. (1991). Intraocular pressure and the rate of visual field loss in chronic open-angle glaucoma. *Am J Ophthalmol* **111**, 491-500.
- Olsson, J., Bengtsson, B., Heijl, A., and Rootzen, H. (1997). An improved method to estimate frequency of false positive answers in computerized perimetry. *Acta Ophthalmol Copenh* **75**, 181-183.
- Olsson, J., Heijl, A., Bengtsson, B., and Rootzen, H. (1993). (P. R. Mills, ed.), pp. 551-556. Kugler & Ghendini, Amsterdam.
- Papermaster, D. S., and Nir, I. (1994). In "Apoptosis" (E. Milhich and R. H. Schimke, eds.), pp. 15-30. Plenum.
- Pederson, J. E., and Anderson, D. R. (1980). The mode of progressive disc cupping in ocular hypertension and glaucoma. *Arch Ophthalmol* **98**, 490-5.
- Pederson, J. E., and Gaasterland, D. E. (1984). Laser-induced primate glaucoma. I. Progression of cupping. *Arch Ophthalmol* **102**, 1689-92.
- Perry, V. H., Oehler, R., and Cowey, A. (1984). Retinal ganglion cells that project to the dorsal lateral geniculate nucleus in the macaque monkey. *Neuroscience* **12**, 1101-23.
- Phelps, C. D., and Corbett, J. J. (1985). Migraine and low-tension glaucoma. A case-control study. *Invest Ophthalmol Vis Sci* **26**, 1105-8.
- Pillunat, L. E., Stodtmeister, R., and Wilmanns, I. (1987). Pressure compliance of the optic nerve head in low tension glaucoma. *Br J Ophthalmol* **71**, 181-187.

Piltz, J. R., Drance, S. M., Douglas, G. R., and Milkelbergh, F. S. (1991). In "Perimetry Update" (R. Mills and A. Heijl, eds.), pp. 465-472. Kugler, Amsterdam/New York.

Potts, A. M., Hodges, D., Shelman, C. B., Fritz, K. J., Levy, N. S., and Mangnall, Y. (1972). Morphology of the primate optic nerve. I. Method and total fiber count. *Invest Ophthalmol* **11**, 980-8.

Quigley, H. A., Addicks, E. M., and Green, W. R. (1982). Optic nerve damage in human glaucoma. III. Quantitative correlation of nerve fiber loss and visual field defect in glaucoma, ischemic neuropathy, papilledema, and toxic neuropathy. *Arch Ophthalmol* **100**, 135-46.

Quigley, H. A., Addicks, E. M., Green, W. R., and Maumenee, A. E. (1981). Optic nerve damage in human glaucoma. II. The site of injury and susceptibility to damage. *Arch Ophthalmol* **99**, 635-49.

Quigley, H. A., Dunkelberger, G. R., and Green, W. R. (1988). Chronic human glaucoma causing selectively greater loss of large optic nerve fibers. *Ophthalmology* **95**, 357-63.

Quigley, H. A., Dunkelberger, G. R., and Green, W. R. (1989). Retinal ganglion cell atrophy correlated with automated perimetry in human eyes with glaucoma. *Am J Ophthalmol* **107**, 453-64.

Quigley, H. A., Enger, C., Katz, J., Sommer, A., Scott, R., and Gilbert, D. (1994). Risk factors for the development of glaucomatous visual field loss in ocular hypertension. *Arch Ophthalmol* **112**, 644-9.

Quigley, H. A., Katz, J., Derick, R. J., Gilbert, D., and Sommer, A. (1992). An evaluation of optic disc and nerve fiber layer examinations in monitoring progression of early glaucoma damage. *Ophthalmology* **99**, 19-28.

Quigley, H. A., Miller, N. R., and George, T. (1980). Clinical evaluation of nerve fiber layer atrophy as an indicator of glaucomatous optic nerve damage. *Arch Ophthalmol* **98**, 1564-71.

Quigley, H. A., Nickells, R. W., Kerrigan, L. A., Pease, M. E., Thibault, D. J., and Zack, D. J. (1995). Retinal ganglion cell death in experimental glaucoma and after axotomy occurs by apoptosis. *Invest Ophthalmol Vis Sci* **36**, 774-86.

Quigley, H. A., Sanchez, R. M., Dunkelberger, G. R., L'Hernault, N. L., and Baginski, T. A. (1987). Chronic glaucoma selectively damages large optic nerve fibers. *Invest Ophthalmol Vis Sci* **28**, 913-20.

Regan, D., Milner, B. A., and Heron, J. R. (1976). Delayed visual perception and delayed visual evoked potentials in the spinal form of multiple sclerosis and in retrobulbar neuritis. *Brain* **99**, 43-66.

Robert, Y., Steiner, D., and Hendrickson, P. (1989). Papillary circulation dynamics in glaucoma. *Graefes Arch Clin Exp Ophthalmol* **227**, 436-439.

Rönne, H. (1909). Ueber das Gesichtsfeld beim Glaukom. *Klin Mbl Augenheilk* **47**, 12-33.

Rossetti, L., Marchetti, I., Orzalesi, N., Scorpiglione, N., Torri, V., and Liberati, A. (1993). Randomized clinical trials on medical treatment of glaucoma. Are they appropriate to guide clinical practice? *Arch Ophthalmol* **111**, 96-103.

Ruben, S., and Fitzke, F. (1994). Correlation of peripheral displacement thresholds and optic disc parameters in ocular hypertension. *Br J Ophthalmol* **78**, 291-4.

Ruben, S. T., Hitchings, R. A., Fitzke, F., and Arden, G. B. (1994). Electrophysiology and psychophysics in ocular hypertension and glaucoma evidence for different pathomechanisms in early glaucoma. *Eye* **8**, 516-20.

Rudnicka, A. R., Steele, C. F., Crabb, D. P., and Edgar, D. F. (1992). Repeatability, reproducibility and intersession variability of the Allergan Humphrey ultrasonic biometer. *Acta Ophthalmol Copenh* **70**, 327-34.

Safran, A. B., Halfon, A., Safran, E., and Mermoud, C. (1995). Angioscotomata and morphological features of related vessels in automated perimetry. *Br J Ophthalmol* **79**, 118-24.

Sample, P. A., Ahn, D. S., Lee, P. C., and Weinreb, R. N. (1992). High-pass resolution perimetry in eyes with ocular hypertension and primary open-angle glaucoma. *Am J Ophthalmol* **113**, 309-16.

Sample, P. A., Madrid, M. E., and Weinreb, M. D. (1994a). Evidence for a variety of functional defects in glaucoma suspect eyes. *J. Glaucoma* **3**, S5-S18.

Sample, P. A., Martinez, G. A., and Weinreb, R. N. (1994b). Short-wavelength automated perimetry without lens density testing. *Am J Ophthalmol* **118**, 632-41.

Sample, P. A., Taylor, J. D., Martinez, G. A., Lusky, M., and Weinreb, R. N. (1993). Short-wavelength color visual fields in glaucoma suspects at risk. *Am J Ophthalmol* **115**, 225-33.

Sample, P. A., and Weinreb, R. N. (1992). Progressive color visual field loss in glaucoma. *Invest Ophthalmol Vis Sci* **33**, 2068-71.

Schiller, P. H., Logothetis, N. K., and Charles, E. R. (1990a). Functions of the colour-opponent and broad-band channels of the visual system. *Nature* **343**, 68-70.

Schiller, P. H., Logothetis, N. K., and Charles, E. R. (1990b). Role of the color-opponent and broad-band channels in vision. *Vis Neurosci* **5**, 321-46.

Schulzer, M. (1992). Intraocular pressure reduction in normal-tension glaucoma patients. The Normal Tension Glaucoma Study Group. *Ophthalmology* **99**, 1468-70.

Sheffield, V. C., Stone, E. M., Alward, W. L., Drack, A. V., Johnson, A. T., Streb, L. M., and Nichols, B. E. (1993). Genetic linkage of familial open angle glaucoma to chromosome 1q21-q31. *Nat Genet* **4**, 47-50.

Shingleton, B. J., Richter, C. U., Dharma, S. K., Tong, L., Bellows, A. R., Hutchinson, B. T., and Glynn, R. J. (1993). Long-term efficacy of argon laser trabeculoplasty. A 10-year follow-up study. *Ophthalmology* **100**, 1324-9.

Silverman, S. E., Trick, G. L., and Hart, W. M., Jr. (1990). Motion perception is abnormal in primary open-angle glaucoma and ocular hypertension. *Invest Ophthalmol Vis Sci* **31**, 722-9.

Sloan, I. (1939). Instruments and techniques for the clinical testing of light sense. III. an apparatus studying regional differences in light sense. *Arch Ophthalmol* **22**, 233-251.

Smith, R. J. (1986). The Lang lecture 1986. The enigma of primary open-angle glaucoma. *Trans Ophthalmol Soc UK* **105**, 618-33.

Smith, S. D., Katz, J., and Quigley, H. A. (1996). Analysis of progressive change in automated visual fields in glaucoma. *Invest Ophthalmol Vis Sci* **37**, 1419-28.

Sommer, A., Katz, J., Quigley, H. A., Miller, N. R., Robin, A. L., Richter, R. C., and Witt, K. A. (1991a). Clinically detectable nerve fiber atrophy precedes the onset of glaucomatous field loss. *Arch Ophthalmol* **109**, 77-83.

Sommer, A., Tielsch, J. M., Katz, J., Quigley, H. A., Gottsch, J. D., Javitt, J., and Singh, K. (1991b). Relationship between intraocular pressure and primary open angle glaucoma among white and black Americans. The Baltimore Eye Survey. *Arch Ophthalmol* **109**, 1090-5.

Spahr, J. (1973). Zur Automatisierung der Perimetrie: I. Die Anwendung eines computergesteuerten Perimeters. *Graefe's Arch Clin Exp Ophthalmol* **188**, 323-338.

Sturmer, J. (1985). What do glaucomatous visual fields really look like in fine-grid computerized profile perimetry? .: *Dev Ophthalmol* **12**, 1-47.

Teikari, J. M., and Airaksinen, J. P. (1992). Twin study on cup/disc ratio of the optic nerve head .: *Br J Ophthalmol* **76**, 218-20.

Thylefors, B., and Negrel, A. D. (1994). The global impact of glaucoma. *Bull World Hlth Org* **72**, 323-326.

Tielsch, J. M., Katz, J., Quigley, H. A., Javitt, J. C., and Sommer, A. (1995). Diabetes, intraocular pressure, and primary open-angle glaucoma in the Baltimore Eye Survey .: *Ophthalmology* **102**, 48-53.

Tielsch, J. M., Katz, J., Sommer, A., Quigley, H. A., and Javitt, J. C. (1994). Family history and risk of primary open angle glaucoma. The Baltimore Eye Survey .: *Arch Ophthalmol* **112**, 69-73.

Tielsch, J. M., Sommer, A., Katz, J., Royall, R. M., Quigley, H. A., and Javitt, J. (1991). Racial variations in the prevalence of primary open-angle glaucoma. The Baltimore Eye Survey .: *Jama* **266**, 369-74.

Traquair, H. M. (1931). Perimetry in the study of glaucoma .*Trans Ophthalmol Soc UK* , 585-599.

Trick, G. L., Steinman, S. B., and Amyot, M. (1995). Motion perception deficits in glaucomatous optic neuropathy .: *Vision Res* **35**, 2225-33.

Tuulonen, A., Lehtola, J., and Airaksinen, P. J. (1993). Nerve fiber layer defects with normal visual fields. Do normal optic disc and normal visual field indicate absence of glaucomatous abnormality? .: *Ophthalmology* **100**, 587-97.

Vingrys, A. J., and Demirel, S. (1993). In "Perimetry Update" (R. P. Mills, ed.), pp. 521-526. Kugler, Amsterdam.

Vogel, R., Crick, R. P., Newson, R. B., Shipley, M., Blackmore, H., and Bulpitt, C. J. (1990). Association between intraocular pressure and loss of visual field in chronic simple glaucoma. *Br J Ophthalmol* **74**, 3-6.

von Graefe, A. (1856). Ueber die Untersuchung des Gesichtsfeldes bei amblyopischen Affectionen. *Archive für Ophthalmologie* **II**, 258-298.

von Graefe, A. (1857). Ueber die Iridectomie bei Glaucom und uber den glaucoatosen prozess. *Graefe's Arch Ophthalmol* **3**, 456-560.

Wall, M., Jennisch, C. S., and Munden, P. M. (1997). Motion perimetry identifies nerve fiber bundlelike defects in ocular hypertension. *Arch Ophthalmol*. **115**, 26-33.

Wall, M., and Ketoff, K. M. (1995). Random dot motion perimetry in patients with glaucoma and in normal subjects. *Am J Ophthalmol* **120**, 587-96.

Wall, M., Maw, R. J., Stanek, K. E., and Chauhan, B. C. (1996). The psychometric function and reaction times of automated perimetry in normal and abnormal areas of the visual field in patients with glaucoma. *Invest Ophthalmol Vis Sci* **37**, 878-85.

Wall, M., and Montgomery, E. B. (1995). Using motion perimetry to detect visual field defects in patients with idiopathic intracranial hypertension a comparison with conventional automated perimetry. *Neurology* **45**, 1169-75.

Wang, J. J., Mitchell, P., and Smith, W. (1997). Is there an association between migraine headache and open-angle glaucoma? Findings from the Blue Mountains Eye Study. *Ophthalmology* **104**, 1714-9.

Weber, J., and Dobek, K. (1986). What is the most suitable grid for computer perimetry in glaucoma patients? *Ophthalmologica* **192**, 88-96.

Weber, J., Koll, W., and Kriegelstein, G. K. (1993). Intraocular pressure and visual field decay in chronic glaucoma. *Ger J Ophthalmol* **2**, 165-9.

Weber, J., and Rau, S. (1992). The properties of perimetric thresholds in normal and glaucomatous eyes .: *Ger J Ophthalmol* **1**, 79-85.

Weber, J., Schultze, T., and Ulrich, H. (1989). The visual field in advanced glaucoma .: *Int Ophthalmol* **13**, 47-50.

Werner, E. B., Saheb, N., and Thomas, D. (1982). Variability of static visual threshold responses in patients with elevated IOPs .: *Arch Ophthalmol* **100**, 1627-31.

Wessing, A., and Von Noorden, G. K. (1969). "Fluorescein Angiography of the Retina." C.V. Mosby, Saint Louis.

Whitaker, D., and Buckingham, T. (1987). Oscillatory movement displacement thresholds resistance to optical image degradation .: *Ophthalmic Physiol Opt* **7**, 121-5.

Wild, J. M., Cubbidge, R. P., and Pacey, E. (1996). Pointwise analysis of short-wavelength automated perimetry thresholds in a normal population .: *Invest Ophthalmol Vis Sci* **37**, S1087.

Wild, J. M., Hosking, S. L., Hutchings, N., Flanagan, J. G., and O'Donoghue, E. P. (1997). Long-term fluctuation in short-wavelength automated perimetry .: *Invest Ophthalmol Vis Sci* **38**, S571.

Wild, J. M., Moss, I. D., Whitaker, D., and O'Neill, E. C. (1995). The statistical interpretation of blue-on-yellow visual field loss .: *Invest Ophthalmol Vis Sci* **36**, 1398-410.

Wilson, M. R., Hertzmark, E., Walker, A. M., Childs, S.-K., and Epstein, D. L. (1987). A case-control study of risk factors in open angle glaucoma .: *Arch Ophthalmol* **105**, 1066-71.

Young, R. W. (1984). Cell death during differentiation of the retina in the mouse .: *J Comp Neurol* **229**, 362-73.

Zadnik, K., Mutti, D. O., and Adams, A. J. (1992). The repeatability of measurement of the ocular components .: *Invest Ophthalmol Vis Sci* **33**, 2325-33.

Zeyen, T. G., and Caprioli, J. (1993). Progression of disc and field damage in early glaucoma .: *Arch Ophthalmol* **111**, 62-5.

STIMULUS ORIENTATION CAN AFFECT MOTION SENSITIVITY IN GLAUCOMA

MARK C. WESTCOTT¹, FREDERICK W. FITZKE¹ and
ROGER A. HITCHINGS²

¹Institute of Ophthalmology; ²Moorfields Eye Hospital; London, UK

Abstract

Purpose: To investigate the effect of stimulus orientation on motion detection thresholds in primary open-angle glaucoma (POAG) patients and controls.

Methods: Line displacement thresholds were measured for a $2^\circ \times 2$ min arc stimulus moving parallel, perpendicularly, or at 45° to the orientation of the retinal nerve fiber layer (NFL), in a randomized order in eight normal controls and 17 POAG patients with reproducible glaucomatous Humphrey 24-2 field defects. Motion measurements were made at one of two locations in the visual field at an eccentricity of 15° .

Results: There was no effect of orientation on the motion detection thresholds in the controls. At the test location, the patients showed a range of motion displacement thresholds from normal to severely elevated. There was more marked threshold elevation for stimulus movement perpendicular to the NFL, compared to movement parallel to the NFL. This difference was significantly greater for patients with more pronounced threshold elevations (Spearman rank correlation coefficient of the difference in the thresholds at perpendicular orientation and parallel orientation versus the mean threshold was significant: $r = 0.55$, $p < 0.005$).

Conclusion: The authors have identified an orientation dependence sensitivity to motion in some patients with glaucoma. This effect may be useful in improving the sensitivity and specificity of motion sensitivity testing in identifying early glaucomatous damage.

Introduction

Abnormalities of motion detection have been shown to occur early in glaucoma using a variety of different stimuli.¹⁻⁵ We have previously identified significantly elevated motion detection thresholds in glaucoma patients using a line displacement test.^{1,2} We have also detected line displacement sensitivity losses in glaucoma in areas of the visual field which appear normal using conventional Humphrey luminance testing and these findings have been confirmed by other workers.^{1,5} Furthermore, we have demonstrated that elevated displacement thresholds can predict the future development of conventional visual field loss at the same locality with good sensitivity and specificity in initially normal fellow eyes of normal-tension glaucoma patients.⁶ These investigations of displacement thresholds in glaucoma have been obtained

Address for correspondence: F.W. Fitzke, Department of Visual Science, Institute of Ophthalmology, 11-43 Bath Street, London EC1V 9EL, UK

Perimetry Update 1996/1997, pp. 35-42
Proceedings of the XIIth International Perimetric Society Meeting
Würzburg, Germany, June 4-8, 1996
edited by M. Wall and A. Heijl
© 1997 Kugler Publications bv, Amsterdam/New York

using vertical line stimuli undergoing horizontal displacements. Other stimuli that have been used are random dot kinetograms, using stimuli in which the signal component moves in either a horizontal direction or one of four cardinal directions.^{3,4,7} The aim of this study was to investigate the effect of the orientation of the stimulus motion on the displacement thresholds in normals and glaucoma, as we are not aware of any previous studies specifically directed at this question.

Although mediated by motion sensitive pathways, line displacement thresholds may in addition be influenced by local luminance loss. Previous investigators have identified the existence of fine slit-like scotomas, beyond the resolution of conventional perimetry, that correspond to the orientation of retinal nerve fiber layer defects.⁸⁻¹⁰ We postulate that displacements of a line stimulus into a slit-like scotoma would contribute to impaired motion sensitivity, and that this effect would depend on the orientation of the line stimulus relative to the orientation of the slit-like scotoma. We hypothesize that the motion sensitivity of a line stimulus moving in a parallel direction to the nerve fiber layer would be less influenced by an underlying fine slit-like scotoma orientated along the axis of the nerve fiber, as illustrated by Figure 1a, than a stimulus moving perpendicular to the NFL and thus into the slit-like scotoma (Fig. 1b).

The aim of this study is to test the hypothesis.

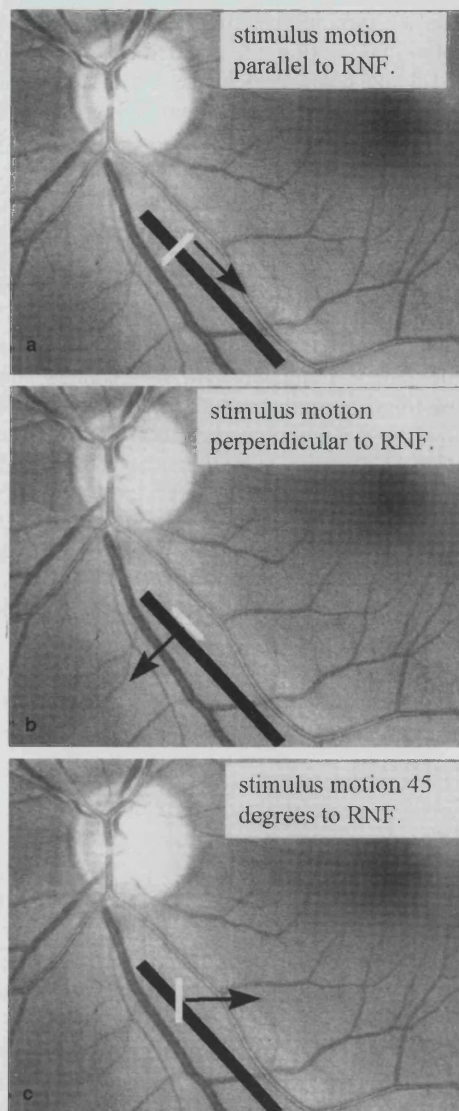
Patients and methods

Seventeen patients with an established diagnosis of primary open-angle glaucoma (POAG) and eight age-matched normal controls were prospectively recruited for this study. All patients had documented intraocular pressures above 21 mm Hg, glaucomatous optic disc cupping and early but reproducible glaucomatous visual field defects on Program 24-2 of the Humphrey Visual Field Analyzer. All controls had a normal ocular examination, intraocular pressures under 21 mm Hg and normal Humphrey 24-2 fields (normal glaucoma hemifield test and global indices within 95% CI for normal subjects) in both eyes.

All patients and controls had a corrected visual acuity in both eyes of $>6/9$ achieved with less than ± 4 diopters (D) spherical equivalent and less than 2 D of astigmatism. Patients with significant ocular pathology other than glaucoma were excluded.

The glaucoma patients had a mean age of 64.9 years with an SD of 7.4, and the control group 58.9 with an SD of 9.8 (non-significant difference at 0.05 level).

Peripheral line displacement thresholds were measured using a test described previously.^{1,2} A PC-generated $2^\circ \times 2$ min line is projected on a green phosphor display viewed at 1.24 meters. The background luminance is set at 7 C/m^2 and the stimulus luminance at 27 C/m^2 . The stimulus is presented in the superotemporal or inferotemporal fields at 15° eccentricity on the 30 or 330 meridian. The line stimulus undergoes instantaneous oscillatory displacements of magnitudes 0–18 min arc at a fixed constant frequency of 2.5 Hz. The subject is instructed to press a response button if movement is seen. Frequency of seeing curves are generated for ten magnitudes of displacement from 0 to 18 min arc, each presented ten times. A Probit fit analysis is applied and the displacement corresponding to 50% seen is taken as the threshold. A gimbal system was constructed to enable the monitor to be rotated through 360° . This allowed us to alter the orientation of the line and hence the



Figs. 1a to c. Left eye motion test in superotemporal field: vertical line stimulus shown in white superimposed on fundus image. The arrow shows the direction of the stimulus displacement, in relation to hypothetical slit-like scotoma orientated along the axis of the retinal nerve fiber layer shown in black. *a.* Stimulus motion parallel to orientation of retinal nerve fibers. *b.* Stimulus motion perpendicular to orientation of retinal nerve fibers. *c.* Stimulus motion 45° to orientation of retinal nerve fibers.

direction of the stimulus motion to an accuracy of within 1°, whilst keeping all other properties of the test constant. Patients underwent motion measurements in one glaucomatous eye in either the superotemporal location (14 patients) or in the inferotemporal location (three patients). Controls underwent motion sensitivity testing in one randomly chosen eye, all in the superotemporal location. All subjects

underwent an initial baseline motion sensitivity test with the stimulus in the vertical position undergoing horizontal motion (designated 0° axis). This was followed by tests with the stimulus rotated counterclockwise by 45° , 135° and 0° (*i.e.*, baseline again) with appropriate rest breaks, in a randomized order to avoid any consistent bias in learning or fatigue.

Analysis

Motion measurements were classified according to the direction of stimulus movement with respect to the orientation of the retinal nerve fibers at the test site. Figures 1a, b and c show the position of the stimulus for a motion test in the superotemporal field of the left eye: movement along the 135° meridian is labeled as 'motion parallel' to the retinal nerve fibers, stimulus movement along the 45° meridian is labeled as 'motion perpendicular' to the retinal nerve fibers, and stimulus movement along the 0° meridian is labeled as 'motion at 45° ' to the retinal NFL. This analysis is a valid supposition, assuming that the orientation of the retinal nerve fibers at the test location lies between 22.5° and 90° from the horizontal reference line.

We evaluated the Humphrey 24-2 luminance at the test site by examining the threshold sensitivities at the four Humphrey 24-2 test locations closest to the motion site. We defined the Humphrey 24-2 luminance at the motion test site as being abnormal if at least one of these four locations was contiguous with a hemifield cluster of depressed locations consisting of at least three adjacent depressed points on the STATPAC-2 pattern deviation plot with one point having a probability of $p < 1\%$ and two adjacent points having a probability of $p < 2\%$.¹¹

Results

The patients had early glaucomatous Humphrey 24-2 field loss with repeatable focal arcuate losses or a nasal step usually limited to one hemifield. The mean of the MDs of the Humphrey 24-2 fields of the glaucoma group was -4.87 dB, $SD \pm 3.37$ dB, (range $+3.37$ to -10.10 dB) which was significantly different from the control mean MD of -0.65 dB, $SD \pm 1.11$ dB (range $+1.11$ to -2.24 dB). (t test significant at $p < 0.001$.)

Fifteen of the seventeen patients had normal Humphrey luminances of the four closest Humphrey test locations to the motion test site, according to our definition (see analysis section), whilst two patients had scotomas extending into the motion test site.

Table 1 shows the mean motion displacement thresholds for the glaucoma and control groups for the orientations tested. The motion tests are classified according to the direction of the stimulus movement relative to the orientation of the retinal nerve fibers (RNF).

The means of the motion thresholds of the controls lie within our normal range of values for this test for all orientations tested.²

The means of the motion displacement thresholds of the glaucoma group were significantly elevated compared to the means of the control group for all orientations tested. There was a statistically significant negative linear correlation between the motion thresholds and the mean of the luminance thresholds at the four Humphrey

Table 1. Mean motion displacement thresholds and standard deviations in min arc for glaucoma and control groups by orientation, with statistical comparison between groups using Student's *t* test

Direction of motion relative to RNF	Controls (min arc)	Glaucoma (min arc)	Controls versus glaucoma
45° (1st measurement)	6.4 ± 1.2	11.7 ± 3.8	<i>t</i> = 5.18 <i>p</i> < 0.001
45° (2nd measurement)	5.0 ± 1.5	10.0 ± 4.3	<i>t</i> = 4.25 <i>p</i> < 0.001
Perpendicular	5.2 ± 1.8	11.3 ± 5.2	<i>t</i> = 4.32 <i>p</i> < 0.001
Parallel	5.6 ± 1.5	9.8 ± 3.7	<i>t</i> = 3.04 <i>p</i> = 0.006

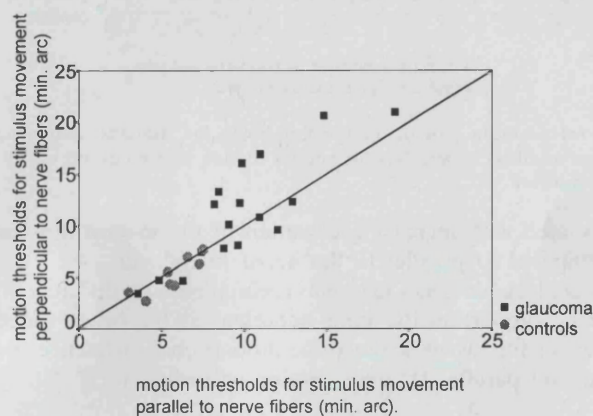


Fig. 2. Scatterplot of subject's thresholds for stimulus motion perpendicular versus motion parallel to retinal nerve fibers, with the line of unity.

24-2 test locations nearest the test site although the degree of correlation was poor ($r^2 = 0.22$, $p = 0.02$). There was no significant linear correlation between the motion thresholds and the Humphrey MD.

To illustrate the individual orientation-dependent variability we plotted the thresholds for stimulus motion perpendicular to the RNF against stimulus motion parallel to the RNF for all subjects (Fig. 2).

For quantitative analysis, we plotted the difference in the thresholds for stimulus motion perpendicular and parallel to the RNF versus the mean of the thresholds (Fig. 3). The zero on the *y* ordinate represents no difference between the motion threshold for motion perpendicular and parallel to the retinal NFL.

For subjects with normal motion thresholds (up to 8.6 min arc, equivalent to mean + 2 SD of controls), there is no orientation dependence, with all differences lying close to the zero ordinate.

In contrast, in patients with abnormally elevated motion thresholds (above 8.6 min arc), a number of the patients lie a considerable distance above the zero ordinate, with the motion threshold for stimulus motion perpendicular to the NFL more severely elevated compared to motion parallel to the NFL. Figure 3 also shows a trend of increasing elevation of motion threshold for stimulus motion perpendicular compared to parallel to the NFL (data points above zero ordinate) in patients with more pronounced threshold elevations. A Spearman rank correlation test showed that this was highly statistically significant ($r = 0.55$, $p < 0.005$). Thus increasing threshold

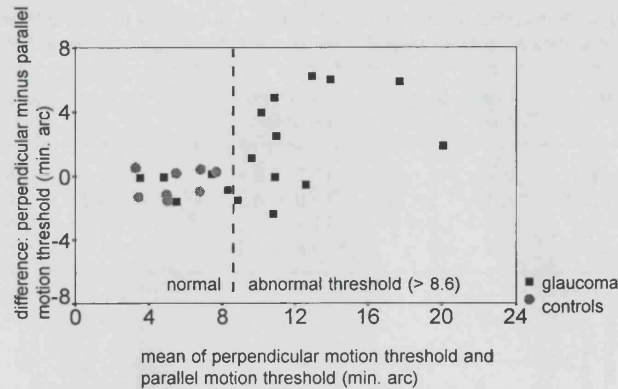


Fig. 3. Difference versus mean plot of motion thresholds for stimulus motion perpendicular and parallel to retinal nerve fibers. Subjects with normal motion thresholds lie to left of vertical reference lines of 8.6 min arc.

elevation is associated with increasing elevation of the motion threshold for motion perpendicular compared to parallel to the nerve fiber layer.

However, this analysis does not take into account smaller differences in the thresholds which may be proportionally more important at the lower range of threshold values. To correct for this, we calculated the proportional difference in the thresholds for perpendicular and parallel stimulus motion according to:

$$\text{Proportional difference (Pn)} = \frac{\text{perpendicular} - \text{parallel motion threshold}}{\text{perpendicular} + \text{parallel motion threshold}}$$

A proportional difference value of 0 represents no difference between the perpendicular and parallel thresholds, +1 represents maximally elevated perpendicular threshold relative to parallel, -1 maximally elevated parallel threshold relative to perpendicular.

Figure 4 is a plot of the proportional difference versus the mean of the perpendicular and parallel thresholds for all subjects. A ranked Spearman correlation test again showed a significant positive correlation between the proportional difference (Pn) and the mean. For all subjects (Spearman ranked correlation coefficient $r = 0.555$, $p = 0.004$). Reference lines indicate the mean ± 2 SD of the controls, with no controls lying outside this range. However, five of the glaucoma patients lie above the control mean +2 SD. These patients have a proportionally elevated motion threshold of at least 15% for stimulus motion perpendicular to the RNF compared to stimulus motion parallel to the RNF. No patients have a proportional difference below the mean -2 SD of the controls. We reviewed the results to identify any distinguishing characteristics of these five patients who showed the most pronounced orientation effect. There was no consistent order in the sequence of the tests performed in the five which may have influenced the results. Of these five patients with the most pronounced orientation effect, one had a scotoma extending to the four Humphrey 24-2 test locations closest to the site of motion testing, one had a nasal Humphrey field defect distant to the motion test site, and three patients had normal Humphrey field in the hemifield of the motion test. Although there was a weak correlation between the motion threshold and the Humphrey luminance at the motion test site,

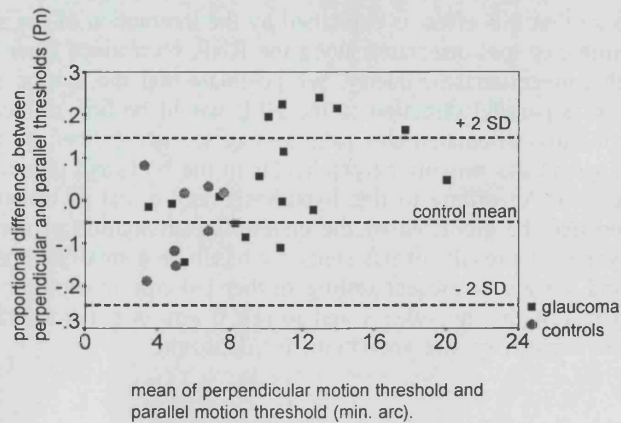


Fig. 4. Proportional difference versus mean plot of motion thresholds for stimulus motion perpendicular and parallel to retinal nerve fibers.

there was no significant correlation between the difference in the motion thresholds of the orientations tested and the Humphrey luminance at the motion test site.

Discussion

The aim of this study is to investigate the effect of stimulus orientation on motion detection thresholds in controls and patients with POAG. We performed tests of motion sensitivity using a line displacement test, with the line stimulus orientated parallel or perpendicularly to the orientation of the retinal NFL corresponding to the site of motion testing. We did not identify any clinically significant differences between the thresholds at perpendicular and parallel orientations in the controls, or in patients with normal motion thresholds. In patients with elevated motion thresholds, there was more marked threshold elevation for stimulus movement perpendicular to the NFL, compared to movement parallel to the NFL. This difference was statistically significantly greater for patients with more pronounced threshold elevations.

In five patients the motion thresholds for stimulus motion perpendicular to the retinal NFL were proportionately elevated by over 15%, compared with motion parallel to the NFL. This proportional elevation exceeded the 95% confidence limits we obtained with our controls. We did not identify any patients who demonstrated a proportional elevation of the threshold for motion parallel compared to perpendicular of this magnitude.

Although factors such as fatigue and learning may affect an individual's performance during the tests we think this is unlikely to explain this affect as the order in which the motion tests were performed was randomized, and we could not find any consistent order effects in the test sequence in these patients. There were no differences in the degree of astigmatic and spherical error in these patients (which was low in all groups) nor were there marked differences in the Humphrey luminance at the test site between the patients who showed an orientation effect and those who did not.

We hypothesize that this effect is explained by the interaction of the stimulus with fine slit-like luminance loss orientated along the RNF, on a much finer scale than is identifiable with conventional perimetry. We postulate that the motion sensitivity of a line stimulus in a parallel direction to the NFL would be less influenced by fine slit-like luminance loss orientated along the axis of the nerve fiber, as illustrated by Figure 1a, than a stimulus moving perpendicular to the NFL and thus into the luminance loss (Fig. 1b). According to this hypothesis, any effect of orientation on the motion threshold may be predicted by the underlying orientation of the retinal NFL at the site of testing. The results of this study are based on a small number of subjects tested so far, and we are at present testing further patients in multiple locations of the visual field to test this hypothesis and to see if any orientation effect is useful in improving the sensitivity and specificity in glaucoma.

Acknowledgments

Supported by the Friends of Moorfields, International Glaucoma Association and the Medical Research Council.

References

1. Fitzke FW, Poinoosawmy D, Ernst W, Hitchings RA: Peripheral displacement thresholds in normals, ocular hypertensives and glaucoma. In: Greve EL, Heijl A (eds) Seventh International Visual Field Symposium, pp 447-452. Dordrecht: Martinus Nijhoff/Dr W Junk Publ 1987
2. Fitzke FW, Poinoosawmy D, Nagasubramanian S, Hitchings RA: Peripheral displacement thresholds in glaucoma and ocular hypertension. In: Heijl A (ed) Perimetry Update 1988/89, pp 399-405. Amsterdam/Milano: Kugler & Ghedini 1989
3. Silverman SE, Trick GL, Hart WM: Motion perception is abnormal in primary open-angle glaucoma and ocular hypertension. *Invest Ophthalmol Vis Sci* 31/4:722-729, 1990
4. Bullimore MA, Wood JM, Svenson K: Motion perception in glaucoma. *Invest Ophthalmol Vis Sci* 34/13:3526-3533, 1993
5. Johnson CA, Marshall D, Eng KM: Displacement threshold perimetry in glaucoma using a Macintosh computer system and a 21-inch monitor. In: Mills RP, Wall M (eds) Perimetry Update 1994/1995, pp 103-110. Amsterdam/New York: Kugler Publ 1995
6. Baez KA, McNaught AI, Dowler JGF, Poinoosawmy D, Fitzke FW, Hitchings RA: Motion detection threshold and field progression in normal tension glaucoma. *Br J Ophthalmol* 79:125-128, 1995
7. Wall M, Ketoff K: Random dot motion perimetry in patients with glaucoma and in normal subjects. *Am J Ophthalmol* 120:587-596, 1995
8. Åsman P, Heijl A, Olsson J, Rootzén H: Spatial analyses of glaucomatous visual fields: a comparison with traditional field indices. *Acta Ophthalmol (Kbh)* 70:679-686, 1992
9. Weber J, Ulrich H: A perimetric nerve fibre bundle map. *Int Ophthalmol* 15:193-200, 1991
10. Tuulonen A, Lehtola J, Airaksinen PJ: Nerve fiber layer defects in normal visual fields. *Ophthalmology* 100:587-598 1993
11. Plitz JR, Drance SM, Douglas GR, Milkelbergh FS. The relationship of peripheral vasospasm, diffuse and localized visual field defects, and intraocular pressure in glaucomatous eyes. In: Mills RP, Heijl A (eds) Perimetry Update 1990/1991, pp 465-472. Amsterdam/New York/Milano: Kugler & Ghedini 1991.

High spatial resolution automated perimetry in glaucoma

Mark C Westcott, Andrew I McNaught, David P Crabb, Frederick W Fitzke, Roger A Hitchings

Abstract

Background—Automated perimetry is of fundamental importance in assessing visual function in glaucoma. A technique was evaluated to perform high spatial resolution automated perimetry to allow a more detailed assessment of the luminance sensitivity in selected regions of the visual field than is possible with conventional perimetry.

Method—High spatial resolution perimetry was performed using a Humphrey automated perimeter by measuring luminance sensitivity across a 9 by 9 degree custom grid of 100 test locations with a separation between adjacent locations of 1 degree. Quantitative analysis of the raw and Gaussian filtered thresholds was performed to assess the repeatability of the technique in normals, glaucoma suspects, and glaucoma patients.

Results—The testing protocol was well tolerated by all subjects. High spatial resolution perimetry in glaucomatous eyes demonstrated fine luminance sensitivity loss not suspected with conventional perimetry. High spatial resolution perimetry also demonstrated reproducible areas of sensitivity loss in some glaucomatous eyes in areas of the visual field which appear normal with conventional programmes. The repeatability of the technique correlated with mean threshold sensitivity and was substantially improved to clinically acceptable levels by Gaussian filtering the thresholds.

Conclusion—This technique of high spatial resolution perimetry allows the practical assessment of selected regions of the visual field at higher resolution than conventional perimetry, and may be clinically useful in glaucoma.

(*Br J Ophthalmol* 1997;81:452-459)

Conventional automated perimetry threshold examinations have a relatively low spatial resolution with 6 degrees separating adjacent test locations in the Humphrey 24-2 or 30-2 programs. Perimetry performed at higher resolution may obtain a more detailed picture of the luminance sensitivity in selected areas of the visual field which may be of particular interest to the clinician. We have performed automated threshold perimetry at higher spatial resolution in selected areas of the visual field by using test locations separated by a 1

degree field. This has allowed us to investigate scotomas in much finer detail than is possible with conventional perimetry. Previous investigators have performed perimetry at higher spatial resolution than conventional perimetry, and have identified subtle scotomas beyond the resolution of conventional perimetry.^{1,2} High spatial resolution perimetry has also been shown to identify scotomas that correspond to retinal nerve fibre layer defects in glaucoma suspects who have normal conventional perimetry.^{3,4} This suggests that high spatial resolution perimetry may have a number of distinct clinical advantages over conventional perimetry in the detection of the earliest glaucomatous field defects. However, previous techniques of high spatial resolution perimetry have been arduous for patients and have been limited by long testing times.^{1,3}

Another recognised problem of high spatial resolution perimetry has been a high intratest variability, with a corresponding poor repeatability of the threshold measurements.¹ We have developed a technique to perform high spatial resolution perimetry using a Humphrey perimeter to generate a fine matrix map (FMM) of a specified region of the visual field within an acceptable test time. This technique of fine matrix mapping has been applied to the study of a number of diseases.⁵⁻⁸

The aim of this study was to investigate the use of fine matrix mapping in glaucoma. We then investigated the use of image processing techniques to improve the repeatability of the high spatial resolution luminance measurements, as these techniques have already been shown to substantially improve the repeatability of conventional perimetry, with no additional cost in test time.^{8,9}

Patients and methods

SUBJECTS

The study was approved by the Moorfields Hospital ethics committee. We prospectively recruited patients with an established diagnosis of primary open angle glaucoma, Glaucoma suspects, and suitably age matched normal controls. All subjects were phakic and had uncorrected visual acuity of >6/9 in at least one eye. All glaucoma patients had documented intraocular pressure >21 mm Hg on at least one occasion before treatment, and evidence of asymmetrical glaucomatous field loss relative to the horizontal meridian on the most recent Humphrey 24-2 or 30-2 field. Glaucoma suspects had documented intraocular pressure >21 mm Hg on at least one occasion, and a

Department of Visual Science, Institute of Ophthalmology, London
M C Westcott
D P Crabb
F W Fitzke

Glaucoma Unit, Moorfields Eye Hospital, City Road, London
A I McNaught
R A Hitchings

Correspondence to:
F W Fitzke, Department of Visual Science, Institute of Ophthalmology, 11-43 Bath Street, London EC1V 9EL.

Accepted for publication
12 February 1997

normal visual field. A field was defined as normal if there were no clusters of significantly depressed locations in either hemifield on the pattern deviation plot of the 24-2 or 30-2 programs of the Humphrey field analyser. According to previously established criteria,¹⁰ a cluster was defined as being significantly depressed if it contained a minimum of three adjacent depressed test locations on the pattern standard deviation plot, with at least one location having a probability of abnormality of $p < 0.01$ and two locations of $p < 0.05$, excluding the peripheral ring of the HFA 30-2. Suitably age matched controls were recruited if they had no significant ocular history, had a normal ocular examination with an IOP less than 21 mm Hg and had normal Humphrey HFA 24-2 fields, according to the above criteria.

TECHNIQUE OF FINE MATRIX MAPPING

To perform fine matrix mapping perimetry the coordinates of four interlaced 5×5 grids of 25 locations (with a separation between adjacent points of 2 degrees) are entered in the 'custom grid' feature of a Humphrey automated perimeter. Each grid is offset relative to the other grids by 1 degree—in the x, y, or x and y axes. The patient undergoes examination using each of the four grids sequentially, using a target size III on a standard Humphrey bowl illumination of 31.5 apostilbs. Accuracy of fixation is monitored in the same way as conventional perimetry.

The data are converted into IBM format files which are merged using custom software to produce a single matrix with a separation between test locations of 1 degree. This FMM of 100 locations subtends a visual angle of 9 degrees by 9 degrees, approximately the area occupied by four locations in the 30-2 program. The numerical matrix is then used to generate a surface or contour plot showing the size and location of luminance sensitivity gradients across the grid. In addition to analysis of the raw data, the FMM thresholds underwent spatial processing using a 3 by 3 Gaussian (normal) filter. This technique has been used to filter conventional Humphrey 30-2 field data and FMMs, and has been described in detail previously.^{8,9}

EXAMINATION PROTOCOLS

High spatial resolution perimetry of the blind spot

We investigated the resolution of our technique by obtaining FMMs of the blind spot of a normal control. Luminance contour plots were superposed to the corresponding fundal landmarks, imaged with a confocal laser scanning ophthalmoscope (CLSO), using argon 488 nm light (Zeiss instruments).

High spatial resolution perimetry in patients with retinal nerve fibre layer defects

Two glaucoma patients with clinical evidence of focal retinal nerve fibre layer defects which did not correspond to a scotoma on conventional perimetry underwent high spatial resolution perimetry. Contour plots of the luminance sensitivity were superposed to CLSO images of the retinal nerve fibre layer defects.

Clinical evaluation of high spatial resolution perimetry

Further evaluation of high spatial resolution perimetry was performed in glaucomatous eyes, glaucoma suspect eyes, and normal controls. Each glaucoma patient underwent Humphrey field examination using the 30-2 program. One eye only was chosen for examination. If both eyes satisfied the above inclusion requirements, the eye showing the greatest contrast in defect depth/sizes across the horizontal midline was chosen. The two sites of fine matrix mapping were chosen as mirror image pairs across the horizontal meridian, and were performed at two eccentricities: the supero and inferotemporal site (Fig 3A), or the superior paracentral (Fig 5A) and inferior paracentral sites.

Each subject underwent examination first at one site with each of the four constituent 25 location grids performed successively with a short, standardised rest between each. The patient was then tested at the mirror image retinal location using the same protocol of four successive grids of 25 locations. The patient was then allowed a rest of at least 2 hours and then the whole protocol was repeated at the original retinal locations to assess intertest fluctuation and reproducibility. The time required for each constituent grid varied

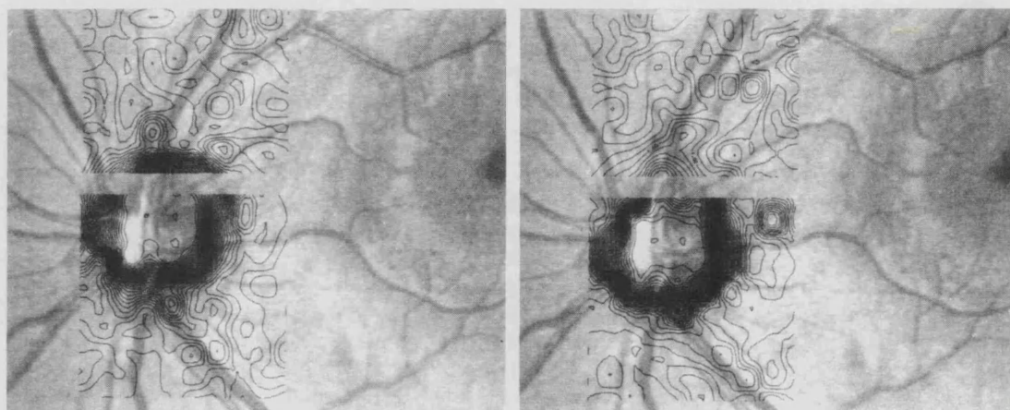


Figure 1 Contour plots of luminance sensitivity obtained from fine matrix maps (FMMs) performed over a blind spot of a normal control, superposed with a fundal scanning laser ophthalmoscope image (inverted) of the subject. Contour lines represent isoluminant points, in 1 dB increments. Note steep sensitivity gradients at the edge of the blind spot as well as more subtle linear defects corresponding in location and extent to the major retinal vascular trunks exiting the optic disc.

between each patient depending on the number of questions asked, related to defect size and depth. Excluding the brief rest between grids, the test time required on the Humphrey field analyser to obtain a FMM in the glaucoma patients was clinically acceptable and ranged from 8 to 26 minutes, with a mean of 20 minutes.

Glaucoma suspects were tested according to the same protocol using the mirror image pair of FMMs in the supero and inferotemporal site. In the absence of conventional field abnormalities, we chose this site as it has been reported to be one of the locations of early visual field defects in glaucoma suspects. We investigated the repeatability of the FMMs in age matched normal controls, using the same test sites, except that the testing was confined to either the superior or the inferior location of the mirror image pair.

Three dimensional surface plots of the FMMs for matched locations in the visual field were compared between groups. Quantitative analysis of the raw and Gaussian filtered

thresholds was performed, and the repeatability of the FMMs was assessed using the technique described by Bland and Altman (see below).

STATISTICAL ANALYSIS

The repeatability of the FMMs was investigated using the technique described by Bland and Altman.¹¹ This technique has been applied to investigate the repeatability of a number of measurements of ocular components,^{12,13} and has also been used to assess the repeatability of visual field measurements.^{9,14} To assess the repeatability of the first and second FMMs, the numeric difference between the first and second threshold sensitivities is calculated for each test location and plotted versus the mean of the sensitivities for that location. This graphical plot illustrates the spread and distribution of the pointwise differences. The repeatability of the FMMs is defined as the SD of the pointwise differences between the first and second FMM.

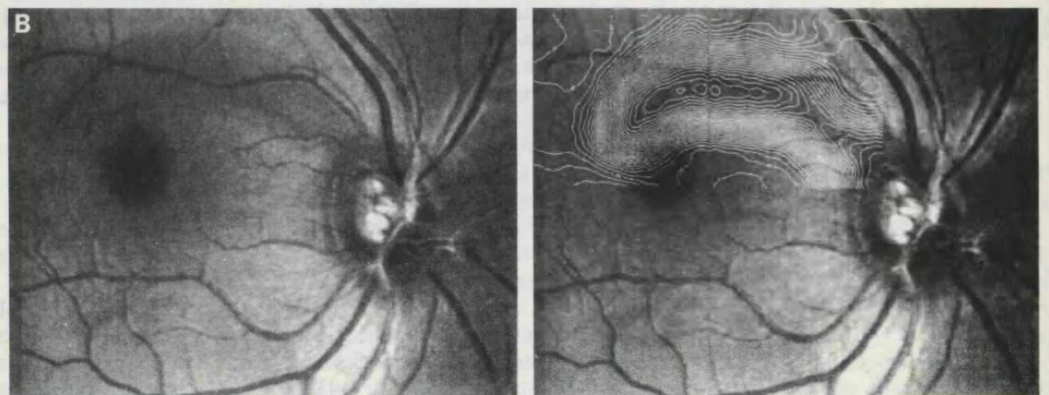
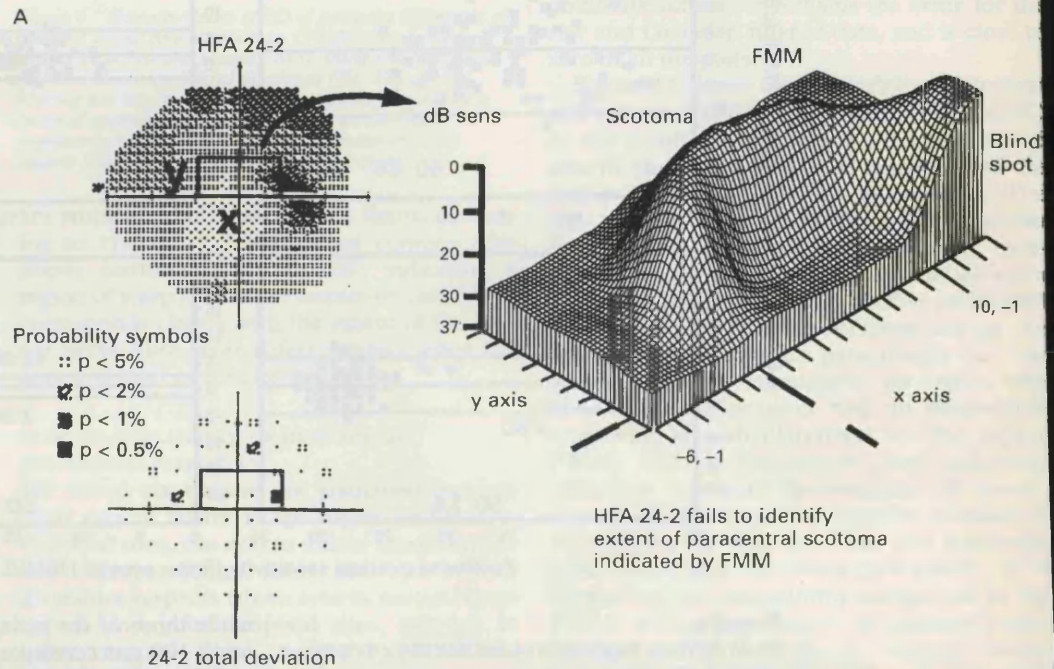


Figure 2 (A) Humphrey 24-2 grey scale and STATPAC 2 total deviation plot from glaucoma suspect right eye. Box indicates the site of two adjacent fine matrix maps (FMMs), which reveal an obvious superior arcuate extending from the blind spot, not shown by the Humphrey 24-2. Contour plots (B) have been superposed with a fundal scanning laser ophthalmoscope image (inverted) obtained from the patient. The sensitivity loss corresponds closely with the extent of a retinal nerve fibre layer defect.

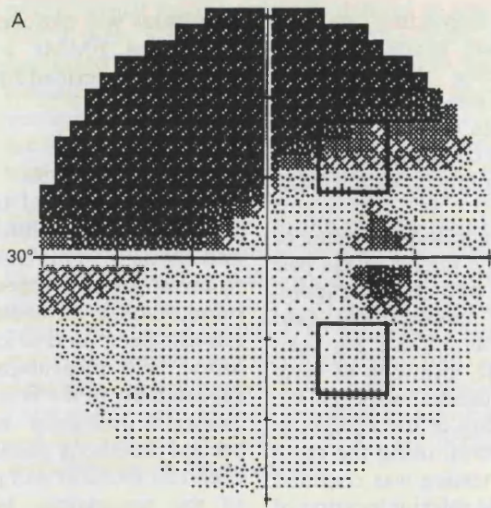
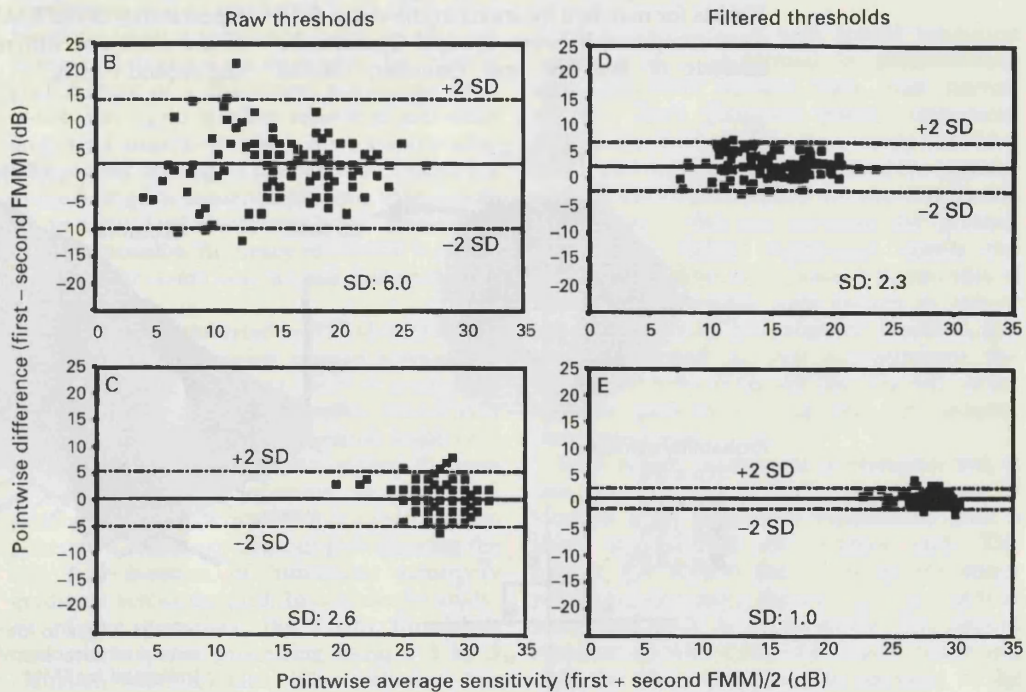


Figure 3 (A) Humphrey 30-2 of glaucomatous eye. Boxes indicate superior and inferior sites of fine matrix map (FMM). (B and D) show pointwise difference versus mean plots for first and second FMM in the superior location, for raw (B) and Gaussian filtered (D) thresholds. (C and E) show corresponding plots for raw (C) and filtered (E) thresholds of the FMMs in the inferior location. Broken lines indicate pointwise limits of agreement, represented as 2 SD, between the first and second FMMs.



Results

HIGH SPATIAL RESOLUTION PERIMETRY OF THE BLIND SPOT

Figure 1 shows the results of performing high spatial resolution perimetry around the blind spot of a normal subject. A contour map of the luminance sensitivity profile has been superposed to a fundal CFLO image (using argon 488 nm light, Zeiss instruments), obtained from the same eye. Accurate superposition was achieved by aligning anatomical landmarks such as the centre of the disc and fovea with the corresponding perimetric landmarks such as centre of the blind spot and fixation, which are plotted by the Humphrey field analyser. The resulting aligned contour map reveals well defined steep luminance sensitivity gradients at the edge of the blind spot as well as more subtle linear relative defects corresponding in location and extent to the major retinal vascular trunks exiting the optic disc. The diameters of the retinal arterioles at the disc margin are approximately 100 μ m,

while those of the retinal veins are about 130 μ m¹⁵; 100 μ m corresponds to a visual angle of approximately 0.3 degrees. This degree of resolution compares well with other reported techniques of high spatial resolution perimetry, which have also identified angioscotoma associated with the major retinal vascular trunks.¹⁶

HIGH SPATIAL RESOLUTION PERIMETRY IN PATIENTS WITH RETINAL NERVE FIBRE LAYER DEFECTS

Figure 2 illustrates the results of high spatial resolution perimetry performed in a glaucoma patient in an area of the visual field corresponding to a clinically visible focal retinal nerve fibre layer defect. A three dimensional surface plot of the luminance sensitivity (Fig 2A) reveals an obvious scotoma which is not apparent on the conventional Humphrey 24-2. The scotoma extends into the nasal field, in a region where the threshold sensitivities of the corresponding Humphrey 24-2 test locations

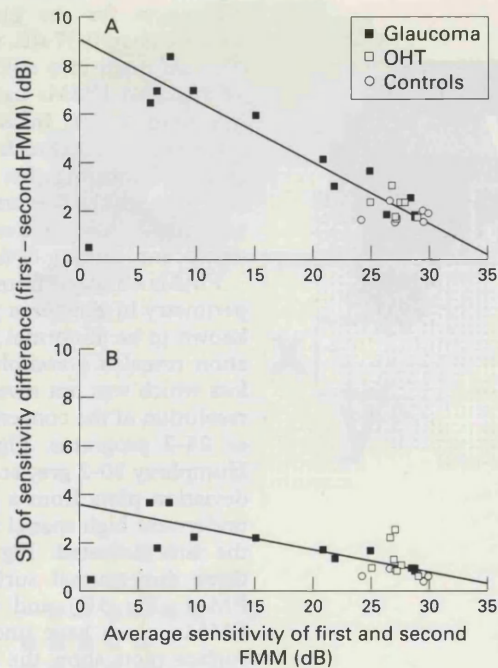


Figure 4 Summary plots of SD of pointwise differences of first and second fine matrix map (FMM) versus mean sensitivity of first and second FMM, using raw thresholds (A) and Gaussian filtered thresholds (B). The effect of filtering has been to reduce the magnitude of the SD by a factor of approximately 2, representing an twofold improvement in repeatability. Lines indicates the least squares linear fit of the data, excluding 1 outlier.

are within the 95% population limits, according to STATPAC 2. The aligned contour map shows contour lines (Fig 2B) indicating a region of steep luminance sensitivity loss which corresponds closely with the extent of the retinal nerve fibre layer defect imaged using the scanning laser ophthalmoscope.

CLINICAL EVALUATION OF HIGH SPATIAL RESOLUTION PERIMETRY

We tested six eyes of six glaucoma patients (four eyes in mirror image supero and inferotemporal sites, two eyes in mirror image supero and inferoparacentral sites), four eyes of four glaucoma suspects (three eyes in mirror image supero and inferotemporal sites, one eye in inferotemporal only), and six eyes of six normal subjects (four eyes in superotemporal site, one eye in inferotemporal site, one eye in inferoparacentral site). The mean ages by group were 64 (SD 4) years for the glaucoma patients, 58 (7) years for the glaucoma suspects, and 65 (6) years for the controls. These differences were not statistically significantly different.

Bland-Altman plots of the pointwise differences versus the pointwise means between the baseline and the repeat FMM were plotted for each subject at each location tested. The mean of the pointwise differences and the SD of the pointwise differences were calculated to provide summary statistics of repeatability for each individual. The mean of the pointwise differences reflects any systematic difference (bias) between the baseline and the subsequent FMM as might be expected if there was a considerable fatigue effect or learning effect. The

repeatability of the first and second FMM defined as the SD of the pointwise difference with lower values indicating better repeatability. The mean plus or minus 2 SD indicates the limits of agreement between the first and the second FMM.

Figures 3B-E are examples of the Bland-Altman plots of the first and second FMM performed for one glaucoma patient in two mirror image locations (Fig 3A) of the field. The superotemporal FMM overlaps an area of depressed threshold sensitivity on the Humphrey 30-2, while the inferotemporal FMM overlaps an area of normal Humphrey 30-2 threshold sensitivity.

The repeatability between the first and second FMMs is poorest, as indicated by the higher pointwise SD, in the location of depressed threshold sensitivity (Fig 3B) compared with the location of normal threshold sensitivity (Fig 3C). The effect of Gaussian filtering of the FMMs has been to substantially reduce the SDs (Fig 3D, E) representing an improved repeatability by a factor of 2 between the baseline and the second FMMs. The mean pointwise difference remains the same for the raw and Gaussian filtered data, and is close to zero in all the plots.

Figure 4A shows the repeatability of the first and second FMMs for all the subjects: the SD of the pointwise differences has been plotted against the mean threshold sensitivity of the first and second FMMs for each subject. The SD values are highest for the glaucoma patients, indicating poorer repeatability, compared with the controls. The one outlier was a glaucoma patient who had FMMs performed in a region of absolute sensitivity loss on the Humphrey 30-2. In this patient only one test location had a measurable sensitivity, the remaining test locations had no measurable sensitivity in either baseline or the repeat FMM, with a consequent zero pointwise difference between the majority of points. Figure 4A illustrates the negative correlation between the SD and the mean grid sensitivity which was highly significant ($p = 0.0001$, $R^2 = 0.91$); thus, the repeatability was poorest in the FMMs with greater degrees of luminance sensitivity loss. Figure 4B shows a similar correlation between the pointwise SD and the mean threshold sensitivity for the Gaussian filtered thresholds. Note that the values of the SD have been reduced by a factor of approximately 2. Designated limits of pointwise agreement between the first and the second FMMs can be defined as the mean plus or minus 2 SD, according to Bland and Altman.¹¹ The limits of agreement for all the Gaussian filtered FMM pairs are below 5 dB; thus, for each FMM pair, the difference between the first and second (repeat) sensitivity thresholds will be less than 5 dB at 95 out of 100 test locations, which we believe is clinically acceptable.

Calculated values for the means of the pointwise differences between the first and second FMMs, representing any overall bias between the first and the second grids were smallest for controls (mean -0.09 dB, range -0.58 dB to 0.50 dB). The means of the pointwise

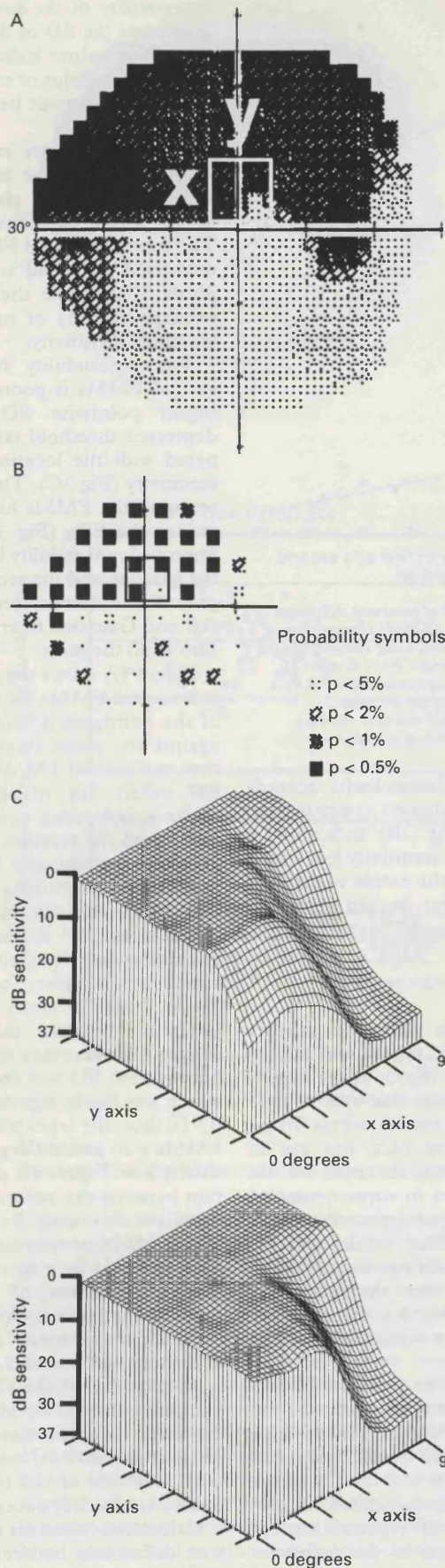


Figure 5 (A, B) show Humphrey 30-2 grey scale and STATPAC 2 total deviation plot from glaucomatous eye, with site of fine matrix map (FMM) indicated by box. (C, D) show three dimensional plots of Gaussian filtered luminance sensitivity thresholds of first and second FMMs. Note reproducible luminance profiles which reveal a steep sensitivity gradient from severely depressed sensitivity, represented as elevated area, to normal sensitivity.

differences for the glaucoma patients were higher (mean 0.37 dB, range -6.70 dB to 3.00 dB), although they still remained small; 11 of 12 repeated FMMs had a mean difference of less than 4 dB. In addition, there was no systematic departure from zero in any of the groups, indicating that there is no significant bias between the first and second FMMs which we might have expected if there was a significant learning or fatigue effect.

FMMs obtained from high spatial resolution perimetry in glaucoma patients at sites already known to be abnormal from the 30-2 examination revealed a complex profile of sensitivity loss which was not revealed by the low spatial resolution of the conventional Humphrey 30-2 or 24-2 programs. Figures 5A and B show Humphrey 30-2 grey scale and STATPAC 2 total deviation plots from a glaucoma patient who underwent high spatial resolution perimetry at the site indicated. Figures 5C and D show three dimensional surface plots of the first FMM (Fig 5C) and the second (Fig 5D) FMMs which have undergone filtering. Both surface plots show the complex profile of the scotoma, which reveals a steep sensitivity gradient from severely depressed to normal sensitivity. Much of the detail is reproducible. In two glaucomatous eyes of two patients fine matrix mapping in an area of normal sensitivity on the Humphrey 30-2 revealed an obvious reproducible defect that was not apparent with conventional perimetry. One example is shown by Figures 6A-E. High spatial resolution perimetry identified a localised reproducible scotoma, represented as an elevated area on the first FMM (Fig 6C) and second FMM (Fig 6D). The FMMs were performed in an area of field overlapped by four Humphrey 24-2 test locations which have normal threshold sensitivity (Fig 6A, B). Figure 6E shows a surface plot of a FMM from a normal control for comparison, which shows a uniform luminance profile.

Discussion

A number of investigators have used high spatial resolution perimetry to detect scotomas beyond the resolution of conventional perimetry.^{1,2} Airaksinen *et al* have used high spatial resolution perimetry to identify scotomas corresponding to retinal nerve fibre layer defects in glaucoma suspects who have normal conventional perimetry.³ In addition, high spatial resolution perimetry has also been shown to be clinically useful in defining residual small central isles of field in advanced glaucoma, which may be too small for conventional perimetry to map.^{17,18} However, a major disadvantage of some of these studies is that they have been arduous for patients and have required an extremely long test time. We have performed high resolution perimetry in a group of normal, glaucoma, and glaucoma suspect eyes using the technique of fine matrix mapping, performed on a Humphrey automated perimeter. We have identified glaucomatous luminance loss which was not revealed by the lower spatial resolution of the conventional Humphrey 30-2 or 24-2 programs. The testing

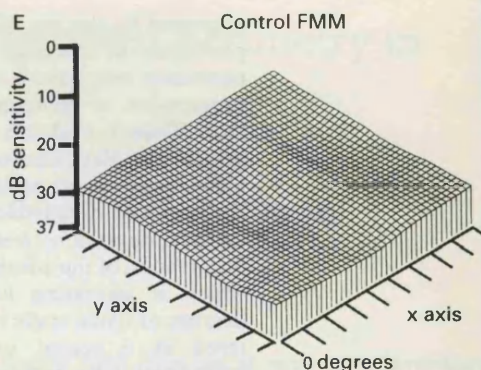
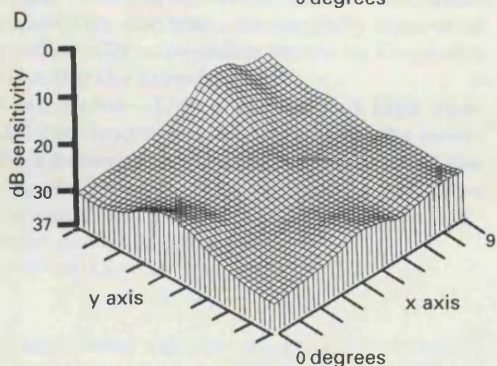
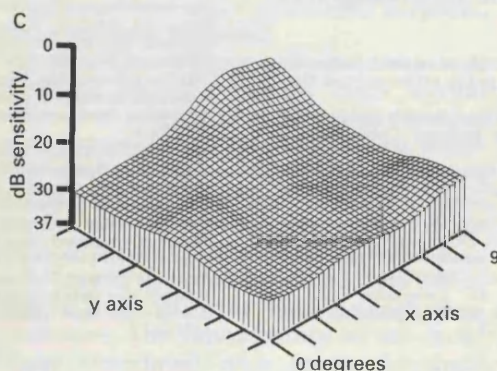
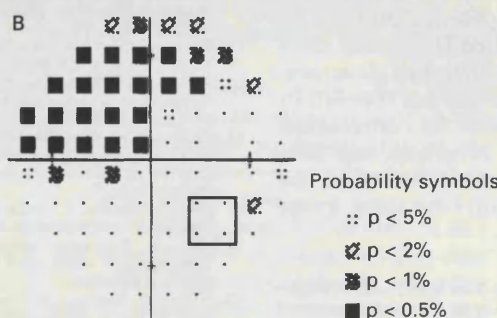
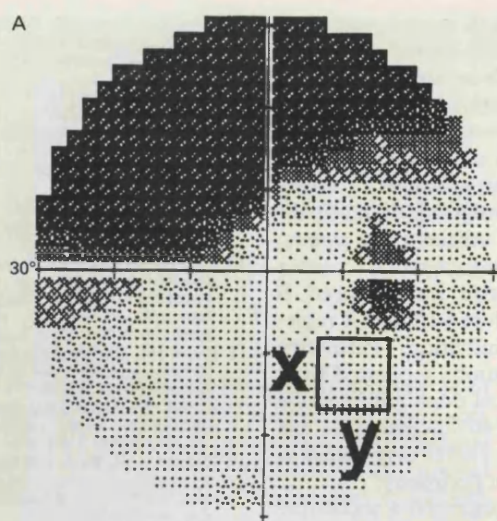


Figure 6 (A, B) Humphrey 30-2 grey scale and STATPAC2 total deviation plot from glaucomatous eye. Box indicates site of FMM which overlaps four Humphrey 30-2 test locations with normal threshold sensitivity. (C, D) show three dimensional plots of Gaussian filtered luminance sensitivity thresholds of first and second FMMs. Elevated areas indicate repeatable luminance defects, not seen in the FMM of an equivalent area of field from age matched normal controls (E).

protocol was well tolerated and all subjects performed the test within a test time of 30 minutes, which we believe is clinically acceptable. Previous investigations of high spatial resolution perimetry have demonstrated that one of the earliest perimetric disturbances in glaucoma is an elevated intratest variability, in some regions, even though the mean threshold sensitivity at the location may still remain

normal.¹⁹ A number of studies have shown that the intertest variability of conventional threshold perimetry is higher in glaucoma patients than in normals.²⁰⁻²³ In addition, the degree of intertest variability has been found to correlate with the degree of sensitivity loss.²² Our results confirm that a similar correlation exists between intertest variability and sensitivity loss in high spatial resolution perimetry, as has been suggested by other workers.¹ To date, the high intertest variability, and consequently low repeatability, in areas of glaucomatous sensitivity loss has been a significant limitation to the usefulness of high spatial resolution perimetry. Attempts to improve the precision of the threshold measurements by repeating the measurements is unlikely to be practical in high spatial resolution perimetry because of the already lengthy test times. We have investigated an alternative method to improve the repeatability using image processing techniques,⁸ which have already been shown to improve the repeatability of conventional automated perimetry.⁹ We have been able to obtain a marked improvement (by a factor of 2) in the repeatability of the technique, by applying a Gaussian filter to the high spatial resolution perimetry threshold data. This improvement in repeatability has been achieved at no extra cost in test time. We have obtained good reproducibility of the luminance profiles using this technique, and this has allowed us to obtain finer details of sensitivity loss which were not apparent on the lower spatial resolution of conventional perimetry. We believe that high spatial resolution perimetry fine matrix mapping may be a useful clinical tool, and may have a diagnostic role in the more detailed evaluation of equivocal areas of visual field of glaucoma patients and suspects. Previous studies have suggested that the test point density of conventional perimetry is not a limiting factor for the identification of the earliest glaucomatous field change. However, these studies used conversion criteria based on the development of field defects measured at conventional resolution.¹⁹ It remains to be determined whether the detection of conversion is

improved by the use of high spatial resolution perimetry. In addition, high spatial resolution perimetry may have a role in identifying early progression of glaucomatous visual field defects. There is evidence to suggest that the progression of glaucomatous defects, as detected using conventional perimetry, is slow.^{24 25} Using conventional perimetric programs with a spacing of 6 degrees between adjacent test points, progression of the advancing edge of a scotoma which is increasing in size must exceed 6 degrees of visual angle before a change is registered at a repeat examination. Perimetry performed using test locations separated by 1 degree offers the theoretical possibility that we may be able to identify advancement at the edge of a scotoma at an earlier stage than is possible with conventional perimetry.

In summary, we have described a technique for performing high spatial resolution perimetry which is clinically practical and can be performed on an unmodified Humphrey automated perimeter. We have identified glaucomatous luminance loss which was not revealed by the lower spatial resolution of the conventional Humphrey 30-2 or 24-2 programs, and have obtained a substantial improvement in the repeatability of the technique by using image processing techniques.

This work was supported by grants from the Friends of Moorfields, the Medical Research Council, the International Glaucoma Association, and the Royal National Institute for the Blind.

- 1 Sturmer J. What do glaucomatous visual fields really look like in fine-grid computerized profile perimetry? *Dev Ophthalmol* 1985;12:1-47.
- 2 Weber J, Dobek K. What is the most suitable grid for computer perimetry in glaucoma patients? *Ophthalmologica* 1986;192:88-96.
- 3 Airaksinen PJ, Heijl A. Visual field and retinal nerve fibre layer in early glaucoma after optic disc haemorrhage. *Acta Ophthalmol (Copenh)* 1983;61:186-94.
- 4 Tuulonen A, Lehtola J, Airaksinen PJ. Nerve fiber layer defects with normal visual fields. Do normal optic disc and normal visual field indicate absence of glaucomatous abnormality? *Ophthalmology* 1993;100:587-97.
- 5 Chen JC, Fitzke FW, Bird AC. Long-term effect of acetazolamide in a patient with retinitis pigmentosa. *Invest Ophthalmol Vis Sci* 1990;31:1914-8.
- 6 Chen JC, Fitzke FW, Pauleikhoff D, Bird AC. Functional loss in age-related Bruch's membrane change with choroidal perfusion defect. *Invest Ophthalmol Vis Sci* 1992;33:334-40.
- 7 Chuang EL, Sharp DM, Fitzke FW, Kemp CM, Holden AL, Bird AC. Retinal dysfunction in central serous retinopathy. *Eye* 1987;1 (Pt 1):120-5.
- 8 Fitzke FW, Kemp CM. Probing visual function with psychophysics and photochemistry. *Eye* 1989;3 (Pt 1):84-9.
- 9 Fitzke FW, Crabb DP, McNaught AI, Edgar DF, Hitchings RA. Image processing of computerised visual field data. *Br J Ophthalmol* 1995;79:207-12.
- 10 Plitz JR, Drance SM, Douglas GR, Milkelbergh FS. The relationship of peripheral vasospasm, diffuse and localized visual field defects, and intraocular pressure in glaucomatous eyes. In: Mills R, Heijl A, eds. *Perimetry update*. Amsterdam/New York: Kugler, 1990/1991:465-72.
- 11 Bland JM, Altman DG. Statistical methods for assessing agreement between two methods of clinical measurement. *Lancet* 1986;1:307-10.
- 12 Zadnik K, Mutti DO, Adams AJ. The repeatability of measurement of the ocular components. *Invest Ophthalmol Vis Sci* 1992;33:2325-33.
- 13 Rudnicka AR, Steele CF, Crabb DP, Edgar DF. Repeatability, reproducibility and interession variability of the Allergan Humphrey ultrasonic biometer. *Acta Ophthalmol Copenh* 1992;70:327-34.
- 14 Flanagan JG, Wild JM, Trope GE. The visual field indices in primary open-angle glaucoma. *Invest Ophthalmol Vis Sci* 1993;34:2266-74.
- 15 Wessing A, Von Noorden GK. *Fluorescein angiography of the retina*. St Louis: CV Mosby, 1969.
- 16 Safran AB, Halfon A, Safran E, Mermoud C. Angioscotomata and morphological features of related vessels in automated perimetry. *Br J Ophthalmol* 1995;79:118-24.
- 17 McNaught AI, Westcott MC, Viswanathan AC, Fitzke FW, Hitchings RA. Fine matrix mapping of foveal sensitivity loss in glaucoma. *Invest Ophthalmol Vis Sci* 1995;36(suppl)(1579).
- 18 Weber J, Schultze T, Ulrich H. The visual field in advanced glaucoma. *Int Ophthalmol* 1989;13:47-50.
- 19 Heijl A. Perimetric point density and detection of glaucomatous visual field loss. *Acta Ophthalmol Copenh* 1993;71:445-50.
- 20 Holmin C, Krakau CE. Variability of glaucomatous visual field defects in computerized perimetry. *Graefes Arch Klin Exp Ophthalmol* 1979;210:235-50.
- 21 Werner EB, Saheb N, Thomas D. Variability of static visual threshold responses in patients with elevated IOPs. *Arch Ophthalmol* 1982;100:1627-31.
- 22 Flammer J, Drance SM, Fankhauser F, Augustiny L. Differential light threshold in automated static perimetry. Factors influencing short-term fluctuation. *Arch Ophthalmol* 1984;102:876-9.
- 23 Flammer J, Drance SM, Zulauf M. Differential light threshold. Short- and long-term fluctuation in patients with glaucoma, normal controls, and patients with suspected glaucoma. *Arch Ophthalmol* 1984;102:704-6.
- 24 Smith SD, Katz J, Quigley HA. Analysis of progressive change in automated visual fields in glaucoma. *Invest Ophthalmol Vis Sci* 1996;37:1419-28.
- 25 Migdal C, Gregory W, Hitchings R. Long-term functional outcome after early surgery compared with laser and medicine in open-angle glaucoma. *Ophthalmology* 1994;101:1651-6.



Abnormal motion displacement thresholds are associated with fine scale luminance sensitivity loss in glaucoma

Mark C. Westcott ^{a,*}, Frederick W. Fitzke ^a, Roger A. Hitchings ^b

^a *Department of Visual Science, Institute of Ophthalmology, 11–43 Bath Street, London EC1 V9EL, UK*

^b *Moorfields Eye Hospital, London, UK*

Received 7 April 1997; received in revised form 11 August 1997; accepted 5 January 1998

Abstract

This study tests the hypothesis that abnormal motion displacement thresholds coexist with scotomas on a finer spatial scale than is measurable by conventional Humphrey perimetry. Eighteen patients with primary open angle glaucoma in one eye, and 18 age matched normal controls underwent motion displacement threshold testing and high spatial resolution perimetry. The motion displacement thresholds were significantly elevated in the glaucoma eyes, in 73% this exceeded normal limits. Ten glaucoma eyes had normal Humphrey 24-2 field nearest the motion test site: of these seven had abnormally elevated motion displacement thresholds and six had fine scale threshold depressions detected with high spatial resolution perimetry. This result suggests that glaucomatous elevations of motion displacement threshold may be present in areas of normal Humphrey 24-2 field, and this may coexist with measurable scotomas beyond the resolution of conventional Humphrey perimetry in some, but not all patients. © 1998 Elsevier Science Ltd. All rights reserved.

Keywords: Motion perception; Glaucoma; Perimetry

1. Introduction

Histological evidence has shown that a substantial number of retinal ganglion cell axons may be lost in glaucoma before a visual field defect can be detected using conventional methods of both manual and full threshold automated perimetry [1,2].

This finding has prompted the search for more sensitive tests of early glaucomatous visual damage. A variety of functional deficits have been identified in early glaucoma using psychophysical tests to isolate a particular aspect of visual function. Differences between normals and glaucoma patients have been reported in short wavelength sensitivity using short wavelength automated perimetry [3–5], temporal sensitivity using flicker and temporal modulation perimetry [6–8], visual resolution using high-pass resolution perimetry [9], and motion perception [10–19]. This evidence supports the suggestion that tests that isolate one particular function may identify the earliest losses, because other spared

visual systems are prevented from compensating for those compromised in glaucoma (Section 4).

We have previously used a line displacement test to show that motion displacement thresholds (MDTs) are significantly elevated in glaucoma [10,11,20]. Experimental work in primates has shown that the perception of line displacement motion is primarily a function of magnocellular ganglion cells [21,22]. This is consistent with evidence from other studies that the magnocellular system is primarily responsible for the perception of motion [23,24], although recent work by Merigan and colleagues suggests that this may be an oversimplification [25].

Other investigators have used random dot kinetograms to test motion perception. Initial studies used random dot kinetograms to simultaneously test large areas of the central visual field, and have reported significantly elevated coherence thresholds in glaucoma patients [12,16]. One criticism of this type of testing is that it may perform poorly in patients with early focal scotomas [18]. Graham and colleagues recently reported that random dot kinetogram testing of motion coherence thresholds of the central field performed little

* Corresponding author. Fax: +44 171 6086834.

better than chance in identifying patients with early focal glaucomatous field defects [26]. This finding supports previous work by Bullimore and colleagues, who found that random dot kinetogram testing of coherence thresholds and maximum displacement thresholds did not discriminate between patients and controls. Instead they reported better results using smaller field sizes to measure minimum displacement thresholds, which were elevated outside the normal range in 10 of 15 glaucoma patients.

Wall and colleagues have used random dot kinetograms to test focal areas of field, and have reported early motion losses in glaucoma [17]. Recently Bosworth and colleagues performed focal random dot kinetogram testing on 14 patients, and were able to show that motion coherence thresholds were significantly poorer in areas of known visual field loss compared to eccentrically matched areas of relative field sparing [18]. However they did not comment on whether coherence thresholds in areas of relative field sparing differed from controls. One limitation of random dot kinetograms is the inherently low spatial resolution of the test, which is limited by the size of the smallest area that can be tested. In the test described by Bosworth and colleagues, the size of the test region was 7.4° , which may encompass one, two, or up to four points on the standard Humphrey test. An alternative approach we have taken is to use line stimuli to measure motion displacement thresholds. The higher spatial resolution of a line stimulus has the advantage of making it possible to evaluate small localized regions of field.

We have previously used a line displacement test to demonstrate elevated motion displacement thresholds in glaucoma [10,11,20]. This test has also identified elevated motion displacement thresholds in glaucoma in areas of normal Humphrey 24-2 visual field, which correspond in location to nerve fiber layer defects [10]. These findings have been confirmed by other workers using both line displacement tests [15] and random dot kinetograms [17,19].

In addition, we have shown that elevated motion displacement thresholds, as measured by a line displacement test, can predict the future development of conventional visual field loss at the same locality in normal tension glaucoma patients [27]. Elevated motion displacement thresholds have also been correlated with glaucomatous optic disc changes in ocular hypertensive patients, before scotomata can be detected using conventional visual field assessment [14].

Although there is considerable evidence that abnormal motion sensitivity can be identified in areas of normal Humphrey 24-2 field, there may be field threshold losses on a finer scale than can be measured by the spacing of the test locations on the Humphrey 24-2. This raises the question of whether motion abnormalities coexist with fine scale depressions of Humphrey

threshold, which may not be identifiable with conventional Humphrey field testing.

The aim of this study is to test the hypothesis that elevated motion displacement thresholds coexist with fine scale depressions of Humphrey threshold, which may predate the appearance of scotomas detected with conventional perimetry.

Previous investigators have used high spatial resolution perimetry to identify fine scale scotomas in apparently normal areas of the field on the Humphrey 24-2, although these results were not examined in the context of other psychophysical abnormalities [28,29].

We have carried out high spatial resolution perimetry using a technique we have previously used in the study of number of diseases [30–33].

2. Methods

2.1. Subjects

The study was approved by the Moorfields Hospital Ethics Committee and followed the tenets of the Declaration of Helsinki. After informed consent was obtained, 18 primary open angle glaucoma (POAG) patients and 18 normal controls agreed to participate in the study.

Patients with an established diagnosis of POAG were prospectively recruited for this study if they had at least two Humphrey 24-2 fields with a localized glaucomatous visual field defect in one eye, and a normal Humphrey HFA 24-2 field in the fellow eye. To define a scotoma we used the pattern deviation plot on the Humphrey 24-2, according to a cluster definition used in a number of previous studies [17,26]. A scotoma required a minimum cluster of three adjacent points depressed on the pattern deviation plot at the $P < 0.02$ level (or at least 5 dB), with one of the points depressed at the $P < 0.01$ level (or at least 10 dB); or two adjacent points depressed $P < 0.01$ level (or at least 10 dB). In addition, the selection criteria included that the cluster of abnormal points could not cross the horizontal meridian.

All fields had to meet standard reliability criteria of $< 20\%$ fixation losses, $< 33\%$ false negatives, $< 33\%$ false positives. All patients had documented evidence of an intra-ocular pressure > 21 mm Hg. on at least one occasion in the glaucoma eye with glaucomatous optic disc cupping characterized by a vertical cup/disc ratio ≥ 0.6 , or cup disc asymmetry between the two eyes of greater than 0.2.

Fifteen out of eighteen glaucomatous eyes, and 10/18 of the glaucoma suspect fellow eyes were being treated with topical antihypertensives. Patients currently using miotics were excluded, as were patients with significant ocular pathology other than glaucoma or evidence of secondary glaucoma.

Suitably age matched controls were recruited if they had no significant ocular history, had a normal ocular examination with an IOP less than 21 mmHg and had normal Humphrey HFA 24-2 fields, with no identifiable clusters of depressed points according to the above definition.

The mean Humphrey 24-2 MD for the glaucoma eyes was -5.8 ± 2.5 dB, range -11.1 to -3.0 dB, which was significantly different ($P < 0.0001$) from the glaucoma suspect eyes (mean MD -1.7 ± 1.7 dB, range -4.2 to $+1.3$ dB) and the controls (mean MD -0.5 ± 1.3 dB, range -2.7 to $+2.5$ dB). The mean MD of the glaucoma suspect eyes was not statistically different from the control mean MD. A brief description of the site of the field defects on the Humphrey 24-2 fields of the glaucoma eyes is given Table 1. In summary, eight of 18 glaucoma eyes had scotomas involving the Humphrey test locations closest to the MDT test site, whilst the remaining ten glaucoma eyes had no scotomas extending to those test locations closest to the MDT test site.

The mean age of the 18 patients was 59.7 ± 12.2 years, with a range 30.6–78.8 years. The mean age of the 18 controls was 57.8 ± 11.5 years, with a range of 31.3–74.9 years. This difference was not statistically significant ($P = 0.63$).

All patients and controls had a corrected visual acuity in both eyes of $\geq 6/9$ achieved with less than ± 4 dioptres spherical equivalent and less than two dioptres of astigmatism.

2.2. Motion displacement testing

We measured motion displacement thresholds using a single line displacement test presented at 15° eccentricity in the superotemporal field. This site was chosen as previous results have identified significantly elevated motion displacement thresholds at this location in glaucoma patients [10,11]. This location also corresponds to an area of retina which is a common site of glaucoma-

tous retinal nerve fiber layer defects, and we have previously reported that these defects can be associated with elevated motion displacement thresholds, even in areas of normal Humphrey 24-2 visual field [10].

The MDT test is performed using a computer generated 2° by 2 min line stimulus presented on a green phosphor screen. The stimulus was presented in the superotemporal field at 15° eccentricity on the 30° meridian. The stimulus undergoes brief lateral displacements from 0 to 18 min of arc and the subject is instructed to press a response button when movement is seen. All subjects were given a suitable instruction period and then underwent a test which consisted of ten presentations each of ten different displacements in 2 min arc intervals from 0 to 18 min of arc presented in a random order. The subject was observed for the duration of the test by the experimenter to ensure reliable fixation throughout the test. Frequency-of-seeing curves were generated, and the data were fit by probit analysis. The motion displacement threshold (MDT) was taken as the displacement corresponding to a 50% frequency-of-seeing of the fitted curve.

2.3. High spatial resolution perimetry

High spatial resolution perimetry (HSRP) was performed in the same region of the superotemporal field by measuring the Humphrey visual field thresholds across a 10×10 matrix of 100 Humphrey test locations separated by 1° . The site of motion displacement testing falls within this area (Fig. 1(a)). To perform high spatial resolution perimetry we used the 'custom grid' program of the Humphrey to define four custom test programs, each consisting of five by five locations separated by 2° , with the coordinates of each custom test program offset to the other by 1° in the x , y , or x - and y -axis. The four custom test programs were applied in succession in a randomized order using target size III on a standard Humphrey bowl illumination of 31.5 apostilbs. Each custom test program lasts approximately 4–5 min with a standardized rest between programs of 2 min. Accuracy of fixation is monitored in the same way as conventional perimetry.

Custom software was used to merge the custom test programs to generate a single fine matrix map of the thresholds of 100 test locations separated by 1 degree covering an area of $9 \times 9^\circ$ and extending from Humphrey coordinates $7x, 7y$ to $16x, 16y$ (for a Right Eye).

The high spatial resolution perimetry was performed without near correction, as the refraction at this eccentricity is difficult to ascertain and near correction could induce prismatic and edge effects which would be difficult to standardize during the test procedure. However the distribution of refractive errors were closely comparable between the glaucoma and control eyes

Table 1
Description of type of glaucomatous field defect on entry Humphrey 24-2 of glaucoma eyes

Type of glaucomatous field loss on entry Humphrey 24-2 fields of 18 glaucoma eyes	Eyes
Superior scotoma involving locations closest to MDT test site. Normal inferior hemifield	1
Superior scotoma not involving locations closest to MDT test site. Normal inferior hemifield	3
Inferior scotoma. Normal superior hemifield with normal thresholds closest to MDT site	5
Inferior scotoma and superior hemifield scotoma not involving locations closest to MDT test site	2
Inferior scotoma and superior hemifield scotoma involving locations closest to MDT test site	7

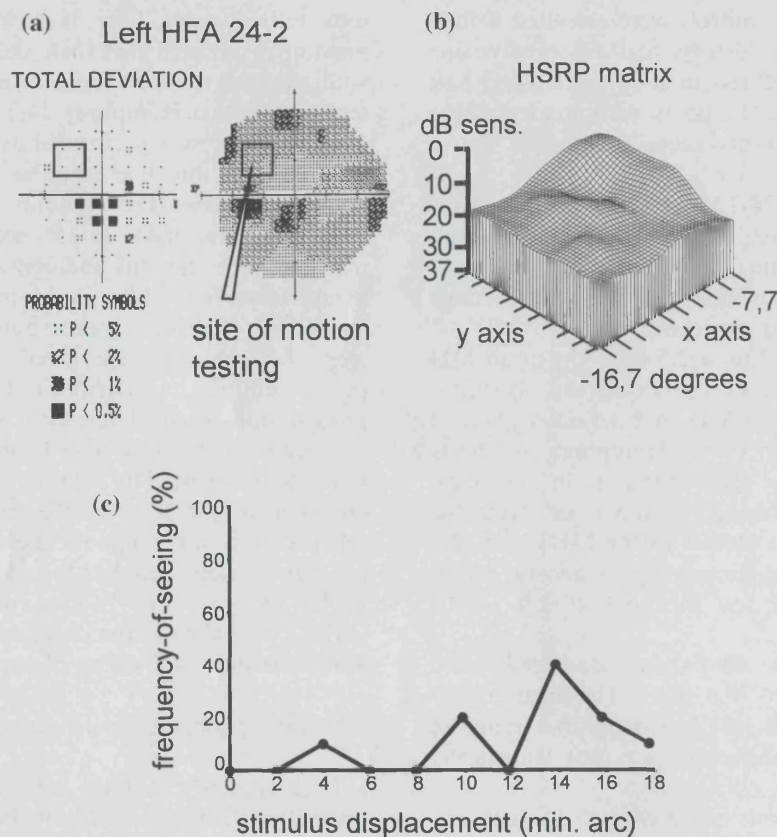


Fig. 1. (a) Humphrey 24-2 from a glaucoma subject showing inferior arcuate scotoma. Arrow indicates site of motion testing within area of normal Humphrey 24-2 field, overlapped by site of high spatial resolution perimetry (box). (b) Abnormal HSRP matrix map: elevations represent area of depressed thresholds. (c) Motion frequency-of-seeing curve shows grossly abnormal motion response.

tested: the median distance refraction (spherical equivalent) of the control eyes was 0 dioptres, range: -1.75 to $+2.13$ D, and for glaucoma eyes 0 D, range: -2.13 to $+2.00$ D. We have previously shown that at such low degrees of refractive error, the effect on threshold is minimal [34].

We analyzed each subject's fine matrix map by calculating the mean threshold sensitivity of the 100 test locations. We derived an additional measure to describe the uniformity of thresholds within each matrix map. This uniformity index (UI) was calculated as the standard deviation (S.D.) of the threshold values.

In addition, spatial image processing of the HSRP thresholds using a Gaussian filter was performed and three dimensional surface plots were generated for display purposes (Fig. 1(b); Fig. 2(b); Fig. 3(b); Fig. 4(b)).

Patients underwent motion displacement threshold testing and high spatial resolution testing in both eyes, tested in a randomized order. Because of the well known difficulties of assuming non independence of a patient's two eyes, only the data of the glaucoma eye was included in the analysis. Therefore each patient only contributed data from one eye (the glaucoma eye) to the study. The controls underwent motion displace-

ment threshold testing and high spatial resolution in one randomly chosen eye. All testing was performed at a single session.

2.4. Statistical Analysis

All variables were tested for normality, and two sample *t*-tests were used to identify significant differences between the glaucoma eyes and control eyes. For variables that failed tests for normality and equivalence of variances, we used the equivalent non-parametric statistical tests. We set the level of statistical significance at $P < 0.05$.

3. Results

3.1. Motion Displacement Thresholds (MDTs)

We were able to record Motion Displacement Thresholds in all 18 control eyes and 15/18 glaucoma eyes. The remaining three glaucoma eyes had such grossly impaired motion perception that the patients did not perceive motion in any of the stimuli presented.

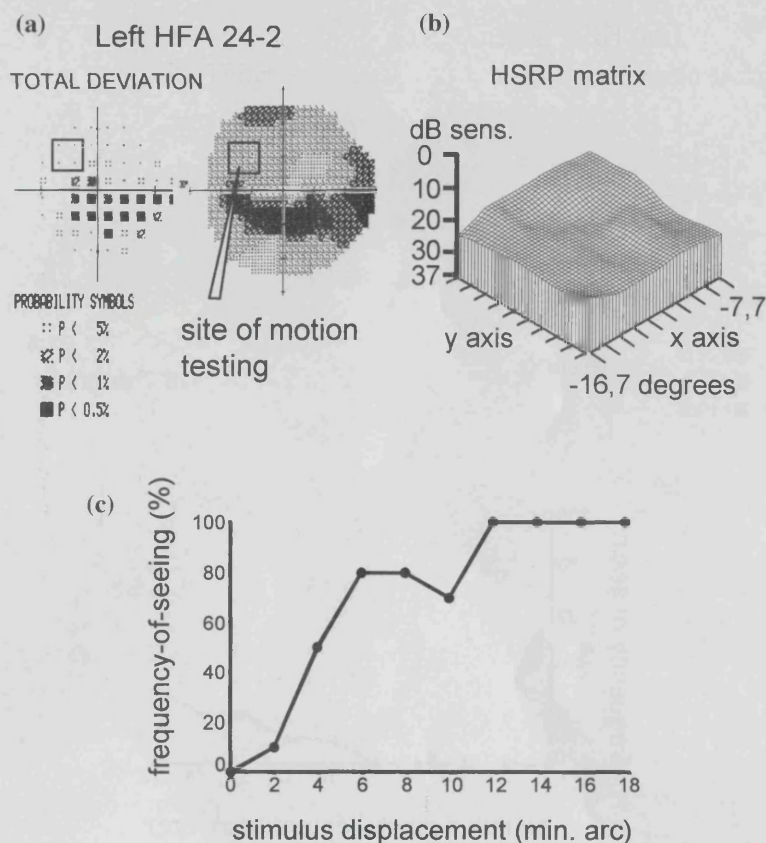


Fig. 2. (a) Humphrey 24-2 from a glaucoma subject showing inferior arcuate scotoma. Arrow indicates site of motion testing within area of normal Humphrey 24-2 field, overlapped by site of high spatial resolution perimetry (box). (b) Abnormal HSRP matrix map. Subtle elevations represent areas of abnormally depressed thresholds. (c) Motion frequency-of-seeing curve shows dip at 10 min arc. The 50% seen threshold is 4.2 min arc, within the control range.

All three of these eyes with an absent motion response had a scotoma on the Humphrey 24-2 at the MDT test location.

Table 2 shows the mean and S.D. of the MDTs by group. Because the variances in the glaucoma eyes and controls were dissimilar (Levene test for homogeneity of variances $P < 0.05$), a non-parametric Mann-Whitney U -test was performed which showed a significant elevation of the MDTs of the glaucoma eyes compared to the controls ($P < 0.0001$).

Fig. 5(a) shows the individual motion thresholds within each group with the reference line indicating mean + 1.96 S.D. of the controls (= 9.2 min. arc). Using this as a cut-off, 11/15 (73%) of the glaucoma eyes had abnormally elevated MDTs above mean + 1.96 S.D. of the controls at the location tested. Only 5/15 (33%) of these eyes had a scotoma cluster on the Humphrey 24-2 field involving the test locations closest to the MDT site.

There were no controls with MDT thresholds above the mean + 1.96 S.D. of the control group.

3.2. High spatial resolution perimetry thresholds

Mean sensitivities for each fine matrix map were calculated (Table 3). This mean sensitivity was significantly lower in the glaucoma patients compared to the controls ($P < 0.001$, unpaired t -test).

The control group mean was found to be 27.9 dB. We defined abnormal as 1.96 S.D. below this (23.5 dB). Fig. 5(b) shows the individual matrix map mean thresholds within each group, with the reference line indicating this normal cut off. Using this cut-off, 13/18 of glaucoma patients had mean matrix thresholds below this level.

We derived a 'uniformity index' (UI) to assess the degree of uniformity of the matrix thresholds, which was calculated as the S.D. of the matrix thresholds.

In normals, the threshold plots were flat, and as a consequence the UIs were low. Areas of scotoma would result in hills and valleys on the threshold plot, and would give rise to a high UI. The UIs of the glaucoma group were significantly higher than controls ($P = 0.0001$, Mann-Whitney U -test) indicating greater spa-

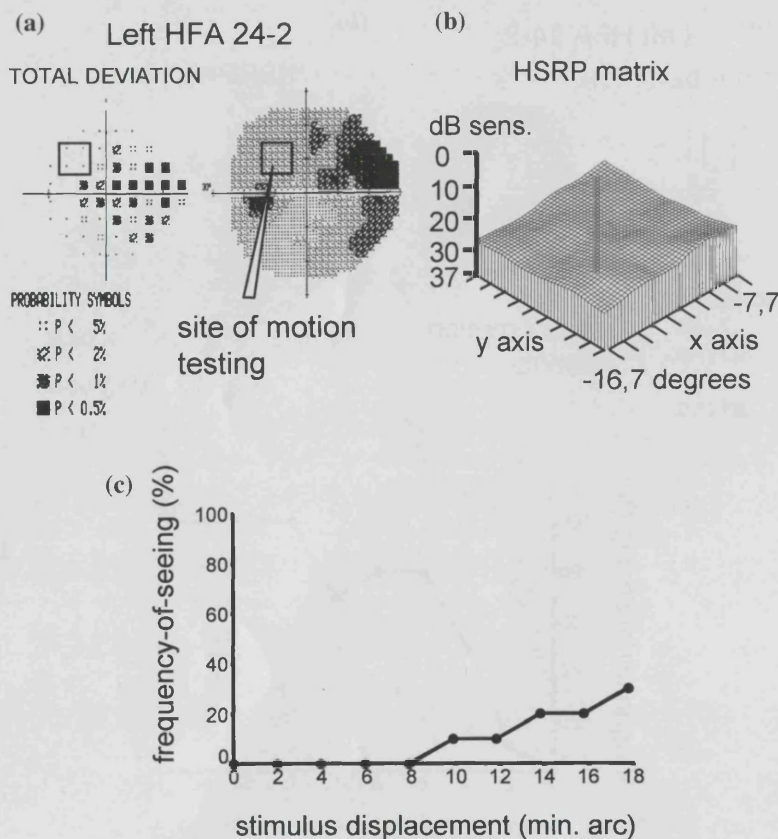


Fig. 3. (a) Humphrey 24-2 from a glaucoma subject showing superior arcuate scotoma. Arrow indicates site of motion testing within area of normal Humphrey 24-2 field, overlapped by site of high spatial resolution perimetry (box). (b) HSRP matrix map is normal, with normal mean threshold sensitivities, and uniform threshold profile (normal uniformity index). (c) Motion frequency-of-seeing curve shows grossly abnormal motion response.

tial variability in the high spatial resolution thresholds in the glaucoma patients. The control values for the UI ranged from 1.3 to 2.5 dB, mean 1.8 dB, S.D. 0.33 dB. We defined the UI as abnormal if it exceeded the control mean + 1.96 S.D. (= 2.4 dB). Fig. 5(c) shows the individual matrix map uniformity indices within each group, with the reference line indicating this normal cut off.

Twelve of the 13 eyes previously identified as having abnormally low mean matrix threshold had an abnormal UI index. We identified one additional glaucoma eye with an abnormal UI, in the presence of normal mean threshold.

3.3. Comparison between abnormal motion displacement thresholds and abnormal high spatial resolution perimetry thresholds

Comparison between Fig. 5(a–c) shows a similar degree of overlap between the control and glaucoma eyes for both the MDTs, and the HSRP mean threshold and uniformity indices. In the glaucoma eyes we then investigated the coexistence of motion abnor-

malities with HSRP abnormalities in relation to the presence or absence of scotoma on the Humphrey 24-2 at the test site.

Eight glaucoma eyes had scotomas on the Humphrey 24-2 field involving the test locations closest to the MDT site. All were abnormal with high spatial resolution perimetry.

Of these eight glaucoma eyes, seven had abnormally elevated MDTs.

The remaining ten glaucoma eyes had no scotomas on the Humphrey 24-2 field which involved any of the test locations closest to the MDT site. (Table 4). Six of the ten eyes had abnormal High Spatial Resolution Perimetry, and of these four had abnormally elevated MDTs. An example is shown in Fig. 1(b), which shows an abnormal HSRP matrix map (abnormally depressed mean sensitivity and an abnormally high uniformity index). This eye has an abnormally elevated motion displacement threshold at the location tested (Fig. 1(c)). Two glaucoma eyes had abnormal high spatial resolution perimetry, with normal MDTs (Fig. 2(a–c)).

Four of the ten eyes had normal High Spatial Resolution Perimetry. Of these four eyes, we identified three

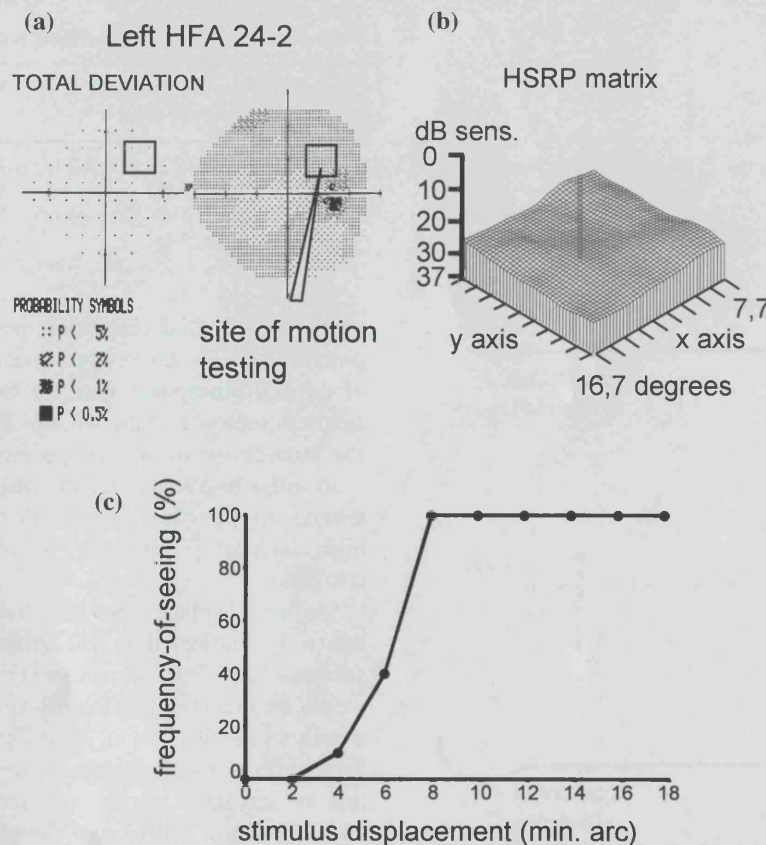


Fig. 4. (a) Humphrey 24-2 from a normal control. Arrow indicates site of motion testing within area of normal Humphrey 24-2 field, overlapped by site of high spatial resolution perimetry (box). (b) HSRP matrix map is normal with uniform luminance profile (mean threshold sensitivity and uniformity index within control range). (c) Normal motion frequency-of-seeing curve with 50% seen threshold within control range.

with abnormally elevated MDTs. Thus these three eyes had abnormal motion sensitivity in the presence of a normal HSRP. An example is shown in Fig. 3(b), which shows a normal HSRP matrix map (normal mean sensitivity and a normal uniformity index) with a coexisting elevated MDT (Fig. 3(c)). For comparison, Fig. 4(a–c) show a normal HSRP matrix map and normal MDT obtained from a control eye.

One glaucoma eye had normal high spatial resolution perimetry and normal motion displacement thresholds at the site tested.

For the controls, one out of eighteen eyes had abnormally depressed HSRP mean threshold sensitivity of 22.8 dB, below our cut-off of 23.5, and 2.3 S.D. below the control group mean. The subject's motion tests and

Table 2
Summary statistics for the motion detection thresholds (MDTs) by group

Group	Mean MDT (min. arc)	S.D.	Minimum	Maximum
Glaucoma	15.3	12.9	4.2	57.6
Controls	6.1	1.6	2.3	8.2

Humphrey 24-2 were both normal. None of the remaining controls had MDTs and HSRP outside the control group mean ± 2 S.D..

There was a statistically significant correlation between the motion thresholds and the mean high spatial resolution perimetry matrix thresholds ($P < 0.0001$, $r^2 = 0.35$) (Fig. 6).

4. Discussion

This aim of this study is to test the hypothesis that abnormal motion displacement thresholds coexist with scotomas on a finer scale than is measurable by conventional Humphrey perimetry. We identified ten glaucoma eyes with normal Humphrey 24-2 field nearest the MDT test site. Of these seven had abnormally elevated motion displacement thresholds and six had fine scale scotomas detected with high spatial resolution perimetry. This result suggests that glaucomatous elevations of motion displacement threshold may be present in areas of normal Humphrey 24-2 field, and this may coexist with measurable scotomas beyond the resolution of conventional Humphrey perimetry in some, but not all patients.

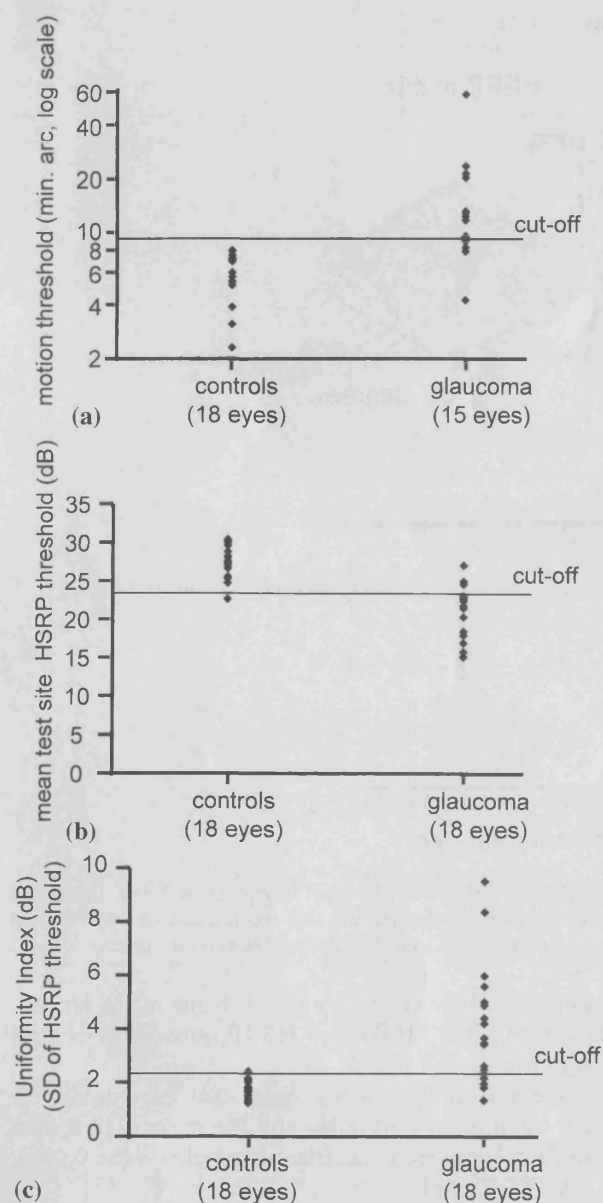


Fig. 5. Plots of individual values of MDT (a), HSRP matrix map mean threshold (b) and HSRP matrix map uniformity index (c) for controls and glaucoma eyes, with horizontal reference lines indicating cut-off of mean + 1.96 S.D. of controls.

We identified two glaucoma eyes with abnormal HSRP in the presence of a normal motion displacement threshold. Whilst it is possible that these defects may be non-glaucomatous and secondary to other factors, we were unable to identify this in our patients. Further studies will be required to confirm this and to examine for additional unrecognized factors which may be responsible for this. A further proportion of the glaucoma patients (30%) had abnormal motion displacement thresholds in areas of field with no detectable scotomas, measured with conventional prime-

Table 3

Summary statistics of high resolution perimetry thresholds by group.

Group	Matrix map mean threshold (dB)	Matrix map uniformity index (dB)
Controls	Mean 27.9, S.D. 2.2 (<i>r</i> 22.8–30.5)	Mean 1.8, S.D. 0.33 (<i>r</i> 1.3–2.5)
Glaucoma	Mean 21.6, S.D. 3.4 (<i>r</i> 15.2–27.1)	Mean 4.1, S.D. 2.25 (<i>r</i> 1.4–9.5)

try or high spatial resolution perimetry. Thus in some patients motion sensitivity abnormalities occur in areas of normal Humphrey field, in the absence of even the smallest scotomas that we can practically detect using the Humphrey automated perimeter.

In order to avoid artefacts due to the trial frame, we elected to perform motion displacement testing and high spatial resolution perimetry without near correction.

Motion displacement thresholds have been shown relatively unaffected by refractive errors [11,35], and the subjects had low refractive errors. Refractive error would be expected to globally suppress Humphrey field threshold sensitivity [36]. The uniformity index (UI) we used reflects focal threshold depression, which would not be expected to be affected by refractive error. Thirteen out of fourteen of the glaucoma eyes identified as abnormal with the HSRP had an abnormal uniformity index. Refractive changes would not be expected to account for these localized threshold abnormalities, as in general the effect of refractive error is to smear out localized abnormalities.

One major hypothesis to account for the occurrence of early abnormalities of motion perception before conventional field defects is the 'selective cell loss hypothesis'.

Quigley and colleagues hypothesized that there is selective damage to the larger diameter optic nerve fibers in early glaucoma [37]. Since magnocellular cells are associated with larger mean diameters, the 'selective loss hypothesis' would imply a preferential loss of magnocellular function. This has received support from a number of histological studies [37–39].

Table 4

Number of eyes with respective MDT and HSRP abnormalities, out of ten glaucoma eyes that had no scotomas on the Humphrey 24-2 field which involved any of the test locations closest to the MDT site

	Normal HSRP (eyes)	Abnormal HSRP(eyes)
Normal MDT (eyes)	1	2
Abnormal MDT (eyes)	3	4

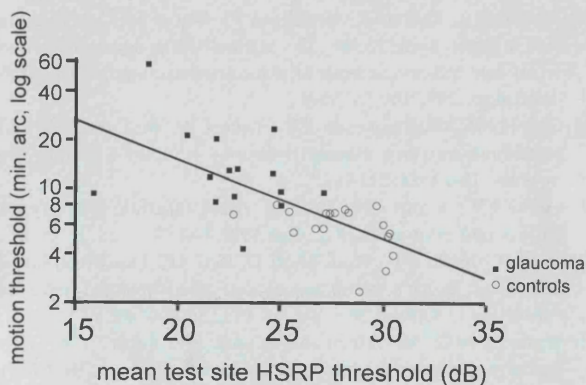


Fig. 6. Relationship between motion displacement threshold and HSRP matrix map mean threshold. The MDTs are presented on a log scale. The solid line represents the least-squares linear fit through the data.

Johnson has proposed an alternative hypothesis based on the concept of reduced redundancy to explain the presence of a variety of psychophysical abnormalities of visual function, including motion perception, in glaucoma before conventional perimetric field defects [40]. According to the reduced redundancy theory, the poor performance of conventional perimetry may be a consequence of the non selective nature of the stimulus, which stimulates a broad spectrum of retinal ganglion cells. The large overlap in ganglion cell receptive fields results in considerable redundancy, that may mask early losses if all classes of ganglion cells are stimulated [40]. Tests that stimulate only a subpopulation of ganglion cells to isolate one aspect of visual function may identify the earliest losses. This is because the ability of spared visual systems from compensating for those compromised in glaucoma is reduced.

Psychophysical evidence for both the selective cell loss hypothesis and the reduced redundancy hypothesis depends upon comparisons of the extent and the sequence of occurrence of selective losses of visual function, compared with non selective losses identified with conventional perimetry [40,41]. Our findings that elevations of motion displacement threshold may coexist with scotomas beyond the resolution of conventional Humphrey perimetry demonstrate the importance of considering the spatial resolution of the tests, which must be taken into account when making comparisons between tests. Although intrinsic differences may exist in the sensitivity of a broad spectrum stimulus such as the Humphrey stimulus, compared with more selective stimuli such as motion stimuli, our results suggest that a principal limitation of conventional Humphrey 24-2 perimetry in detecting early glaucoma is its inadequate spatial resolution.

Acknowledgements

MC Westcott is supported by research grants from the Friends of Moorfields and the International Glaucoma Association. FW Fitzke is supported by a grant from the Medical Research Council. We are grateful to the reviewers for their comments on an earlier version of this manuscript, which have now been incorporated into this manuscript.

References

- [1] Quigley HA, Addicks EM, Green WR. Optic nerve damage in human glaucoma. III. Quantitative correlation of nerve fiber loss and visual field defect in glaucoma, ischemic neuropathy, papilledema, and toxic neuropathy. *Arch Ophthalmol* 1982;100:135–46.
- [2] Quigley HA, Dunkelberger GR, Green WR. Retinal ganglion cell atrophy correlated with automated perimetry in human eyes with glaucoma. *Am J Ophthalmol* 1989;107:453–64.
- [3] Sample PA, Weinreb RN. Progressive color visual field loss in glaucoma. *Invest Ophthalmol Vis Sci* 1992;33:2068–71.
- [4] Johnson CA, Adams AJ, Casson EJ, Brandt JD. Progression of early glaucomatous visual field loss as detected by blue-on-yellow and standard white-on-white automated perimetry. *Arch Ophthalmol* 1993;111:651–6.
- [5] Johnson CA, Adams AJ, Casson EJ, Brandt JD. Blue-on-yellow perimetry can predict the development of glaucomatous visual field loss. *Arch Ophthalmol* 1993;111:645–50.
- [6] Lachenmayr BJ, Drance SM, Douglas GR, Mikelberg FS. Light-sense, flicker and resolution perimetry in glaucoma a comparative study. *Graefes Arch Clin Exp Ophthalmol* 1991;229:246–51.
- [7] Casson EJ, Johnson CA, Shapiro LR. Longitudinal comparison of temporal-modulation perimetry with white-on-white and blue-on-yellow perimetry in ocular hypertension and early glaucoma. *J Opt Soc Am A* 1993;10:1792–806.
- [8] Tyler CW, Hardage L, Stamper RL. The temporal visuogram in ocular hypertension and its progression to glaucoma. *J Glaucoma Suppl* 1994;3:S65–72.
- [9] Frisen L. High-pass resolution perimetry. A clinical review. *Doc Ophthalmol* 1993;83:1–25.
- [10] Fitzke FW, Poinoosawmy D, Ernst W, Hitchings RA. Peripheral displacement thresholds in normals, ocular hypertensives and glaucoma. In: Greve EL, Heijl A, editors. Seventh International Visual Field Symposium. Dordrecht: Martinus Nijhoff, 1987:447–52.
- [11] Fitzke FW, Poinoosawmy D, Nagasubramanian S, Hitchings RA. Peripheral displacement thresholds in glaucoma and ocular hypertension. In: Kriegelstein GK, editor. *Perimetry Update*. Amsterdam: Kugler, 1989:399–405.
- [12] Silverman SE, Trick GL, Hart WM Jr. Motion perception is abnormal in primary open-angle glaucoma and ocular hypertension. *Invest Ophthalmol Vis Sci* 1990;31:722–9.
- [13] Bullimore MA, Wood JM, Swenson K. Motion perception in glaucoma. *Invest Ophthalmol Vis Sci* 1993;34:3526–33.
- [14] Ruben S, Fitzke F. Correlation of peripheral displacement thresholds and optic disc parameters in ocular hypertension. *Br J Ophthalmol* 1994;78:291–4.
- [15] Johnson CA, Marshall D, Eng KM. Displacement threshold perimetry in glaucoma using a Macintosh computer system and a 21-inch monitor. In: Mills R, Wall M, editors. *Perimetry Update*. Amsterdam: Kugler, 1995:103–10.

- [16] Trick GL, Steinman SB, Amyot M. Motion perception deficits in glaucomatous optic neuropathy. *Vis Res* 1995;35:2225–33.
- [17] Wall M, Ketoff KM. Random dot motion perimetry in patients with glaucoma and in normal subjects. *Am J Ophthalmol* 1995;120:587–96.
- [18] Bosworth CF, Sample PA, Weinreb RN. Motion perception thresholds in areas of glaucomatous visual field loss. *Vis Res* 1997;37:355–64.
- [19] Joffe KM, Raymond JE, Chrichton A. Motion coherence perimetry in glaucoma and suspected glaucoma. *Vision Res* 1997;37:955–64.
- [20] Ruben ST, Hitchings RA, Fitzke F, Arden GB. Electrophysiology and psychophysics in ocular hypertension and glaucoma evidence for different pathomechanisms in early glaucoma. *Eye* 1994;8:516–20.
- [21] Lee BB. Macaque ganglion cells and spatial vision. *Prog Brain Res* 1993;95:33–43.
- [22] Lee BB, Wehrhahn C, Westheimer G, Kremers J. Macaque ganglion cell responses to stimuli that elicit hyperacuity in man detection of small displacements. *J Neurosci* 1993;13:1001–9.
- [23] Livingstone MS, Hubel DH. Psychophysical evidence for separate channels for the perception of form, color, movement, and depth. *J Neurosci* 1987;7:3416–68.
- [24] Merigan WH, Maunsell JH. Macaque vision after magnocellular lateral geniculate lesions. *Vis Neurosci* 1990;5:347–52.
- [25] Merigan WH, Byrne CE, Maunsell JH. Does primate motion perception depend on the magnocellular pathway? *J Neurosci* 1991;11:3422–9.
- [26] Graham SL, Drance SM, Chauhan BC, Swindale NV, Hnik P, Mikelberg FS, Douglas RG. Comparison of psychophysical and electrophysiological testing in glaucoma. *Invest Ophthalmol Vis Sci* 1996;37:2651–62.
- [27] Baez KA, McNaught AI, Dowler JG, Poinoosawmy D, Fitzke FW, Hitchings RA. Motion detection threshold and field progression in normal tension glaucoma. *Br J Ophthalmol* 1995;79:125–8.
- [28] Sturmer J. What do glaucomatous visual fields really look like in fine-grid computerized profile perimetry? *Dev Ophthalmol* 1985;12:1–47.
- [29] Tuulonen A, Lehtola J, Airaksinen PJ. Nerve fiber layer defects with normal visual fields. Do normal optic disc and normal visual field indicate absence of glaucomatous abnormality? *Ophthalmology* 1993;100:587–97.
- [30] Capon MR, Polkinghorne PJ, Fitzke FW, Bird AC. Sorsby's pseudoinflammatory macula dystrophy—Sorsby's fundus dystrophies. *Eye* 1988;2:114–22.
- [31] Fitzke FW, Kemp CM. Probing visual function with psychophysics and photochemistry. *Eye* 1989;3:84–9.
- [32] Chen JC, Fitzke FW, Pauleikhoff D, Bird AC. Functional loss in age-related Bruch's membrane change with choroidal perfusion defect. *Invest Ophthalmol Vis Sci* 1992;33:334–40.
- [33] Westcott MC, McNaught AI, Crabb DP, Fitzke FW. High spatial resolution automated perimetry in glaucoma. *Br J Ophthalmol* 1997;81:452–9.
- [34] Wu J, Bird AC, McNaught A, Buckland MS, Fitzke FW. Fine matrix mapping of the macular region in normal subjects. *Chung-Hua-Yen-Ko-Tsa-Chih* 1995;31:243–9.
- [35] Whitaker D, Buckingham T. Oscillatory movement displacement thresholds resistance to optical image degradation. *Ophthalmic Physiol Opt* 1987;7:121–5.
- [36] Goldstick BJ, Weinreb RN. The effect of refractive error on automated global analysis program G-1. *Am J Ophthalmol* 1987;104:229–32.
- [37] Quigley HA, Dunkelberger GR, Green WR. Chronic human glaucoma causing selectively greater loss of large optic nerve fibers. *Ophthalmology* 1988;95:357–63.
- [38] Glovinsky Y, Quigley HA, Dunkelberger GR. Retinal ganglion cell loss is size dependent in experimental glaucoma. *Invest Ophthalmol Vis Sci* 1991;32:484–91.
- [39] Chaturvedi N, Hedley W-ET, Dreyer EB. Lateral geniculate nucleus in glaucoma. *Am J Ophthalmol* 1993;116:182–8.
- [40] Johnson CA. Selective versus nonselective losses in glaucoma. *J Glaucoma* 1994;3:S32–44.
- [41] Sample PA, Madrid ME, Weinreb MD. Evidence for a variety of functional defects in glaucoma suspect eyes. *J Glaucoma* 1994;3:S5–S18.



Characteristics of frequency-of-seeing curves for a motion stimulus in glaucoma eyes, glaucoma suspect eyes, and normal eyes

Mark C. Westcott^a, Frederick W. Fitzke^{a,*}, David P. Crabb^a, Roger A. Hitchings^b

^a *Institute of Ophthalmology, Department of Visual Science, 11–43 Bath Street, London EC1 9EL, UK*

^b *Moorfields Eye Hospital, London, UK*

Received 8 April 1997; received in revised form 17 November 1997; accepted 2 June 1998

Abstract

This study compared frequency-of-seeing curves for a line displacement test in glaucoma patients and normals. Probit analysis of the frequency-of-seeing curves provided the motion thresholds and the slopes of the frequency-of-seeing curves, represented by the interquartile range. The thresholds and interquartile ranges were significantly elevated in the glaucoma eyes and suspect eyes, compared to controls. A logistic regression model incorporating both the interquartile range and threshold significantly improved the sensitivity of the motion test in the suspects. Abnormal shallowing of the slope of the motion frequency-of-seeing curve may represent one of the earliest changes in glaucoma. © 1998 Elsevier Science Ltd. All rights reserved.

Keywords: Glaucoma; Motion perception; Frequency-of-seeing curves; Psychometric-function; Perimetry

1. Introduction

Histological evidence has shown that a substantial number of retinal ganglion cell axons may be lost in glaucoma before a visual field defect can be detected using conventional methods of full threshold automated perimetry (Quigley, Addicks & Green, 1982; Quigley, Dunkelberger & Green, 1989). This finding has prompted the development of alternative tests, including motion detection, which may be more sensitive in detecting early glaucomatous visual damage. We have previously demonstrated glaucomatous loss of motion sensitivity using a line displacement test (Fitzke, Poinosawmy, Ernst & Hitchings, 1987; Fitzke, Poinosawmy, Nagasubramanian & Hitchings, 1989; Ruben & Fitzke, 1994; Baez, McNaught, Dowler, Poinosawmy, Fitzke & Hitchings, 1995), and a number of workers have confirmed these findings using line stimuli (Johnson, 1994; Johnson, Marshall & Eng, 1995) and random dot kinetograms (Silverman, Trick & Hart, 1990; Bullimore, Wood & Swenson, 1993; Trick, Steinman & Amyot, 1995; Wall & Ketoff, 1995; Bosworth, Sample & Weinreb, 1997; Joffe, Raymond & Chrichton, 1997).

Experimental work in primates has shown that magnocellular ganglion cells are primarily responsible for the perception of motion elicited by small line displacements (Lee, 1993; Lee, Wehrhahn, Westheimer & Kremers, 1993). This is consistent with evidence from other studies which suggests that primate perception of motion to a variety of stimuli is primarily a function of the magnocellular system (Livingstone & Hubel, 1987; Merigan & Maunsell, 1990; Merigan, Byrne & Maunsell, 1991). However motion sensitivity may not be exclusively a property of the magnocellular system, as parvocellular mechanisms have also been shown to participate in such functions (Lee, Wehrhahn, Westheimer & Kremers, 1993; Anderson, Drasdo & Thompson, 1995).

A principal hypothesis to account for the early occurrence of motion sensitivity defects is the concept of preferential loss of larger diameter magnocellular ganglion cells, in early glaucoma, which has received support from a number of histological studies (Quigley, Dunkelberger & Green, 1988, 1989; Glovinsky, Quigley & Dunkelberger 1991; Chaturvedi, Hedley & Dreyer, 1993; Glovinsky, Quigley & Pease, 1993). An alternative hypothesis to account for a variety of early deficits of visual function in glaucoma is based on the concept of reduced redundancy (Johnson, 1994).

* Corresponding author. Fax: +44 171 6086834.

The reduced redundancy theory postulates that those tests which isolate a very sparse population of ganglion cells, with little physiological redundancy, will identify the earliest loss in glaucoma. Such selective tests have identified deficits of motion sensitivity (a test of magnocellular ganglion cell function) (Fitzke, Poinoosawmy, Ernst & Hitchings, 1987; Fitzke, Poinoosawmy, Nagasubramanian & Hitchings, 1989; Silverman, Trick & Hart, 1990; Bullimore, Wood & Swenson, 1993; Ruben & Fitzke, 1994; Johnson, 1994; Johnson, Marshall & Eng, 1995; Trick, Steinman, & Amyot, 1995; Wall & Ketoff, 1995; Bosworth, Sample & Weinreb, 1997; Joffe, Raymond & Chrichton, 1997), blue-on-yellow sensitivity (a test of the short wavelength sensitive ganglion cells) (Sample & Weinreb, 1992; Johnson, Adams, Casson & Brandt, 1993b,a), and flicker sensitivity (Lachenmayr, Drance, Douglas & Mikelberg, 1991; Casson, Johnson & Shapiro, 1993; Tyler, Hardage & Stamper, 1994).

Previously published investigations of motion sensitivity losses in glaucoma have concentrated on differences in the motion thresholds between groups. Although Silverman, Trick & Hart (1990) reported a qualitative lessening of the slope of the psychometric curve of motion in some patients with glaucoma, there has been no detailed analysis of frequency-of-seeing curves for a motion response in glaucoma to date. Frequency-of-seeing curves describe the relationship between the probability of seeing a stimulus and a stimulus parameter such as intensity (luminance stimulus) or stimulus displacement (motion stimulus). The S-shaped frequency-of-seeing curve has been shown to describe the relationship between luminance sensitivity and variability in automated perimetry (Chauhan & House, 1991; Weber & Rau, 1992; Olsson, Heijl, Bengtsson & Rootzen, 1993; Chauhan, Tompkins, LeBlanc & McCormick, 1993; Henson, Evans, Chauhan & Lane, 1996; Wall, Maw, Stanek & Chauhan, 1996). The threshold is usually defined as the stimulus intensity at which 50% of the stimuli will be seen. In addition the steepness of the frequency-of-seeing curve can be calculated to provide a measure of the intratest variability around the threshold at that test location. A steep gradient represents little variability, whilst shallow gradients indicate large intratest variability. A number of workers have found a significant correlation between threshold and the slope of the frequency-of-seeing curve for luminance stimuli (Chauhan & House, 1991; Weber & Rau, 1992; Olsson, Heijl, Bengtsson & Rootzen, 1993; Chauhan, Tompkins, LeBlanc & McCormick, 1993; Henson, Evans, Chauhan & Lane, 1996; Wall, Maw, Stanek & Chauhan, 1996). These studies have reported a shallowing of the slope of the frequency-of-seeing curve in glaucoma patients with decreased sensitivities, reflecting an abnormally high intratest variability. In addition, Chauhan, Tompkins, LeBlanc

& McCormick (1993) have shown that glaucoma patients have widely differing frequency-of-seeing curves for similar thresholds and were able to identify patients who had normal Humphrey field thresholds, but who had an abnormally shallow slope of the frequency-of-seeing curve. This study tests the hypothesis that frequency-of-seeing analysis can characterise additional differences between the motion response of normal subjects and glaucoma patients, beyond that achieved by measuring thresholds alone. The identification of these differences may allow us to improve the sensitivity and specificity of motion testing in glaucoma.

2. Methods

2.1. Testing strategy

We measured motion sensitivity using a line displacement test presented in the superotemporal field to obtain Motion Displacement Thresholds (MDT). This site was chosen as previous results have identified significantly elevated Motion Displacement Thresholds at this location in glaucoma patients, with good separation between patients and controls (Fitzke, Poinoosawmy, Ernst & Hitchings, 1987; Fitzke, Poinoosawmy, Nagasubramanian & Hitchings, 1989). The MDT test was performed using a computer generated line stimulus presented on a monochrome monitor (Phillips green monochrome P31 monitor, model number 750205, pixelation 300×920 , frame rate 50 Hz). The view distance was 1.24 m. The width of the stimulus was formed by addressing two horizontal pixels. The stimulus subtended $2^\circ \times 2$ min arc in size and the background $8 \times 10^\circ$, as measured directly from the display. The line stimulus was presented in the superotemporal field at 15° eccentricity on the 30° meridian. The luminance of the background was 7 cd/m^2 and the stimulus was 27 cd/m^2 .

The subject viewed a fixation target and was instructed to press a response button when movement was seen. A warning tone was sounded which was followed by 1.5 s during which the stimulus was stationary. During the following 2 s, the stimulus (if it were to move), would undergo sudden oscillatory displacements at 2.5 Hz, beginning at a random time after the start of this interval. If the subject pressed the response button before stimulus movement had begun, then this was counted as a false positive response.

After a suitable instruction period, subjects underwent a test which consisted of ten presentations each of ten different displacements in 2 min arc intervals from 0 to 18 min arc presented in a random order. The test includes ten presentations of a 0 min arc displacement (stationary target catch trials) and if the subject presses the button to 0 min arc displacement then this was

recorded as a false positive response. The experimenter observed the subject for the duration of the test to ensure reliable fixation throughout the test.

2.2. Subjects

The study was approved by the Moorfields Hospital Ethics Committee and followed the tenets of the Declaration of Helsinki. All patients and controls gave informed consent prior to agreeing to participate. We defined a glaucoma eye as primary open-angle glaucoma (POAG) if it fulfilled the following diagnostic criteria:

1. Documented evidence of an intra-ocular pressure > 21 mmHg on at least one occasion in the presence of an open angle.
2. Abnormal optic disc with glaucomatous optic disc cupping.
3. Previously documented glaucomatous visual field defect on the Humphrey 24-2 field test.

A field was defined as glaucomatous on the Humphrey 24-2 if at least one hemifield contained a cluster of a minimum of three adjacent depressed points on the STATPAC2 pattern deviation plot with one point having a probability of $P < 1\%$ and two adjacent

points having a probability of $P < 2\%$ (Piltz, Drance, Douglas & Mikelbergh, 1991). We evaluated the Humphrey 24-2 field at the MDT test site using the field thresholds of the four locations nearest the MDT test site (see Fig. 1A). We defined the Humphrey 24-2 field at the motion test site as being abnormal if the field thresholds of at least one of these four locations was contiguous with a hemifield cluster of depressed locations, according to the above criteria.

Glaucoma suspect eyes were eligible if they had at least one of the following: glaucomatous optic disc cupping, clinical evidence of retinal nerve fiber layer defects, or a documented intra-ocular pressure > 21 mmHg on at least one occasion, in the presence of a normal Humphrey 24-2 field (defined as normal or borderline Glaucoma Hemifield Test in the absence of any clusters of depressed locations in either hemifield). We excluded any eyes with significant ocular pathology other than glaucoma, including evidence of cataract or secondary glaucoma, and eyes which were being treated with topical miotics. We recruited suitably age matched controls if they had no significant ocular history, had a normal ocular examination with an IOP less than 21 mmHg and had normal Humphrey HFA 24-2 fields (defined as a normal Glaucoma Hemifield Test with

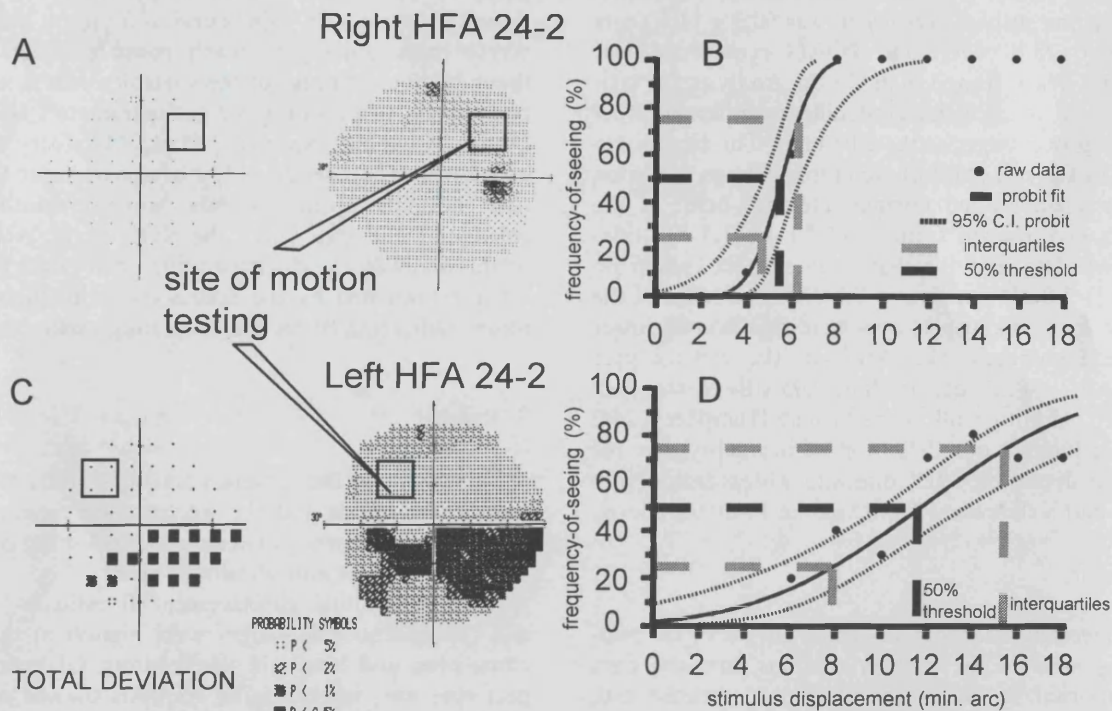


Fig. 1. (A) Humphrey 24-2 greyscale and Statpac2 total deviation plot from normal control aged 69, showing site of motion testing (arrow) with four closest Humphrey test locations; (B) normal subject's motion frequency-of-seeing curve. Black circles represent raw data points with probit-fitted curve (solid black curve), and 95% CI (dashed black curves). Dashed black line indicates normal 50% seen threshold of $5.5 \pm SE 0.4$ min arc with normal interquartile range of $1.5 \pm SE 0.5$ min arc (dashed grey lines); (C) Humphrey 24-2 of a glaucoma patient aged 69 with an inferior arcuate scotoma. Arrow indicates site of motion testing on greyscale plot, with four closest Humphrey 24-2 test locations (box) showing normal threshold sensitivity, within 95% population limits on Statpac2 output; and (D) motion frequency-of-seeing curve of same patient, with elevated threshold ($11.6 \pm SE 0.9$ min arc) and abnormally shallow slope, indicated by elevated interquartile range of $7.6 \pm SE 1.3$ min arc.

global indices within 95% CI for normal subjects with no hemifield clusters of depressed points). All Humphrey 24-2 fields met standard reliability criteria of <20% fixation losses, <33% false negatives, <33% false positives. All patients and controls had a corrected visual acuity in the tested eye of $\geq 6/9$ achieved with less than ± 4 dioptres spherical equivalent and less than 2 dioptres of astigmatism. We tested 29 control subjects and 42 patients. The controls underwent testing in one randomly selected eye. Twenty-seven patients had one eye meeting either POAG ($n = 14$) or glaucoma suspect criteria ($n = 13$) and underwent testing in this eye only. Fifteen patients had POAG in one eye and a glaucoma suspect fellow eye, and underwent testing of both eyes in a randomised order. Because these patients were contributing both eyes to the study, we performed two independent analyses of the data: the first using data from both eyes of these patients, then reanalysing using data from only one eye selected at random from each of these patients. We present the data using both eyes of these patients, as all statistically significant results reported in this study were confirmed using both analyses, and did not differ at the $P = 0.005$ level of significance.

The mean age of the controls was 58.7 ± 10.5 years, with a range 31.3–74.9 years. The mean age of patients with glaucoma suspect eyes tested was 60.9 ± 11.5 years (range 30.6–78.8 years) and POAG eyes tested was 62.9 ± 10.7 years (range 30.6–78.8). Analysis of variance showed no statistically significant differences between the group's ages at the 0.05 level. The Humphrey 24-2 Mean Defects (MD or weighted average deviation from the age-corrected normal reference field) of the glaucoma eyes ranged from -14.2 to -1.3 dB, (median -4.6 dB), and the glaucoma suspect eyes from -4.2 to $+1.8$ dB (median -0.7 dB). The MDs of the glaucoma eyes and suspect eyes were significantly lower than the Humphrey 24-2 MDs of the control eyes (range -2.7 – $+2.5$ dB, median 0.05 dB) at the $P < 0.05$ level. Although all suspects had Humphrey 24-2 fields that fulfilled our definition of normality, five (of 28) had a depressed MD, one had a depressed PSD, and five had a depressed CPSD at the $P < 0.05\%$ level.

2.3. Analysis

We generated frequency-of-seeing curves of the subject's responses to the motion stimulus, and the data were imported to SPSS for Windows, (release 6.0, SPSS, Chicago, IL) for further analysis. We performed probit analysis of the data using SPSS and the motion displacement threshold (MDT) was defined as the displacement corresponding to a 50% frequency-of-seeing of the probit fitted curve. We used the interquartile range as a measure of the slope of the frequency-of-seeing curve, as this measure has previously been used by

other investigators (Chauhan, Tompkins, LeBlanc & McCormick, 1993). The interquartile range is the stimulus displacement interval that corresponds to 25–75% frequency-of-seeing of the probit fitted curve. Fig. 1B shows the motion frequency-of-seeing curve from a normal control, with the calculated parameters. Fig. 1A shows the site of motion testing, superposed to the subject's Humphrey 24-2 plot. Because the variances of the groups were dissimilar for both the motion thresholds and interquartile ranges (Levene Test for Homogeneity of Variances $P < 0.05$), non parametric Kruskal–Wallis tests were performed to identify for significant differences between the three groups. Post-hoc Mann–Whitney U tests were then performed to identify the significant differences between pairs of groups.

To characterise the extent to which the slope provides additional information we analysed the data according to a stepwise logistic regression model incorporating both the motion thresholds and the interquartile ranges, and their squared terms. This was performed for normal against glaucoma eyes, and for normal against suspect eyes. The results of the logistic regression analysis were used to generate a receiver operating characteristic (ROC) curve which was compared to the ROC curve generated using the motion threshold alone. The ROC curve is a plot of sensitivity versus one-specificity for each possible cut-off across the measurement range of the variables, and is useful in comparison of two or more test parameters (Graham, Drance, Chauhan, Swindale, Hnik, Mikelberg & Douglas 1996). The overall ability of a parameter to separate normals from patients was summarised by calculating the area under the ROC curve. According to this analysis, the discriminating ability of a parameter is represented by the area score, with higher area scores indicating better discriminating ability.

3. Results

Table 1 shows the summary statistics of the 50% seen motion thresholds and the interquartile ranges of the probit fitted frequency-of-seeing curves for the controls, glaucoma suspect and glaucoma eyes.

Both the motion displacement thresholds (MDTs) and the interquartile ranges were highest in the glaucoma eyes, and lowest in the controls. Glaucoma suspect eyes were intermediate. Analysis showed a highly significant ranked difference between the groups for both variables (Kruskal–Wallis test $P < 0.0001$). Post hoc two sample Mann–Whitney U tests identified significantly elevated MDTs in the glaucoma eyes ($P < 0.0001$) and in the glaucoma suspect eyes ($P < 0.001$), compared to controls. The interquartile ranges were also significantly elevated in the glaucoma eyes ($P <$

Table 1
Summary of the statistics for the frequency-of-seeing curves

Group	Normals (29 eyes)	Glaucoma suspects (28 eyes)	Glaucoma patients (29 eyes)
Motion threshold	5.9 ± 1.7 (2.6–8.9)	8.7 ± 3.4 (5.0–17.6)	12.9 ± 5.8 (5.2–34.2)
Interquartile range	3.3 ± 1.4 (1.0–5.9)	5.3 ± 2.3 (2.1–9.60)	8.4 ± 4.7 (4.2–25.5)

Values shown are mean ± 1 SD in min arc.

Figures in brackets indicate minimum and maximum values.

0.0001) and in the glaucoma suspect eyes ($P < 0.005$) compared to the controls. The MDTs in the glaucoma eyes were also significantly raised compared to the suspect eyes ($P = 0.0001$), as were the interquartile ranges ($P < 0.01$).

Subgroup analysis did not show any significant difference between the glaucoma suspect fellow eyes of glaucoma patients and eyes of glaucoma suspects or ocular hypertensives in terms of motion threshold, interquartile range, or Humphrey MD.

Logistic regression analysis incorporating both the motion thresholds and the interquartile ranges was performed for normal against glaucoma eyes, and for normal against suspect eyes. In both cases, the interquartile ranges (slope) and the threshold were found to contribute to the model significantly ($P > 0.05$).

To investigate the separation between the glaucoma eyes and the controls we plotted a ROC curve (Fig. 2A) of the motion threshold compared with the logistic regression model incorporating the interquartile range. A motion threshold cut-off of 9.0 min arc identified 22/29 glaucoma eyes as abnormal, with a sensitivity of 76% and a specificity of 100%. The logistic regression model incorporating both the threshold and interquartile range identified 24/29 glaucoma eyes as abnormal with a sensitivity of 83% at 100% specificity. Consideration of the interquartile range alone identified 23/29 eyes as abnormal, with a sensitivity of 79% at 100% specificity. Thus in the glaucoma eyes, only two additional eyes were identified as abnormal on the basis of an abnormal interquartile range, whereas they would have been classified as normal on the basis of threshold alone. Of the 24/29 eyes classified as abnormal by the regression model, 17/24 eyes had normal Humphrey 24-2 field thresholds at the motion test site. One such example is shown in Fig. 1D, which shows an abnormal frequency-of-seeing curve with an elevated threshold and interquartile range, indicating an abnormally shallow slope, obtained in a region of field with normal Humphrey 24-2 thresholds (Fig. 1C).

In the glaucoma suspects the motion threshold alone identified 6/28 suspect eyes as abnormal, with a sensitivity of 21% at 100% specificity (Fig. 2B). The logistic regression model incorporating the interquartile range identified 15/28 glaucoma eyes as abnormal resulting in a sensitivity of 54% with 100% specificity. The in-

terquartile range alone identified 14/28 eyes as abnormal (sensitivity of 50% at 100% specificity). All 28 suspect eyes had normal Humphrey 24-2 fields according to our enrolment criteria. Thus amongst suspects

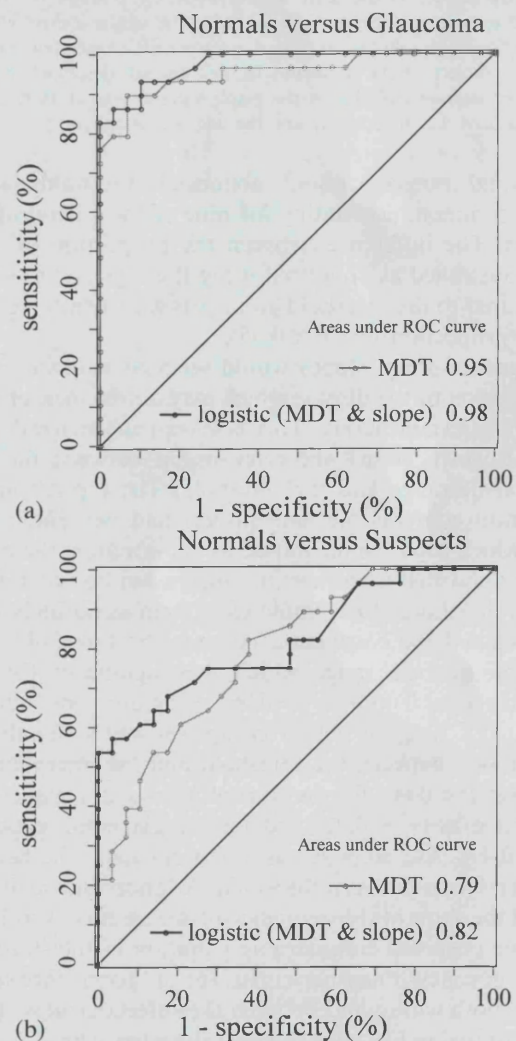


Fig. 2. Receiver operating characteristic (ROC) curves for the motion thresholds (grey line) in comparison to the logistic regression model incorporating the interquartile range (black line). (a) The ROC curve for glaucoma eyes versus controls. Areas under the ROC curve were 0.95 for the motion thresholds, and 0.98 for the logistic regression model. (b) Shows the ROC curve for suspect eyes versus controls. Areas under the ROC curve were 0.79 for the motion thresholds, and 0.82 for the logistic regression model.

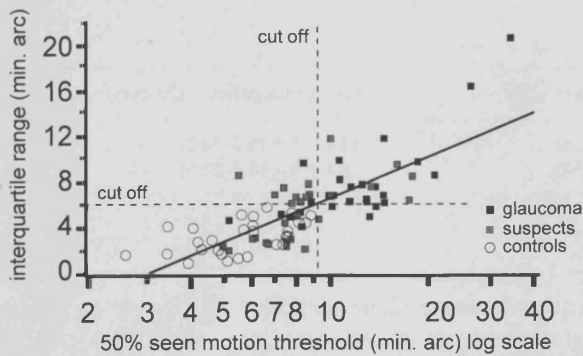


Fig. 3. Relationship between calculated interquartile range and threshold of motion frequency-of-seeing curves for all subjects. The solid line represents the least-squares linear fit through the data. Dashed lines represent cut-offs below which all of the control values for motion threshold (vertical) and interquartile range (horizontal) lie. One subject's data could not be well enough described by the probit to warrant inclusion in the graph because even at 18 min arc displacement the subject only saw the line occasionally.

abnormal ranges without abnormal thresholds were more common, accounting for nine of the 15 abnormal results. The difference between the proportion of suspects identified as abnormal using the regression model compared to the threshold alone was statistically significant (proportion test $P < 0.05$).

Thus abnormal slopes would seem to indicate early progression of the disease which may not be measurable by the threshold alone. This is shown schematically in Fig. 3 which shows the relationship between the interquartile range and the threshold. The top left hand quadrant contains the nine suspect and two glaucoma eyes which could be diagnosed as abnormal on the basis of an abnormal interquartile range when consideration of the threshold alone would class them as normals. We investigated the correlation between the threshold and the interquartile range which was significant for all subjects ($P < 0.0001$, $r^2 = 0.56$, excluding one outlier $r^2 = 0.71$). Analysis within groups showed a significant correlation between the threshold and the interquartile range at $P < 0.005$ for the controls ($r^2 = 0.27$), glaucoma suspect eyes ($r^2 = 0.32$) and for the glaucoma patients ($r^2 = 0.41$). Although statistically significant, the degree of correlation between threshold elevation and shallowing of the slope of the frequency-of-seeing curve was low, and we observed considerable variation in the slope of the frequency-of-seeing curve for a given threshold value, both within and between the subject groups. This is illustrated in Fig. 4A–C which show frequency-of-seeing curves from patients with similar motion thresholds, with markedly different interquartile ranges. Although these subjects had essentially the same thresholds (8.4–8.6 min arc) the interquartile ranges increased roughly in proportion to the seriousness of their glaucoma: extending from a normal value of $4.2 \pm \text{SE } 0.8$ min arc for a suspect eye (Fig. 4A) to $9.6 \pm \text{SE } 2.2$ min arc in a

glaucoma eye (Fig. 4C). In contrast, we identified four eyes that had abnormal motion thresholds with normal interquartile ranges that were within the control range. Fig. 4D illustrates the frequency-of-seeing curve obtained from a glaucoma eye with an abnormal motion threshold (13.2 min arc) and a normal interquartile range ($5.1 \pm \text{SE } 1.0$ min arc).

4. Discussion

The aim of this study was to examine the characteristics of frequency-of-seeing curves for a motion stimulus in normals, glaucoma suspects and glaucomatous eyes. We have found a correlation between the slope of the frequency-of-seeing curve and the motion threshold, with increasing threshold elevation associated with shallowing of the slope of the frequency-of-seeing curve, signifying a higher threshold variability. However the degree of association was low, and we identified considerable variation in the slope of the frequency-of-seeing curves for a given motion threshold.

A significant finding in this study was that the analysis of the interquartile range (slope) in addition to the motion threshold achieved a better separation of suspects from controls than could be obtained by analysing the motion threshold alone. A multivariate logistic regression analysis (using a forward selection procedure) was used to develop a discriminant function to separate glaucomatous eyes from controls, and suspect eyes from controls. In both cases a term using the slope data was found to contribute significantly to the model ($P < 0.05$). This supports the hypothesis that the slope provides extra information allowing for a better discrimination or separation between both suspects and controls, and glaucomatous eyes and controls.

This is reflected by the improvement in the sensitivity of the motion test in the suspects at 100% specificity from 21% using threshold alone to 54% using both variables. The improvement in separation was most marked in patients with only moderately elevated thresholds or with thresholds within the normal range. For example, only 6/28 (21%) of the glaucoma suspects had abnormally elevated motion thresholds outside our normal range. Of the remaining 22 eyes with normal thresholds, analysis of the interquartile range identified an abnormal shallowing of the slope in a further nine eyes.

In the glaucoma eyes, abnormally elevated thresholds and interquartile ranges coexisted in a high proportion (72%). Because of the greater proportion of threshold abnormalities in this group, analysis of the interquartile range only identified two additional eyes as abnormal, compared with the threshold analysis alone.

A caveat of this analysis is that whilst we have developed a discriminant function or classification rule

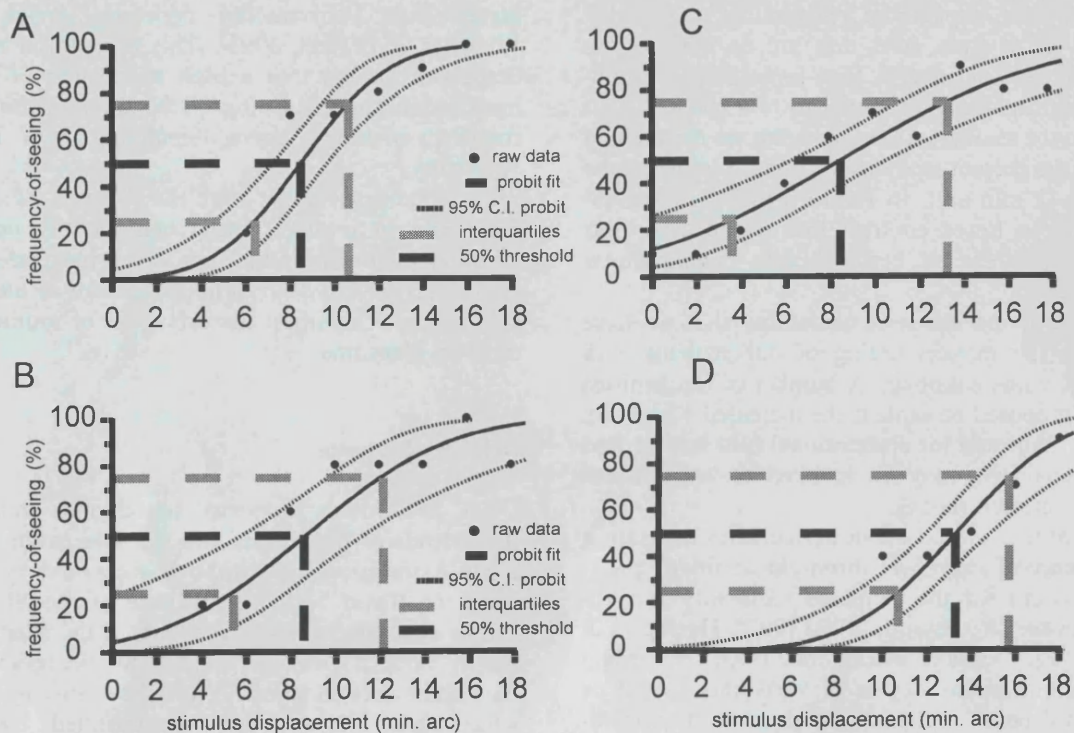


Fig. 4. Frequency-of-seeing curves from three patients with near identical normal motion thresholds (8.4–8.6 min arc), with differing slopes: (A) glaucoma suspect eye from patient aged 63 with normal interquartile range of $4.2 \pm \text{SE } 0.8$ min arc; (B) glaucoma suspect eye from patient aged 68 with abnormally shallow slope and elevated interquartile range of $6.8 \pm \text{SE } 2.2$ min arc; and (C) POAG eye from patient aged 31 with marked shallowing of the slope, with elevated interquartile range of $9.6 \pm \text{SE } 2.2$ min arc. The threshold remains within normal limits. Frequency-of-seeing curve of POAG eye from patient aged 75 with elevated threshold ($13.2 \pm \text{SE } 0.7$ min arc) and normal slope, indicated by interquartile range of $5.1 \pm \text{SE } 1.0$ min arc.

we cannot comment on its performance on an independent set of data. Moreover, the multivariate logistic regression model not only considered the threshold and the slope but also their squared terms. A different result would be obtained if we had, for example, not included the squared (quadratic) terms in the model. In fact, the squared terms were not significant ($P < 0.05$) or included for the separation of glaucomatous eyes from controls but did affect the separation of suspects from controls. The sensitivity of a discriminant function based on the threshold and slope alone (without the squared terms) in separating suspects from controls would be 43% (12 out of 28 suspect eyes identified as abnormal) at 100% specificity. Nevertheless, this is still superior to using the threshold information alone (21% sensitivity at 100% specificity) and the analysis employed does characterise the extent to which the slope provides new diagnostic information. Subsequent studies may validate it as a usable method.

Our findings of a correlation between the motion threshold and slope of the frequency-of-seeing curve is analogous to that for conventional perimetry, which has been reported by a number of researchers (Chauhan & House, 1991; Weber & Rau, 1992; Olsson,

Heijl, Bengtsson & Rootzen, 1993; Chauhan, Tompkins, LeBlanc & McCormick, 1993; Henson, Evans, Chauhan & Lane, 1996; Wall, Maw, Stanek & Chauhan, 1996). The considerable individual differences that we identified in the motion frequency-of-seeing curves of patients with similar motion thresholds are similar to the findings of Chauhan, Tompkins, LeBlanc & McCormick (1993) for a luminance stimulus.

Our results indicate that an abnormal shallowing of the slope of the motion frequency-of-seeing curve may represent one of the earliest changes in glaucoma, and may occur before identifiable threshold elevation. This finding suggests that measures of intratest variability may be an important component of future motion tests in glaucoma. Further longitudinal studies are required to investigate whether frequency-of-seeing analysis can improve the sensitivity and specificity of motion testing in predicting conventional field deterioration.

In addition to the use of frequency-of-seeing analysis, a further improvement in our line displacement test may be achieved with the use of lower contrast stimuli. Lee, Wehrhahn, Westheimer & Kremers (1993) have shown that individual parvocellular cells (at 8° retinal

eccentricity) were capable of responding to line displacements of as little as 2 min arc as long as the contrast was 40% or greater. They reported parvocellular mediated displacement thresholds of 4 min arc. This is similar to the smallest sized thresholds we obtained in normals in the present study using a line stimulus of the same width (2 min arc). In future it may be advantageous to use a lower contrast line stimulus for our MDT test in order to better isolate magnocellular responses.

The cause of the increased variability that we have observed in the motion testing of our patients with glaucoma remains unknown. A number of mechanisms have been proposed to explain the increased variability reported in glaucoma for conventional field testing, and similar mechanisms may be invoked to explain our findings for motion testing.

One hypothesis is that small inaccuracies of fixation in the presence of steep field threshold sensitivity profiles may account for the increased variability in glaucoma (Henson & Bryson, 1990/1991; Haefliger & Flammer, 1991; Vingrys & Demirel, 1993). According to this hypothesis, the degree of variability would be expected to depend on the magnitude of fixation instability and the number and steepness of the sensitivity gradients. However Henson, Evans, Chauhan & Lane (1996) have recently cast doubt on this hypothesis by measuring perimetric frequency-of-seeing curves both with and without fixation error correction in 14 glaucoma patients. They identified a positive correlation between the sensitivity and the slope of the frequency of seeing curve, with a shallowing of the curve associated with locations of lowered sensitivity. A reanalysis using only those responses with good fixation had no significant effect on reducing the variability, either at normal locations or damaged field locations (Henson, Evans, Chauhan & Lane, 1996).

Alternative mechanisms which are not dependent on fixation losses have been proposed to explain the changes in the slope of the psychophysical function. These include neural mechanisms related to factors such as fatigue (Brenton & Argus, 1987) and reduced number of nerve fibres (Flammer, Drance & Zulauf, 1984). We have considered our findings in terms of the concept of reduced redundancy, as proposed by Johnson (1994).

One prediction of the reduced redundancy hypothesis is that selective tests should exhibit greater threshold variability than non selective tests. This is because a selective test stimulates a sparser subpopulation of ganglion cells with minimal overlapping receptive fields, compared with more non-selective tests (Johnson, 1994). This prediction of the reduced redundancy hypothesis has been supported by Wild, Moss, Whitaker & O'Neill (1995), who have shown that the short term variability of selective blue-on-yellow testing (SWAP) is

higher than conventional perimetry (Wild, Moss, Whitaker & O'Neill, 1995). This mechanism may underlie our finding that a high proportion of patients have significant shallowing of the slope of the motion frequency-of-seeing curve, signifying high intratest variability.

Our findings suggest that the analysis of intratest variability in motion testing can identify important additional differences between glaucoma patients and controls. This may lead to improvements in our understanding of the earliest abnormalities of motion sensitivity in glaucoma.

Acknowledgements

MC Westcott is supported by research grants from the Friends of Moorfields and the International Glaucoma Association. DP Crabb is supported by a grant from the Royal National Institute of the Blind. FW Fitzke is supported by a grant from the Medical Research Council. We are grateful to the reviewers for their comments on an earlier version of this manuscript, which have now been incorporated into this manuscript.

References

- Anderson, S. J., Drasdo, N., & Thompson, C. M. (1995). Parvocellular neurons limit motion acuity in human peripheral vision. *Proceedings of the Royal Society of London B*, 261, 129–138.
- Baez, K. A., McNaught, A. I., Dowler, J. G., Poinosawmy, D., Fitzke, F. W., & Hitchings, R. A. (1995). Motion detection threshold and field progression in normal tension glaucoma. *British Journal of Ophthalmology*, 79, 125–128.
- Bosworth, C. F., Sample, P. A., & Weinreb, R. N. (1997). Motion perception thresholds in areas of glaucomatous visual field loss. *Vision Research*, 37, 355–364.
- Brenton, R. S., & Argus, W. A. (1987). Fluctuations on the Humphrey and Octopus perimeters. *Investigative Ophthalmology & Visual Science*, 28, 767–771.
- Bullimore, M. A., Wood, J. M., & Swenson, K. (1993). Motion perception in glaucoma. *Investigative Ophthalmology & Visual Science*, 34, 3526–3533.
- Casson, E. J., Johnson, C. A., & Shapiro, L. R. (1993). Longitudinal comparison of temporal-modulation perimetry with white-on-white and blue-on-yellow perimetry in ocular hypertension and early glaucoma. *Journal of the Optical Society of America A*, 10, 1792–1806.
- Chaturvedi, N., Hedley, W. E. T., & Dreyer, E. B. (1993). Lateral geniculate nucleus in glaucoma. *American Journal of Ophthalmology*, 116, 182–188.
- Chauhan, B. C., & House, P. H. (1991). Intratest variability in conventional and high-pass resolution perimetry. *Ophthalmology*, 98, 79–83.
- Chauhan, B. C., Tompkins, J. D., LeBlanc, R. P., & McCormick, T. A. (1993). Characteristics of frequency-of-seeing curves in normal subjects, patients with suspected glaucoma, and patients with glaucoma. *Investigative Ophthalmology & Visual Science*, 34, 3534–3540.

- Fitzke, F. W., Poinosawmy, D., Ernst, W., & Hitchings, R. A. (1987). Peripheral displacement thresholds in normals, ocular hypertensives and glaucoma. In E. L. Greve, & A. Heijl, *Seventh international visual field symposium*. Dordrecht: Martinus Nijhoff, 447–452.
- Fitzke, F. W., Poinosawmy, D., Nagasubramanian, S., & Hitchings, R. A. (1989). Peripheral displacement thresholds in glaucoma and ocular hypertension. In A. Heijl, *Perimetric update*. Amsterdam: Kugler and Ghedini, 399–405.
- Flammer, J., Drance, S. M., & Zulauf, M. (1984). Differential light threshold. Short- and long-term fluctuation in patients with glaucoma, normal controls, and patients with suspected glaucoma. *Archives of Ophthalmology*, 102, 704–706.
- Glovinsky, Y., Quigley, H. A., & Dunkelberger, G. R. (1991). Retinal ganglion cell loss is size dependent in experimental glaucoma. *Investigative Ophthalmology & Visual Science*, 32, 484–491.
- Glovinsky, Y., Quigley, H. A., & Pease, M. E. (1993). Foveal ganglion cell loss is size dependent in experimental glaucoma. *Investigative Ophthalmology & Visual Science*, 34, 395–400.
- Graham, S. L., Drance, S. M., Chauhan, B. C., Swindale, N. V., Hnik, P., Mikelberg, F. S., & Douglas, R. G. (1996). Comparison of psychophysical and electrophysiological testing in glaucoma. *Investigative Ophthalmology & Visual Science*, 37, 2651–2662.
- Haefliger, I. O., & Flammer, J. (1991). Fluctuation of the differential light threshold at the border of absolute scotomas. Comparison between glaucomatous visual field defects and blind spots. *Ophthalmology*, 98, 1529–1532.
- Henson, D. B., & Bryson, H. (1990). Is variability in glaucomatous field loss due to poor fixation control. In R. P. Mills, & A. Heijl, *Perimetric Update*. Amsterdam: Kugler & Ghedini, 217–220.
- Henson, D. B., Evans, J., Chauhan, B. C., & Lane, C. (1996). Influence of fixation accuracy on threshold variability in patients with open angle glaucoma. *Investigative Ophthalmology & Visual Science*, 37, 444–450.
- Joffe, K. M., Raymond, J. E., & Chrichton, A. (1997). Motion coherence perimetry in glaucoma and suspected glaucoma. *Vision Research*, 37, 955–964.
- Johnson, C. A. (1994). Selective versus nonselective losses in glaucoma. *Journal of Glaucoma*, 3(1), S32–S44.
- Johnson, C. A., Adams, A. J., Casson, E. J., & Brandt, J. D. (1993a). Blue-on-yellow perimetry can predict the development of glaucomatous visual field loss. *Archives of Ophthalmology*, 111, 645–650.
- Johnson, C. A., Adams, A. J., Casson, E. J., & Brandt, J. D. (1993b). Progression of early glaucomatous visual field loss as detected by blue-on-yellow and standard white-on-white automated perimetry. *Archives of Ophthalmology*, 111, 651–656.
- Johnson, C. A., Marshall, D., & Eng, K. M. (1995). Displacement threshold perimetry in glaucoma using a Macintosh computer system and a 21-in monitor. In R. Mills, & M. Wall, *Perimetry update*. Amsterdam: Kugler and Ghedini, 103–110.
- Lachenmayr, B. J., Drance, S. M., Douglas, G. R., & Mikelberg, F. S. (1991). Light-sense, flicker and resolution perimetry in glaucoma a comparative study. *Graefes's Archive for Clinical and Experimental Ophthalmology*, 229, 246–251.
- Lee, B. B. (1993). Macaque ganglion cells and spatial vision. *Progress in Brain Research*, 95, 33–43.
- Lee, B. B., Wehrhahn, C., Westheimer, G., & Kremers, J. (1993). Macaque ganglion cell responses to stimuli that elicit hyperacuity in man detection of small displacements. *Journal of Neuroscience*, 13, 1001–1009.
- Livingstone, M. S., & Hubel, D. H. (1987). Psychophysical evidence for separate channels for the perception of form, color, movement, and depth. *Journal of Neuroscience*, 7, 3416–3468.
- Merigan, W. H., Byrne, C. E., & Maunsell, J. H. (1991). Does primate motion perception depend on the magnocellular pathway? *Journal of Neuroscience*, 11, 3422–3429.
- Merigan, W. H., & Maunsell, J. H. (1990). Macaque vision after magnocellular lateral geniculate lesions. *Visual Neuroscience*, 5, 347–352.
- Olsson, J., Heijl, A., Bengtsson, B., & Rootzen, H. (1993). Frequency-of-seeing in computerised perimetry. In P. R. Mills, *Perimetry update*. Amsterdam: Kugler & Ghedini, 551–556.
- Piltz, J. R., Drance, S. M., Douglas, G. R., & Mikelberg, F. S. (1991). The relationship of peripheral vasospasm, diffuse and localized visual field defects, and intraocular pressure in glaucomatous eyes. In R. Mills, & A. Heijl Jr., *Perimetry update*. Amsterdam/New York: Kugler, 465–472.
- Quigley, H. A., Addicks, E. M., & Green, W. R. (1982). Optic nerve damage in human glaucoma. III. Quantitative correlation of nerve fiber loss and visual field defect in glaucoma, ischemic neuropathy, papilledema, and toxic neuropathy. *Archives of Ophthalmology*, 100, 135–146.
- Quigley, H. A., Dunkelberger, G. R., & Green, W. R. (1988). Chronic human glaucoma causing selectively greater loss of large optic nerve fibers. *Ophthalmology*, 95, 357–363.
- Quigley, H. A., Dunkelberger, G. R., & Green, W. R. (1989). Retinal ganglion cell atrophy correlated with automated perimetry in human eyes with glaucoma. *American Journal of Ophthalmology*, 107, 453–464.
- Ruben, S., & Fitzke, F. (1994). Correlation of peripheral displacement thresholds and optic disc parameters in ocular hypertension. *British Journal of Ophthalmology*, 78, 291–294.
- Sample, P. A., & Weinreb, R. N. (1992). Progressive color visual field loss in glaucoma. *Investigative Ophthalmology & Visual Science*, 33, 2068–2071.
- Silverman, S. E., Trick, G. L., & Hart, W. M. Jr. (1990). Motion perception is abnormal in primary open-angle glaucoma and ocular hypertension. *Investigative Ophthalmology & Visual Science*, 31, 722–729.
- Trick, G. L., Steinman, S. B., & Amyot, M. (1995). Motion perception deficits in glaucomatous optic neuropathy. *Vision Research*, 35, 2225–2233.
- Tyler, C. W., Hardage, L., & Stamper, R. L. (1994). The temporal visuogram in ocular hypertension and its progression to glaucoma. *Journal of Glaucoma*, 3, 65–72.
- Vingrys, A. J., & Demirel, S. (1993). The effect of fixational loss on perimetric thresholds and reliability. In R. P. Mills, *Perimetry update*. Amsterdam: Kugler & Ghedini, 521–526.
- Wall, M., & Ketoff, K. M. (1995). Random dot motion perimetry in patients with glaucoma and in normal subjects. *American Journal of Ophthalmology*, 120, 587–596.
- Wall, M., Maw, R. J., Stanek, K. E., & Chauhan, B. C. (1996). The psychometric function and reaction times of automated perimetry in normal and abnormal areas of the visual field in patients with glaucoma. *Investigative Ophthalmology & Visual Science*, 37, 878–885.
- Weber, J., & Rau, S. (1992). The properties of perimetric thresholds in normal and glaucomatous eyes. *German Journal of Ophthalmology*, 1, 79–85.
- Wild, J. M., Moss, I. D., Whitaker, D., & O'Neill, E. C. (1995). The statistical interpretation of blue-on-yellow visual field loss. *Investigative Ophthalmology & Visual Science*, 36, 1398–1410.